

FORMULATION AND EVALUATION OF COLON TARGETED ORAL DRUG DELIVERY SYSTEM USING NATURAL POLYMERS AND METHACRYLIC ACID CO-POLYMERS

A Thesis submitted to Gujarat Technological University

for the Award of

Doctor of Philosophy

in

Pharmacy

by

Patel Jayminkumar Manilal

189999901011

under supervision of

Dr. Shreeraj H. Shah



GUJARAT TECHNOLOGICAL UNIVERSITY

AHMEDABAD

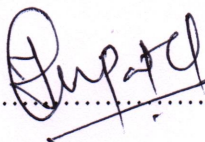
February-2024

© Patel Jayminkumar Manilal

DECLARATION

I declare that the thesis entitled "**FORMULATION AND EVALUATION OF COLON TARGETED ORAL DRUG DELIVERY SYSTEM USING NATURAL POLYMERS AND METHACRYLIC ACID CO-POLYMERS**" submitted by me for the degree of Doctor of Philosophy is the record of research work carried out by me during the period from **2018** to **2023** under the supervision of **Dr. Shreeraj H. Shah** and this has not formed the basis for the award of any degree, diploma, associateship, fellowship, titles in this or any other University or other institution of higher learning. I further declare that the material obtained from other sources has been duly acknowledged in the thesis. I shall be solely responsible for any plagiarism or other irregularities, if noticed in the thesis.

Signature of the Research Scholar:



Date.....


17/02/24

Name of Research Scholar: **Patel Jayminkumar Manilal**

Place: **Ahmedabad**

CERTIFICATE

I certify that the work incorporated in the thesis "**FORMULATION AND EVALUATION OF COLON TARGETED ORAL DRUG DELIVERY SYSTEM USING NATURAL POLYMERS AND METHACRYLIC ACID CO-POLYMERS**" submitted by **Mr. Jayminkumar Manilal Patel** was carried out by the candidate under my supervision/ guidance. To the best of my knowledge: (i) the candidate has not submitted the same research work to any other institution for any degree/diploma, Associateship, Fellowship or other similar titles (ii) the thesis submitted is a record of original research work done by the Research Scholar during the period of study under my supervision, and (iii) the thesis represents independent research work on the part of the Research Scholar.

Signature of Supervisor: 

Date: 

Name of Supervisor: **Dr. Shreeraj H. Shah**

Place: **Ahmedabad**

Course-work Completion Certificate

This is to certify that Mr. **Jayminkumar Manilal Patel** enrolment no. **189999901011** is enrolled for PhD program in the branch **Pharmacy** of Gujarat Technological University, Ahmedabad.

(Please tick the relevant option(s))

☐ He has been exempted from the course-work (successfully completed during M.Phil Course)

☐ He has been exempted from Research Methodology Course only (successfully completed during M.Phil. Course)

☒ He has successfully completed the PhD course work for the partial requirement for the award of PhD Degree. His performance in the course work is as follows-

Grade Obtained in Research Methodology [PH001]	Grade Obtained in Self-Study Course (core Subject) [PH002]
BB	AB


Supervisor's Sign

(Dr. Shreeraj H. Shah)

Originality Report Certificate

It is certified that PhD Thesis titled "**FORMULATION AND EVALUATION OF COLON TARGETED ORAL DRUG DELIVERY SYSTEM USING NATURAL POLYMERS AND METHACRYLIC ACID CO-POLYMERS**" by **Patel Jayminkumar Manilal** has been examined by us. We undertake the following:

- a. Thesis has significant new work / knowledge as compared already published or are under consideration to be published elsewhere. No sentence, equation, diagram, table, paragraph or section has been copied verbatim from previous work unless it is placed under quotation marks and duly referenced.
- b. The work presented is original and own work of the author (i.e., there is no plagiarism). No ideas, processes, results or words of others have been presented as Author own work.
- c. There is no fabrication of data or results which have been compiled / analyzed.
- d. There is no falsification by manipulating research materials, equipment or processes, or changing or omitting data or results such that the research is not accurately represented in the research record.
- e. The thesis has been checked using **Drill Bit Anti-Plagiarism software** (copy of originality report attached) and found within limits as per GTU Plagiarism Policy and instructions issued from time to time (i.e., permitted similarity index $\leq 10\%$).

Signature of the Research Scholar:

Date: 17/02/24

Name of Research Scholar: **Patel Jayminkumar Manilal**

Signature of Supervisor:

Date: 13/02/2024

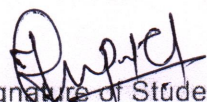
Name of Supervisor: **Dr. Shreeraj H. Shah**

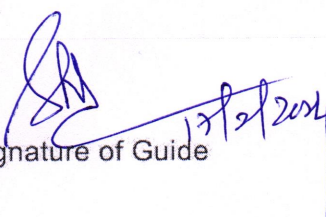
Place: **Ahmedabad**



Gujarat Technological University
Certificate of Plagiarism Check for Thesis

Author Name	PATEL JAYMINKUMAR MANILAL
Course of Study	Ph.D.
Name of Guide	Dr. Shreeraj H. Shah
Department	Pharmacy
Acceptable Maximum Limit	10 %
Submitted By	pateljaymin9@gmail.com
Paper Title	PHD THESIS
Similarity	8%
Paper ID	1044552
Submission Date	2023-10-25 09:19:54


Signature of Student


Signature of Guide

Head of the Department

University Librarian

Director of Post Graduate Studies

* This report has been generated by DrillBit Anti-Plagiarism Software



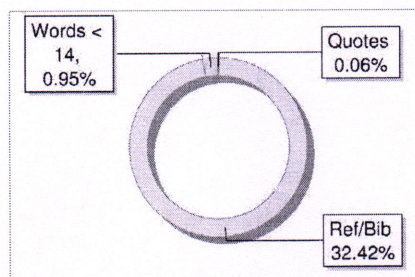
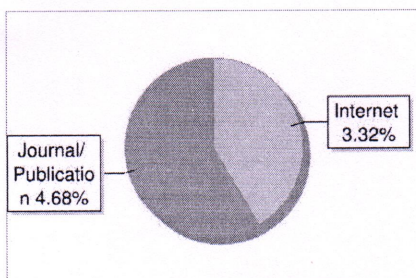
The Report is Generated by DrillBit Plagiarism Detection Software

Submission Information

Author Name	PATEL JAYMINKUMAR MANILAL
Title	PHD THESIS
Paper/Submission ID	1044552
Submitted by	pateljaymin9@gmail.com
Submission Date	2023-10-25 09:19:54
Total Pages	187
Document type	Thesis

Result Information

Similarity 8 %

*Exclude Information*

Quotes	Not Excluded
References/Bibliography	Excluded
Sources: Less than 14 Words Similarity	Excluded
Excluded Source	4 %
Excluded Phrases	Not Excluded

A Unique QR Code use to View/Download/Share Pdf File



Ph.D. Thesis Non-Exclusive License to GUJARAT TECHNOLOGICAL UNIVERSITY

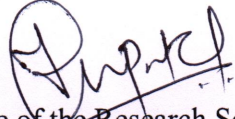
In consideration of being a Research Scholar at Gujarat Technological University, and in the interests of the facilitation of research at the University and elsewhere, I, **Patel Jayminkumar Manilal** having **189999901011** hereby grant a non-exclusive, royalty free and perpetual license to the University on the following terms:

- a. The University is permitted to archive, reproduce and distribute my thesis, in whole or in part, and/or my abstract, in whole or in part (referred to collectively as the “Work”) anywhere in the world, for non-commercial purposes, in all forms of media;
- b. The University is permitted to authorize, sub-lease, sub-contract or procure any of the acts mentioned in paragraph (a);
- c. The University is authorized to submit the Work at any National / International Library, under the authority of their “Thesis Non-Exclusive License”;
- d. The Universal Copyright Notice (©) shall appear on all copies made under the authority of this license;
- e. I undertake to submit my thesis, through my university, to any Library and Archives. Any abstract submitted with the thesis will be considered to form part of the thesis.
- f. I represent that my thesis is my original work, does not infringe any rights of others, including privacy rights, and that I have the right to make the grant conferred by this non-exclusive license.
- g. If third party copyrighted material was included in my thesis for which, under the terms of the Copyright Act, written permission from the copyright owners is required, I have obtained such permission from the copyright owners to do the acts mentioned in paragraph (a) above for the full term of copyright protection.
- h. I understand that the responsibility for the matter as mentioned in the paragraph (g) rests with the authors / me solely. In no case shall GTU have any liability for any acts / omissions / errors / copyright infringement from the publication of the said thesis or otherwise.
- i. I retain copyright ownership and moral rights in my thesis, and may deal with the copyright in my thesis, in any way consistent with rights granted by me to my university in this non-exclusive license.
- j. GTU logo shall not be used /printed in the book (in any manner whatsoever) being

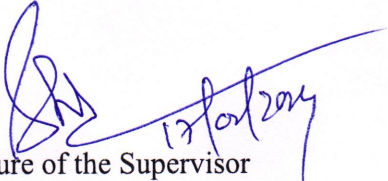
- published or any promotional or marketing materials or any such similar documents.
- k. The following statement shall be included appropriately and displayed prominently in the book or any material being published anywhere: "The content of the published work is part of the thesis submitted in partial fulfilment for the award of the degree of Ph.D. in **Pharmacy** of the Gujarat Technological University".
- l. I further promise to inform any person to whom I may hereafter assign or license my copyright in my thesis of the rights granted by me to my university in this nonexclusive license. I shall keep GTU indemnified from any and all claims from the Publisher(s) or any third parties at all times resulting or arising from the publishing or use or intended use of the book / such similar document or its contents.
- m. I am aware of and agree to accept the conditions and regulations of Ph.D. including all policy matters related to authorship and plagiarism.

Date: 17/02/24

Place: Al Bad


Signature of the Research Scholar

Recommendation of the Supervisor: Yes


Signature of the Supervisor

Thesis Approval Form

The viva-voce of the PhD Thesis submitted by Shri. **Jayminkumar Manilal Patel**, **189999901011** entitled "**FORMULATION AND EVALUATION OF COLON TARGETED ORAL DRUG DELIVERY SYSTEM USING NATURAL POLYMERS AND METHACRYLIC ACID CO-POLYMERS**" was conducted on at Graduate School of Pharmacy, Gujarat Technological University, Gandhinagar.

(Please tick any one of the following options)

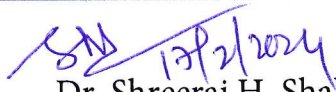
☒ The performance of the candidate was satisfactory. We recommend that he/she be awarded the PhD degree.

☐ Any further modifications in research work recommended by the panel after 3 months from the date of first viva-voce upon request of the Supervisor or request of Independent Research Scholar after which viva-voce can be re-conducted by the same panel again.

(Briefly specify the modifications suggested by the panel)

☐ The performance of the candidate was unsatisfactory. We recommend that he/she should not be awarded the PhD degree.

(The panel must give justifications for rejecting the research work)


Dr. Shreeraj H. Shah

Name and Signature of Supervisor with Seal


Dr. Jayvadan K. Patel

1) (External Examiner 1) Name and Signature


Dr. Juturi Ravikumar Reddy

2) (External Examiner 2) Name and Signature

ABSTRACT

This research aimed to develop a colon-targeted Budesonide drug delivery system using microbial and pH triggers within the framework of Quality by Design (QbD). Natural gums were screened for their potential to create a colon-targeted drug delivery system based on viscosity analysis and enzyme sensitivity studies. Tamarind Gum was selected as the primary candidate based on its excellent viscosity characteristics. For tablet dosage forms, carboxymethyl (CM) Tamarind Gum was chosen, and these tablets were coated with Eudragit S 100 to delay drug release in the upper gastrointestinal tract. Pellet dosage forms were optimized using critical process parameters and formulation variables, super-coated with Eudragit S100 for enhanced colon targeting. Through the Box Behnken Design and Response Surface Optimization methods, the research identified the Design Space (DS) and optimal formulations meeting specific criteria. The results showed that these formulations released less than 10% of the drug in the first 5 hours and over 80% within 9 hours, aligning with colon-targeted drug delivery goals. Histopathology and biochemical analyses of IL-6 and TNF- α confirmed the efficiency of the optimized pellet formulation in treating induced ulcerative colitis in rats compared to standard Budesonide solution. Roentgenography demonstrated that the optimized formulation remained intact for 5 hours and fully disseminated after 7 hours. This research presents a systematic approach to developing colon-targeted Budesonide formulations with delay drug release characteristics, promising clinical applications for colon-related disorders.

Key words: Budesonide, Tamarind gum, Carboxymethyl tamarind gum, Eudragit S 100, pH and Microbial Approach, Quality by Design.

Acknowledgement

It is the moment of happiness for me and my family as the dreams seen come true with completion of the PhD degree course, key mile stone in my education. "Research is to see what everybody has seen but nobody has thought"

This research work is a journey accompanied by the synergistic efforts and involvement of a lot of people. This doctoral work had its own set of challenges; therefore, I would like to grab this opportunity to extend my sincere gratitude to all the people, directly or indirectly, involved in the success of my research work,

*From the start, I want to express my gratitude to **The Almighty God** for enabling me to showcase my abilities and for giving me the courage to persevere through whatever difficulties I may encounter.*

*A successful outcome in any research endeavour is greatly influenced by the selfless guidance of the mentor. I am immensely grateful to my honourable guide, **Dr. Shreeraj Shah**, Principal & Director, L. J. Institute of Pharmacy, LJ University, for his valuable advice & support throughout the course; and having the much-needed faith & confidence in me during the entire duration of Ph.D. I am thankful to him for his valuable time and untiring efforts.*

*I am grateful to **Gujarat Technological University** for granting me a wonderful opportunity to conduct my Ph.D. research under its esteemed affiliation. I am extremely grateful to **all the staff members of Ph.D. Section, Gujarat Technological University**, for their timely co-operation and support in ensuring the smooth execution of all the procedures of my Dissertation work. I am extremely grateful to **L. J. Institute of Pharmacy and LJ University** for their unwavering support, motivation, and provision of excellent facilities, incentives, and financial assistance that have greatly contributed to the successful conduction of my research work,*

*I am eternally thankful to my DPC members **Dr. Anita Lalwani**, Professor, K. B institute of pharmaceutical research, Gandhinagar; and **Dr. D. M. Patel**, Associate Professor, Graduate School of Pharmacy, Gandhinagar, for their invaluable suggestions, generous time during the entire research work, and moulding the project into an outstanding research endeavour.*

*I am incredibly grateful to **Zydus Cadila, Ahmedabad, India**, for generously providing me with a gift sample of the Budesonide drug. I am also thankful to **Exim Pvt. Ltd** for their kind gesture of providing a natural gums sample and their prompt cooperation.*

*Special thanks to **Dr. Paresh Patel** and **Ms. Kaushika Patel**, two of my closest colleagues and trusted friends, have been an endless source of motivation and encouragement throughout the completion of my thesis and the subsequent publication of the research-based articles.*

*I would like to express my gratitude to **Mr. Mihir Patel**, **Dr. Aashish Panchal**, **Dr. Shruti Rawal** and **Dr. Tosha Pandya** for their encouragement and unwavering support throughout my journey.*

*I am thankful to **Dr. K. Pundarikakshudu**, Founder Director, L. J. Institute of Pharmacy, for the persistent support. I would like to express my appreciation to my colleague, **Mr. Vijay Kevlani**, for his unwavering assistance in the successful completion of the animal study. Additionally, I would like to acknowledge the valuable support provided by the members of the Pharmaceutical Technology Department, namely **Dr. Sheetal Acharya**, **Mr. Mangesh Kulkarni**, **Ms. Shital Trivedi**, and **Ms. Disha Joshi**.*

*I am also thankful to my students **Momin Faiz**, **Dhruv**, **Bhargav**, **Sahil** and **Parth** for their help in my work.*

*I am grateful for the invaluable assistance provided by the non-teaching staff members of the Pharmaceutical Technology department, **Mr. Danabhai Parmar**, **Mr. Dajibhai Thakor**, and **Mr. Tulsiram Pasi**, during the successful conduction of our experimental work.*

*Finally, the words of thanks would be insufficient for the pacemaker of my work – my elder brother- **Jayesh Bhai**, My wife-**Alpa**, my **mother** and all other family members. Their unending care, motivation and encouragement have helped me to complete the project successfully.*

List of Contents

DECLARATION.....	iii
CERTIFICATE	iv
Course-work Completion Certificate	v
Originality Report Certificate.....	vi
Ph.D. Thesis Non-Exclusive License to.....	ix
Thesis Approval Form	xi
ABSTRACT	xii
Acknowledgement	xiii
List of Contents	xv
List of Abbreviations	xx
List of Figures.....	xxi
List of Tables	xxiii
List of appendices.....	xxv
1. Introduction.....	1
<i>1.1 Introduction to inflammatory bowel disease.....</i>	<i>1</i>
1.1.1 Intestinal barrier in Inflammatory Bowel Disease	4
1.1.2 Diagnosis of Inflammatory Bowel Disease	5
1.1.3 Treatment of Inflammatory bowel disease.....	7
1.1.3.1 Medical Management of Ulcerative Colitis and Crohn's Disease.....	7
<i>1.2 Introduction to Colon Targeted Drug delivery system</i>	<i>9</i>
1.2.1 Advantages of CDDS over Conventional Drug Delivery	10
1.2.2 Approaches of colon targeted drug delivery system.....	11
1.2.2.1 Coating with pH dependent polymers.....	11
1.2.2.2 Timed-Release Systems	12
1.2.2.3 Microbial Triggered Systems.....	13
1.2.3 Colonic microflora and metabolic activity	15
<i>1.3 Introduction to Polysaccharides.....</i>	<i>17</i>
1.3.1 Polysaccharides selected for the present study:.....	17
<i>1.4 Introduction to drug</i>	<i>23</i>

1.5 Introduction to Quality by Design (QbD)	24
1.5.1 Elements of Pharmaceutical Quality by Design	24
1.6 References.....	29
2. Review of Literature	37
2.1 Review of literature for budesonide	37
2.2 Literature Review for Natural Polymers.....	42
2.3 Review of literature for microbial approach-based colon targeted drug delivery system.....	48
2.4 Review of literature for modified dissolution methodology.....	52
2.5 References.....	54
3. Aim, Objectives and Rationale of Present investigation.....	59
3.1 Aim of the Present Investigation.....	59
3.2 Objectives of Present Investigation	60
3.3 Rationale of Present Investigation	61
3.3.1 Rationale for the selection of Budesonide as drug.....	61
3.3.2 Rationale for the selection of combination of pH and Microbial Approach for colon targeted drug delivery system	61
4. Preformulation Studies.....	63
4.1 Materials and Equipments	63
4.2 Preformation studies.....	64
4.2.1 Drug identification	64
4.2.1.1 Physical characterization	65
4.2.1.2 Melting point (MP) determination	65
4.2.1.3 Solubility	65
4.2.1.4 Identification of Drug by FTIR and UV scanning	65
4.2.2 Drug – excipient compatibility study.....	66
4.2.3 Development of calibration curve for Budesonide by UV spectrophotometric method in 0.1 N HCl, Phosphate Buffer (pH 7.4), and Phosphate buffer (pH 6.8)	66
4.2.4 Calibration Curve of budesonide in 0.1 N HCl.....	66
4.2.5 Calibration Curve of budesonide in phosphate buffer pH 7.4	67
4.2.6 Calibration Curve of budesonide in phosphate buffer pH 6.8	68
4.2.7 Screening of Natural Gums by Viscometric Procedure:.....	68
4.2.8 Preparation of 4% rat cecal content solution and Probiotic Culture Medium:	69
4.2.9 Enzymatic susceptibility for natural gums:	70
4.3 Results and Discussion:.....	70
4.3.1 Identification of Drugs.....	70

4.3.1.1 Identification of Drugs by Description, Solubility and Melting Point	70
4.3.1.2 Identification of drugs by FTIR and UV scanning	71
4.3.2 Drug – Excipient compatibility study	72
4.3.3 Standard Calibration Curve of Budesonide in 0.1N HCl, Phosphate Buffer pH 7.4 & 6.8 ...	77
4.3.4 Screening of Natural Gums:	80
4.4 References:	84
5. Colon Targeted Tablet dosage form	87
5.1 Experimental Methods	87
5.1.1 Precompression parameters	87
5.1.1.2: Bulk density	87
5.1.1.2: Tapped density	87
5.1.1.3 Compressibility Index	88
5.1.1.4 Hausner ratio	88
5.1.1.5 Angle of Repose	88
5.1.2 Preliminary batches of Tablets by Direct Compression method and wet granulation	89
5.1.3 Post compression parameters for uncoated tablets dosage form	90
5.1.3.1 Weight Variation test	90
5.1.3.2 Friability	91
5.1.3.3 Hardness	91
5.1.3.4 Thickness	91
5.1.3.5 % Assay (Drug Content)	92
5.1.4 Coating of Tablets	92
5.1.4.1 Method of preparation of coating solution	92
5.1.5 Designing the Formulations by using Box-Behnken factorial design	93
5.1.6 Dissolution Method	96
5.1.7 Release kinetics of the formulations prepared by the experimental design	96
5.1.7.1 Zero-order kinetics	97
5.1.7.2 First order kinetics	97
5.1.7.3 Higuchi model	98
5.1.7.4 Hixon -Crowell model	98
5.1.7.5 Korsmeyer – Peppas model (Power Law)	99
5.1.7.6 Weibull Model	99
5.1.8 Roentgenography study	100
5.1.9 Stability Study	100

5.2. Result and Discussion	101
5.2.1 Precompression parameters of lubricated powder mass/granules	101
5.2.2 Post compression parameters of tablet dosage form	102
5.2.3 In-Vitro release studies	103
5.2.4 <i>In vitro</i> release profile of batches prepared by the Box-Behnken Experimental Design	106
5.2.5 Statistical Assessment of Box-Behnken Experimental Design	110
5.2.5.1 Effect of X_1 , X_2 , and X_3 on % drug release at 2 (Y2) hrs.	110
5.2.5.2 Effect of X_1 , X_2 , and X_3 on % drug release at 5 (Y5) hrs.	113
5.2.5.3 Effect of X_1 , X_2 , and X_3 on % drug release at 8 (Y8) hrs.	115
5.2.6 Release kinetics of formulation batches	120
5.2.7 <i>In-vivo</i> study in rabbit	124
5.2.8 Stability Study	125
5.3. References	126
6. Colon Targeted Pellets-based dosage form	129
6.1 Experimental Methods	129
6.1.1 Preparation of Pellets dosage form	129
6.1.2 Risk assessment	129
6.1.3 Screening of Pellets Parameters (Formulation and Process) by using 2^4 full factorial design	130
6.1.3.1 Aspect Ratio of Pellets.	132
6.1.3.2 Average Particle size.	132
6.1.3.3 In-vitro drug release at 2 hours	132
6.1.4 Coating of Pellets	132
6.1.5 Formulation optimization by using Box-Behnken Factorial Design	134
6.1.6 Dissolution Method	135
6.1.7 Release kinetics of the formulations prepared by the experimental design	136
6.1.8 <i>In vivo</i> study	136
6.1.8.1 Animals and ethical approval	136
6.1.8.2 Induction of ulcerative colitis	137
6.1.8.3 Histopathological evaluation	138
6.1.8.4 Preparation of tissue homogenate for biochemical estimation	140
6.1.9 Roentgenography study	141
6.1.10 Stability Study	142
6.2. Result and Discussion	142
6.2.1 Risk assessment study for core pellets	142

6.2.2 Influence of formulation parameters and process parameters on dependent variables by using 2⁴ screening factorial Design for core pellets	144
6.2.2.1 Aspect Ratio of Pellets	145
6.2.2.2 Particle size distribution	148
6.2.2.3 Percentage Cumulative Drug Release (% CDR) at 2 Hrs.	152
6.2.3 Creating the Design Space and reducing numbers and the range of independent variables for next Experimental Design	155
6.2.4 Box-Behnken Design	156
6.2.4.2 percentage cumulative drug release (% CDR) at 5 hours	160
6.2.4.3 percentage cumulative drug release (% CDR) at 9 hours	163
6.2.5 Release kinetics of formulation batches	166
6.2.6 In vivo study	169
6.2.6.1 Histopathological assessment of the colon	169
6.2.6.2 Biochemical estimation of cytokines, IL 6 and TNF- α	172
6.2.7 SEM analysis for optimised Formulation	176
6.2.8 Stability Study	176
6.3 References	178
7. Comparison of dissolution profiles between Tablet and Pellets dosage form	181
7.1 Statistical Methods	181
7.1.1 Model Independent Models [4]:	181
7.1.2 Model dependent Models:	184
7.2 Result and Discussion	184
7.3 References	189
8. Conclusion	191
List of publications	193
Appendix A- CPCSEA Approval protocol for in vivo study	196

List of Abbreviations

CD	= Crohn's Disease
UC	= Ulcerative Colitis
QbD	= Quality by Design
CPPs	= Critical Process Parameters
CQAs	= Critical Quality attributes
QTPP	= Quality Target Product Profile
BBD	= Box-Behnken Design
CM	= Carboxymethyl
GI	= Gastrointestinal
ICH	= International conference on Harmonisation
IPA	= Isopropyl Alcohol
% CDR	= percentage Cumulative Drug Release
mL	= millilitre
ppm	= Part per millions
ANOVA	= Analysis of Variance
API	= Active Pharmaceutical Ingredients
FTIR	= Fourier transform infrared Spectroscopy
R ²	= Regression Coefficients
λ_{max}	= The wavelength at maximum absorbance
RPN	= Risk Priority Number
FMEA	= Failure Mode and Effects Analysis
DS	= Design Space
SEM	= Scanning Electro-Microscopy
TNF- α	= Tumour Necrosis factor - alpha
IL-6	= Interleukin-6
% DE	= percentage Dissolution efficiency
MDT	= mean Dissolution time
MSD	= Multivariant Statistical Distance

List of Figures

Figure 1.1 Inflammatory bowel disease (a) Crohn's disease (b) Ulcerative colitis	1
Figure 1.2: Connection between input CMAs and CPPs and output CQAs	28
Figure 4.1: FTIR spectra of budesonide (a) observed (b) Reported in Indian pharmacopeia 2010 .	72
Figure 4.2: UV scanning of the Budesonide (λ_{max} -244)	72
Figure 4.3 FTIR spectra of (a) budesonide (b) Budesonide + Khaya gum	73
Figure 4.4: FTIR spectra of budesonide +(a) Pectin gum(b)Ghatti gum(c) Xanthan gum	74
Figure 4.5: FTIR spectra of budesonide + (a) Karaya (b) Gellan (c) Tamarind gum	75
Figure 4.6: FTIR spectra of budesonide + (a) Locust Bean gum (b) Eudragit S 100	76
Figure 4.7: Standard calibration curve of Budesonide in 0.1 N HCl	78
Figure 4.8: Standard calibration curve of Budesonide in Phosphate buffer pH 7.4.....	79
Figure 4.9: Standard calibration curve of Budesonide in Phosphate buffer pH 6.8.....	80
Figure 4.10: Viscosity profile of 1 % solution of different gums in Phosphate buffer pH 6.8.	81
Figure 4.11: Enzymatic degradation of gums in presence of probiotic culture medium (a) Tamarind gum (b) Locust bean gum without CO ₂ aeration.....	82
Figure 4.12: Enzymatic degradation of Natural gums in presence of 4 % rat cecal content and probiotic culture with respect to time (a) Tamarind gum (b) Locust bean gum (c) Karaya Gum (d) Gellan gun	83
Figure 5.1: Coating pan assembly for coating of tablet dosage form.....	93
Figure 5.2 Dissolution assembly with Insta CO ₂ disposable set for creating the anaerobic environment in dissolution medium.....	96
Figure 5.3: <i>In –Vitro</i> Drug Release study of Preliminary trial batches.....	104
Figure 5.4: <i>In –Vitro</i> Drug Release of Tablets prepared by PVP K 30 in IPA and water.....	105
Figure 5.5: <i>In vitro</i> release of experimental batches F1 to F5.....	107
Figure 5.6: <i>In vitro</i> release of experimental batches F6 to F10.....	108
Figure 5.7: <i>In vitro</i> release of experimental batches F11 to F15.....	109
Figure 5.8: 3D Response Graph (a) and Contour Plot (b) for % CDR at 2 hrs	112
Figure 5.9: 3D Response Graph (a) and Contour Plot (b) for % CDR at 5 hrs	114
Figure 5.10: 3D Response Graph (a) and Contour Plot (b) for CDR at 8 hrs	117
Figure 5.11: Design space (Overlay plot) of prepared with Operating ranges of B (% Ratio of Water: IPA content) at 100 (3 rd level).....	118
Figure 5.12: Design space (Overlay plot) of prepared with Operating ranges of A (Quantity of CM Tamarind gum) at 100 (2 nd level)	118
Figure 5.13: X – Ray imaging of Rabbit for Tablet dosage form	124

Figure 6.1: Catheter (Size: 6FG) used for instillation of 4% acetic acid in rectal cavity of rat	138
Figure 6.2 Protocol of In-vivo study	139
Figure 6.3: A Fishbone diagram illustrating factors that may have impact on the critical quality attributes (CQA).....	142
Figure 6.4: RPN score after FMEA risk assessment. RPN threshold of 60 was considered for selection of risk factor as potential high-risk factor.	144
Figure 6.5: Pareto Charts for Aspect Ratio	146
Figure 6.6: 3D Response Graph (a) and Contour Plot (b) for Aspect Ratio	148
Figure 6.7: Pareto Charts for Particle Size Distribution.....	149
Figure 6.8: 3D Response Graph (a) and Contour Plot (b) for Particle size Distribution	151
Figure 6.9: Pareto Charts for % CDR at 2 hours.....	153
Figure 6.10: 3D Response Graph (a) and Contour Plot (b) for % CDR at 2 hours.....	155
Figure 6.11: Design Space Generated By 2^4 Factorial Design.....	156
Figure 6.12: 3D Response Graph (a) and Contour Plot (b) for % CDR at 2 hrs.....	159
Figure 6.13: 3D Response Graph (a) and Contour Plot (b) for % CDR at 5 hrs.....	162
Figure 6.14: 3D Response Graph (a) and Contour Plot (b) for % CDR at 5 hrs.....	164
Figure 6.15: Design space (Overlay plot) of prepared with Operating ranges of X3 (% weight gain) at (a) 2.5 % weight gain (b) % 4.8 weight gain (c) % 6 weight gain (d) 7.5 % weight gain.....	165
Figure 6.16: Histopathological Evaluation for different animal groups	171
Figure 6.17: Standard calibration curve of TNF- α	173
Figure 6.18: Standard calibration curve of IL-6.....	173
Figure 6.19: Biochemical estimation of (a) IL 6 and (b) TNF- α in different animal group.....	175
Figure 6.20: SEM Picture of surface of Optimized Pellets (1) Magnification with 97X (b) Magnification with 250X (c) Magnification with 1000X	176

List of Tables

Table 4.1: List of Materials used in present study with supplier	63
Table 4.2: List of Equipment's used in present study with supplier	64
Table 4.3: Drug identification based on characterization, solubility, and melting point	71
Table 4.4: FTIR charactered peaks for drug and its mixtures with polymers	76
Table 4.5: standard calibration curve f Budesonide in 0.1 N HCl	77
Table 4.6: standard calibration curve f Budesonide in Phosphate buffer pH 7.4.....	78
Table 4.7: standard calibration curve f Budesonide in Phosphate buffer pH 6.8.....	79
Table 4.8: Viscosity profile of 1 % solution of different gums.....	80
Table 5.1: Composition of Tablets for Preliminary formulation.....	89
Table 5.2: Tablets prepared by PVP K 30 in IPA and water using tamarind gum and CM tamarind gum	90
Table 5.3: Weight variation limit as per IP	90
Table 5.4: compositions of coating solution	92
Table 5.5: Process parameters Fixed for coating of Tablets	93
Table 5.6: Independent variables and Dependent variables of Box Behnken design	94
Table 5.7: Formulation batches (F1 to F8) as per the Box Behnken Design	95
Table 5.8: Formulation batches (F1 to F8) as per the Box Behnken Design	95
Table 5.9: Precompression parameters of premixture of Preliminary formulations	101
Table 5.10: Precompression parameters of premixture of Preliminary formulation batches.....	102
Table 5.11: In vitro release data of batches prepared by direct compression	103
Table 5.12: In vitro release data of batches prepared by Wet granulation	103
Table 5.13: Dissolution profile of tablets prepared by the PVP K 30 in IPA and Water as bridging agent.....	105
Table 5.14: In vitro release studies of experimental batches F1 to F5	107
Table 5.15: In vitro release studies of experimental batches F6 to F10.....	108
Table 5.16: In vitro release studies of experimental batches F11 to F15	109
Table 5.17: Box-Behnken Experimental design Matrix and their responses.....	110
Table 5.18: Analysis of variance of independent variable Y2 (% CDR at 2 hours)	111
Table 5.19: Analysis of variance of independent variable Y5 (% CDR at 5 hours)	113
Table 5.20: Analysis of variance of independent variable Y8 (% CDR at 8 hours)	115
Table 5.21: Predicated and Observed values for Dependent Variables of Checkpoint Batches	120
Table 5.22: statistical parameter of all mathematical models (F1 to F8).....	121
Table 5.23: statistical parameter of all mathematical models (F9 to F15)	122
Table 5.24: Stability Study of Optimized Batch (F3) under accelerated Conditions as per ICH guideline.....	125
Table 6.1: Dependent variables and independent variables with levels.....	130
Table 6.2: Experiment Batches as per 2 ⁴ factorial Design (FP1 TO FP8)	131
Table 6.3: Experiment Batches as per 2 ⁴ factorial Design (FP1 TO FP8)	131
Table 6.4: Composition of enteric polymer Coating Solution	133
Table 6.5: Process Parameters for pan coating of pellets.....	133
Table 6.6 Independent variables and Dependent variables of Box Behnken design	134
Table 6.7: Experimental batches as per Box-Behnken Design (F1 to F8)	135
Table 6.8: Experimental batches as per Box-Behnken Design (F1 to F8)	135
Table 6.9: RPN score of possible risk factors by Initial risk assessment study	143
Table 6.10: Experimental runs obtained from 2 ⁴ Factorial design and their responses.	144
Table 6.11: Aspect ratio of all factorial batches.....	145

Table 6.12: Analysis of variance for the Aspect Ratio (dependent variable).....	146
Table 6.13: Particle Size Distribution data of batches as per 2 ⁴ factorial designs	149
Table 6.14: Analysis of variance for the Particle size distribution (dependent variable)	150
Table 6.15: % CDR at 2 hours for of the batches as per 2 ⁴ factorial designs.....	152
Table 6.16: Analysis of variance for the % cumulative drug release at 2 hours (dependent variable)	153
Table 6.17: Experimental runs obtained from Box-Behnken Experimental design and their responses.	157
Table 6.18: Analysis of variance for the % cumulative drug release at 2 hours (dependent variable)	157
Table 6.19: Analysis of variance for the % cumulative drug release at 5 hours (dependent variable)	160
Table 6.20: Analysis of variance for the % cumulative drug release at 9 hours (dependent variable)	163
Table 6.21: Predicated and Observed values for Dependent Variables of Confirmatory batches .	166
Table 6.22: Statistical parameter of all mathematical models (F1 to F8)	167
Table 6.23: Statistical parameter of all mathematical models (F9 to F15)	168
Table 6.24: Standard calibration curve data for the TNF- α	172
Table 6.25: Standard calibration curve data for the IL-6	173
Table 6.26: Values of IL6 for each experimental animal group	173
Table 6.27: Values of TNF- α for each experimental animal group	174
Table 6.28: Stability Study of Optimized Batch (F12) under accelerated Conditions as per ICH guideline.....	177
Table 7.1: In-vitro Dissolution Profile Comparison using Fit Factors (Pairwise Procedures).....	185
Table 7.2: % Dissolution efficiency (%DE) comparison using One way ANOVA study	186
Table 7.3: One way ANOVA study for the % DE and MDT	187
Table 7.4: In-vitro Dissolution Profile Comparison using MSD (Multivariate Statistical distance) test	187

List of appendices

Appendix A- CPCSEA Approval protocol for *in vivo* study

CHAPTER 1

Introduction

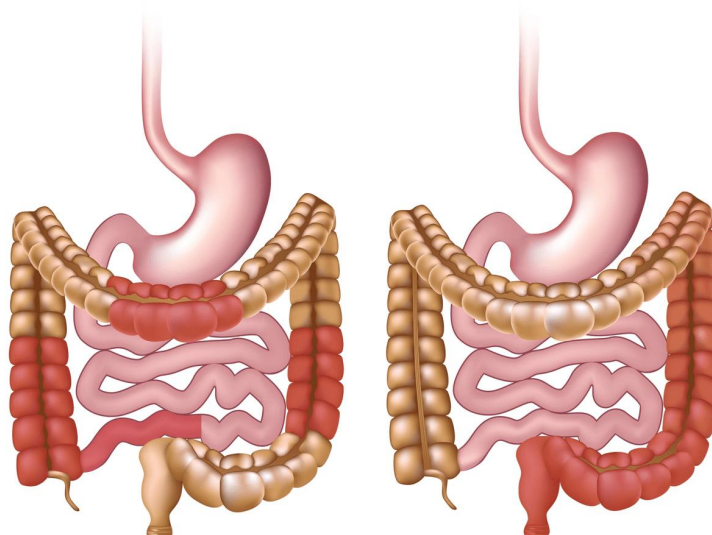
CHAPTER 1

1. Introduction

1.1 Introduction to inflammatory bowel disease

Inflammatory bowel diseases (IBDs) comprise ulcerative colitis and Crohn's disease predominately. IBDs that induce inflammation along the membrane of the digestive tract include Crohn's disease and ulcerative colitis as shown in Figure 1.1. Ulcerative colitis is characterised by chronic inflammation in the colon, among other areas of the digestive tract[1]. Prominent gastrointestinal manifestations are linked to inflammatory bowel disease (IBD), including but not limited to diarrhoea, abdominal pain, rectal haemorrhage, anaemia, and inadvertent weight loss[2].

Inflammatory Bowel Disease



Crohn's disease

Ulcerative colitis

Figure 1.1 Inflammatory bowel disease (a) Crohn's disease (b) Ulcerative colitis

Ulcerative Colitis (UC) is a pathological condition distinguished by inflammation and morphological changes that are confined to the colon. In 95% of instances, involvement of the rectum is observed, accompanied by a range of proximal extension degrees[3]. The

inflammatory reaction primarily affects the inner lining of the large intestine and is categorized by the presence of ulcers, swelling, and bleeding, with varying levels of severity[4]. The histological observations in this study encompass both acute and long-term inflammation in the mucosal lining, which is defined by the existence of mononuclear cells and polymorphonuclear leukocytes[3]. Additionally, the study noted the presence of crypt lesions, distortion of mucosal glands, and a reduction in goblet cells[4].

One of the salient features of ulcerative colitis (UC) is a condition characterized by the frequent coexistence of blood and mucous with fecal matter, followed by severe lower abdominal discomfort that is at its most intense during the process of defecation[3]. A differentiation is made between diarrhoea characterized by the absence of blood and mucus and diarrhoea accompanied by the presence of mucus. Within a therapeutic context, it is important to establish a clear differentiation between ulcerative colitis (UC) and Crohn's disease[5]. The detection of ulcerative colitis (UC) often occurs at an earlier stage after the appearance of symptoms in comparison to Crohn's disease (CD)[6]. The primary reason for this phenomenon is the conspicuous observation of blood in the faeces, which functions as a clear sign for individuals that a digestive ailment may be present[7]. The location of stomach pain is determined by the extent to which the colon is affected. The patient has discomfort specifically localized in the left lower quadrant, which then extends across the whole abdomen as a result of pancolitis[8].

Children have a difficult incidence of pancolonic connection, an increased probability of disease proliferation towards the proximal area with time, and a heightened vulnerability to colectomy as compared to adult persons[5]. Vigilant observation is necessary for those displaying abdominal cramping, recurrent discomfort upon palpation, and a reduction in bowel movements. The presence of a possible risk for the progress of toxic megacolon is the underlying reason for this concern[9].

Crohn's disease (CD), unlike ulcerative colitis (UC), stands out for its capacity to affect any part of the gastrointestinal tract, even including the peri-anal area and oropharynx[10]. Frequently, affected sections of the intestine are separated by healthy regions, resulting in the expression "skip areas." This condition involves irritation that can penetrate through the entire intestinal wall, potentially leading to the formation of fistulas or sinus tracts. Histologically, it's characterized by the presence of tiny depressions known as Peyer's patch phthoid ulcers[11]. Furthermore, there are signs of chronic inflammation extending into the

submucosal layer, and sometimes noncaseating granulomas can be observed. The most common locations for CD, in decreasing order, are the ileocecal section, subsequent to the terminal small intestines in isolated, extensive involvement of the small intestine, and isolated colonic inflammation.[3].

In contrast to the clinical presentation commonly perceived in ulcerative colitis (UC), Crohn's disease (CD) is often marked by its intricacy, which can potentially lead to delays in making an accurate diagnosis[3]. The way gastrointestinal symptoms manifest themselves depends on the specific site, level, and harshness of the condition. Patients with association with the ileocolonic area frequently experience abdominal discomfort after eating, which can sometimes extend to the area around the belly button, a particular concern in paediatric patients[12]. During the examination, it is possible to identify pain, especially in the lower right abdomen, which may occasionally suggest the presence of an inflammatory mass. Symptoms of gastroduodenal Crohn's disease (CD) encompass difficulties with swallowing (dysphagia), feeling full soon after eating (early satiety), nausea, vomiting, and discomfort in the upper abdomen (epigastric distress)[10].

In an attempt to alleviate the discomfort linked to gastroduodenal Crohn's disease, patients often restrict their calorie intake[13]. This condition is characterized by issues such as delayed stomach emptying and abdominal pain. When there is extensive disease in the small bowel, it can lead to a series of indications, including generalized stomach pain, reduced appetite, diarrhoea, and loss of weight. Additionally, lactose malabsorption may occur. The physical examination confirms the presence of general abdominal discomfort. Although the clubbing of the fingertips is rare, it is primarily observed in infants with severe small intestine disease[14].

Colonic Crohn's disease (CD) displays symptoms that may resemble those of ulcerative colitis (UC). These symptoms encompass a combination of abdominal cramps accompanied by the presence of mucus and blood in the stool, along with irritation in the lower abdomen that is often relieved by bowel movements[15]. In clinical practice, perianal conditions like anal tags, deep anal fissures, and fistulas are frequently identified. When combined with borborygmi (stomach rumbling), the presence of increased abdominal discomfort, bloating, and vomiting indicates the progression of the inflammatory process toward localized stenosis, which can manifest as either complete or partial obstruction[16].

Approximately 5% of individuals diagnosed with inflammatory bowel disease (IBD) that specifically impacts the colon cannot be classified definitively based on clinical, radiological, endoscopic, and pathological criteria. This is due to the presence of certain characteristics that exhibit overlapping aspects of both illnesses. The current designation for this condition is referred to as "'IBD, type unclassified (IBDU)". The designation of 'indeterminate colitis (IC)' should be only used in instances when a colectomy has been conducted and the pathologist, after a comprehensive investigation, is unable to definitively define the illness[17]. If all patients are consistently defined in this standardised manner, it is expected that this would enhance the process of data collecting for an Inflammatory Bowel Disease (IBD) registry and promote clinical research[18].

1.1.1 Intestinal barrier in Inflammatory Bowel Disease

A thorough understanding of the features and attributes of the gastrointestinal tract can enhance our knowledge of the biological processes involved in the development of inflammatory bowel disease (IBD). This knowledge can also inspire fresh ideas for the development of therapeutic approaches aimed at addressing these chronic diseases[1].

Numerous defence mechanisms are employed to mitigate infections resulting from inflammatory bowel disease (IBD). These mechanisms encompass physical barriers, such as closely bound epithelial cells, as well as peptides that inhibit bacteria secreted by bowel cell membranes. Additionally, the mucosal innate and adaptive immune systems play a crucial role in eradicating exotic infections[19]. The digestive tract is comprised of four distinct layers that exhibit specialisation in functional composition. These layers include the mucosa, submucosa, muscularis externa, and adventitious tissue[20].

The mucosa, found as the innermost layer within the digestive tract, contributes significantly to the process of dietary digestion. This structure serves as a protective barrier that separates the internal organs from the inner space of the gastrointestinal system. The primary makeup of this layer mostly comprises of interconnected epithelial cells firmly held together by dense junctions. These cells have a crucial role in facilitating the movement of essential nutrients through the epithelium, all the while serving as a protective shield against the passage of potentially harmful substances into the host organism. Additionally, besides their composition of epithelial linings, these structures also include goblet cells and endocrine cells[21].

Goblet cells possess the exclusive role of secreting mucin, a substance that, upon dissolution in water, gives rise to mucus. Endocrine cells, which are often located inside the epithelial lining, are responsible for the secretion of hormones that have an active function in the control of digestive processes[22]. The capacity of external bacteria to penetrate the epithelial barrier allows them unhindered access to the circulatory system, significantly contributing to the onset of gastrointestinal conditions. A substantial amount of research, including investigations in both humans and mice, has consistently shown that inflammatory bowel diseases (IBDs), like Crohn's disease, are marked by a reduction in mucus production and a weakened epithelial barrier. Consequently, this leads to heightened intestinal permeability and the adherence of toxins to the cells that line the digestive tract[23].

1.1.2 Diagnosis of Inflammatory Bowel Disease

Eliminating intestinal pathogens before diagnosing or during exacerbations of inflammatory bowel disease (IBD) is of utmost importance. Many infections have the potential to mimic IBD, such as *Clostridium difficile*, *Giardia lamblia*, *Salmonella*, *Shigella*, *Campylobacter*, *Aeromonas*, *Plesiomonas*, *Yersinia*, *Escherichia coli* O157:H7, *Histoplasma*, *Mycobacterium tuberculosis*, and *Entamoeba histolytica*. Individuals initially diagnosed with IBD may also have concurrent contaminations[24]. However, even when treated for the identified pathogen, people with this condition often experience persistent symptoms that are resistant to resolution or tend to reappear within a relatively short timeframe, ranging from days to weeks[25].

Different diagnostic tests are used for identification of Inflammatory bowel disease as follows.

Hematologic Tests:

Screening examinations for inflammatory bowel disease (IBD) include a comprehensive analysis of blood components, such as a complete blood count, as well as the assessment of inflammatory indicators and liver enzymes comprise a metabolic description[26]. The presence of an raised white blood count accompanied by an increase in band formations, microcytic anaemia, and thrombocytosis may indicate the presence of inflammatory bowel disease (IBD)[27]. Approximately 90% of paediatric patients with Crohn's disease have higher levels of acute-phase reactants including C-reactive protein, and blood orosomucoid[28]. However, these markers are less often raised in paediatric patients with ulcerative colitis. The presence of hypoalbuminemia and a decreased amount of plasma iron

may be seen. The presence of raised liver enzyme values should initiate an assessment to determine the presence of any related liver disease. Additional serologic assays that have been developed contain perinuclear anti-neutrophilic cytoplasmic antibody (P-ANCA) and anti-Saccharomyces cerevisiae antibodies (ASCA)[29]. The aforementioned assays serve as diagnostic evidence of inflammatory bowel disease (IBD) or to assist in differentiating between ulcerative colitis (UC) and Crohn's disease (CD), however they should not be utilised as a sole means of diagnosing IBD. The presence of anti-Saccharomyces cerevisiae antibodies (ASCA) has been seen in a range of 44% to 54% of children diagnosed with Crohn's disease (CD). However, it is worth noting that when ASCA is discovered[29], it has a high level of specificity, ranging from 89% to 97%. The presence of perinuclear antineutrophil cytoplasmic antibodies (P-ANCA) has been seen in a range of 66 to 83% among children diagnosed with ulcerative colitis (UC), and children in range of 14 to 19% children diagnosed by Crohn's disease (CD). The confirmation of the perinuclear staining pattern in UC is established by the observed removal of this pattern subsequent to DNase treatment of the neutrophils[30].

Endoscopic Examination:

When considering an analysis of Inflammatory Bowel Disease (IBD), it is recommended to do an endoscopic examination accompanied by biopsies in order to establish a definitive diagnosis[31]. Histologic examination is often effective in distinguishing between ulcerative colitis (UC) and Crohn's disease (CD). However, there are situations when the characteristics of colitis may deviate from the conventional presentation, resulting in a analysis of unknown colitis[32].

Radiologic examination:

Radiographic assessments are often limited to individuals diagnosed with Crohn's disease in order to assess the extent of small intestine loop and terminal ileum involvement, using a small intestine follow-through X-ray procedure. The utilisation of enteroclysis, which involves the direct administration of contrast dye into the small intestine, is infrequent due to patient distress and the necessity of introducing a tube[33]. However, it is employed in cases where conventional follow-through X-ray examinations have failed to provide sufficient visualisation of small bowel loops. CD is characterised by the presence of stiff stenotic segments, skip regions, as well as sinus tracts or fistulae. The use of barium enemas for the purpose of diagnosing ulcerative colitis is not recommended, particularly in individuals with moderate or severe colitis, since it may potentially trigger the development of toxic megacolon. Nevertheless, the use of barium enemas may be advantageous in the

identification and characterization of stenosis, fistulae, or sinus tracts in individuals diagnosed with Crohn's disease[34].

1.1.3 Treatment of Inflammatory bowel disease

1.1.3.1 Medical Management of Ulcerative Colitis and Crohn's Disease

Mild disease

The use of oral sulfasalazine, either as a standalone therapy or in conjunction with topical treatments, is employed for the management of moderate illness. The use of more recent 5-aminosalicylic acid (5-ASA) drugs, such as mesalamine, olsalazine, and balsalazide, is beneficial for those who have adverse reactions to sulfasalazine, rendering them unable to tolerate its usage[2]. Topical therapies such as mesalamine and enemas, mesalamine suppositories, and corticosteroid froth have been shown to potentially alleviate symptoms in individuals with restricted distal colonic illness[35].

Corticosteroids administered at a quantity of 1 mg/kg/day have revealed efficacy in reducing disease activity and facilitating remission in the majority of patients. Nevertheless, the use of corticosteroids for an extended period is discouraged owing to the presence of unfavourable side effects such as aesthetic alterations, inhibition of linear growth in children, and the development of osteopenia[36]. In addition, the efficacy of corticosteroids in maintaining remission has not been shown. Budesonide, a very powerful corticosteroid subject to significant hepatic metabolism during its first pass, has therapeutic efficacy; nonetheless, it is noteworthy that about one-third of patients encounter side effects associated with its use[37].

Metronidazole and ciprofloxacin have shown efficacy in managing mild to moderate illness, especially in those presenting with perianal ailment and communicable sequelae. Sensory neuropathy, a condition that might develop as a result of prolonged metronidazole use, often exhibits full resolution or improvement with cessation of the medication[38].

Moderate to severe disease.

Hospitalisation is recommended for patients who exhibit notable symptoms such as severe stomach cramps, bloody diarrhoea, abdominal soreness, anaemia, and hypoalbuminemia. During their hospital stay, these patients will undergo thorough clinical monitoring and receive IV administration of corticosteroids, fluids, and nutrition[39, 40]. It is advisable to refrain from using antispasmodic medicines due to their potential to increase the likelihood of toxic megacolon occurrence in patients. The monitoring of blood counts and chemistries

is conducted with meticulous attention. The administration of intravenous steroids is maintained until the cessation of stomach cramps and hematochezia. The dietary limitations, initially include the avoidance of foods rich in fibre, residue, and spiciness, are gradually relaxed as the disease's activity diminishes in response to medical management[41]. The initiation of concomitant therapy with sulfasalazine/5-aminosalicylic acid preparations occurs after the subsiding of initial symptoms in order to sustain remission[42].

Immunosuppressive treatment

Azathioprine and 6-mercaptopurine are used for their steroid-sparing properties, since corticosteroids are related with adverse effects in around 50% of patients. The use of these medicines for the treatment of acute colitis is limited due to their delayed start of action[43, 44]. Cyclosporine and tacrolimus have been used as therapeutic agents for the management of acute steroid-refractory ulcerative colitis in cases when surgical intervention was imminent[44]. Patients who establish remission often see clinical improvement within a period of 7 to 10 days. Nevertheless, a significant proportion of individuals have a recurrence of symptoms upon discontinuation of these therapeutic medications. The duration of remission may be extended by starting therapy with azathioprine or 6-mercaptopurine at minimum four weeks before ceasing cyclosporine medication[45].

Prognosis

It has been shown that a significant proportion, ranging from 25% to 40%, of people diagnosed with severe ulcerative colitis (UC) may ultimately need the surgical intervention of colectomy. Individuals who were diagnosed with proctosigmoiditis prior to reaching the age of 21 had a higher likelihood of illness development beyond the splenic flexure and eventual colectomy compared to those whose condition remained localised[46, 47]. The consensus among the medical community is that individuals diagnosed with severe colitis often require monitoring colonoscopy in order to identify dysplasia, typically around 8 years after the initial diagnosis. Following the commencement of surveillance colonoscopy, further tests should be conducted at intervals of 1 to 2 years[48]. The incidence of colon cancer among individuals in Sweden who were diagnosed before the age of 15 was found to be 1% after a 15-year period, 6.5% after a 20-year period, and 15% after a 25-year period[49].

1.2 Introduction to Colon Targeted Drug delivery system

The localization of drug delivery specifically to the colon is a much-desired objective in drug, as it offers significant advantages for the treatment of several bowel disorders including ulcerative colitis, Crohn's disease, amebiasis, colonic cancer, as well as the local therapy of colonic pathologies[50]. Additionally, it enables the efficient systemic distribution of protein and peptide drug[51]. The colon-specific drug delivery system (CDDS) must possess the ability to protect the drug during its transit to the colon[52]. This entails ensuring that drug release and absorption do not take place in the stomach or small intestine. Furthermore, it is imperative that the bioactive agent remains intact and is not degraded in either of these dissolution sites[53]. Upon reaching the colon, the drug should solely be released and integrated via the delivery system. The colon is considered to be a favourable location for the absorption of peptides and protein drugs due to several explanations[54]. In contrast to the small intestine, the pH and variety of digestive enzymes in the colon are comparatively reduced[54]. This reduced enzymatic activity in the colon helps protect peptide drugs from being hydrolysed and enzymatically degraded in the duodenum and jejunum. Consequently, controlled drug delivery systems (CDDS) can effectively shield peptide drugs from degradation, allowing them to be released in the ileum or colon[55]. This targeted release mechanism ultimately enhances the systemic bioavailability of the drugs. Lastly, it is worth noting that the colon has a prolonged retention period of up to five days and displays a high degree of sensitivity towards absorption enhancers[56].

The oral route is often regarded as the most convenient and preferable method for administering drugs. However, other routes may also be used for the delivery of drugs to the colon. The administration of drugs via the rectum provides a direct and efficient means of targeting the colon. Nevertheless, achieving access to the proximal region of the colon by rectal administration poses challenges[57]. The administration of drug via the rectum might elicit discomfort in patients, perhaps leading to suboptimal compliance[57]. Drug formulations intended for intrarectal administration are available in the form of liquids, foam, and suppositories. The intrarectal route is used for both systemic administration and the targeted delivery of topically active drugs to the large intestine. Rectal administration of corticosteroids, namely hydrocortisone and prednisolone, is used as a therapeutic approach to treat ulcerative colitis[58]. While the absorption of these drugs mostly occurs in the large colon, it is widely accepted that their effectiveness is primarily attributed to their topical

administration. The concentration of drugs that reaches the colon is contingent upon many dosage form parameters, the extent of reversing diffusion, and the duration of stay. Research studies have revealed that foam and suppositories tend to be typically maintained inside the rectum and sigmoid colon, but enema solutions have a notable ability to disperse across a larger area[55].

The human colon contains a diverse array of bacterial species, including more than 400 distinctive species, which serve as resident flora. The estimated population density of these bacteria inside the colonic contents may reach up to 10^{10} bacteria per gramme[59]. The gut microbiota is responsible for several processes, including azoreduction and enzymatic cleavage, such as the cleavage of glycosides. These metabolic pathways have the potential to play a significant role in drug metabolism and may potentially be used for the targeted distribution of peptide-based macromolecules, such as insulin, through oral route[60].

1.2.1 Advantages of CDDS over Conventional Drug Delivery

Chronic colitis, specifically ulcerative colitis, and Crohn's disease are presently medicated with the use of glucocorticoids and other anti-inflammatory medications[61]. The systemic use of glucocorticoids, namely dexamethasone and methyl prednisolone, via oral and intravenous methods, leads to the occurrence of several adverse effects at the systemic level. These side effects include Adeno-suppression, immunosuppression, and bone resorption[62]. Consequently, targeted medication delivery to the colon has the potential to not only decrease the necessary dosage but also mitigate the adverse systemic effects associated with elevated dosages[63].

In order to achieve efficient drugs delivery to the colon via the gastrointestinal (GI) tract, it is necessary to protect the drug against early release in the stomach and small intestine, and afterwards facilitate its targeted release in the colon[64]. Several approaches have been suggested for the purpose of delivering drugs specifically to the colon, with the majority of them capitalising on the subsequent four key characteristics of the gastrointestinal (GI) tract and colon[65]:

1. The estimation of the duration of transit in the small intestine.
2. Variation in biological circumstances throughout various segments of the gastrointestinal tract.
3. The distinctive nature of bacterial enzymes that are localised in the colon.

4. The use of targeting moieties particular to the colon for the purpose of drug delivery system targeting.

1.2.2 Approaches of colon targeted drug delivery system

1.2.2.1 Coating with pH dependent polymers

Eudragit is a suitable choice for coating the tablet core in order to provide a dosage form that achieves selective release of drugs in the colon[64]. Eudragit polymers are synthesised from esters of acrylic and methacrylic acid, with their physicochemical characteristics being influenced by the presence of functional groups (R). These substances exhibit several forms, including aqueous dispersion, organic solution, granules, and powders. The effective treatment of bowel diseases the targeted delivery of drugs to the inflamed region in the colon, while minimising any loss in the upper part of gastrointestinal tract. The use of a pH-dependent polymer, namely Eudragit S100, to coat the tablet core is capable of achieving the desired outcome[66]. However, it is important to note that this approach may result in untimely release of the drug in the distal small intestine. In order to address this concern, a coating solution including a combination of Eudragit L100 and Eudragit S100 is used[67]. The solubility properties of these anionic polymers vary, and their proportion in the coating aids in achieving regulated medication release. The polymer covering maintains its structural integrity inside the stomach, but begins to degrade in the distal small intestine (pH 7.5), resulting in the controlled release of a limited quantity of medication. Upon reaching the colon, the complete dissolution of the coat occurs, resulting in an increased release of the medication. Nevertheless, a significant drawback of the drug's early release is seen, and this might be mitigated by optimising the thickness of the polymeric coating[52].

Khan et al. (1999) [68] used a coating technique to apply two methacrylic acid polymers, namely Eudragit® L100-55 and Eudragit® S100, onto mesalazine tablets. This coating process included spraying the polymers from aqueous solutions. The combinations of Eudragit® L100-55 and Eudragit® S100 that were investigated in different ratio. The findings from dissolution experiments conducted on coated tablets have shown that the release patterns of the medication may be altered by adjusting the ratios of Eudragit® L100-55 and Eudragit® S100 within the pH range of 5.5 to 7.0, since these specific polymers exhibit solubility within this range. The use of a composite coating formulation including a blend of the aforementioned copolymers has the potential to address the challenge of significant variations in gastric pH levels seen among different people[69].

The pH-dependent controlled drug delivery systems (CTDDS) using copolymers of methacrylic acid have been documented for several drugs, including 5-aminosalicylic acid [70], budesonide [71], and prednisolone [72].

1.2.2.2 Timed-Release Systems

Timed-release formulations are predicated on the controlled release of the drug inside the colon after a certain duration[73]. This technique relies on the duration of transit through the small intestine, a variable that has been seen to fluctuate between 3 and 4 hours. The duration of gastric emptying exhibits variability across individuals and is further influenced by dietary consumption [74]. Moreover, it has been shown that some disorders, including irritable bowel syndrome and ulcerative colitis, might have an impact on the duration of transit through the colon. In their study, Gazzaniga et al. used a strategy including the utilisation of pH-sensitive polymers and a timed-dependent mechanism in order to accomplish targeted distribution specifically to the colon [75]. A drug-containing core surrounded by three polymeric layers, comprising of a hydrophilic layer positioned between two pH sensitive layers, was created. The findings of the *in vitro* test demonstrated a prolonged release of the medication, which may be attributed to the protective effect of pH and the creation of a hydrogel[76].

A further investigation[77] was conducted to examine the use of a composite coating consisting of pH-dependent and time-dependent polymers as an integrated approach for delivering indomethacin pellets to the colon. The pH-dependent polymers Eudragit S100 and Eudragit L100 were used, whereas the time-dependent polymer Eudragit RS was utilised in the study. The conducted dissolution experiments on pellets immersed in liquids with varying pH levels (1.2, 6.5, 6.8, and 7.2) revealed that the introduction of Eudragit RS to pH-dependent polymers may effectively regulate the release of drugs in the colon.

Mastiholimath et al. (2007) [78] examined a colon focused device that delivers theophylline in a pulsatile manner, taking into consideration the effects of pH and time. The fundamental structure included of a non-soluble hard gelatin capsule shell, which was inside packed with eudragit microcapsules containing theophylline. The capsule was then sealed using a hydrogel plug. The device was fully coated with an enteric coating to mitigate the impact of variations in stomach emptying time. The *in vitro* release investigations conducted on the pulsatile device confirmed that a rise in the eudragit content led to a delayed release of theophylline from the microcapsules. The capsule device has successfully accomplished

programmable pulsatile release that is unique to the colon, within a time frame of 2-24 hours. This aligns with the requirements of chronotherapeutic drug delivery.

1.2.2.3 Microbial Triggered Systems

Prodrug

Prodrugs refer to inert derivatives of a pharmaceutical compound that experience enzymatic hydrolysis, often in the colon, to liberate the active component [79]. To attain optimal delivery of drugs targeted to the colon, it is essential to reduce the amount of hydrolysis in the upper areas of the gastrointestinal tract while significantly increasing it in the colon.

Azo conjugates are a well investigated class of chemicals within this particular category. Nevertheless, this approach lacks flexibility since it heavily depends molecular structure of the drug[80].

Kim et al. successfully synthesised a prodrug of metronidazole that proceeded metabolism to produce the active drug, metronidazole, upon exposure to the cecal contents of rats. In contrast to metronidazole, it was shown that this particular prodrug did not undergo metabolism in the small intestine. Additionally, the prodrug absorption was much reduced compared to oral metronidazole, as indicated by a previous study[81].

In a separate investigation, Kim et al. conducted an experiment whereby they synthesised a prodrug of metronidazole by including a sulphate group. The researchers demonstrated that this particular formulation stayed unchanged in the upper intestine. However, upon exposure to rat cecal contents, the prodrug underwent cleavage, resulting in the release of active metronidazole. In a manner similar to the initial prodrug, a much lower proportion of the conjugated prodrug underwent degradation and absorption in the small intestine relative to the active drug subsequent to oral administration. Consequently, a negligible quantity was assimilated into the systemic distribution[82].

Vaidya and colleagues used the prodrug strategy, whereby metronidazole was chemically linked to pectin. They then compared the release of the drug from available formulation to prepared microsphere-based pectin containing formulation that physically retained the drug. The prodrug pectin based metronidazole exhibited a significant decrease in drug release throughout the upper gastrointestinal tract (GIT) as compared to pectin microspheres that contained metronidazole[83].

Another strategy for enhancing the stability of a drug formulation throughout its transit through the stomach and small intestine involves the covalent attachment of the medication to a carrier molecule[84].

Various carrier molecules, including cyclodextrin, glucuronide, dextran, and amino acids, have the ability to form complexes with drugs via binding interactions. Additionally, it is possible to establish a connection between it and a carrier through an azo bond. The breakdown of these bonds is facilitated by colonic bacteria[85].

Polysaccharide-Based Delivery Systems

Polysaccharide-based delivery systems has numerous benefits, rendering them more favoured as an operative approach for the targeted administration of drugs to the colon. Polysaccharides provide many benefits in various applications, including their widespread availability, ease of modification, inherent stability, safety, and potential to undergo biodegradation [86].

Mundargi et al. [87] conducted a comparative analysis of several polysaccharides to assess their efficacy in delivering metronidazole specifically to the colon. The findings indicate that the pace at which metronidazole is released is influenced by both the kind and amount of the polysaccharide used in the formulation. The tablets were subjected to *in vitro* assessment in various solutions, including 0.1 N hydrochloric acid (HCl), phosphate buffer pH 7.4, and phosphate buffer pH 6.8 containing 4% weight/volume of rat cecal content. The results indicated that the drug release from the matrix tablets within the initial 5-hour period, corresponding to the duration consumed in the stomach and small intestine, varied between 12% and 33%.

The use of a blend of polysaccharides in colon-specific drug delivery systems (CDDS) has shown superior efficacy in delivering specifically to the colon, as opposed to the utilisation of a singular polysaccharide. Derivatives of cellulose are often used in conjunction to formulate these delivery methods due to the fact that cellulose exhibits limited systemic absorption upon oral administration. There are two distinct categories of cellulose esters that find use in the formulation of pharmaceutical drugs. Cellulose esters, such as cellulose acetate, that are non-enteric in nature exhibit insolubility in water, with their solubility being unaffected by changes in pH levels. Insoluble and permeable coatings may use these materials. The solubilities of enteric cellulose esters, such as cellulose acetate phthalate (CAP) and hydroxypropyl methylcellulose phthalate (HPMCP), exhibit pH-dependent

characteristics. The solubility of these substances is limited in very acidic environments; yet, their dissolution occurs within a certain pH range. The dissolution of the polymer is contingent upon the degree of esterification, hence resulting in variations in pH. Several carbohydrate mixes have been investigated in research studies[88–90].

As previously discussed, some polysaccharides, including pectin, chondroitin sulphate, chitosan, and galactomannan, possess desirable characteristics for facilitating targeted transport to the colon. These polysaccharides may undergo degradation by colonic enzymes and do not pose any damage to organisms. It is hypothesised that the incorporation of polysaccharides in thin film coatings may enhance the efficiency of drug delivery to specific locations at an accelerated pace, in contrast to other formulations that use these ingredients in matrix systems or as compression coatings. Pectin has the capacity to alter medication release as a result of its inherent gelling properties. In order to mitigate water permeability and safeguard the medication core, it is common practise to include an hydrophobic polymer, like ethyl cellulose (EC), into the coating layer together with pectin [91].

Wakerly et al. used Ethyl cellulose and pectin based aqueous dispersion for a coating onto paracetamol tablets. The film coatings were prepared with different pectin/EC ratios. Subsequent *in vitro* evaluation of the coated tablets revealed a positive correlation between the quantity of pectin in the film and the rate of medication release. The medication permeated both the extracellular matrix (EC) and the film coating through the formation of holes resulting from the degradation of pectin by pectinolytic enzymes [92].

1.2.3 Colonic microflora and metabolic activity

The term "gut" as an adjective is often associated with the intestinal flora, specifically referring to the microbiota and microflora.

The gut flora (colonic microflora) includes a collection of microorganisms that colonize the gastrointestinal tracts of animals. It serves as the principal reservoir of human flora and has the capacity to metabolize certain nutrients, such as carbohydrates, that would otherwise remain indigestible. The gut of a healthy adult typically contains around 2 kg of these bacteria.

Bacterial microorganisms constitute the majority of the microbial population occupying the colon, including a significant proportion of the fecal matter's dry weight, estimated to be as high as 60%. The stomach contains a diverse array of species, ranging from between 300 to

1000, while the majority of estimates converge around 500. Nevertheless, it is quite likely that around 99% of the bacterial population originates from a relatively small number of species, estimated to be around 30 or 40. Fungi and protozoa are also present among the gut microbiota, but with comparatively lesser functional roles. The predominant proportion of these prevalent bacteria are classified as anaerobes, indicating their ability to thrive in an environment absent of oxygen. The indigenous microbes, often referred to as normal flora bacteria, have the potential to emerge as real pathogens during periods of compromised immune function[93].

The majority of bacteria may be classified into many genera, including *Fusobacterium*, *Eubacterium*, *Ruminococcus*, *Peptococcus*, *Bacteroides*, *Clostridium*, *Peptostreptococcus*, and *Bifidobacterium* [94].

Genera and families like as *Escherichia* and *Lactobacillus* have a comparatively lower degree of abundance. Species belonging to the genus *Bacteroides* comprise around 30% of the total bacterial population inside the gastrointestinal tract, so highlighting the significant role played by this species in the host's physiological processes[95]. The extant fungal organisms identified inside the gastrointestinal microbiota including *Candida*, *Saccharomyces*, *Aspergillus*, and several more[96]. Several bacteria that are commonly found in the large intestine of humans include *Bacteroides fragilis* (100), *Bacteroides melaninogenicus* (100), *Bacteroides oralis* (100), *Lactobacillus* (20-60), *Clostridium perfringens* (25-35), *Clostridium tetani* (1-35), *Bifidobacterium bifidum* (30-70), *Staphylococcus aureus* (30-50), *Enterococcus faecalis* (100), *Escherichia coli* (100), *Salmonella enteritidis* (3-7), *Klebsiella sp.* (40-80), *Enterobacter sp.* (40-80), *Proteus mirabilis* (5-55), and *Pseudomonas aeruginosa* (3-11)[94, 97].

The energy needed by the colonic bacterial flora to sustain cellular activity is obtained via the process of fermenting different substrates that remain intact in the small intestine[98].

The substrates involve a range of di and trisaccharides, such as cellobiose, raffinose, stachyose, and lactulose. Additionally, they include residues derived from partially digested polysaccharides like starch, as well as polysaccharides originating from endogenous sources such as mucopolysaccharides [99, 100].

In addition to mucopolysaccharides, dietary fibers serve as additional substrates for fermentation. These fibers that are derived from the cell wall of plant, including cellulose,

hemicellulose, and pectin compounds[101]. Several enzymes are synthesized by the microorganisms present in the colon in order to ease the fermentation process [102, 103]

1.3 Introduction to Polysaccharides

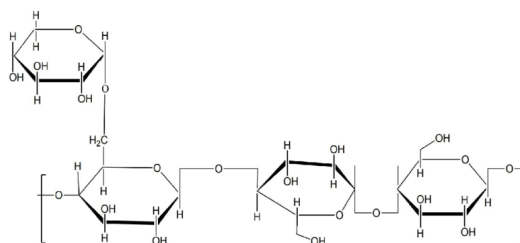
Polysaccharide-based drug delivery approach to the colon exhibit advantages over other approaches.

Polysaccharides effectively maintain their structural integrity and serve as a barrier to hinder the premature release of drugs as they traverse the gastrointestinal tract. However, upon exposure to colonic fluid, the drug is released due to the activity of microorganisms [103, 104].

1.3.1 Polysaccharides selected for the present study:

(1)Tamarind gum[105, 106]

Structural formula:



CAS NO. 39386-78-2

Chemical name: Tamarind gum, Tamarind seed polysaccharide

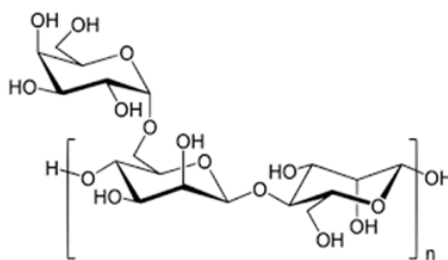
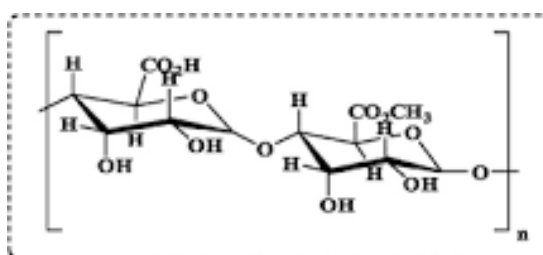
Molecular weight: 52,350 Daltons

Functional category: Food compounds, Antioxidant

Solubility: soluble in hot water

Description: It is composed of a β -(1,4)-d-glucan backbone by α -(1,6)-d-xylose branches which is partially replaced with β -(1,2)-d-galactose

Use: Tamarind gum powder is utilized in the production of ketchups, spices, baked compounds, meat products, instant noodles, and ice cream. It is also utilized as an additive in pet food. In Indian curries, tamarind puree is one of the souring agents.

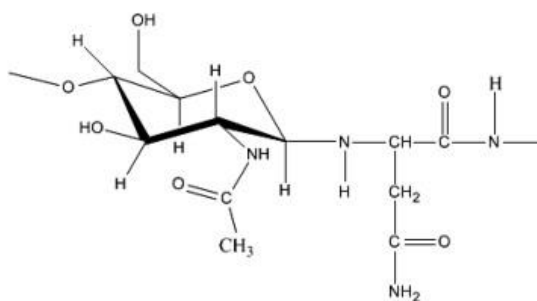
(2)Khaya gum[107–110]**Structural formula:****CAS NO.** 69106-62-3**Chemical name:** khaya gum**Molecular weight:** 52,350 Daltons**Functional category:** Food compounds, binding agent**Solubility:** Water-soluble, ethanol-sparingly soluble, and acetone and chloroform insoluble.**Description:** It is known to contain significantly branched polysaccharides composed of D -galactose, L -rhamnose, D-galacturonic acid, and 4- α -methyl- D-glucuronic acid.**Use:** as a binder, film coating, disintegrant, and controlled release polymer.**(3)Pectin gum**[111]**Structural formula:****CAS NO.** 69106-62-3**Chemical name:** Pectin gum**Molecular weight:** 150 KDaltons**Functional category:** gelling agent, emulsifying agent**Solubility:** soluble in pure water

Description: Pectin is a linear polysaccharide consisting of (1,4)- α -D-galacturonic acid units interspersed at random with neutral sugars and (1,2)-linked L-rhamnoside chains.

Use: Pectin is utilized as a stabilizer and gelling agent in food. Considerable attention has been devoted to its prospective applications as a pharmaceutical agent, including its capacity to regulate lipid and cholesterol levels, serum glucose and insulin levels, and gastric emptying delay. A number of recent studies have investigated the viability of utilizing pectin to create nanoparticles that could serve as drug delivery vehicles.

(4)Ghatti gum[112, 113]

Structural formula:



CAS NO. 9000-28-6

Chemical name: Indian gum, ghatti gum, gum ghati

Molecular weight: 12,000 Daltons

Functional category: Thickening agent, stabilizer

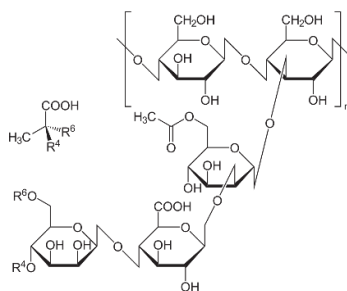
Solubility: Water-soluble, ethanol-insoluble

Description: The compound consists of D-galactose, D-arabinose, D-mannose, D-xylose, and D-glucuronic acid in a molar ratio of 10:6:2:1:2, with minor amounts of 6-deoxyhexose also present.

Use: Used as an emulsifier in pharmaceuticals, oils, and waxes; Used as a flavor enhancer, emulsifier, solvent, and stabilizer or thickener for foods;

(5)Xanthan gum[114]

Structural formula:



CAS NO.: 11138-66-2

Chemical name: Xanthan gum

Molecular weight: 200 KDaltons

Functional category: thickening agent, emulsifier, and stabilizer

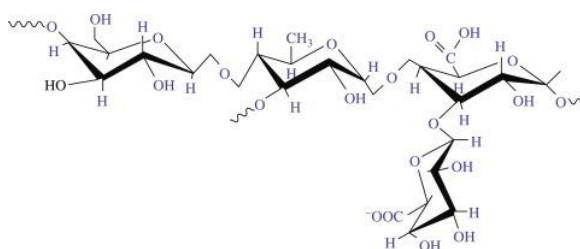
Solubility: soluble in cold and hot water

Description: Xanthan is a long-chain polysaccharide composed of d-glucose, d-mannose, and d-glucuronic acid in a molecular ratio of 3:3:2, with a significant quantity of trisaccharide side chains attached to each component.

Use: In manufacturing, xanthan gum is used as a thickening, stabilizing agent, matrixing agent in foods, toothpastes, and pharmaceuticals.

(6) Karaya gum[115]

Structural formula:



CAS NO. 9000-36-6

Chemical name: gum tragacanth, Indian gum, Karaya gum, sterculia gum

Molecular weight: 16000 Daltons

Functional category: Food compounds, thickening agent

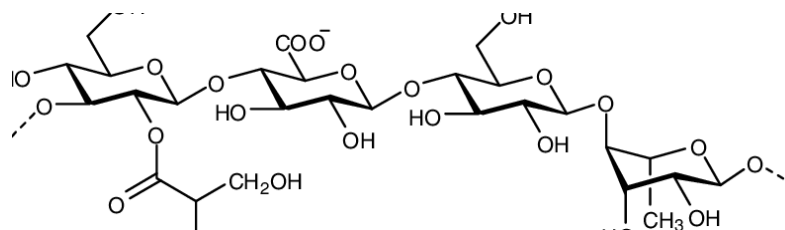
Solubility: Water-soluble, ethanol-sparingly soluble, and acetone and chloroform insoluble.

Description: Gum karaya is a polysaccharide that is highly acetylated and is formed from α -d-galacturonic acid and α -l-rhamnose chains.

Use: It is utilized in foods as an emulsifier and thickener, laxative, denture adhesive, and in stomas's closures.

(7) Gellan gum[116]

Structural formula:



CAS NO. 71010-52-1

Chemical name: Gellan Gum

Molecular weight: 1000000 Daltons

Functional category: binding agent, and stabilizing agent

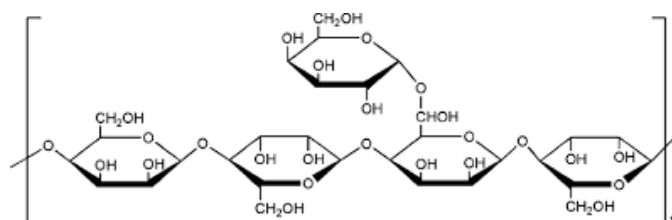
Solubility: hot water-soluble, cold water-insoluble

Description: Tetrasaccharide is a repeating unit of monomers consisting of two D-glucose residues, one D-glucuronic acid residue, and one L-rhamnose residue.

Use: as a binder, stabilizer, and thickener. Primarily, it stabilizes gels composed of water, including desserts and swallowing gelatin.

Locust bean gum[117]

Structural formula:



CAS NO. 9000-40-2

Chemical name: carob gum, locust bean gum

Molecular weight: 50000 Daltons

Functional category: Thickening agent

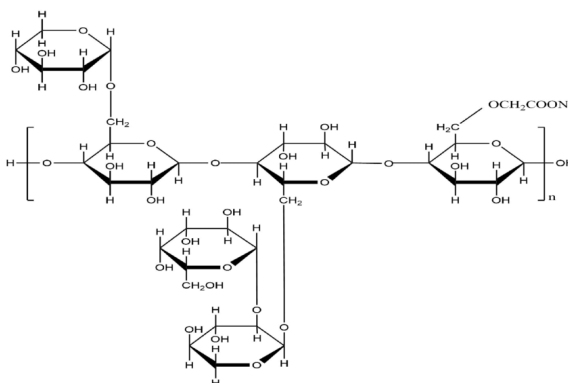
Solubility: incompletely soluble in cold water, soluble in hot water

Description: It consists of a D-mannopyranose backbone chain that is linear in shape, supplemented by a D-galactopyranose side-branching unit, which branches an average of one D-galactopyranose unit for every four D-mannopyranose units.

Use: As a Food stabilizers, thickeners, and fat substitutes. Additionally, it is employed as a texturizer and adjunct gelling agent to other hydrocolloids.

Carboxymethyl Tamarind gum[118]

Structural formula:



CAS NO. 68647-15-4

Chemical name: Carboxymethyl Tamarind gum (CMTKG)

Molecular weight: 914000 Daltons

Functional category: Thickening agent

Solubility: soluble in cold water and hot water

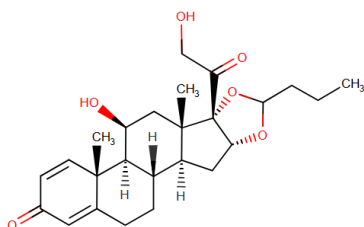
Description: It is composed of D-xylose, D-galactose, and D-glucose in the molar ratio of 1:2:3.

Use: As a thickener for textile printing. Additionally employed for expanding cotton warp and jute fibers. It finds widespread application in the paper and explosives industries as a viscosity enhancer.

1.4 Introduction to drug

Budesonide[119, 120]

Budesonide is a corticosteroid that is prescribed for the treatment of ulcerative colitis, asthma, COPD, hay fever, and allergies.



IUPAC Name:

(1S,2S,4R,8S,9S,11S,12S,13R)-11-hydroxy-8-(2-hydroxyacetyl)-9,13-dimethyl-6-propyl-5,7-dioxapentacycloicosa-14,17-dien-16-one

Physical Properties:

Appearance	: white to off-white, tasteless, odourless powder
Melting Point	: 221-232°C (dec.)
Solubility (Water)	: 0.0457 mg/mL

Chemical properties:

Molecular Formula	: C ₂₅ H ₃₄ O ₆
Molecular Weight	: 430.5 g/mol
pKa Value	: 13.74 (acidic), -2.9 (basic)
Log P	: 2.42
Dose of Drug	: 9 mg

Pharmacokinetic Properties:

Bioavailability	: 10 to 20 %
Volume of Distribution	: 2–3 litre/kg
Plasma Protein Binding	: 85 to 90 %
Elimination half-life	: 2.0-3.6 hours

Metabolism : Liver CYP4A4

Pharmacological and Pharmacodynamic Properties:

Category : Anti-inflammatory agents

Pharmacodynamic Properties:

Budesonide, a glucocorticoid composed of a 22R and 22S epimer, is prescribed for the treatment of inflammatory pulmonary and intestinal disorders, including ulcerative colitis, asthma, COPD, and Crohn's disease.

The therapeutic index is broad, given the substantial variation in dosage among patients.

Mechanism of action

Glucocorticoids exert their effects by impeding neutrophil apoptosis and demargination, phospholipase A2 inhibition, which consequently reduces the synthesis of arachidonic acid derivatives, NF-Kappa B and other transcription factors associated with inflammation, and interleukin-10 promotion of anti-inflammatory genes.

1.5 Introduction to Quality by Design (QbD)

The idea of Quality by Design (QbD) was first formulated by Dr. Joseph M. Juran, a renowned figure in the field of quality management. Dr. Juran asserts that incorporating quality considerations into the product design process is crucial, as numerous occurrences of quality crises and problems can be attributed to shortcomings in the preliminary design phase[121].

Risk-based approaches and the implementation of QbD principles are promoted by the US Food and Drug Administration (FDA) throughout the processes of drug product development, manufacturing, and regulation. The FDA initially prioritized QbD after realizing that increased testing does not invariably result in enhanced product quality. Incorporate quality into the product[122].

1.5.1 Elements of Pharmaceutical Quality by Design

In the context of pharmaceutical Quality by Design (QbD) approach for product development, the applicant participates in the identification of quality characteristics that hold significant importance from the perspective of the patient. These identified

characteristics are then transformed into critical quality attributes (CQAs) of the drug product[123]. Furthermore, the applicant establishes a correlation between the variables associated with formulation and manufacturing processes and the aforementioned CQAs. The ultimate objective is to consistently provide the patient with a drug product that possesses the desired CQAs[124]. Quality by Design (QbD) encompasses many key factors, which include:

1. A Quality target product profile (QTPP) outlining the essential quality characteristics of the pharmaceutical product.
2. Development and comprehension of the product, encompassing the recognition of critical material attributes (CMAs).
3. Design and comprehension of the manufacturing process, incorporating the identification of critical process parameters (CPPs) and a deep grasp of scalability principles, while establishing the interconnection between CMAs and CPPs with CQAs.
4. An encompassing control strategy that encompasses specific requirements for the drug substance(s), excipient(s), and the drug product, along with regulations governing each stage of the production process.
5. The evaluation of process capability and the continuous enhancement of procedures.

The Quality Target Product Profile (QTPP) is a comprehensive document that outlines the critical quality attributes (CQAs) of a drug product. The Quality Target Product Profile (QTPP) is a progressive description of the quality attributes that a pharmaceutical product should ideally possess in order to assure the intended quality, with due consideration to the safety and effectiveness of the product[125]. The Quality Target Product Profile (QTPP) serves as the fundamental framework for designing the product's development process. Several factors should be taken into account when determining what should be included in the Quality Target Product Profile (QTPP). These considerations may include the following aspects[125]:

1. The intended clinical application, method of administration, dosage form, and delivery mechanisms that are applicable.
2. Drug's potency.
3. The container and closure system.

4. The manner in which the therapeutic component is released or dispensed, as well as characteristics that impact pharmacokinetic properties that are pertinent to the specific dosage form being developed.
5. Appropriate quality standards for the ultimate product on the market, including characteristics such as sterility, purity, stability, and drug release. As the subsequent step in the development process, critical quality attributes (CQAs) for the medicinal product are identified.

A critical quality attribute (CQA) pertains to a feature or trait of an end product, such as a finished pharmaceutical item, and can encompass physical, chemical, biological, or microbiological aspects. To ensure the desired product quality, a CQA should adhere to a predefined threshold, span, or distribution[126].

Identity, assay, content uniformity, residual solvents, degradation products, drug release or dissolution, moisture content, microbial limits, and physical attributes including shape, size, shape, Odor, score configuration, and friability are all potential quality attributes of a pharmaceutical product. These characteristics may or may not be critical. Patient injury severity is the primary determinant of an attribute's criticality; should the product deviate from the permissible range for that attribute, it would cause severe consequences[127].

The criticality of a property is not influenced by the probability of occurrence, detectability, or controllability. It is evident that prior to initiating any development efforts, it is essential to establish a comprehensive definition for a novel product. Nevertheless, the significance of predefining the target qualities of the therapeutic product has often been undervalued throughout time. As a consequence, the absence of a clearly defined Quality Target Product Profile (QTPP) has led to the inefficient use of time and precious resources.

A recent paper by Raw et al. [128] demonstrates the importance of establishing the proper QTPP prior to beginning development. QbD examples also serve to illustrate the recognition and application of QTPPs [125].

Ever since its introduction, Quality by Design (QbD) has highlighted the importance of design, understanding, and overseeing processes, as elucidated in the ICH Q8 (R2) directives. It is essential to emphasize the equitable significance of product design, understanding, and regulation. Clinical trials serve as validation that product design is crucial in determining whether a product can adequately satisfy the needs and demands of patients. Furthermore, it determines whether the product retains its efficacy throughout its designated

period of storage, as confirmed by stability investigations. Such a profound understanding of the product might have prevented specific instances of stability issues in the past[129].

Product understanding and design hinge on the development of a durable product that can consistently meet the desired quality target product profile (QTPP) over its entire shelf life. Product design is a versatile field that allows for various design paths.

In order to create and cultivate a robust pharmaceutical product that possesses the desired critical quality attributes (CQAs), a product development scientist must carefully contemplate the physical, chemical, and biological characteristics of the active pharmaceutical ingredient[130].

Investigations into formulation optimization provide significant insights into the subsequent sides:

- By establishing a functional relationship between critical quality attributes (CQAs) and critical material attributes (CMAs), the formulation's robustness can be enhanced.
- The identification and characterization of CMAs present in the drug substance, excipients, and manufacturing materials.
- The development of control strategies encompassing excipients as well as the drug substance.

The QbD approach prioritizes the utility of the knowledge acquired and the relevance of the optimization studies rather than the quantity of such studies. These factors are crucial in order to ensure that the designed drug product is of high quality.

Hence, although Quality by Design (QbD) and Design of Experiments (DoE) are not interchangeable, the latter can hold a substantial role within the framework of QbD. The drug substance, excipients, and materials used during production may encompass various critical material attributes (CMAs). A critical material attribute (CMA) pertains to a feature or characteristic of an input material, spanning physical, chemical, biological, or microbiological aspects, and it must adhere to predefined limits, ranges, or distributions to ensure the desired quality of the excipient, drug substance, or in-process material. The connection between input CMAs and CPPs and output CQAs is shown in Fig. 1.

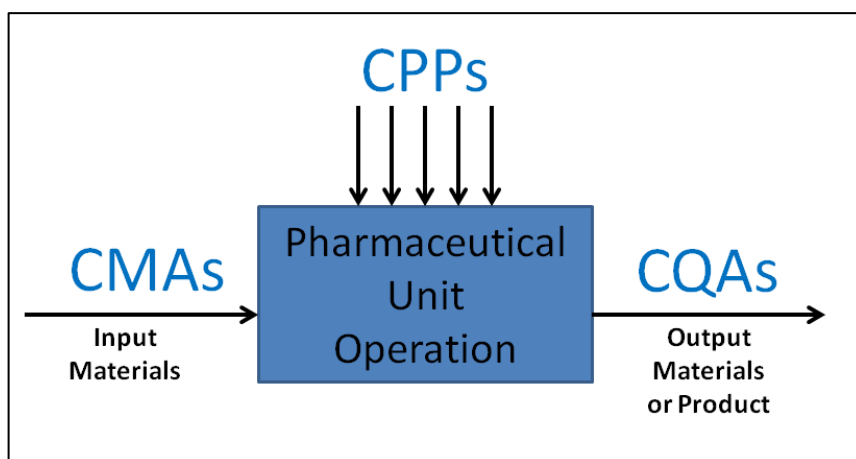


Figure 1.2: Connection between input CMAs and CPPs and output CQAs

In the context of this study, CMAs are distinguished from CQAs by the fact that CQAs pertain to output materials, such as completed drug products and product intermediates, whereas CMAs concern input materials, with the drug substance and other ingredients. The CMA of an intermediate may be converted from its CQA to its CMA for a subsequent manufacturing step. Since there are numerous drug substance and excipient characteristics that could strongly affect the CQAs of the preliminary product and final drug product, it is impracticable for a researcher to explore all of the recognized material characteristics during dosage form optimization studies. Consequentially, a risk assessment would be beneficial for determining which ingredient characteristics demand additional investigation.

In preparation a plan to investigate both product design and understanding, research initiatives can be organized to concurrently achieve the goals of understanding both the product and the associated processes.

Moreover, the establishment of an interactive or interconnected relationship between material properties, process variables, and product attributes is tremendously facilitated by experimental studies that are executed with great accuracy and purpose.

A design space is defined as the intricate relationship and coordination between process parameters and input factors, including material attributes, as per ICH Q8 (R2). It has been demonstrated that this combination ensures the integrity of the final product[121].

Regulatory notification is not required for parameter adjustments made within the designated design space. However, any deviation from this predetermined area is generally regarded as a change, which would normally initiate a regulatory post-approval change process[127].

The design space is submitted for regulatory evaluation and approval by the applicant. As a consequence, the design space is established through the analysis of validated models, such as first-principal models, or Design of Experiments (DoE) data.

1.6 References

1. Fakhoury, M., Negrulj, R., Mooranian, A., & Al-Salami, H. (2014). Inflammatory bowel disease: Clinical aspects and treatments. *Journal of Inflammation Research*, 7(1), 113–120. <https://doi.org/10.2147/JIR.S65979>
2. Pithadia, A. B., & Jain, S. (2011). Treatment of inflammatory bowel disease (IBD). *Pharmacological Reports*, 63(3), 629–642. [https://doi.org/10.1016/S1734-1140\(11\)70575-8](https://doi.org/10.1016/S1734-1140(11)70575-8)
3. Hendrickson, B. A., Gokhale, R., & Cho, J. H. (2002). Clinical aspects and pathophysiology of inflammatory bowel disease. *Clinical Microbiology Reviews*, 15(1), 79–94. <https://doi.org/10.1128/CMR.15.1.79-94.2002>
4. Sairenji, T., Collins, K. L., & Evans, D. V. (2017). An Update on Inflammatory Bowel Disease. *Primary Care - Clinics in Office Practice*, 44(4), 673–692. <https://doi.org/10.1016/j.pop.2017.07.010>
5. Khor, B., Gardet, A., & Xavier, R. J. (2011). Genetics and pathogenesis of inflammatory bowel disease. *Nature*, 474(7351), 307–317. <https://doi.org/10.1038/nature10209>
6. Ramos, G. P., & Papadakis, K. A. (2019). Mechanisms of Disease: Inflammatory Bowel Diseases. *Mayo Clinic Proceedings*, 94(1), 155–165. <https://doi.org/10.1016/j.mayocp.2018.09.013>
7. Zhang, Y. Z., & Li, Y. Y. (2014). Inflammatory bowel disease: Pathogenesis. *World Journal of Gastroenterology*, 20(1), 91–99. <https://doi.org/10.3748/wjg.v20.i1.91>
8. Casati, J., Toner, B. B., De Rooy, E. C., Drossman, D. A., & Maunder, R. G. (2000). Concerns of patients with inflammatory bowel disease: A review of emerging themes. *Digestive Diseases and Sciences*, 45(1), 26–31. <https://doi.org/10.1023/A:1005492806777>
9. Langholz, E., Munkholm, P., Davidsen, M., & Binder, V. (1992). Colorectal cancer risk and mortality in patients with ulcerative colitis. *Gastroenterology*, 103(5), 1444–1451. [https://doi.org/10.1016/0016-5085\(92\)91163-X](https://doi.org/10.1016/0016-5085(92)91163-X)
10. Blumberg, R. S., & Strober, W. (2001). Prospects for research in inflammatory bowel disease. *Jama*, 285(5), 643–647. <https://doi.org/10.1001/jama.285.5.643>
11. Brooke, M. A., & Miraflor, E. (2018). Inflammatory Bowel Disease. *Abernathy's Surgical Secrets: Seventh Edition*, 230–233. <https://doi.org/10.1016/B978-0-323-47873-1.00052-8>
12. Podolsky, D. K. (2002). The current future understanding of inflammatory bowel disease. *Bailliere's Best Practice and Research in Clinical Gastroenterology*, 16(6), 933–943. <https://doi.org/10.1053/bega.2002.0354>
13. Kornum, D. S., Terkelsen, A. J., Bertoli, D., Klinge, M. W., Høyer, K. L., Kufaishi, H. H. A., ... Krogh, K. (2021). Assessment of Gastrointestinal Autonomic Dysfunction: Present and Future Perspectives. *Journal of Clinical Medicine*, 10(7), 1392. <https://doi.org/10.3390/jcm10071392>
14. Feuerstein, J. D., & Cheifetz, A. S. (2017). Crohn Disease: Epidemiology, Diagnosis, and Management. *Mayo Clinic Proceedings*, 92(7), 1088–1103. <https://doi.org/10.1016/j.mayocp.2017.04.010>
15. Ha, F., & Khalil, H. (2015). Crohn's disease: a clinical update. *Therapeutic Advances in Gastroenterology*, 8(6), 352–359. <https://doi.org/10.1177/1756283X15592585>
16. Roda, G., Chien Ng, S., Kotze, P. G., Argollo, M., Panaccione, R., Spinelli, A., ... Danese, S. (2020). Crohn's disease. *Nature Reviews Disease Primers*, 6(1), 22. <https://doi.org/10.1038/s41572-020-0156-2>

17. Silverberg, M. S., Satsangi, J., Ahmad, T., Arnott, I. D., Bernstein, C. N., Brant, S. R., ... Warren, B. F. (2005). Toward an Integrated Clinical, Molecular and Serological Classification of Inflammatory Bowel Disease: Report of a Working Party of the 2005 Montreal World Congress of Gastroenterology. *Canadian Journal of Gastroenterology*, 19(suppl a), 5A-36A. <https://doi.org/10.1155/2005/269076>
18. Mowat, C., Cole, A., Windsor, A., Ahmad, T., Arnott, I., Driscoll, R., ... Bloom, S. (2011). Guidelines for the management of inflammatory bowel disease in adults. *Gut*, 60(5), 571–607. <https://doi.org/10.1136/gut.2010.224154>
19. Swidsinski, A., Ladhoff, A., Pernthaler, A., Swidsinski, S., Loening-Baucke, V., Ortner, M., ... Lochs, H. (2002). Mucosal flora in inflammatory bowel disease. *Gastroenterology*, 122(1), 44–54. <https://doi.org/10.1053/gast.2002.30294>
20. Sarriá, R., Latorre, R., Henroteaux, M., Henroteaux, N., Soria, F., Pérez-Cuadrado, E., & López Albors, O. (2012). Morphometric study of the layers of the canine small intestine at five sampling sites. *The Veterinary Journal*, 192(3), 498–502. <https://doi.org/10.1016/j.tvjl.2011.06.041>
21. Hawiger, J. (2001). Innate Immunity and Inflammation: A Transcriptional Paradigm. *Immunologic Research*, 23(2–3), 099–110. <https://doi.org/10.1385/IR:23:2-3:099>
22. Moore, W. F., Bentley, R. C., Kim, K.-R., Olatidoye, B., Gray, S. R., & Robboy, S. J. (1998). Goblet-Cell Mucinous Epithelium Lining the Endometrium and Endocervix. *International Journal of Gynecological Pathology*, 17(4), 363–367. <https://doi.org/10.1097/00004347-199810000-00011>
23. Schreiber, O., Petersson, J., Waldén, T., Ahl, D., Sandler, S., Phillipson, M., & Holm, L. (2013). iNOS-Dependent Increase in Colonic Mucus Thickness in DSS-Colitic Rats. *PLoS ONE*, 8(8), e71843. <https://doi.org/10.1371/journal.pone.0071843>
24. Semrad, C. E. (2012). Approach to the Patient with Diarrhea and Malabsorption. In *Goldman's Cecil Medicine* (pp. 895–913). Elsevier. <https://doi.org/10.1016/B978-1-4377-1604-7.00142-1>
25. Bellizzi, A., Barucca, V., Fioriti, D., Colosimo, M. T., Mischitelli, M., Anzivino, E., ... Pietropaolo, V. (2010). Early years of biological agents therapy in Crohn's disease and risk of the human polyomavirus JC reactivation. *Journal of Cellular Physiology*, 224(2), 316–326. <https://doi.org/10.1002/jcp.22146>
26. Cioffi, M. (2015). Laboratory markers in ulcerative colitis: Current insights and future advances. *World Journal of Gastrointestinal Pathophysiology*, 6(1), 13. <https://doi.org/10.4291/wjgp.v6.i1.13>
27. Yan, S. L. S., Russell, J., Harris, N. R., Senchenkova, E. Y., Yildirim, A., & Granger, D. N. (2013). Platelet Abnormalities during Colonic Inflammation. *Inflammatory Bowel Diseases*, 19(6), 1245–1253. <https://doi.org/10.1097/MIB.0b013e318281f3df>
28. Cappello, M., & Morreale, G. C. (2016). The Role of Laboratory Tests in Crohn's Disease. *Clinical Medicine Insights: Gastroenterology*, 9, CGast.S38203. <https://doi.org/10.4137/CGast.S38203>
29. Anand, V., Russell, A. S., Tsuyuki, R., & Fedorak, R. (2008). Perinuclear Antineutrophil Cytoplasmic Autoantibodies and Anti- *Saccharomyces Cerevisiae* Antibodies as Serological Markers Are Not Specific in the Identification of Crohn's Disease and Ulcerative Colitis. *Canadian Journal of Gastroenterology*, 22(1), 33–36. <https://doi.org/10.1155/2008/974540>
30. Tesija Kuna, A. (2013). Serological markers of inflammatory bowel disease. *Biochemia Medica*, 23(1), 28–42. <https://doi.org/10.11613/BM.2013.006>
31. Spiceland, C. M., & Lodhia, N. (2018). Endoscopy in inflammatory bowel disease: Role in diagnosis, management, and treatment. *World Journal of Gastroenterology*, 24(35), 4014–4020. <https://doi.org/10.3748/wjg.v24.i35.4014>
32. Jung, S.-A. (2012). Differential Diagnosis of Inflammatory Bowel Disease: What Is the Role of Colonoscopy? *Clinical Endoscopy*, 45(3), 254. <https://doi.org/10.5946/ce.2012.45.3.254>
33. Saibeni, S. (2007). Imaging of the small bowel in Crohn's disease: A review of old and new techniques. *World Journal of Gastroenterology*, 13(24), 3279. <https://doi.org/10.3748/wjg.v13.i24.3279>

34. Griffin, N., Grant, L. A., Anderson, S., Irving, P., & Sanderson, J. (2012). Small bowel MR enterography: problem solving in Crohn's disease. *Insights into Imaging*, 3(3), 251–263. <https://doi.org/10.1007/s13244-012-0154-3>
35. Sands, B. E. (2007). Inflammatory bowel disease: Past, present, and future. *Journal of Gastroenterology*, 42(1), 16–25. <https://doi.org/10.1007/s00535-006-1995-7>
36. Kornbluth, A., Marion, J. F., Salomon, P., & Janowitz, H. D. (1995). How effective is current medical therapy for severe ulcerative and crohn's colitis?: An analytic review of selected trials. *Journal of Clinical Gastroenterology*. <https://doi.org/10.1097/00004836-199506000-00004>
37. Campieri, M., Ferguson, A., Doe, W., Persson, T., & Nilsson, L. G. (1997). Oral budesonide is as effective as oral prednisolone in active Crohn's disease. *Gut*, 41(2), 209–214. <https://doi.org/10.1136/gut.41.2.209>
38. Nikolaus, S., & Schreiber, S. (2007). Diagnostics of Inflammatory Bowel Disease. *Gastroenterology*, 133(5), 1670–1689. <https://doi.org/10.1053/j.gastro.2007.09.001>
39. Nimmons, D. (2016). Elderly patients and inflammatory bowel disease. *World Journal of Gastrointestinal Pharmacology and Therapeutics*, 7(1), 51. <https://doi.org/10.4292/wjgpt.v7.i1.51>
40. Arasaradnam, R. P., Brown, S., Forbes, A., Fox, M. R., Hungin, P., Kelman, L., ... Walters, J. R. F. (2018). Guidelines for the investigation of chronic diarrhoea in adults: British Society of Gastroenterology, 3rd edition. *Gut*, 67(8), 1380–1399. <https://doi.org/10.1136/gutjnl-2017-315909>
41. Bateman, L., & Conrad, K. (2016). Inpatient Medicine. In *Absolute Hospital Medicine Review* (pp. 1–105). Cham: Springer International Publishing. https://doi.org/10.1007/978-3-319-23748-0_1
42. Murray, A., Nguyen, T. M., Parker, C. E., Feagan, B. G., & MacDonald, J. K. (2020). Oral 5-aminosalicylic acid for induction of remission in ulcerative colitis. *Cochrane Database of Systematic Reviews*, 2020(8), 1–129. <https://doi.org/10.1002/14651858.CD000543.pub5>
43. Büning, C., & Lochs, H. (2006). Conventional therapy for Crohn's disease. *World Journal of Gastroenterology*, 12(30), 4794. <https://doi.org/10.3748/wjg.v12.i30.4794>
44. Dubinsky, M. C. (2004). Azathioprine, 6-mercaptopurine in inflammatory bowel disease: Pharmacology, efficacy, and safety. *Clinical Gastroenterology and Hepatology*, 2(9), 731–743. [https://doi.org/10.1016/S1542-3565\(04\)00344-1](https://doi.org/10.1016/S1542-3565(04)00344-1)
45. Panaccione, R., Ghosh, S., Middleton, S., Márquez, J. R., Scott, B. B., Flint, L., ... Rutgeerts, P. (2014). Combination Therapy With Infliximab and Azathioprine Is Superior to Monotherapy With Either Agent in Ulcerative Colitis. *Gastroenterology*, 146(2), 392–400.e3. <https://doi.org/10.1053/j.gastro.2013.10.052>
46. Liu, S., & Eisenstein, S. (2021). State-of-the-art surgery for ulcerative colitis. *Langenbeck's Archives of Surgery*, 406(6), 1751–1761. <https://doi.org/10.1007/s00423-021-02295-6>
47. Bohl, J. L., & Sobba, K. (2015). Indications and Options for Surgery in Ulcerative Colitis. *Surgical Clinics of North America*, 95(6), 1211–1232. <https://doi.org/10.1016/j.suc.2015.07.003>
48. Le Berre, C., Honap, S., & Peyrin-Biroulet, L. (2023). Ulcerative colitis. *The Lancet*, 402(10401), 571–584. [https://doi.org/10.1016/S0140-6736\(23\)00966-2](https://doi.org/10.1016/S0140-6736(23)00966-2)
49. Kobayashi, T., Siegmund, B., Le Berre, C., Wei, S. C., Ferrante, M., Shen, B., ... Hibi, T. (2020). Ulcerative colitis. *Nature Reviews Disease Primers*, 6(1), 74. <https://doi.org/10.1038/s41572-020-0205-x>
50. Philip, A. K., Dabas, S., & Pathak, K. (2009). Optimized prodrug approach: A means for achieving enhanced anti-inflammatory potential in experimentally induced colitis. *Journal of Drug Targeting*, 17(3), 235–241. <https://doi.org/10.1080/10611860902718656>
51. Renukuntla, J., Vadlapudi, A. D., Patel, A., Boddu, S. H. S., & Mitra, A. K. (2013). Approaches for enhancing oral bioavailability of peptides and proteins. *International Journal of Pharmaceutics*, 447(1–2), 75–93. <https://doi.org/10.1016/j.ijpharm.2013.02.030>
52. Amidon, S., Brown, J. E., & Dave, V. S. (2015). Colon-Targeted Oral Drug Delivery Systems:

- Design Trends and Approaches. *AAPS PharmSciTech*, 16(4), 731–741. <https://doi.org/10.1208/s12249-015-0350-9>
53. Lemmens, G., Van Camp, A., Kourula, S., Vanuytsel, T., & Augustijns, P. (2021). Drug Disposition in the Lower Gastrointestinal Tract: Targeting and Monitoring. *Pharmaceutics*, 13(2), 161. <https://doi.org/10.3390/pharmaceutics13020161>
54. Cao, S., Xu, S., Wang, H., Ling, Y., Dong, J., Xia, R., & Sun, X. (2019). Nanoparticles: Oral Delivery for Protein and Peptide Drugs. *AAPS PharmSciTech*, 20(5), 190. <https://doi.org/10.1208/s12249-019-1325-z>
55. Hua, S. (2020). Advances in Oral Drug Delivery for Regional Targeting in the Gastrointestinal Tract - Influence of Physiological, Pathophysiological and Pharmaceutical Factors. *Frontiers in Pharmacology*, 11. <https://doi.org/10.3389/fphar.2020.00524>
56. Maher, S., & Brayden, D. J. (2021). Formulation strategies to improve the efficacy of intestinal permeation enhancers. *Advanced Drug Delivery Reviews*, 177, 113925. <https://doi.org/10.1016/j.addr.2021.113925>
57. Hua, S. (2019). Physiological and Pharmaceutical Considerations for Rectal Drug Formulations. *Frontiers in Pharmacology*, 10, 1196. <https://doi.org/10.3389/fphar.2019.01196>
58. Philip, A., & Philip, B. (2010). Colon Targeted Drug Delivery Systems: A Review on Primary and Novel Approaches. *Oman Medical Journal*, 25(2), 70–78. <https://doi.org/10.5001/omj.2010.24>
59. De Anda-Flores, Y., Carvajal-Millan, E., Campa-Mada, A., Lizardi-Mendoza, J., Rascon-Chu, A., Tanori-Cordova, J., & Martínez-López, A. L. (2021). Polysaccharide-Based Nanoparticles for Colon-Targeted Drug Delivery Systems. *Polysaccharides*, 2(3), 626–647. <https://doi.org/10.3390/polysaccharides2030038>
60. Sun, C., Chen, L., & Shen, Z. (2019). Mechanisms of gastrointestinal microflora on drug metabolism in clinical practice. *Saudi Pharmaceutical Journal*, 27(8), 1146–1156. <https://doi.org/10.1016/j.jsps.2019.09.011>
61. Philip, A. K., Dubey, R. K., & Pathak, K. (2010). Optimizing delivery of flurbiprofen to the colon using a targeted prodrug approach. *Journal of Pharmacy and Pharmacology*, 60(5), 607–613. <https://doi.org/10.1211/jpp.60.5.0006>
62. Moghadam-Kia, S., & Werth, V. P. (2010). Prevention and treatment of systemic glucocorticoid side effects. *International Journal of Dermatology*, 49(3), 239–248. <https://doi.org/10.1111/j.1365-4632.2009.04322.x>
63. Hua, S., Marks, E., Schneider, J. J., & Keely, S. (2015). Advances in oral nano-delivery systems for colon targeted drug delivery in inflammatory bowel disease: Selective targeting to diseased versus healthy tissue. *Nanomedicine: Nanotechnology, Biology and Medicine*, 11(5), 1117–1132. <https://doi.org/10.1016/j.nano.2015.02.018>
64. Lee, S. H., Bajracharya, R., Min, J. Y., Han, J.-W., Park, B. J., & Han, H.-K. (2020). Strategic Approaches for Colon Targeted Drug Delivery: An Overview of Recent Advancements. *Pharmaceutics*, 12(1), 68. <https://doi.org/10.3390/pharmaceutics12010068>
65. Amidon, S., Brown, J. E., & Dave, V. S. (2015). Colon-Targeted Oral Drug Delivery Systems: Design Trends and Approaches. *AAPS PharmSciTech*, 16(4), 731–741. <https://doi.org/10.1208/s12249-015-0350-9>
66. Nikam, A., Sahoo, P. R., Musale, S., Pagar, R. R., Paiva-Santos, A. C., & Giram, P. S. (2023). A Systematic Overview of Eudragit® Based Copolymer for Smart Healthcare. *Pharmaceutics*, 15(2), 587. <https://doi.org/10.3390/pharmaceutics15020587>
67. Pawar, P., Sharma, P., Chawla, A., & Mehta, R. (2013). Formulation and *in vitro* evaluation of Eudragit S-100 coated naproxen matrix tablets for colon-targeted drug delivery system. *Journal of Advanced Pharmaceutical Technology & Research*, 4(1), 31. <https://doi.org/10.4103/2231-4040.107498>
68. Khan, M. Z. I., Štedul, H. P., & Kurjaković, N. (2000). A pH-Dependent Colon-Targeted Oral Drug

- Delivery System Using Methacrylic Acid Copolymers. II. Manipulation of Drug Release Using Eudragit® L100 and Eudragit S100 Combinations. *Drug Development and Industrial Pharmacy*, 26(5), 549–554. <https://doi.org/10.1081/DDC-100101266>
69. Kumar, P., & Mishra, B. (2008). Colon Targeted Drug Delivery Systems -An Overview. *Current Drug Delivery*, 5(3), 186–198. <https://doi.org/10.2174/156720108784911712>
70. Rudolph, M. (2001). A new 5-aminosalicylic acid multi-unit dosage form for the therapy of ulcerative colitis. *European Journal of Pharmaceutics and Biopharmaceutics*, 51(3), 183–190. [https://doi.org/10.1016/S0939-6411\(01\)00134-5](https://doi.org/10.1016/S0939-6411(01)00134-5)
71. Fedorak, R. N., & Bistriz, L. (2005). Targeted delivery, safety, and efficacy of oral enteric-coated formulations of budesonide. *Advanced Drug Delivery Reviews*, 57(2), 303–316. <https://doi.org/10.1016/j.addr.2004.08.009>
72. Kumari, A., Jain, A., Hurkat, P., Tiwari, A., & Jain, S. K. (2018). Eudragit S100 coated microsponges for Colon targeting of prednisolone. *Drug Development and Industrial Pharmacy*, 44(6), 902–913. <https://doi.org/10.1080/03639045.2017.1420079>
73. Gazzaniga, A., Moutaharrik, S., Filippin, I., Foppoli, A., Palugan, L., Maroni, A., & Cerea, M. (2022). Time-Based Formulation Strategies for Colon Drug Delivery. *Pharmaceutics*, 14(12), 2762. <https://doi.org/10.3390/pharmaceutics14122762>
74. Goyal, R. K., Guo, Y., & Mashimo, H. (2019). Advances in the physiology of gastric emptying. *Neurogastroenterology & Motility*, 31(4). <https://doi.org/10.1111/nmo.13546>
75. Gazzaniga, A., Iamartino, P., Maffione, G., & Sangalli, M. E. (1994). Oral delayed-release system for colonic specific delivery. *International Journal of Pharmaceutics*, 108(1), 77–83. [https://doi.org/10.1016/0378-5173\(94\)90418-9](https://doi.org/10.1016/0378-5173(94)90418-9)
76. Rizwan, M., Yahya, R., Hassan, A., Yar, M., Azzahari, A., Selvanathan, V., ... Abouloula, C. (2017). pH Sensitive Hydrogels in Drug Delivery: Brief History, Properties, Swelling, and Release Mechanism, Material Selection and Applications. *Polymers*, 9(12), 137. <https://doi.org/10.3390/polym9040137>
77. Krishnaiah, Y. S. R., Bhaskar Reddy, P. R., Satyanarayana, V., & Karthikeyan, R. S. (2002). Studies on the development of oral colon targeted drug delivery systems for metronidazole in the treatment of amoebiasis. *International Journal of Pharmaceutics*, 236(1–2), 43–55. [https://doi.org/10.1016/S0378-5173\(02\)00006-6](https://doi.org/10.1016/S0378-5173(02)00006-6)
78. Mastiholimath, V. S., Dandagi, P. M., Jain, S. S., Gadad, A. P., & Kulkarni, A. R. (2007). Time and pH dependent colon specific, pulsatile delivery of theophylline for nocturnal asthma. *International Journal of Pharmaceutics*, 328(1), 49–56. <https://doi.org/10.1016/j.ijpharm.2006.07.045>
79. Rabito, M. F., Reis, A. V., Reis Freitas, A. dos, Tambourgi, E. B., & Cavalcanti, O. A. (2012). A pH/enzyme-responsive polymer film consisting of Eudragit® FS 30 D and arabinoxylane as a potential material formulation for colon-specific drug delivery system. *Pharmaceutical Development and Technology*, 17(4), 429–436. <https://doi.org/10.3109/10837450.2010.546409>
80. Jain, A., Gupta, Y., & Jain, S. (2006). Azo Chemistry and Its Potential for Colonic Delivery. *Critical Reviews™ in Therapeutic Drug Carrier Systems*, 23(5), 349–400. <https://doi.org/10.1615/CritRevTherDrugCarrierSyst.v23.i5.10>
81. Kim, D., Hong, S., Jung, S., Jung, Y., & Kim, Y. M. (2009). Synthesis and Evaluation of N-Nicotinoyl-2-{2-(2-Methyl-5-Nitroimidazol-1-yl)Ethoxy}-D,L-Glycine as a Colon-Specific Prodrug of Metronidazole. *Journal of Pharmaceutical Sciences*, 98(11), 4161–4169. <https://doi.org/10.1002/jps.21720>
82. Kim, H., Lee, Y., Yoo, H., Kim, J., Kong, H., Yoon, J.-H., ... Kim, Y. M. (2012). Synthesis and evaluation of sulfate conjugated metronidazole as a colon-specific prodrug of metronidazole. *Journal of Drug Targeting*, 20(3), 255–263. <https://doi.org/10.3109/1061186X.2011.639024>
83. Vaidya, A., Jain, S., Agrawal, R. K., & Jain, S. K. (2015). Pectin–metronidazole prodrug bearing microspheres for colon targeting. *Journal of Saudi Chemical Society*, 19(3), 257–264. <https://doi.org/10.1016/j.jscs.2012.03.001>

-
84. Bruno, B. J., Miller, G. D., & Lim, C. S. (2013). Basics and recent advances in peptide and protein drug delivery. *Therapeutic Delivery*, 4(11), 1443–1467. <https://doi.org/10.4155/tde.13.104>
 85. Roldo, M., Barbu, E., Brown, J. F., Laight, D. W., Smart, J. D., & Tsibouklis, J. (2007). Azo compounds in colon-specific drug delivery. *Expert Opinion on Drug Delivery*, 4(5), 547–560. <https://doi.org/10.1517/17425247.4.5.547>
 86. Ibrahim, I. M. (2023). Advances in Polysaccharide-Based Oral Colon-Targeted Delivery Systems: The Journey So Far and the Road Ahead. *Cureus*. <https://doi.org/10.7759/cureus.33636>
 87. Mundargi, R. C., Patil, S. A., Agnihotri, S. A., & Aminabhavi, T. M. (2007). Development of Polysaccharide-Based Colon Targeted Drug Delivery Systems for the Treatment of Amoebiasis. *Drug Development and Industrial Pharmacy*, 33(3), 255–264. <https://doi.org/10.1080/03639040600897127>
 88. Kosaraju, S. L. (2005). Colon Targeted Delivery Systems: Review of Polysaccharides for Encapsulation and Delivery. *Critical Reviews in Food Science and Nutrition*, 45(4), 251–258. <https://doi.org/10.1080/10408690490478091>
 89. Shukla, R. K., & Tiwari, A. (2012). Carbohydrate polymers: Applications and recent advances in delivering drugs to the colon. *Carbohydrate Polymers*, 88(2), 399–416. <https://doi.org/10.1016/j.carbpol.2011.12.021>
 90. Bassi, P., & Kaur, G. (2010). pH modulation: a mechanism to obtain pH-independent drug release. *Expert Opinion on Drug Delivery*, 7(7), 845–857. <https://doi.org/10.1517/17425247.2010.491508>
 91. Liu, L., Fishman, M. L., Kost, J., & Hicks, K. B. (2003). Pectin-based systems for colon-specific drug delivery via oral route. *Biomaterials*, 24(19), 3333–3343. [https://doi.org/10.1016/S0142-9612\(03\)00213-8](https://doi.org/10.1016/S0142-9612(03)00213-8)
 92. Wakerly, Z., Fell, J. ., Attwood, D., & Parkins, D. (1997). Studies on drug release from pectin/ethylcellulose film-coated tablets: a potential colonic delivery system. *International Journal of Pharmaceutics*, 153(2), 219–224. [https://doi.org/10.1016/S0378-5173\(97\)00110-5](https://doi.org/10.1016/S0378-5173(97)00110-5)
 93. VARSHOSAZ, J., EMAMI, J., TAVAKOLI, N., FASSIHI, A., MINAIYAN, M., AHMADI, F., & DORKOOSH, F. (2009). Synthesis and evaluation of dextran–budesonide conjugates as colon specific prodrugs for treatment of ulcerative colitis. *International Journal of Pharmaceutics*, 365(1–2), 69–76. <https://doi.org/10.1016/j.ijpharm.2008.08.034>
 94. Jain, V., Shukla, N., & Mahajan, S. C. (2015). Polysaccharides in colon specific drug delivery, 1(1), 3–11. <https://doi.org/10.15761/JTS.1000103>
 95. Thursby, E., & Juge, N. (2017). Introduction to the human gut microbiota. *Biochemical Journal*, 474(11), 1823–1836. <https://doi.org/10.1042/BCJ20160510>
 96. Rowland, I., Gibson, G., Heinken, A., Scott, K., Swann, J., Thiele, I., & Tuohy, K. (2018). Gut microbiota functions: metabolism of nutrients and other food components. *European Journal of Nutrition*, 57(1), 1–24. <https://doi.org/10.1007/s00394-017-1445-8>
 97. Syromyatnikov, M., Nesterova, E., Gladkikh, M., Smirnova, Y., Gryaznova, M., & Popov, V. (2022). Characteristics of the Gut Bacterial Composition in People of Different Nationalities and Religions. *Microorganisms*, 10(9), 1866. <https://doi.org/10.3390/microorganisms10091866>
 98. Kho, Z. Y., & Lal, S. K. (2018). The Human Gut Microbiome – A Potential Controller of Wellness and Disease. *Frontiers in Microbiology*, 9(1), 1835. <https://doi.org/10.3389/fmicb.2018.01835>
 99. Cummings, J. H., & Englyst, H. N. (1987). Fermentation in the human large intestine and the available substrates. *The American Journal of Clinical Nutrition*, 45(5), 1243–1255. <https://doi.org/10.1093/ajcn/45.5.1243>
 100. Levitt, M. D., Hirsh, P., Fetzer, C. A., Sheahan, M., & Levine, A. S. (1987). H₂ excretion after ingestion of complex carbohydrates. *Gastroenterology*, 92(2), 383–389. [https://doi.org/10.1016/0016-5085\(87\)90132-6](https://doi.org/10.1016/0016-5085(87)90132-6)
 101. Zhang, B., Gao, Y., Zhang, L., & Zhou, Y. (2021). The plant cell wall: Biosynthesis, construction, and functions. *Journal of Integrative Plant Biology*, 63(1), 251–272.
-

- <https://doi.org/10.1111/jipb.13055>
102. Joseph, S. K., Sabitha, M., & Nair, S. C. (2019). Stimuli-Responsive Polymeric Nanosystem for Colon Specific Drug Delivery. *Advanced Pharmaceutical Bulletin*, 10(1), 1–12. <https://doi.org/10.15171/apb.2020.001>
 103. Chourasia, M. K., & Jain, S. K. (2004). Polysaccharides for Colon Targeted Drug Delivery. *Drug Delivery*, 11(2), 129–148. <https://doi.org/10.1080/10717540490280778>
 104. Barclay, T. G., Day, C. M., Petrovsky, N., & Garg, S. (2019). Review of polysaccharide particle-based functional drug delivery. *Carbohydrate Polymers*, 221(1), 94–112. <https://doi.org/10.1016/j.carbpol.2019.05.067>
 105. Veluraja, K., Ayyalnarayanassubburaj, S., & Paulraj, A. J. (1997). Preparation of gum from Tamarind seed — and its application in the preparation of composite material with sisal fibre. *Carbohydrate Polymers*, 34(4), 377–379. [https://doi.org/10.1016/S0144-8617\(97\)00128-8](https://doi.org/10.1016/S0144-8617(97)00128-8)
 106. Malviya, R., Sundram, S., Fuloria, S., Subramaniam, V., Sathasivam, K. V., Azad, A. K., ... Fuloria, N. K. (2021). Evaluation and Characterization of Tamarind Gum Polysaccharide: The Biopolymer. *Polymers*, 13(18), 3023. <https://doi.org/10.3390/polym13183023>
 107. Odeku, O. A., & Itiola, O. A. (2003). Evaluation of the Effects of Khaya Gum on the Mechanical and Release Properties of Paracetamol Tablets. *Drug Development and Industrial Pharmacy*, 29(3), 311–320. <https://doi.org/10.1081/DDC-120018205>
 108. Ozoude, C. H., Azubuike, C. P., Ologunagba, M. O., Tonuewa, S. S., & Igwilo, C. I. (2020). Formulation and development of metformin-loaded microspheres using Khaya senegalensis (Meliaceae) gum as co-polymer. *Future Journal of Pharmaceutical Sciences*, 6(1), 120. <https://doi.org/10.1186/s43094-020-00139-6>
 109. Aspinall, G. O., Johnston, M. J., & Stephen, A. M. (1960). 955. Plant gums of the genus Khaya. Part II. The major component of Khaya senegalensis gum. *Journal of the Chemical Society (Resumed)*, 4918. <https://doi.org/10.1039/jr9600004918>
 110. Odeku, O. A., & Fell, J. T. (2010). Evaluation of khaya gum as a directly compressible matrix system for controlled release. *Journal of Pharmacy and Pharmacology*, 56(11), 1365–1370. <https://doi.org/10.1211/0022357044652>
 111. Vaclavik, V. A., & Christian, E. W. (2014). Pectins and Gums. In Vaclavik V.; Christian E. W. (Ed.), *Essentials of Food Science* (pp. 53–61). spingernature. https://doi.org/10.1007/978-1-4614-9138-5_5
 112. Hobbs, C. A., Swartz, C., Maronpot, R., Davis, J., Recio, L., & Hayashi, S. (2012). Evaluation of the genotoxicity of the food additive, gum ghatti. *Food and Chemical Toxicology*, 50(3–4), 854–860. <https://doi.org/10.1016/j.fct.2011.11.021>
 113. Deshmukh, A. S., Setty, C. M., Badiger, A. M., & Muralikrishna, K. S. (2012). Gum ghatti: A promising polysaccharide for pharmaceutical applications. *Carbohydrate Polymers*, 87(2), 980–986. <https://doi.org/10.1016/j.carbpol.2011.08.099>
 114. Nasrollahzadeh, M., Nezafat, Z., Shafiei, N., & Soleimani, F. (2021). Polysaccharides in food industry. In *Biopolymer-Based Metal Nanoparticle Chemistry for Sustainable Applications* (pp. 47–96). Elsevier. <https://doi.org/10.1016/B978-0-323-89970-3.00002-0>
 115. Williams, P. A. (2016). Gums: Properties and Uses. In *Encyclopedia of Food and Health* (pp. 283–289). Elsevier. <https://doi.org/10.1016/B978-0-12-384947-2.00364-0>
 116. Sworn, G., & Stouby, L. (2021). Gellan gum. In *Handbook of Hydrocolloids* (pp. 855–885). Elsevier. <https://doi.org/10.1016/B978-0-12-820104-6.00009-7>
 117. Philp, K. (2018). Polysaccharide Ingredients. In *Reference Module in Food Science* (p. 32). Elsevier. <https://doi.org/10.1016/B978-0-08-100596-5.22367-6>
 118. Khushbu, & Warkar, S. G. (2020). Potential applications and various aspects of polyfunctional macromolecule- carboxymethyl tamarind kernel gum. *European Polymer Journal*, 140(July), 110042. <https://doi.org/10.1016/j.eurpolymj.2020.110042>

-
119. Gavins, F., & Flower, R. J. (2008). Budesonide. In *xPharm: The Comprehensive Pharmacology Reference* (pp. 1–5). Elsevier. <https://doi.org/10.1016/B978-008055232-3.61350-9>
 120. Papich, M. G. (2016). Budesonide. In *Saunders Handbook of Veterinary Drugs* (pp. 84–85). Elsevier. <https://doi.org/10.1016/B978-0-323-24485-5.00112-1>
 121. Yu, L. X., Amidon, G., Khan, M. A., Hoag, S. W., Polli, J., Raju, G. K., & Woodcock, J. (2014). Understanding pharmaceutical quality by design. *AAPS Journal*, 16(4), 771–783. <https://doi.org/10.1208/s12248-014-9598-3>
 122. Mohurle, M. S. M., J. Asnani, M. D. A., R. Chaple, D. D., Kurian, M. J., & G. Bais, M. A. (2019). Quality by Design (QbD): An Emerging Trend in Improving Quality and Development of Pharmaceuticals. *Saudi Journal of Medical and Pharmaceutical Sciences*, 05(12), 1132–1138. <https://doi.org/10.36348/sjmps.2019.v05i12.019>
 123. Testas, M., da Cunha Sais, T., Medinilha, L. P., Niwa, K. N. I., de Carvalho, L. S., Maia, S. D., ... Yamakawa, C. Y. (2021). An industrial case study: QbD to accelerate time-to-market of a drug product. *AAPS Open*, 7(1), 12. <https://doi.org/10.1186/s41120-021-00047-w>
 124. Han, J. K., Shin, B. S., & Choi, D. H. (2019). Comprehensive Study of Intermediate and Critical Quality Attributes for Process Control of High-Shear Wet Granulation Using Multivariate Analysis and the Quality by Design Approach. *Pharmaceutics*, 11(6), 252. <https://doi.org/10.3390/pharmaceutics11060252>
 125. Namjoshi, S., Dabbaghi, M., Roberts, M. S., Grice, J. E., & Mohammed, Y. (2020). Quality by Design: Development of the Quality Target Product Profile (QTPP) for Semisolid Topical Products. *Pharmaceutics*, 12(3), 287. <https://doi.org/10.3390/pharmaceutics12030287>
 126. Demmon, S., Bhargava, S., Ciolek, D., Halley, J., Jaya, N., Joubert, M. K., ... Tsai, P. (2020). A cross-industry forum on benchmarking critical quality attribute identification and linkage to process characterization studies. *Biologicals*, 67, 9–20. <https://doi.org/10.1016/j.biologicals.2020.06.008>
 127. Parshuramkar, P., Khobragade, D., & Kashyap, P. (2023). Comprehension of Quality by Design in the Development of Oral Solid Dosage Forms. *Journal of Young Pharmacists*, 15(3), 406–418. <https://doi.org/10.5530/jyp.2023.15.56>
 128. Raw, A. S., Lionberger, R., & Yu, L. X. (2011). Pharmaceutical Equivalence by Design for Generic Drugs: Modified-Release Products. *Pharmaceutical Research*, 28(7), 1445–1453. <https://doi.org/10.1007/s11095-011-0397-6>
 129. Simão, J., Chaudhary, S. A., & Ribeiro, A. J. (2023). Implementation of Quality by Design (QbD) for development of bilayer tablets. *European Journal of Pharmaceutical Sciences*, 184(1), 106412. <https://doi.org/10.1016/j.ejps.2023.106412>
 130. Jameel, F., Hershenson, S., Khan, M. A., & Martin-Moe, S. (2015). *Quality by Design for Biopharmaceutical Drug Product Development*. (F. Jameel, S. Hershenson, M. A. Khan, & S. Martin-Moe, Eds.) (1st ed., Vol. 18). New York, NY: Springer New York. <https://doi.org/10.1007/978-1-4939-2316-8>

CHAPTER 2

Review of Literature

CHAPTER 2

2. Review of Literature

2.1 Review of literature for budesonide

Campieri M. et al.[1] conducted a 12-week study to compare two dosage regimens of prednisolone and budesonide in 178 patients who had active Crohn's disease affecting the ascending colon and ileum. Patients received budesonide controlled ileal release (CIR) capsules at 9 mg once daily, 4.5 mg twice daily, or prednisolone tablets at 40 mg once daily. Clinical remission, as defined by a Crohn's Disease Activity Index (CDAI) score of 150 or below, constituted the principal objective. Remission rates for once-daily budesonide or prednisolone were 60% after eight weeks, whereas twice-daily budesonide exhibited a rate of 42% ($p=0.062$). Glucocorticoid-related side effects were similar among groups, but prednisolone caused more moon face ($p=0.0005$) and impaired adrenal function ($p=0.0023$). In conclusion, budesonide CIR, whether once or twice daily, effectively induced remission in Crohn's disease with a simpler, safer approach and fewer side effects compared to prednisolone.

Varshosaz J et al.[2] devised and assessed a reversed-phase HPLC method to analyze budesonide and its synthesized hemiesters in colon-specific dosage form and dissolution media. They used a μ -Bondapak C (18) column at room temperature, with a mobile phase of acetonitrile: potassium phosphate (pH 3.2). Detection was at 244 nm, with dexamethasone as the internal standard. The method exhibited linearity (1-20 $\mu\text{g/ml}$), by a detection limit of 0.05 $\mu\text{g/ml}$. It demonstrated accuracy, selectivity, sensitivity, and precision, effectively separating the drug and its derivatives from excipients. The method was successfully applied to analyse these compounds in dissolution media and oral formulations specific to the colon were achieved using the method.

Rutgeerts P et al.[3] conducted a 10-week trial comparing controlled-release budesonide and prednisolone for treating active Crohn's disease in 176 patients. Budesonide, with its low systemic bioavailability, was administered at 9 mg/day for eight weeks, followed by 6 mg/day for two weeks. Prednisolone was given at 40 mg/day for two weeks, gradually reducing to 5 mg/day in the final week. Remission was obtained by 53% of budesonide-treated patients (CDAI score ≤ 150) after 10 weeks, compared to 66% in the prednisolone group ($p = 0.12$). Both treatments reduced CDAI scores, budesonide caused substantially fewer corticosteroid-related adverse effects (29 patients versus 48 patients, $p = 0.003$). Prednisolone caused more pituitary-adrenal function suppression initially but not at 10 weeks. Both drugs were effective, with prednisolone showing slightly better CDAI score reduction, while budesonide had fewer side effects and less pituitary-adrenal suppression.

Varshosaz J et al.[4] intended to fabricate budesonide pellets for the treatment of inflammatory bowel disease (IBD) using a new colon drug delivery system (CODES). Pellet cores containing lactulose or mannitol were coated sequentially with Eudragit E100, acid-soluble polymer, hydroxypropylmethyl cellulose, and super coated by eudragit FS 30D, enteric coat. *In vitro* tests showed controlled drug release in pH 6.8 with rat cecal contents, influenced by amount and the type of polysaccharide and acid-soluble layer thickness. An optimized formulation effectively treated TNBS-induced colitis in rats. This study suggests that CODES-based pellets hold promise for delivering budesonide to the colon in IBD therapy.

Kane S. V. et al.[5] aimed to evaluate the safety and efficacy of budesonide in the treatment of active Crohn's disease and maintenance of remission, in comparison to corticosteroids, 5-aminosalicylic acid (5-ASA). They selected randomized controlled trials and assessed treatment effectiveness and adverse events. Remission was induced more effectively with budesonide than with placebo (RR=1.82) and 5-ASA (RR=1.73), although only one trial compared it to 5-ASA. For patients with low disease activity, budesonide and conventional corticosteroids showed no significant difference in remission induction. However, budesonide was less likely to cause corticosteroid-related adverse events (RR=0.65). There was an absence of statistically significant variation observed in the incidence of adverse events related to corticosteroids or budesonide compared to 5-ASA or a placebo. Budesonide did not demonstrate efficacy in sustaining remission.

Greenberg, Gordon R. et al.[6] conducted a study to assess the effectiveness and safety of a controlled-ileal-release budesonide formulation in individuals with active Crohn's disease affecting the lower part of small intestine or ileum and proximal colon. A comparison was made between a placebo and three distinct daily concentrations of budesonide (3 mg, 9 mg, and 15 mg) in a 258-patient, randomized, multipoint trial. After eight weeks, remission rates were significantly higher in the budesonide groups (51%, 43%, and 33%) compared to the placebo group (20%). Quality of life improvements were consistent with remission rates. Disease location, previous surgery, and corticosteroid use didn't impact outcomes. While some patients withdrew from the study due to various reasons, budesonide did not induce any notable adverse effects or toxicities associated with corticosteroids. In conclusion, a daily dose of 9 mg of oral controlled-release budesonide was effective and well-tolerated in treatment of active Crohn's disease of the ileum and proximal colon over eight weeks.

Bar-Meir S et al.[7] conducted a study to compare the effectiveness and safety of budesonide (BUD) and prednisone (PRED) in treating active Crohn's disease (CD) affecting the terminal ileum and/or colon. In a randomised, controlled trial with 201 patients, BUD was given at 9 mg once daily for 8 weeks, while PRED was administered at 40 mg daily for 2 weeks, gradually tapering to 5 mg/day by the study's end. Both treatments resulted in similar efficacy (51% for BUD and 52.5% for PRED) in achieving a Crohn's Disease Activity Index of <150. However, BUD had a significantly lower rate of steroid-related adverse reactions (30% vs. 14%). Most improvements in CDAI scores occurred in the first 2 weeks. In conclusion, BUD is as effective as PRED in treating CD involving the terminal ileum and ascending colon but has fewer steroid-related adverse effects.

Song Ivy H. et al.[8] compared the systemic exposure of budesonide from Budesonide Oral Suspension (BOS) and ENTOCORT EC to provide PK bridge data for safety evaluations. BOS is under phase III development for EoE, whereas ENTOCORT EC treats mild-to-moderate Crohn's disease. The trial gave healthy participants a single oral dosage of BOS 2 mg and ENTOCORT EC 9 mg in a random order. BOS was absorbed quicker than ENTOCORT EC, reaching peak concentrations in 1.5 hours against 4 hours. BOS 2 mg decreased systemic budesonide exposure, maximum plasma concentration, and area under the concentration-time curve compared to ENTOCORT EC 9 mg. Despite no significant differences, treatment-emergent side effects were modest and did not cause cessation. PK bridging data for BOS-ENTOCORT EC safety comparisons is provided by these results.

Bhatt H. et al.[9] aimed to improve the aqueous solubility of Budesonide (BUD) for more consistent C max and T max in patients with IBD and targeted delivery to the colon. They used solid dispersion along poloxamer 188 to enhance solubility. A tablet equivalent to 9 mg of Budesonide was prepared from the solid dispersion, then coated with Eudragit S100 and L100 for colon targeting. Statistical design optimized polymer ratio and coating %. Results indicated that modifying drug release in the colon was achievable by optimizing these factors. Accelerated stability testing over three months showed no significant change in drug release, suggesting a promising formulation.

Bruni Giovanna et al.[10] conducted a study to create and analyze electrospun fibers containing budesonide, aiming to regulate its release within the gastrointestinal tract. Budesonide, potent glucocorticosteroid used for treating inflammatory bowel diseases affecting the ileum and colon. They successfully electrospun Eudragit® S 100, a polymer that dissolves at pH > 7, into ultrafine fibers loaded with 9% and 20% (w/w) budesonide. Various analyses confirmed the amorphous character of budesonide in these electrospun systems. As determined by dissolution rate experiments, the drug released minimally at pH 1.0 and maintained a sustained amount at pH 7.2. These fiber-based pharmaceutical systems offer an effective approach for targeting budesonide to the terminal ileum and colon, potentially enhancing its local therapeutic efficacy.

Varshosaz J et al.[11] conducted research with the objective of creating a budesonide delivery system that is specific to the colon in order to improve its efficacy in the treatment of ulcerative colitis. Succinate spacer and dimethylaminopyridine were used to generate dextran–budesonide conjugates. Characterization and analysis of conjugates included degree of substitution (DS), aqueous solubility, and chemical stability. Various rat gastrointestinal system segments were tested for drug release. DS varied from 11.60 to 19.33 mg/100 mg conjugate depending on dextran MW. DS increased solubility, notably in MW 10,000 and 70,000 conjugates. In stomach and intestinal simulations, all conjugates were stable. The stomach and small intestine released less than 10% of the medication, whereas colonic content doubled it, making it appropriate for colonic drug administration. Dextran 70,000 conjugates showed the best promise for ulcerative colitis therapy.

Thomsen O. et al.[12] compared controlled-ileal-release budesonide capsules with slow-release mesalamine tablets in active Crohn's disease involving the ileum and ascending colon using double-blind, multicentre study. For 16 weeks, 93 of 182 patients got 9 mg of

budesonide daily and 89 received 2 g of mesalamine twice daily. Clinical remission—150 or less on the Crohn's Disease Activity Index—was the main endpoint. Budesonide had a 69% remission rate after 8 weeks, compared to 45% for mesalamine. Budesonide had 62% and mesalamine 36% after 16 weeks. Budesonide patients finished the 16-week therapy more often and had fewer serious side effects. Despite relatively different morning cortisol levels, both therapies were beneficial. In conclusion, controlled-ileal-release budesonide was more successful than slow-release mesalamine in producing remission in active Crohn's disease involving the ileum and ascending colon.

Lowry P. W. et al.[13] compared budesonide with mesalamine for remission in mild to moderately active Crohn's disease in a randomized, double-blind, double-dummy research. For 16 weeks, patients with CDAI scores between 200 and 400 were randomized to either budesonide (9 mg daily) or mesalamine (2 g twice daily). The main goal was clinical remission (CDAI \leq 150). Patients on budesonide exhibited greater remission rates than mesalamine at 8 weeks (69% vs. 45%) and 16 weeks (62% vs. 36%). Budesonide shortened the time to remission and increased 16-week study completion. Both groups had comparable treatment-related adverse effects. More budesonide patients exhibited unusually low cortisol (33% vs. 17%) and failed cosyntropin stimulation (10% vs. 0%) after therapy. This research demonstrates that budesonide induces Crohn's disease remission better than mesalamine with better safety.

Abdalla M. I. et al.[14] analysed that Budesonide, a corticosteroid with increased topical efficacy and restricted systemic absorption in the treatment of ulcerative colitis Budesonide was previously only available in rectal form; however, a multi-matrix oral version has been developed. The review analyzes the chemical structure and pharmacological properties of oral and rectal budesonide formulations, clinical studies on their effectiveness and safety in UC, and their present position in UC management. Budesonide induces remission in mild to moderate UC patients but may be less effective than 5-aminosalicylates (5-ASA) and systemic steroids when taken orally. Rectal budesonide works similarly to other rectal steroids but behind 5-ASA. Its significance in maintenance therapy, 5-ASA combos, and oral and rectal budesonide combinations are still unclear.

Levine A. et al.[15] evaluate the effectiveness and tolerability of oral budesonide in comparison to prednisone in children diagnosed with mild to moderately active Crohn's disease in prospective 12-week trial. The 33 patients in both therapy groups had comparable features and disease activity. Both budesonide and prednisone groups had 47% and 50%

remission rates at 12 weeks. Budesonide had less adverse effects (32% vs. 71% in prednisone), including fewer aesthetic side effects. Due to its lesser adverse effects, budesonide may be a better option to prednisone for paediatric patients with mild to moderate Crohn disease activity. The research found that remission rates were comparable.

Turanli Y et al.[16] create controlled-release nanofibers for colonic delivery, utilizing the Eudragit S100, anionic and Eudragit RL100, cationic polymers. Budesonide, a drug commonly used for inflammatory bowel disease (IBD), served as the model drug. The study analysed the polymer solutions' conductivity, surface tension, and viscosity before the electrospinning process. After production, the researchers analyse the surface character, *in vitro* drug release, swelling capacity, water contact angle, and bioadhesion properties. Results showed that the dosage form with ES100:ERL100 (95:5) was the most suitable for colon-specific drug delivery. These nanofibers exhibited minimal drug release at pH 1.2 and 6.8 and a significant release at pH 7.4. The study suggests that the electro spun nanofibers, created by combining anionic and cationic eudragit polymers, hold promise as a drug delivery system for treating IBD and other intestinal diseases.

Prabhu P. et al.[17] conducted a study to explore the colon targeting of the natural polymer khaya gum and compared it with guar gum. They formulated fast-disintegrating core tablets containing budesonide using direct compression, which were then coated with either khaya gum or guar gum. Additionally, these tablets subjected to coating with Eudragit L-100. X-ray imaging was used to track the tablets' movement and integrity in different parts of the gastrointestinal tract in rabbits. The dissolution profiles demonstrated that both khaya gum and guar gum, after used as compression coatings, offered some protection against drug release in the upper part of GI tract. However, the enteric-coated formulations provided complete protection in the upper gastrointestinal tract and released the drug in the large intestine through degradation of the gums by enzymes. The study concluded that while the polysaccharide polymers showed diverse dissolution profiles in the presence and absence of rat cecal contents, additional enteric coating was effective in delivery of the drug to the colon.

2.2 Literature Review for Natural Polymers

Malviya et al.[18] main objective to collect and analyse tamarind gum polysaccharide (TGP) as of *Tamarindus indica* for biomedical applications. For the gum extraction, they

employed distilled water, and for the precipitation, they used ethyl alcohol as an antisolvent. The extracted powder exhibited good flowability with a Hausner ratio of 0.94, Carr's index of 6.25, and an angle of repose of 0.14. Chemical tests confirmed the presence of carbohydrates as the primary constituents. TGP demonstrated a high swelling index of $87 \pm 1\%$, indicating excellent water absorption capacity. A neutral pH of approximately 6.70 ± 0.01 was observed in a 1% gum solution. IR spectra revealed the presence of various functional groups. Contact angle measurements indicated good wetting and liquid spreading on the surface, while SEM showed spherical and irregular particle shapes. DSC analysis indicated crystalline nature with an exothermic peak at 350 °C. Overall, TGP exhibited favourable properties for use as an excipient in biomedical dosage form formulations.

Sirisha et al.[19] used locust bean gum to create a colon-specific drug delivery system for mesalamine. In order to control medication release in the esophagus and stomach, they used ionic gelation to create core microspheres that were then cross-linked with glutaraldehyde and covered with pH-sensitive Eudragit S-100. These microspheres exhibited distinct surface morphologies. The optimized batch (ILBG6) achieved drug release rates of 98.44% for core microspheres, 73.58% for coated microspheres, and 98.28% for coated microspheres in rat cecal contents. All formulations followed Higuchi kinetics, and microsphere prepared by Eudragit S-100 followed Korsmeyer-Peppas kinetics with diffusion mechanism. Stability studies revealed minimal changes, indicating formulation stability. In summary, these locust bean gum-based microspheres hold promise for colon-targeted mesalamine delivery in ulcerative colitis treatment.

Salve et al.[20] created ibuprofen sustained-release tablets that are specifically designed to target the colon using guar and xanthan gum. Drug-excipient compatibility test were performed, and the formulated matrices exhibited controlled release systems, with approximately 50-60% of tablet content comprising polysaccharides degradable by colonic microflora. Biodegradability studies demonstrated a significant decrease in viscosity when exposed to 4% RCC and galactomannase enzyme. *In-vitro* drug release profiles showed that the 4:6 ratio of guar and xanthan gum provided optimal controlled release for 24 hours, making these tablets a potential candidate for colon-targeted drug delivery.

Webster et al.[21] created a more effective oral delivery method for anticancer medicines that specifically target colon cancer. This system incorporates drug-coated nanoparticles, utilizing natural materials like guar gum and xanthan gum, along with probiotics. These

natural gums prevent the drug from breaking down in the upper digestive tract and are then released in the colon where they are most effective. *In vitro* experiments successfully demonstrated the targeted delivery of 5-fluorouracil to the colon. Electron microscopy confirmed spherical nanoparticles with a size of 200 nm. It was shown that 93% of the drug was released in the presence of 4% (w/v) rat cecal material at pH 7.2 and 7.4. *In-vivo* outcomes supported a selected approach for maintaining intestinal/colonic microflora integrity while delivering colon-targeted drugs for treating colon cancer.

Ravi V. et al.[22] utilized natural polysaccharides such as chitosan and guar gum as carriers and diltiazem hydrochloride as the model drug to develop a novel colon-targeted tablet. These tablets had an inulin coating on the inside and a shellac coating on the outside. Evaluation included weight variation, hardness, and % weight gain. *In vitro* release studies involved pH 1.2 HCl for 2 hours, pH 7.4 phosphate buffer for 3 hours, and simulated colonic fluid (SCF) for 6 hours to model the digestive process. The results showed that 4% w/v rat cecal contents in saline phosphate buffer (SCF) after 24 hours provided suitable environments for *in vitro* evaluation. The coated tablets effectively controlled drug release in the upper part of GI tract, releasing the maximum amount in the colonic milieu. Chitosan was identified as the suitable polymer for colon targeting. This study suggests the potential for using polysaccharides and inulin-shellac coatings for colon-targeted drug delivery, addressing both local and systemic disorders.

Singhal et al.[23] intended to create a Guar Gum-based matrix tablet that would exhibit an effective *in vitro* mouth-to-colon release profile and possess appropriate mechanical strength when used as the model drug quercetin. Their aim was to develop an oral colonic delivery method that prevents medication absorption in the stomach and duodenum while allowing full drug release in the colon. Quercetin, known for its antioxidant properties and its potential in treating colon cancer, often has poor absorption in stomach and small intestine. The colon offers an ideal site for drug delivery due to its near-neutral pH, decreased enzymatic activity, longer transit time, and enhanced absorption potential. Achieving colon-targeted drug delivery could enhance quercetin's absorption, leading to improved bioactivity with fewer doses.

Kumar B. et al.[24] devised a system for colon-specific drug delivery using mesoporous silica nanoparticles (MSN). Guar gum, a natural carbohydrate polymer, was employed to seal the mesoporous channels of MSN and encapsulate the model medication 5-fluorouracil

(5FU). Characterization techniques confirmed the successful synthesis of MSN with a size less than 100 nm, belonging to the MCM-41 type. Non-covalent interactions allowed MSN to maintain its nanoparticle structure following guar gum capping. The release of 5FU from guar gum-capped MSN occurred specifically in the presence of enzymes of colonic region, simulating the colonic environment. This released drug demonstrated anticancer action in colon cancer cell lines *in vitro*. Moreover, the GG-MSN system exhibited minimal drug release in the absence of enzymes, making it a promising candidate for further *in vivo* investigations in colon-specific drug delivery.

Newton A.M.J. et al.[25] utilized a variety of natural polymers—chitosan, tamarind gum, and okra gum—to create a drug delivery system that targets the colon for the treatment of early morning hypertension. They incorporated Propranolol HCl as a model drug to measure precise and time-dependent release. Tamarind gum, a novel polymer, was introduced and compared to other leading natural polymers. Matrix tablets of Propranolol HCl were formulated via direct compression and met quality control standards. Carbopol 940 served as a supporting polymer to alter drug release and tablet features. *In vitro* release studies involved testing in 0.1N HCl, pH 6.8 phosphate buffer, and pH 7.4 phosphate buffer. Formulations using Tamarind gum demonstrated extended drug release related to other polymer-based formulations and exhibited favourable compression characteristics. The study suggests the potential of Tamarind gum in developing an effective chronotherapeutic colon-targeted drug delivery system for early morning hypertension management.

Zhang et al.[26] emphasize the development of polysaccharide-based oral colon-targeted drug delivery systems that are activated by the physiological environment of the colon. Polysaccharides offer potential advantages for colon targeting due to their specificity. The review gives an overview of *in vitro* and *in vivo* evaluations of polysaccharide-based molecules for colon targeting and a summary of different kinds of polysaccharides utilized for colon targeting. Not only are polysaccharide-based microspheres emphasized for delivering drugs in the treatment of systemic illnesses like rheumatoid arthritis and chronic stable angina, but they are also highlighted for their use in the treatment of local colon disorders including colon cancer, inflammatory bowel disease (IBD), amoebiasis, and irritable bowel syndrome (IBS). The potential of polysaccharide-based micro/nanocarriers for colon-targeted drug administration is also discussed. These include microbeads, microcapsules, microparticles, nanoparticles, nanogels, and nanospheres.

Prezotti et al.[27] designed biodegradable mucoadhesive beads for colon-targeted delivery of resveratrol (RES) using a composite of gellan gum and pectin. These beads had a circular shape with a mean diameter of 914 μm , a high-RES entrapment rate of 76%, and a regulated drug release time of up to 48 hours at intestinal pH (6.8). According to the Korsmeyer pappas, the drug release exhibited a mixed Fickian diffusion/Case II transport kinetics, indicating that both diffusion and swelling/polymer chain relaxation were involved in regulating release rates. Importantly, these beads were deemed safe for intestinal cell lines (Caco-2 and HT29-MTX), and their use significantly reduced RES permeation in an *in vitro* triple intestinal model. This property, along with the controlled release at acidic pH, supports the potential of these beads for targeted drug delivery to the colon, which could enhance the local therapeutic effects of RES.

Sharma K. et al.[28] created a biodegradable hydrogel composite, gum ghatti-co-poly (acrylic acid-aniline) (Gg-co-poly (AA-ANI)), by employing crosslinkers and initiators to graft copolymerize aniline onto Gg-co-poly (AA) chains. In order to produce the matrix Gg-co-poly (AA), acrylic acid (AA) was polymerized onto the gum ghatti (Gg) backbone. Using an array of methodologies, the crosslinked hydrogels were characterized, providing confirmation that the graft polymerization was effective. Using the decomposing soil method, the biodegradation of the hydrogels was assessed for a duration of two months. This was achieved by quantifying weight changes and computing the degradation percentage. Potential was observed for the hydrogels to function as colon-specific drug delivery systems, and it was determined that optimal drug absorption occurred in the hydrogel exhibiting the greatest percentage enlargement. In order to obtain a deeper understanding of the mechanism by which the model drug, amoxicillin trihydrate, was released from the hydrogels, preliminary kinetic studies were performed.

Khotimchenko et al.[29] highlight the use of biopolymer delivery systems, specifically pectin-based materials, in the treatment of malignant tumors to reduce severe side effects associated with chemotherapy. Pectins are particularly promising for colon-targeted drug delivery due to their stability in varying gastrointestinal conditions and susceptibility to degradation by colonic microflora-produced pectinases. Various pectin-containing delivery systems, including hydrogels, tablets, pellets, films, microspheres, microsponges, and nanoparticles, have been developed. These systems enable the concentration of active drug molecules to be increased at specific sites within the intestine while reducing their blood

levels, thereby lowering the risk of severe side effects. The review compiles and discusses the extensive literature available on the use of pectin biopolymers in drug delivery applications.

Singh V. et al.[30] aimed to achieve precise release of 5-aminosalicylic acid (5-ASA) specifically in the colon, addressing the challenge of its easy permeation in the upper gastrointestinal tract at acidic pH. They developed carboxymethyl cellulose-rosin gum hybrid nanoparticles (CRNP3) with an average size of 267 nm using the nanoprecipitation method. A variety of techniques were employed to characterize CRNP3. According to *in vitro* release investigations, the drug was released at a sluggish rate of 72% over a period of 12 hours in simulated intestinal fluid (SIF), after an initial 2 hours of controlled release in simulated gastric fluid (SGF). In contrast, the complete discharge of 100% was accomplished by natural carboxymethyl cellulose or rosin gum within a duration of 5 hours or 8 hours, respectively. The utilization of CRNPs for delayed release exhibits potential in augmenting the bioavailability of drugs in the colon, owing to its non-Fickian diffusion mechanism and zero-order kinetics.

Sharma et al.[31] created a two-step aqueous polymerization procedure to produce a gum ghatti-graft-poly (methacrylic acid-aniline) interpenetrating network (IPN) hydrogel. To begin, graft co-polymerization of poly (methacrylic acid) (poly (MAA)) chains onto a gum ghatti (Gg) backbone was performed, with the reaction conditions optimized to achieve the highest possible water absorption capacity. The resultant hydrogel demonstrated swelling characteristics that were dependent on pH. Additionally, aniline (ANI) monomer was incorporated via oxidative polymerization into the preformed Gg-g-poly (MAA) network. In addition to analyzing the structure, morphology, and thermal properties of the cross-linked hydrogel, biodegradation studies confirmed its biodegradability. At a temperature of 37°C, the release profiles of the hydrogel networks were investigated using amoxicillin trihydrate as a model drug across various pH conditions. At pH 2.2 and 7.0, drug release from the Gg-g-poly (MAA) matrix was non-Fickian, whereas at pH 9.2, it was Fickian. On the other hand, the Gg-g-poly (MAA-IPN-ANI) matrix demonstrated Fickian behavior across all pH ranges. The hydrogels exhibited regulated drug release characteristics, rendering them prospective vehicles for administering drugs specifically to the colon within the lower gastrointestinal tract.

Pal et al.[32] implemented an innovative and environmentally sustainable sesbania gum-based hydrogel, which was fabricated through microwave-assisted polymerization, to construct a sustained release matrix for 5-fluorouracil. As a monomer and crosslinker, acrylamide and N, N Methylenebisacrylamide were utilized, respectively. Multiple analyses, including FTIR, SEM, XRD, TGA, DSC, and elemental analysis, validated the copolymerization phenomenon. Sorben swelling was employed to encapsulate bioactive 5-fluorouracil, and its rate of release was investigated across various pH dissolution media in accordance with USP standards. Higher crosslinking in hydrogels was associated with delayed release rates, whereas an increase in pH led to an increase in release rates. The hydrogel's non-Fickian release behaviour was indicated by the release kinetics, rendering it a potentially effective system for regulated drug administration.

2. 3 Review of literature for microbial approach-based colon targeted drug delivery system

Hua S. et al[33] review that colon-targeted drug delivery is a key focus of research for treating localized colon diseases, offering enhanced therapeutic effectiveness and reduced systemic side effects. This review highlights its significance, especially for addressing inflammatory bowel diseases (IBD) like Crohn's Disease and ulcerative colitis. Although recent developments in oral drug delivery have improved for colonic delivery, it is important to take into account the changed physiology of the GI tract that occurs during GI inflammation. Drug distribution to inflamed colon tissues has been greatly improved by the use of nanotechnology in the development of oral dosage forms. Recent advances in orally given nano-delivery methods for colon targeting are discussed, as is the anticipated future of this research in offering more effective and localized therapies for colon diseases.

Li D. et al.[34] review that inflammatory bowel disease (IBD) is a challenging group of gastrointestinal disorders characterized by recurrent intestinal inflammation. Effective oral treatment for IBD is hindered by physical barriers in the gastrointestinal tract. Nanoparticle-based drug delivery systems (DDSs) offer a promising solution due to their unique properties and enhanced permeability in inflamed bowel tissues. This review focuses on understanding IBD's pathophysiology and strategies for precise drug delivery to affected areas. Nanoparticles, extracellular vesicles, and plant-derived nanoparticles are only a few examples of the new types of nano-targeted carriers introduced. Recently developed oral

nanoparticles for the treatment of inflammatory bowel disease are reviewed. The relevance of nanomedicines in enhancing drug delivery accuracy in IBD therapy is highlighted, and the review also discusses obstacles in nanotechnology and proposes possible future routes for more successful IBD treatment.

Bansal, V. et al.'s[35] review focuses on targeting drugs to the colon, crucial for both localized and systemic effects of peptides and proteins. Various innovative methods are employed to target drugs with colonic absorption windows. pH-sensitive polymers and prodrugs are utilized for effective colonic drug delivery. Natural polymers are also successfully employed due to their low toxicity, biodegradability, and accessibility in diverse molecular weights and chemical compositions. These natural polymers are recognized pharmaceutical excipients, enhancing their suitability for colonic drug delivery and supporting their use in this context.

Naeem, M. et al.'s[36] review explores nano-drug delivery systems (NDDS) for targeted drug delivery to the colon, primarily for conditions like ulcerative colitis, Crohn's disease, colon cancer, and peptide/protein drug delivery. NDDS offer advantages for colon-specific diseases, enhancing therapeutic efficacy while minimizing systemic toxicity. However, obstacles like premature drug release, stomach degradation, pH fluctuations, mucus entrapment, and upper small intestine uptake pose challenges for successful colon-specific drug delivery. Despite these limitations, developments in NDDS show promise for reshaping medicine delivery for illnesses limited to the colon. The obstacles that orally delivered systems confront are outlined, and important areas of colon-specific drug administration are discussed in this study. It also summarizes recent advancements in NDDS that can be taken orally for colon targeting and gives hints at potential future developments in this area.

De Anda-Flores, Y et al.[37] came to the conclusion that polysaccharide nanomaterials have become very important in making nanoparticles for drug delivery systems that target the gut. These systems constitute an oral non-invasive therapy utilized to treat a wide range of diseases. In order to attain effective colonic delivery, the research underscored the criticality of examining the mucoadhesive, chemical, and enzymatic barriers present in the gastrointestinal tract. The significance of this analysis lies in its capacity to facilitate the passage of nanomaterials through these barriers and their efficient delivery to the colon. The study provided details on the synthesis of nanoparticles composed of diverse polysaccharides, which exhibited the ability to traverse numerous obstacles within the

gastrointestinal tract. It has been demonstrated that the encapsulation efficiency, drug protection, and release mechanisms of these nanoparticles are affected when they reach the colon. Furthermore, the research paper examined the potential impact of nanoparticle size on early drug degradation and release in the digestive tract via diffusion through GI tract barriers². The research presented by De Anda-Flores et al. highlights the importance of nanoparticles based on polysaccharides in the development of drug delivery systems that specifically target the colon. This holds great potential for enhancing the treatment of various diseases.

Arévalo-Pérez, R. et al.[38] have made a significant contribution to the field of colon drug delivery research, an area that is becoming more attention-grabbing owing to its capacity to deliver peptides and drugs specifically to the colon for the purpose of treating diseases, while preventing potential adverse effects and systemic absorption. In order to formulate effective pharmaceuticals for colon drug delivery, an extensive understanding of synthetic/semisynthetic and natural polymers is required. For the development of diverse drug delivery systems for the colon, substances including hydroxypropyl methylcellulose, chitosan, polyethylene oxide, pectin, natural polysaccharides, alginates, and polymethacrylates have demonstrated potential. The variety of formulations encompasses advanced nano systems and incorporated osmotic-like compounds, in addition to conventional tablets and capsules. The objective of this research is to synthesize information regarding the processes and components incorporated into these pharmaceutical formulations, with an emphasis on recent developments in the domain.

Amidon, S et al.[39] highlight the significance of colon-specific drug delivery systems (CDDS) in the management of specific ailments affecting the bowel, including chronic pancreatitis, ulcerative colitis, Crohn's disease, irritable bowel syndrome, and colon cancer. Moreover, for the treatment of conditions other than colonic, the colon can facilitate the absorption of systemic medications, particularly those that are susceptible to degradation in the stomach. Optimal drug delivery to the colon is critical for achieving therapeutic efficacy. In the article, numerous formulation strategies for developing CDDS are discussed. These approaches utilize elements such as fluctuations in pH levels within the gastrointestinal tract, microbiota in the colon, and enzymatic activity to attain accurate colonic targeting. In addition to discussing the determinants of colon-specific drug delivery and colonic bioavailability, the review acknowledges the constraints that are inherent in CDDS. This

article offers an exhaustive analysis of conventional and more recent formulation techniques and technologies that are presently utilized in the development of CDDS.

Vagare, R et al.[40] produced and assessed a drug delivery system tailored for the colon, Tenoxicam, through the utilization of compression-coated tablets. The constituents included Tenoxicam, Avicel pH101, HPMC K4M, and Guar gum. The compression-coated tablets underwent analysis using differential scanning calorimetry (DSC), Fourier-transform infrared (FTIR) spectroscopy, and in-vitro dissolving experiments, both in the presence and absence of rat caecal material. The findings of the study demonstrate the effective development of a targeted drug delivery system for Tenoxicam that specifically targets the colon. This was achieved by formulating the medicine using Guar gum in conjunction with different amounts of HPMC. The tablets demonstrated adherence to the specified criteria for medication content, hardness, thickness, friability, and weight fluctuation. The augmentation of hydroxypropyl methylcellulose (HPMC) content inside the compression coat resulted in a decrease in the release of the medication. According to the findings of in-vitro drug release investigations, it was determined that tablets containing a blend of 90% Guar gum and 10% HPMC exhibited efficacy in delivering Tenoxicam specifically to the colon, while demonstrating low release in the stomach and small intestine.

Mundargi, R et al.[41] wanted to create metronidazole (MTZ) drug delivery system which were formulated by employing a graft copolymer of methacrylic acid and guar gum (GG) as a vehicle, in conjunction with a variety of polysaccharides. An assessment was conducted on various polysaccharides, including GG, xanthan gum, pectin, carrageenan, β -cyclodextrin, and methacrylic acid-g-guar (MAA-g-GG) gum. The tablets' suitability for colon-specific drug delivery was evaluated through *in vitro* experiments. In order to enhance the resistance of certain formulations to acidic environments, an enteric coating of Eudragit-L 100 was applied instead. According to drug release studies conducted in simulated fluids, the rate of release was concentration and type of polysaccharide/polymer. Tablets that were not coated with xanthan gum or a graft copolymer mixture released 30–40% of the drug within the first four to five hours, whereas GG coated with the graft copolymer released 70% of the drug. A coating of enteric decreased discharge by 18–24%. The release was increased in media containing rat caecal contents as a result of solubilization of the polymer or microbial degradation. The drug was transported by super-Case-II for coated formulations

and non-Fickian for uncoated formulations. In general, the selection of enteric coating and polysaccharide had a substantial impact on the release of MTZ.

2.4 Review of literature for modified dissolution methodology

Singh, S et al.[42] investigate the significance of dissolution testing as a means of forecasting the *in-vivo* release kinetics of drug dosage forms that are administered orally. Their particular emphasis is on oral delivery systems that target the colon using polysaccharides, in which the simulation of the complete gastrointestinal pathway is vital. This procedure consists of conducting sequential dissolution tests in simulated colonic fluid (SCF), simulated gastric fluid (SGF), and simulated intestinal fluid (SIF). In contrast to SGF and SIF, which have established and standardized compositions, the production of SCF generally necessitates the incorporation of human fecal slurry or rodent feces. In order to simulate colonic fluid, the authors suggest an alternative technique involving the co-cultivation of five probiotics and a prebiotic in anaerobic conditions. A comparison was made between the drug release profiles of colon-targeted delivery systems in this medium and those of conventionally utilized media containing human faecal sediment and rodent caecal contents. Consistent results indicated that this suggested medium may function as a practical, biologically significant, and animal-friendly method for dissolution testing in the development of drugs with a specific target in the colon.

Webster, T et al.[43] wanted to establish a novel dissolution technique that is animal-free and suitable for the evaluation of nanorough polysaccharide-based micron granules that are intended for drug delivery in the colon. The researchers employed probiotic made from bacteria identified in the colon and conducted a comparative analysis with conventional dissolution methods utilizing media supplemented with rat cecal contents and human excrement. The research investigated the cultivation of prevalent species of colonic bacteria (including *Bacteroides*, *Bifidobacterium*, *Lactobacillus* species, *Eubacterium*, and *Streptococcus*) in a skim milk powder and honey mixture. They then added probiotic cultures to the dissolution media in order to evaluate the release of drugs from formulations containing polysaccharides. A gradient pH dissolution method was implemented utilizing the USP dissolution apparatus I/II. The findings indicated that the outcomes produced by the probiotic-based system were similar to those obtained from the conventional rat cecal and human fecal-based fermentation models. This suggests that the efficacy of probiotic

dissolution methods can be utilized to evaluate oral formulations of polysaccharides intended for colonic drug delivery. A substantial contribution is made to the domain of nanostructured biomaterials through the development of a more straightforward assay for drug delivery to the colon.

Kotla, N et al.[44] discuss the increasing prevalence of colonic diseases such as ulcerative colitis, Crohn's disease, and colon cancer as a result of dietary and lifestyle factors. This has increased interest in drug delivery systems that target the colon, with polysaccharide coating emerging as a successful method. However, the assessment of these systems necessitates a practical, economical, pertinent, and replicable dissolution technique. It is difficult to replicate the intricate characteristics of the colon; therefore, numerous dissolution strategies, including enzymes, rat caecal contents, human fecal slurries, and multistage culture systems, have been attempted. Pharmaceutical scientists continue to face a substantial obstacle in the form of developing colon-specific bio-relevant dissolution media that are both economical and animal-friendly. An assortment of dissolution techniques that replicate the *in vivo* efficacy of dosage forms intended for colon targeting are examined in the article. The constraints and factors that must be taken into account when developing biocompatible dissolution methods for these systems are also emphasized.

Yadav, A et al.[45] proposed an innovative dissolution technique that utilizes microorganisms to assess colon-targeted delivery systems that are administered orally. The authors sought to address the drawbacks associated with traditional methods. The researchers determined that a medium consisting of five distinct microorganisms was universally suitable for this objective. A range of delivery systems, such as microspheres coated with polysaccharide, liquisolid compacts, and mini tablets, were formulated and evaluated for sequential solubility in media containing and lacking microbiota. In comparison to media containing cecal content from rats and goats, the dissolution profiles of all polysaccharide-based formulations in the probiotic medium based on fluid thioglycollate (FTM) were identical. This implies that the probiotic medium formulated using FTM has the capacity to eradicate the necessity for animal sacrifice during dissolution testing of polysaccharide-based colon-targeted delivery systems. This methodology presents a viable and morally sound substitute for evaluating the efficacy of said drug delivery systems.

Yang, L et al.[46] discuss the use of colonic microflora fermentation for achieving colon-specific drug delivery, highlighting its advantages such as independence from gastrointestinal conditions. They mention the COLAL technology, an advanced delivery system. However, *in vitro* testing of these systems is challenging because the key indicator is colonic-specific drug release, which is hard to replicate using standard methods like USP dissolution tests. As a result, alternative dissolution methods involving enzymes, human fecal slurries, rat caecal contents, and multi-stage cultures have been developed to better mimic colonic conditions. The article primarily focuses on summarizing and reviewing these dissolution testing methods for describing colon-specific delivery systems stimulated by colonic bacteria, along with brief insights into relevant colon physiology.

2.5 References

1. Campieri, M., Ferguson, A., Doe, W., Persson, T., & Nilsson, L. G. (1997). Oral budesonide is as effective as oral prednisolone in active Crohn's disease. *Gut*, 41(2), 209–214. <https://doi.org/10.1136/gut.41.2.209>
2. Varshosaz, J., Emami, J., Tavakoli, N., Minaian, M., Rahmani, N., Ahmadi, F., & Dorkoosh, F. (2011). Development and validation of a rapid HPLC method for simultaneous analysis of budesonide and its novel synthesized hemiesters in colon specific formulations. *Research in pharmaceutical sciences*, 6(2), 107–16. Retrieved from <http://www.ncbi.nlm.nih.gov/pubmed/22224094>
3. Rutgeerts, P., Lofberg, R., Malchow, H., Lamers, C., Olaison, G., Jewell, D., ... Seidegard, C. (1994). A Comparison of Budesonide with Prednisolone for Active Crohn's Disease. *New England Journal of Medicine*, 331(13), 842–845. <https://doi.org/10.1056/NEJM199409293311304>
4. Varshosaz, J., Emami, J., Tavakoli, N., Minaian, M., Rahmani, N., Dorkoosh, F., & Mahzouni, P. (2011). Development of novel budesonide pellets based on CODES(TM) technology: *In vitro/in vivo* evaluation in induced colitis in rats. *Daru : journal of Faculty of Pharmacy, Tehran University of Medical Sciences*, 19(2), 107–17. Retrieved from <http://www.ncbi.nlm.nih.gov/pubmed/22615647>
5. Kane, S. V., Schoenfeld, P., Sandborn, W. J., Tremaine, W., Hofer, T., & Feagan, B. G. (2002). Systematic review: the effectiveness of budesonide therapy for Crohn's disease. *Alimentary Pharmacology & Therapeutics*, 16(8), 1509–1517. <https://doi.org/10.1046/j.1365-2036.2002.01289.x>
6. Greenberg, G. R., Feagan, B. G., Martin, F., Sutherland, L. R., Thomson, A., Williams, C. N., ... Persson, T. (1994). Oral Budesonide for Active Crohn's Disease. *New England Journal of Medicine*, 331(13), 836–841. <https://doi.org/10.1056/NEJM199409293311303>
7. Bar-Meir, S., Chowers, Y., Lavy, A., Abramovitch, D., Sternberg, A., Leichtmann, G., ... Mittmann, U. (1998). Budesonide versus prednisone in the treatment of active Crohn's disease. The Israeli Budesonide Study Group. *Gastroenterology*, 115(4), 835–40. Retrieved from <http://www.ncbi.nlm.nih.gov/pubmed/9753485>
8. Song, I. H., Finkelman, R. D., & Lan, L. (2020). A Pharmacokinetic Bridging Study to Compare Systemic Exposure to Budesonide between Budesonide Oral Suspension and ENTOCORT EC in Healthy Individuals. *Drugs in R&D*, 20(4), 359–367. <https://doi.org/10.1007/s40268-020-00324-1>
9. Bhatt, H., Naik, B., & Dharamsi, A. (2014). Solubility Enhancement of Budesonide and Statistical Optimization of Coating Variables for Targeted Drug Delivery. *Journal of Pharmaceutics*, 2014, 1–

13. <https://doi.org/10.1155/2014/262194>
10. Bruni, G., Maggi, L., Tammam, L., Canobbio, A., Di Lorenzo, R., D'aniello, S., ... Marini, A. (2015). Fabrication, Physico-Chemical, and Pharmaceutical Characterization of Budesonide-Loaded Electrospun Fibers for Drug Targeting to the Colon. *Journal of Pharmaceutical Sciences*, 104(11), 3798–3803. <https://doi.org/10.1002/jps.24587>
11. VARSHOSAZ, J., EMAMI, J., TAVAKOLI, N., FASSIHI, A., MINAIYAN, M., AHMADI, F., & DORKOOSH, F. (2009). Synthesis and evaluation of dextran–budesonide conjugates as colon specific prodrugs for treatment of ulcerative colitis. *International Journal of Pharmaceutics*, 365(1–2), 69–76. <https://doi.org/10.1016/j.ijpharm.2008.08.034>
12. Thomsen, O. Ø., Cortot, A., Jewell, D., Wright, J. P., Winter, T., Veloso, F. T., ... Pettersson, E. (1998). A Comparison of Budesonide and Mesalamine for Active Crohn's Disease. *New England Journal of Medicine*, 339(6), 370–374. <https://doi.org/10.1056/NEJM199808063390603>
13. Lowry, P. W., & Sandborn, W. J. (1999). A comparison of budesonide and mesalamine for active Crohn's disease. *Gastroenterology*, 116(5), 1263–1264. [https://doi.org/10.1016/S0016-5085\(99\)70034-X](https://doi.org/10.1016/S0016-5085(99)70034-X)
14. Abdalla, M. I., & Herfarth, H. (2016). Budesonide for the treatment of ulcerative colitis. *Expert Opinion on Pharmacotherapy*, 17(11), 1549–1559. <https://doi.org/10.1080/14656566.2016.1183648>
15. Levine, A., Weizman, Z., Broide, E., Shamir, R., Shaoul, R., Pacht, A., ... Bujanover, Y. (2003). A comparison of budesonide and prednisone for the treatment of active pediatric Crohn disease. *Journal of Pediatric Gastroenterology and Nutrition*, 36(2), 248–252. <https://doi.org/10.1097/00005176-200302000-00017>
16. Turanlı, Y., & Acartürk, F. (2021). Fabrication and characterization of budesonide loaded colon-specific nanofiber drug delivery systems using anionic and cationic polymethacrylate polymers. *Journal of Drug Delivery Science and Technology*, 63, 102511. <https://doi.org/10.1016/j.jddst.2021.102511>
17. Prabhu, P., Ahamed, N., Matapady, H. N., Ahmed, M. G., Narayanacharyulu, R., Satyanarayana, D., & Subrahmanayam, E. (2010). Investigation and comparison of colon specificity of novel polymer khaya gum with guar gum. *Pakistan journal of pharmaceutical sciences*, 23(3), 259–65. Retrieved from <http://www.ncbi.nlm.nih.gov/pubmed/20566437>
18. Malviya, R., Sundram, S., Fuloria, S., Subramaniam, V., Sathasivam, K. V., Azad, A. K., ... Fuloria, N. K. (2021). Evaluation and Characterization of Tamarind Gum Polysaccharide: The Biopolymer. *Polymers*, 13(18), 3023. <https://doi.org/10.3390/polym13183023>
19. Sirisha, V. N. L., Chinna Eswariah, M., & Sambasiva Rao, A. (2018). A novel approach of locust bean gum microspheres for colonic delivery of mesalamine. *International Journal of Applied Pharmaceutics*, 10(1), 86–93. <https://doi.org/10.22159/ijap.2018v10i1.22638>
20. Salve, P. S. (2011). Development and *in vitro* evaluation colon targeted drug delivery system using natural gums. *Asian Journal of Pharmaceutical Research*, 1(4), 91–101.
21. Webster, T. J., Singh, S., Kotla, N., Tomar, S., Maddiboyina, B., Sharma, D., & Sunnapu, O. (2015). A nanomedicine-promising approach to provide an appropriate colon-targeted drug delivery system for 5-fluorouracil. *International Journal of Nanomedicine*, 7175. <https://doi.org/10.2147/IJN.S89030>
22. Ravi, V., Siddaramaiah, & Pramod Kumar, T. M. (2008). Influence of natural polymer coating on novel colon targeting drug delivery system. *Journal of Materials Science: Materials in Medicine*, 19(5), 2131–2136. <https://doi.org/10.1007/s10856-007-3155-x>
23. Singhal, A., Jain, H., Singhal, V., Elias, E., & Showkat, A. (2011). Colon-targeted quercetin delivery using natural polymer to enhance its bioavailability. *Pharmacognosy Research*, 3(1), 35. <https://doi.org/10.4103/0974-8490.79113>
24. Kumar, B., Kulanthaivel, S., Mondal, A., Mishra, S., Banerjee, B., Bhaumik, A., ... Giri, S. (2017).

- Mesoporous silica nanoparticle based enzyme responsive system for colon specific drug delivery through guar gum capping. *Colloids and Surfaces B: Biointerfaces*, 150, 352–361. <https://doi.org/10.1016/j.colsurfb.2016.10.049>
25. Newton, A. M. J., Indana, V. L., & Kumar, J. (2015). Chronotherapeutic drug delivery of Tamarind gum, Chitosan and Okra gum controlled release colon targeted directly compressed Propranolol HCl matrix tablets and in-vitro evaluation. *International Journal of Biological Macromolecules*, 79, 290–299. <https://doi.org/10.1016/j.ijbiomac.2015.03.031>
 26. Zhang, H., Alsarra, I. A., & Neau, S. H. (2002). An *in vitro* evaluation of a chitosan-containing multiparticulate system for macromolecule delivery to the colon. *International Journal of Pharmaceutics*, 239(1–2), 197–205. [https://doi.org/10.1016/S0378-5173\(02\)00112-6](https://doi.org/10.1016/S0378-5173(02)00112-6)
 27. Prezotti, F., Boni, F., Ferreira, N., Silva, D., Campana-Filho, S., Almeida, A., ... Sarmento, B. (2018). Gellan Gum/Pectin Beads Are Safe and Efficient for the Targeted Colonic Delivery of Resveratrol. *Polymers*, 10(1), 50. <https://doi.org/10.3390/polym10010050>
 28. Sharma, K., Kumar, V., Chaudhary, B., Kaith, B. S., Kalia, S., & Swart, H. C. (2016). Application of biodegradable superabsorbent hydrogel composite based on Gum ghatti-co-poly(acrylic acid-aniline) for controlled drug delivery. *Polymer Degradation and Stability*, 124, 101–111. <https://doi.org/10.1016/j.polymdegradstab.2015.12.021>
 29. Khotimchenko, M. (2020). Pectin polymers for colon-targeted antitumor drug delivery. *International Journal of Biological Macromolecules*, 158, 1110–1124. <https://doi.org/10.1016/j.ijbiomac.2020.05.002>
 30. Singh, V., Joshi, S., & Malviya, T. (2018). Carboxymethyl cellulose-rosin gum hybrid nanoparticles: An efficient drug carrier. *International Journal of Biological Macromolecules*, 112, 390–398. <https://doi.org/10.1016/j.ijbiomac.2018.01.184>
 31. Sharma, K., Kumar, V., Kaith, B. S., Som, S., Kumar, V., Pandey, A., ... Swart, H. C. (2015). Synthesis of Biodegradable Gum ghatti Based Poly(methacrylic acid-aniline) Conducting IPN Hydrogel for Controlled Release of Amoxicillin Trihydrate. *Industrial & Engineering Chemistry Research*, 54(7), 1982–1991. <https://doi.org/10.1021/ie5044743>
 32. Pal, P., Pandey, J. P., & Sen, G. (2018). Sesbania gum based hydrogel as platform for sustained drug delivery: An ‘*in vitro*’ study of 5-Fu release. *International Journal of Biological Macromolecules*, 113, 1116–1124. <https://doi.org/10.1016/j.ijbiomac.2018.02.143>
 33. Hua, S., Marks, E., Schneider, J. J., & Keely, S. (2015). Advances in oral nano-delivery systems for colon targeted drug delivery in inflammatory bowel disease: Selective targeting to diseased versus healthy tissue. *Nanomedicine: Nanotechnology, Biology and Medicine*, 11(5), 1117–1132. <https://doi.org/10.1016/j.nano.2015.02.018>
 34. Li, D., Yang, M., Xu, H., Zhu, M., Zhang, Y., Tian, C., ... Wang, L. (2022). Nanoparticles for oral delivery: targeted therapy for inflammatory bowel disease. *Journal of Materials Chemistry B*, 10(31), 5853–5872. <https://doi.org/10.1039/D2TB01190E>
 35. Bansal, V., Malviya, R., Malaviya, T., & Sharma, P. K. (2014). Novel prospective in colon specific drug delivery system. *Polimery w medycynie*, 44(2), 109–118.
 36. Naeem, M., Awan, U. A., Subhan, F., Cao, J., Hlaing, S. P., Lee, J., ... Yoo, J. W. (2020). Advances in colon-targeted nano-drug delivery systems: challenges and solutions. *Archives of Pharmacal Research*, 43(1), 153–169. <https://doi.org/10.1007/s12272-020-01219-0>
 37. De Anda-Flores, Y., Carvajal-Millan, E., Campa-Mada, A., Lizardi-Mendoza, J., Rascon-Chu, A., Tanori-Cordova, J., & Martínez-López, A. L. (2021). Polysaccharide-Based Nanoparticles for Colon-Targeted Drug Delivery Systems. *Polysaccharides*, 2(3), 626–647. <https://doi.org/10.3390/polysaccharides2030038>
 38. Arévalo-Pérez, R., Maderuelo, C., & Lanao, J. M. (2020). Recent advances in colon drug delivery

- systems. *Journal of Controlled Release*, 327, 703–724. <https://doi.org/10.1016/j.jconrel.2020.09.026>
39. Amidon, S., Brown, J. E., & Dave, V. S. (2015). Colon-Targeted Oral Drug Delivery Systems: Design Trends and Approaches. *AAPS PharmSciTech*, 16(4), 731–741. <https://doi.org/10.1208/s12249-015-0350-9>
40. Vagare, R. S. (2015). MICROBIAL TRIGGERED COLON TARGETED COMPRESSION COATED TABLETS OF TENOXICAM: FORMULATION AND EVALUATION. *Journal of Drug Delivery and Therapeutics*, 5(1). <https://doi.org/10.22270/jddt.v5i1.1051>
41. Mundargi, R. C., Patil, S. A., Agnihotri, S. A., & Aminabhavi, T. M. (2007). Development of Polysaccharide-Based Colon Targeted Drug Delivery Systems for the Treatment of Amoebiasis. *Drug Development and Industrial Pharmacy*, 33(3), 255–264. <https://doi.org/10.1080/03639040600897127>
42. Singh, S. K., Yadav, A. K., Prudhviraaj, G., Gulati, M., Kaur, P., & Vaidya, Y. (2015). A novel dissolution method for evaluation of polysaccharide based colon specific delivery systems: A suitable alternative to animal sacrifice. *European Journal of Pharmaceutical Sciences*, 73, 72–80. <https://doi.org/10.1016/j.ejps.2015.03.012>
43. Webster, T., Kotla, N., Singh, S., Sunnapu, O., & Maddiboyina, B. (2016). A novel dissolution media for testing drug release from a nanostructured polysaccharide-based colon specific drug delivery system: an approach to alternative colon media. *International Journal of Nanomedicine*, 11, 1089–1095. <https://doi.org/10.2147/IJN.S97177>
44. Kotla, N. G., Gulati, M., Singh, S. K., & Shivapooja, A. (2014). Facts, fallacies and future of dissolution testing of polysaccharide based colon-specific drug delivery. *Journal of Controlled Release*, 178, 55–62. <https://doi.org/10.1016/j.jconrel.2014.01.010>
45. Yadav, A., Sadora, M., Singh, S., Gulati, M., Maharshi, P., Sharma, A., ... Gowthamrajan, K. (2017). Novel biorelevant dissolution medium as a prognostic tool for polysaccharide-based colon-targeted drug delivery system. *Journal of Advanced Pharmaceutical Technology & Research*, 8(4), 150. https://doi.org/10.4103/japtr.JAPTR_70_17
46. Yang, L. (2008). Biorelevant dissolution testing of colon-specific delivery systems activated by colonic microflora. *Journal of Controlled Release*, 125(2), 77–86. <https://doi.org/10.1016/j.jconrel.2007.10.026>

CHAPTER 3

**Aim, Objectives and
Rationale of Present
Investigation**

CHAPTER 3

3. Aim, Objectives and Rationale of Present investigation

3.1 Aim of the Present Investigation

The development of an oral colonic drug delivery system is a complex undertaking that demands careful consideration of multiple factors. The ideal release profile for the colon should be determined by considering not only the composition and properties of the dosage form, but also the behaviour and environmental conditions that the dosage form experiences before reaching the colon.

While several strategies have been proposed to address these challenges, the systems that rely on the unique degrading ability by the colonic microbial flora to release the drug from the formulation have emerged as a promising solution.

The aim of present study is to formulate colon targeted delivery system by combination of pH & microbial approaches within the framework of Quality by Design (QbD) for the treatment of local disease associated with colon like ulcerative colitis, irritable bowel syndrome.

3.2 Objectives of Present Investigation

- To retard the drug release in the upper part of GI tract and deliver drug in its intact form as close as possible to the target site.
- To assess the strength and enzymatic sensitivity of various natural polymers like karaya gum, khaya gum, gum Ghatti, xanthan gum, gellan gum, locust bean gum, tamarind gum for targeting to colon through viscosity parameter for preliminary Screening.
- To develop gum & pH dependent polymer-based colon targeted tablet-based DDS of Budesonide.
- To develop gum & pH dependent polymer-based colon targeted pellet-based DDS of Budesonide.
- To assess efficiency of optimized formulations in treatment of ulcerative colitis by targeting to the colon through roentgenography and histopathology study.

3.3 Rationale of Present Investigation

3.3.1 Rationale for the selection of Budesonide as drug

Despite the fact that 5-ASA (5-Amino Salicylic Acid) drugs have been the preferred treatment for CD (Crohn's disease) and UC (Ulcerative Colitis), there is contradictory information about their efficacy in individuals with Crohn's Disease, particularly as long-term treatment.

Antibiotics have a minimal role in colonic CD therapy. Corticosteroids remain the preferred therapy for acute diseases unresponsive to more conservative treatment.

Corticosteroids often demonstrating notable efficacy in treatments, but are accompanied by a range of potential side effects.

Budesonide is much more effective than mesalamine in the treatment of severe ulcerative colitis. Budesonide is a relatively recent steroid that minimizes corticosteroid-associated implications.

Budesonide is a corticosteroid possessing considerable anti-inflammatory effect at the site of application but limited systemic activity due to significant hepatic degradation. Because of this, conventional oral formulations of budesonide are less effective than prednisolone, a common corticosteroid with considerable side effects. So, in the present investigation, budesonide was intended to target the colon via a colon-specific approach.

Due to low incidence of adverse effects and high affinity for glucocorticoid receptors, Budesonide is an important choice for treatment of IBD (ulcerative colitis).

3.3.2 Rationale for the selection of combination of pH and Microbial Approach for colon targeted drug delivery system

The development of an oral colonic drug delivery system is considerably challenging task due to different environmental conditions experienced by the dosage form prior to reaching the colon.

Every system has both benefits and drawbacks. Since there are large fluctuations in the pH levels in various parts of the gastrointestinal tract, and since these differences have been widely studied, the absence of site-specificity inspired the development of pH-dependent systems. The effectiveness of timed-release dose forms in colonic locations is deemed

inadequate due to significant fluctuations in stomach emptying time and transit across the ileo-caecal junction.

Amongst all the approaches proposed so far, the systems relying on the unique degrading ability by the colonic microbial flora to release the drug from formulations is preferred.

Polysaccharides, a large class of compounds that remain less affected in the upper part of the GI tract and are not attacked significantly by the enzymes in the *small* intestine but are degraded by bacterial enzymes in the colon, appear to be promising as carriers in the design of the microbially controlled CTDDS. By employing a pH-dependent polymer as an additional coating, drug release in the stomach is effectively inhibited, and a suitable delay in release is also achieved in the small intestine.

CHAPTER 4

Preformulation Studies

CHAPTER 4

4. Preformulation Studies

4.1 Materials and Equipments

List of Materials and equipment used for the present studies are shown in Table 4.1 and 4.2 respectively.

Table 4.1: List of Materials used in present study with supplier

Sr. No	Name of Material	Supplier
1	Budesonide	Zydus Cadila Pvt. Ltd.
2	Tamarind gum	Exim Gum Pvt ltd.
3	CM tamarind gum	Exim Gum Pvt ltd.
4	Lucast Bean gum	Yarow chem Ltd.
5	Karaya Gum	Yarow chem Ltd.
6	Khaya gum	Yarow chem Ltd.
7	Pectin gum	Astron
8	Gum Ghatti	Yarow chem Ltd.
9	Chitosan	Yarow chem Ltd.
10	Xanthan gum	ACS chemical Ltd.
11	Gallan gum	Suvidhinath lab ltd.
12	Micro crystalline cellulose	Astron Pvt. Ltd.
13	Lactose	Pallav enterprise
14	Talc	Qualikems Ltd.
15	Magnesium stearate	Pallav enterprise
16	PVP K 30	Purvi enterprises
17	Eudragit S 100	Evonik Pvt. Ltd.
18	Acetone	Purvi enterprises
19	Iso propyl alcohol	Purvi enterprises
20	Probiotic capsule (bacterial strains)	Eris life science Ltd.

21	Fluid thioglycolic acid	TM media Ltd.
22	Barium sulphate	Pallav enterprise
23	Acetic acid	Purvi enterprises
24	Ether	Pallav enterprise
25	NaOH	Pallav enterprise
26	CO ₂ aerator (INSTA CO ₂ supply set)	Taiwan brand (Insta)

Table 4.2: List of Equipment's used in present study with supplier

Sr. No	Name of Equipment	Supplier
1	Digital Balance	Wensar (an iso 9001)
2	Melting point apparatus	Singhla scientific ltd.
3	Bath Ultra-sonicator	Labman scientific instrument
4	UV spectrophotometer	Shimadzu (uv-1900i)
5	FTIR spectrometer	Shimadzu (irspirit-t)
6	Brookfield viscometer	Brookfield engineering lab.
7	Digital pH meter	Digitronic ltd.
8	Magnetic stirrer	Remi Pvt. Ltd.
9	Veego Dissolution Apparatus	Veego Pvt. Ltd.
10	8 station D-tooling Tablet compression machine	Karnavati Pvt. Ltd.
11	Extruder	Cronimach Pvt. Ltd
12	Spheroniser	Cronimach Pvt. Ltd
13	Tray dryer	Ridhi trading Ltd.
14	Coating pan	Ridhi trading Ltd.
15	Friabilator	Patel scientific Pvt. Ltd.
16	Digital hardness tester	Parisa technology Pvt. Ltd.
17	Stability chamber	Patel scientific Pvt. Ltd.

4.2 Preformulation studies

4.2.1 Drug identification

One of the first steps in ensuring the quality and safety of an acquired drug sample before it is used in a formulation is to identify the drug.

Appearance, solubility, melting point, and Fourier-transform infrared (FT-IR) spectroscopy were all used in this study to definitively recognize the drug[1].

4.1.1.1 Physical characterization

The physicochemical features of drugs, including their state, color, odor, and taste, were subjected to physical examination and afterwards compared to the documented specifications of the drugs[2].

4.2.1.2 Melting point (MP) determination

A melting point apparatus and the capillary method were employed to determine the melting point of budesonide. A glass capillary containing budesonide powder is inserted, with one end of the capillary having been sealed by the flame. Within the Thiele's tube, the capillary containing the budesonide powder was dipped in liquid paraffin and gradually warmed from below with a Bunsen burner until the budesonide powder within the capillary proceeded melting. Observed at the temperature at which it starts to melt down is the melting point. The result was assessed in triplicate[3, 4].

4.1.1.3 Solubility

Solubility tests were conducted in order to ascertain the drug's purity. The drug's solubility was assessed by transferring 10 mg of the drug into a test tube and subsequently adding 0.1 ml of solvent in a sequential manner. Solvent was added in a continuous manner until the sample was completely dissolved. In order to determine the solubility of the drug powder, the solubility of the solvent used was measured and compared to previously reported values[5].

4.2.1.4 Identification of Drug by FTIR and UV scanning

The Fourier transform infrared (FT-IR) technique is often used for the analysis and characterization of pharmaceutical solids in the field of solid-state characterisation. The drug was identified using the Fourier Transform Infrared (FT-IR) spectroscopy approach, using the FTIR spectrophotometer (Model: Inspiarts-T, Shimadzu, Japan). The drug sample was positioned in close proximity to a diamond crystal, which serves as an optimal substrate for Fourier Transform Infrared Spectroscopy (FTIR) due to its high refractive index and chemical inertness. The drug sample was then subjected to transmission mode scanning throughout the spectral range of 4000 to 400 cm^{-1} . The infrared (IR) spectrum of the drug acquired in this study was compared to the established standard spectra of the drug[6, 7].

The UV scanning of drug was performed using UV spectrophotometer in ethanol, in the range of 200 to 400 nm[8].

4.2.2 Drug – excipient compatibility study

For the drug-excipient compatibility study, FTIR spectrophotometer was used [9]. On an FTIR spectrophotometer (Model: Inspiris-T, Shimadzu, Japan) in the range of 4000–500 cm^{-1} , IR spectra of the drug and the combination of the drug and the excipients were performed.

4.2.3 Development of calibration curve for Budesonide by UV spectrophotometric method in 0.1 N HCl, Phosphate Buffer (pH 7.4), and Phosphate buffer (pH 6.8)

Determination of λ_{max} in 0.1 N HCl

10 mg of the drug, which was precisely weighed, was dissolved in 100 ml of 0.1 N HCl using a volumetric flask. A volume of 1 ml of this solution was transferred to an additional 10 ml volumetric flask, and the volume was adjusted to volume with 0.1 N HCl. With a UV/Vis double beam spectrophotometer, the resulted solution was examined in the 200-400 nm range[10].

Determination of λ_{max} in phosphate buffer pH 7.4 and pH 6.8

A 10 mg quantity of the drug was dissolved in 100 ml of phosphate buffer solution with a pH of 7.4/pH of 6.8 in a volumetric vessel with the same capacity. In a 10 ml volumetric flask, 1 ml of this stock solution was pipetted in, and the volume was adjusted to the mark using buffer solution. The solution obtained was subjected to scanning using a UV/Vis double beam spectrophotometer within the wavelength range of 200-400 nm[11].

4.2.4 Calibration Curve of budesonide in 0.1 N HCl

The calibration curve for budesonide in a 0.1 N hydrochloric acid (HCl) solution was used to ascertain the extent of drug release in *in vitro* release studies.

Preparation of stock solution:

A precise measurement of 100 mg of budesonide was carefully placed into a volumetric flask with a capacity of 100 ml. The drug was dissolved and diluted with 0.1 N hydrochloric acid (HCl) until the solution reached the desired concentration of 1000 $\mu\text{g/ml}$. A 10 ml portion

was taken out from the previous solution and then diluted to a volume of 100 ml using 0.1 N HCl. This process produced a stock solution with a concentration of 100 µg/ml[12].

Preparation of samples for the standard calibration curve

Accurate volumes of budesonide stock solution (0.4, 0.8, 1.2, and 1.6 mL) were appropriately extracted and transferred into 10 mL volumetric flasks. These flasks were then diluted to the mark with 0.1 N HCl, resulting in final solution concentrations ranging from 4 to 16 µg/mL. A drug-free solution was used as a blank for spectroscopic testing. In order to determine the value of λ_{max} , a solution with a concentration of 10 µg/ml was subjected to scanning throughout the wavelength range of 200-400 nm using a double beam spectrophotometer. The absorbance of the prepared solutions in the calibration plot was measured at the maximum wavelength (λ_{max}) of budesonide. The process of quantifying absorbance was carried out three times in order to ensure accuracy and reliability. A calibration curve was generated by plotting the mean absorbance values (n=3) against the corresponding concentrations[8].

4.2.5 Calibration Curve of budesonide in phosphate buffer pH 7.4

The calibration curve for budesonide in a Phosphate Buffer with a pH of 7.4 was used to ascertain the extent of drug release in the context of *in vitro* release tests.

Preparation of stock solution:

A precise measurement of 100 mg of budesonide was carefully added into a volumetric flask with a capacity of 100 ml. The drug underwent dissolution and subsequent dilution with Phosphate Buffer pH 7.4 until the desired concentration of 1000 µg/ml was achieved. A 10 ml aliquot was extracted from the aforementioned solution and then diluted to a volume of 100 ml using Phosphate Buffer pH 7.4. This process resulted in the creation of a stock solution with a concentration of 100µg/ml[12].

Preparation of samples to obtain standard calibration curve

Precise volumes of budesonide stock solution (0.4, 0.8, 1.2, and 1.6 mL) were properly collected and transferred into 10 mL volumetric flasks. These aliquots were further diluted with Phosphate Buffer pH 7.4 up to the mark, resulting in final solution concentrations ranging from 4-16 µg/mL. A blank consisting of a drug-free solution was used for spectroscopic measurement. In order to determine the maximum wavelength (λ_{max}), a

solution with a concentration of 10 µg/ml was subjected to scanning throughout the range of 200-400 nm using a double beam spectrophotometer. The absorbance of the prepared solutions in the calibration plot was measured at the maximum wavelength (λ_{max}) of budesonide. The process of measuring absorbance was conducted three times in order to ensure accuracy and reliability of the results. A calibration curve was generated by plotting the average absorbance values (n=3) against the corresponding concentrations[8].

4.2.6 Calibration Curve of budesonide in phosphate buffer pH 6.8

The calibration curve for budesonide in Phosphate Buffer pH 6.8 was used to ascertain the drug release in *in vitro* release studies.

Preparation of stock solution:

A precise measurement of 100 mg of budesonide was carefully added into a volumetric flask with a capacity of 100 ml. The drug was dissolved and then diluted with Phosphate Buffer pH 6.8 till reaching the specified mark, resulting in a solution with a concentration of 1000 µg/ml. A 10 ml aliquot was extracted from the aforementioned solution and then diluted to a volume of 100 ml using Phosphate Buffer pH 6.8. This process yielded a stock solution with a concentration of 100µg/ml.

Preparation of solutions to obtain calibration curve

Precise aliquots (0.4, 0.8, 1.2, and 1.6 mL) were taken out from the budesonide stock solution and transferred to a 10 mL volumetric flask. The aliquots were diluted to the mark using Phosphate Buffer pH 6.8, resulting in a final solution concentration ranging from 4 to 16 µg/mL. As a baseline for spectroscopic analysis, a drug-free solvent was utilized. A double-beam spectrophotometer was employed to analyze a 10 µg/ml solution within the wavelength range of 200-400 nm in order to determine the λ_{max} . The absorbance of solutions prepared for the calibration plot was assessed at the λ_{max} value of budesonide. The absorbance measurement procedure was executed in triplicate. The concentration was plotted against the mean value of absorbance (n=3) in order to generate a calibration curve.

4.2.7 Screening of Natural Gums by Viscometric Procedure:

In order to achieve the optimal colon-targeted drug delivery system, an effective gum with a desired delay time was chosen after screening. The lag time of polymers can be ascertained by analysing the viscosity profile of the gums, which was an appropriate method for

screening the polymers from the options at hand[13]. To determine the viscosity, a 1% solution of each gum was prepared by dissolving it in phosphate buffer with a pH of 6.8[14]. Due to the intricate interconnectivity of their chains, polysaccharides require a substantial amount of time to fully hydrate. Consequently, the solutions containing polysaccharides were allowed to dissolve completely overnight. For measurement of viscosity, the Brookfield viscometer was employed to measure the viscosity of a solution[15]. In accordance with the solution's viscous properties, spindle number 63 was selected[16]. The solution was then subjected to a rotational speed of 12 rotations per minute for viscosity measurement. Based on the viscosity data, a selection was made of several natural polymers that exhibit favourable viscosity properties, which were subsequently chosen for further investigation.

4.2.8 Preparation of 4% rat cecal content solution and Probiotic Culture Medium:

A buffer solution containing rat cecal content at a concentration of 4% is utilised as an *in-vitro* model to replicate the colonic region's environment. This model facilitates the degradation of polysaccharides and simulates the release of drugs.

Cecal content from a total of six Wistar rats weighing between 250-300g was collected through abdominal incisions[17]. Institutional Animal Ethics Committee, L. J. institute of Pharmacy, LJ university, Ahmedabad, Gujarat, India (Proposal No. LJIP/IAEC/2022-23/02) granted approval for the research. The specified quantity of rat cecal content was transferred into a 100 mL solution of phosphate buffer with a pH value of 6.8. To create an appropriate environment for the survival of anaerobic bacteria present in the rat cecal content, continuous CO₂ aeration was implemented[18].

The probiotic culture medium was prepared using Velgut probiotic and probiotic capsules manufactured by Eris Life Science Ltd., India. The capsules consisted of a blend of advantageous bacterial strains, such as *Bifidobacterium longum*, *Bifidobacterium breve*, *Lactobacillus acidophilus*, *Bifidobacterium infantis*, *Lactobacillus casei*, *Lactobacillus rhamnosus*, *Streptococcus thermophilus*, *Lactobacillus plantarum*, and *Saccharomyces boulardi*[19].

In order to stimulate the anaerobic bacteria contained within the probiotic capsule, Fluid Thioglycollate Medium (FTM) was employed. The preparation of FTM involved the agitation of 8.94 g of FTM powder in 300 mL of deionized water, which was subsequently subjected to autoclaving for a duration of 15 minutes at a pressure of 15 pounds and a

temperature of 121°C[19]. The FTM suspension was subsequently inoculated with 325 mg of the probiotic contents extracted from the capsule. The culture was then incubated for a duration of 48 hours at a temperature of 35°C, under anaerobic conditions[20].

4.2.9 Enzymatic susceptibility for natural gums:

The viscometric method was deemed appropriate and utilized to evaluate the enzymatic susceptibility of natural gums. The measurement of viscosity was conducted on 1% (w/v) solutions of natural polysaccharides in phosphate buffer with a pH of 6.8. The experiment involved monitoring the changes in viscosity over a period of time while incorporating probiotic culture medium in different quantity and 4% rat cecal content.

The temperature of the viscometer was controlled at $37 \pm 0.5^\circ\text{C}$, and viscosity measurements were performed at defined time intervals (0, 0.5, 1, 1.5, 2, and 2.5 hours) utilizing the Brookfield viscometer[15]. The experimental procedure involved conducting measurements utilising 1% natural gum solutions and varying volumes (1 ml, 2 ml, 3 ml, 4 ml, and 5 ml) of probiotic culture medium. To check the influence of anaerobic conditions, the culture medium was continuously aerated with CO₂ using an INSTA 95g CO₂ Disposable Supply. In addition, the specific viscosity-time profile of 1% natural gums in the 4% rat cecal content solution was compared to the specific viscosity-time profile of 1% (w/v) solutions of natural polysaccharides in phosphate buffer with a pH of 6.8, using varying volumes (1 ml, 2 ml, 3 ml, 4 ml, and 5 ml) of probiotic culture medium. The observed decreases in viscosity over time in the presence of enzymes with and without CO₂ aeration, in comparison to the control without enzymes, indicated the enzymatic degradation of natural polymers (polysaccharides)[14].

4.3 Results and Discussion:

4.3.1 Identification of Drugs

4.3.1.1 Identification of Drugs by Description, Solubility and Melting Point

The results of a physical examination and determination of budesonide's melting point are detailed in Table 4.3.

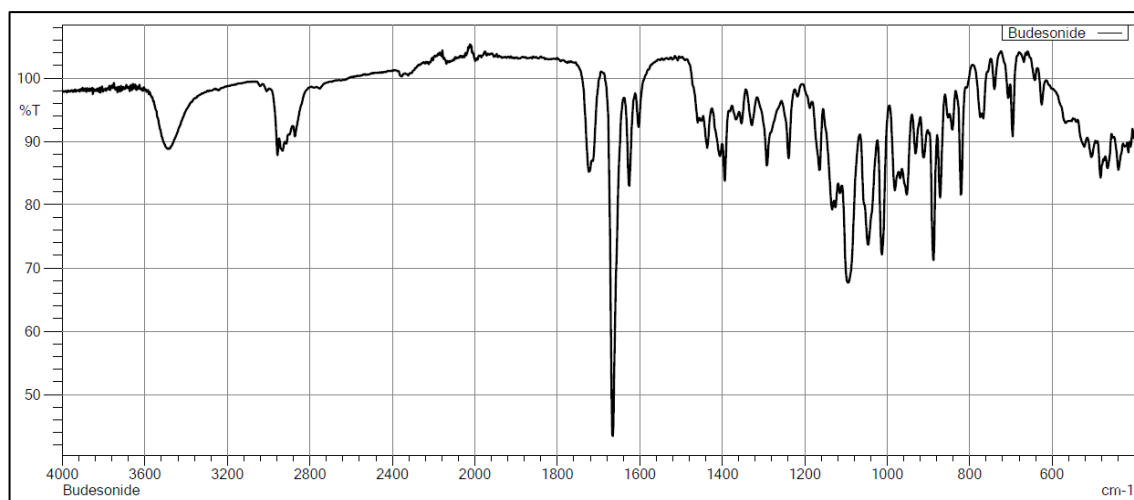
Table 4.3: Drug identification based on characterization, solubility, and melting point

Sr. no.	Identification Parameters	Standard criteria	Observation	Remarks
1	State	Solid (crystalline)	Solid Crystalline	Complies
2	Colour	White	White	Complies
3	Melting point	228-232 °C	229 °C	Complies
4	Solubility	Practically insoluble in water	Practically insoluble in water (0.038 mg/ml)	Complies

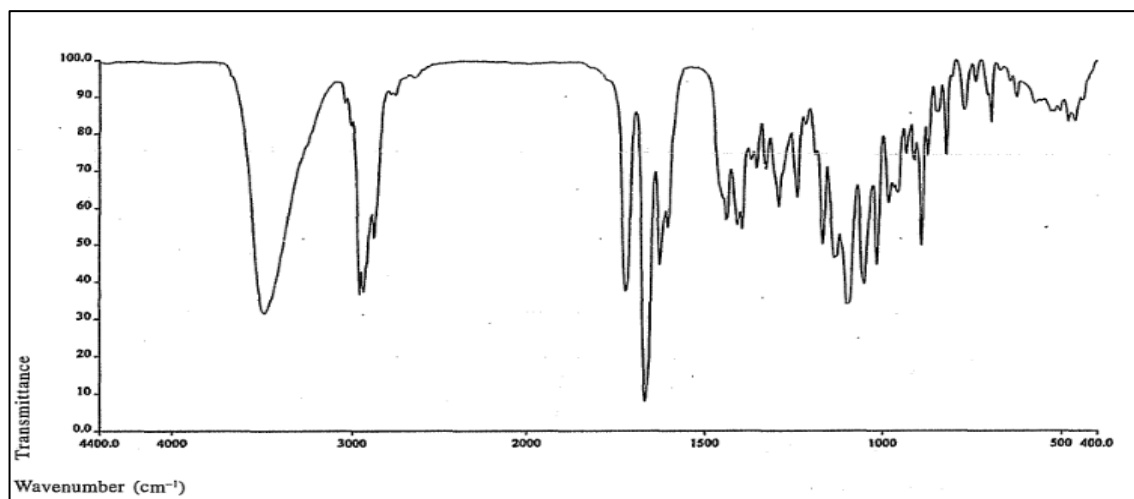
It was determined from Tables 4.3 that the obtained value of the drug's melting point was comparable to the reported value, indicating that the drug samples show resembled the reported properties. In the presence of any impurity, the melting point of a particular drug substance will fluctuate. The previously mentioned test revealed that the sample substance meets the criteria of the budesonide standard.

4.3.1.2 Identification of drugs by FTIR and UV scanning

A comparison was made between the budesonide FTIR spectra and reference IR spectra in order to identify and validate different functional groups. The budesonide spectra, both as reported and as observed, are illustrated in Figure 4.1. From the figure, it was concluded that given sample of budesonide shows all the peak reported by the FTIR of drug in Indian pharmacopeia 2010. The λ_{max} was found to be 244nm as shown in figure 4.2, which complies with the standard 242 nm as per BP.

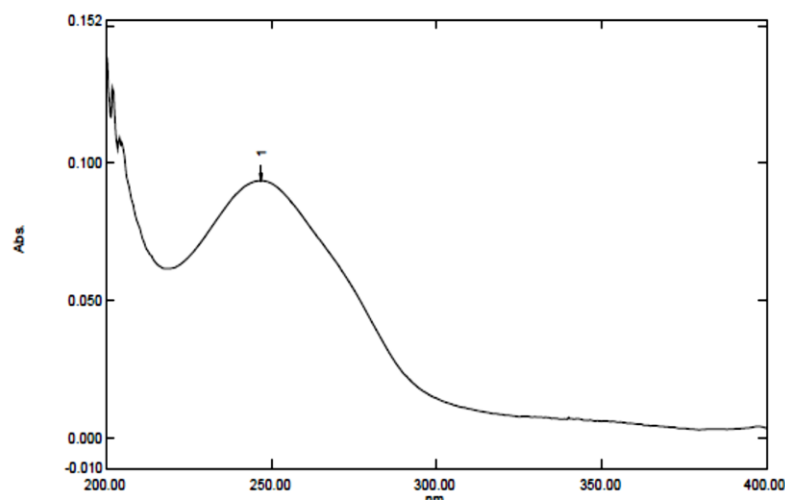


(a)



(b)

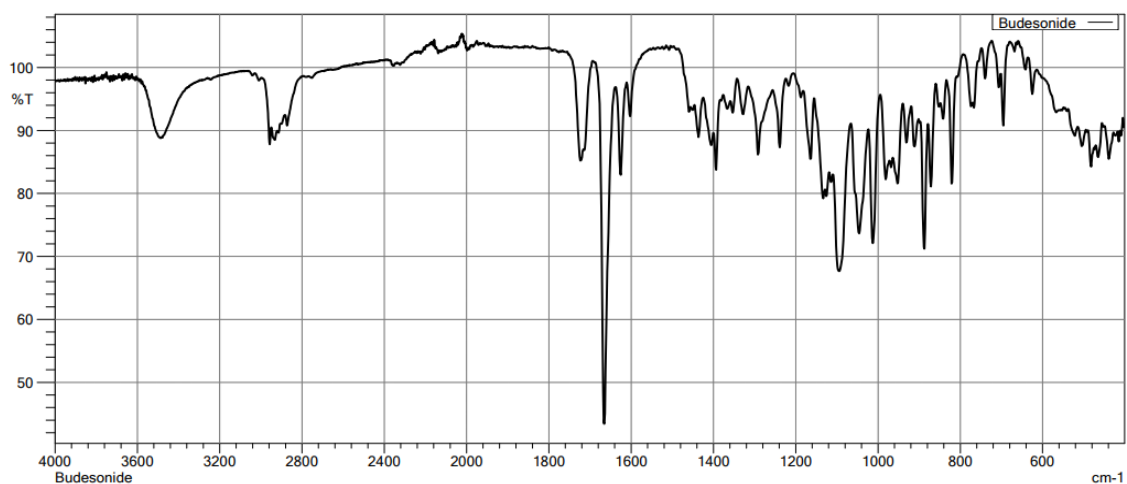
Figure 4.1: FTIR spectra of budesonide (a) observed (b) Reported in Indian pharmacopeia 2010

Figure 4.2: UV scanning of the Budesonide (λ_{max} -244)

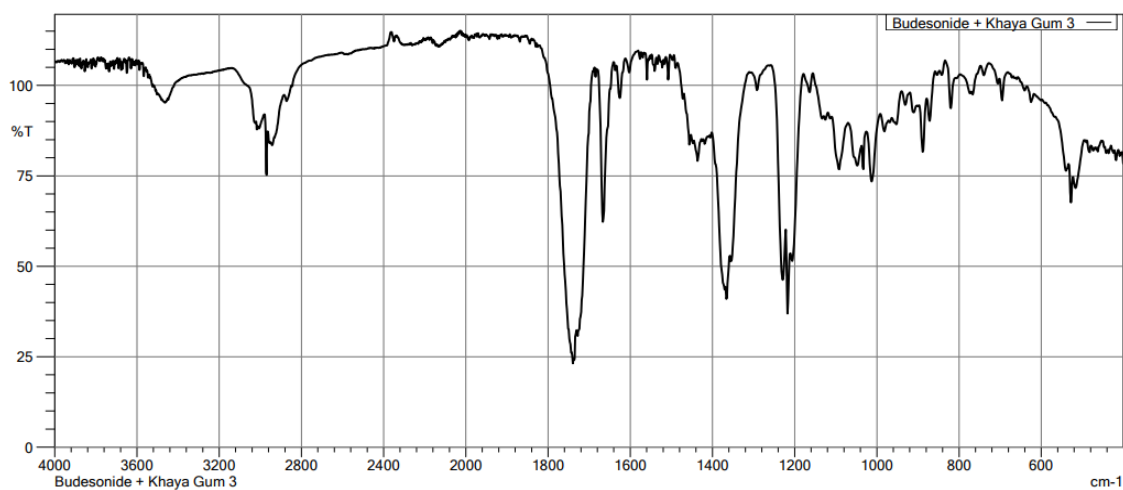
4.3.2 Drug – Excipient compatibility study

In the FTIR Spectra of plain drug and with polymer mixtures for drug excipient compatibility studies were reflected in Figure 4.3, 4.4, 4.5, and 4.6.

The peaks of functional groups such as O-H stretching, C-H aromatic stretching, C=C aromatic stretching, O-H stretching of carboxyl, C=O stretching of carboxyl and N-H bending of amine were determined

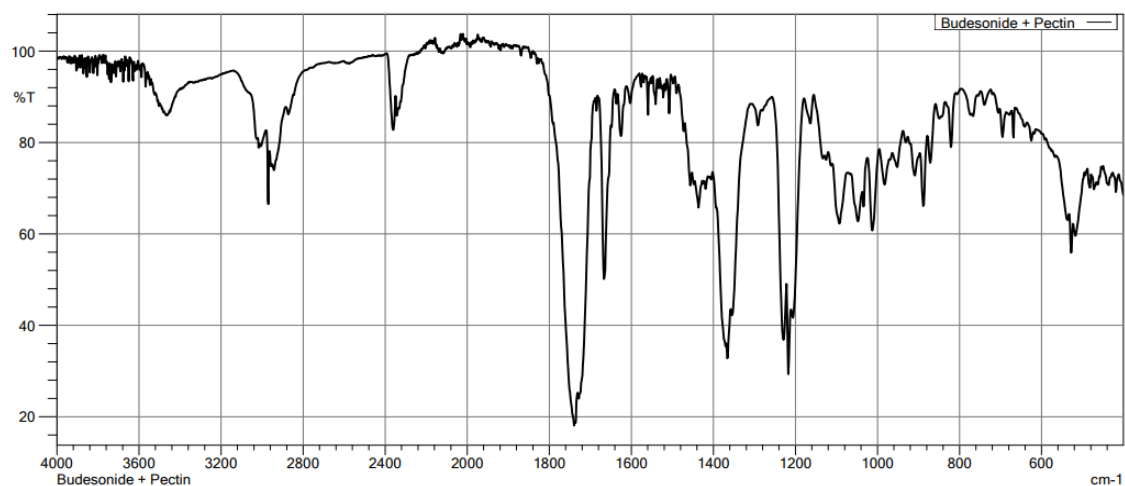


(a)

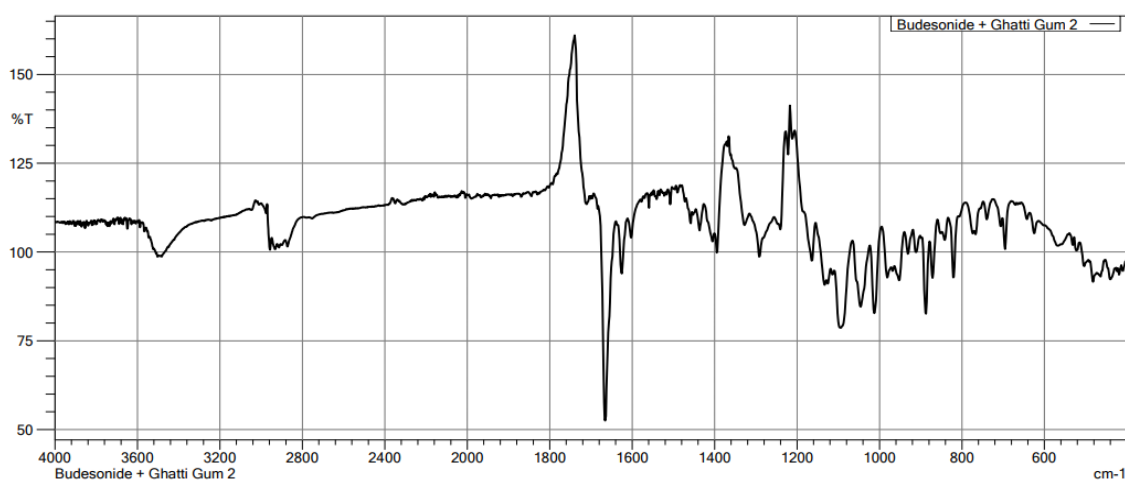


(b)

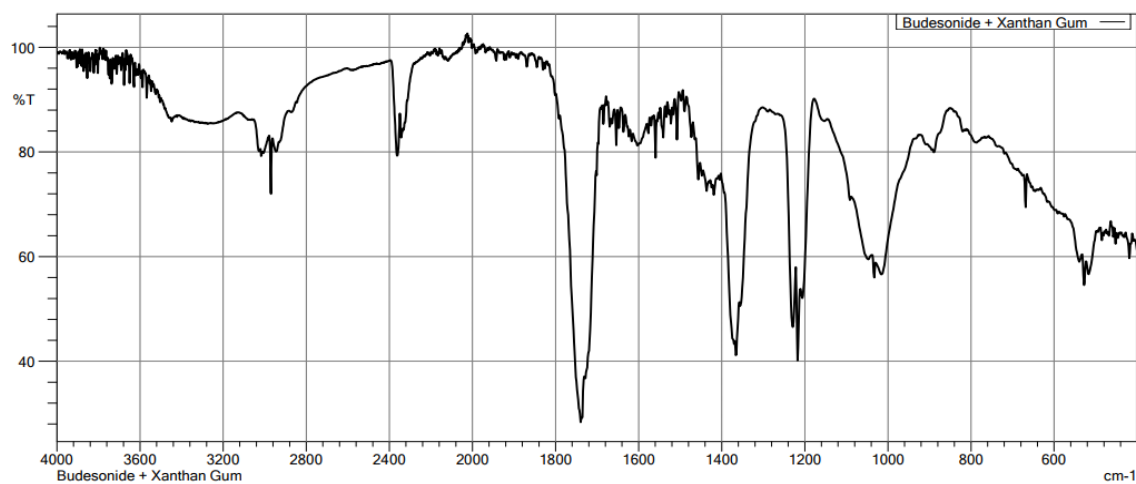
Figure 4.3 FTIR spectra of (a) budesonide (b) Budesonide + Khaya gum



(a)

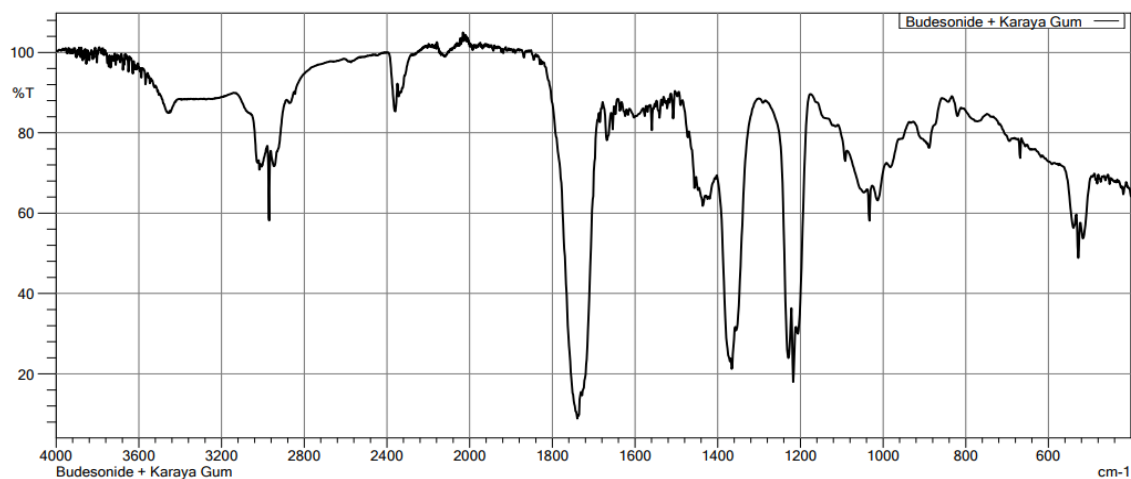


(b)

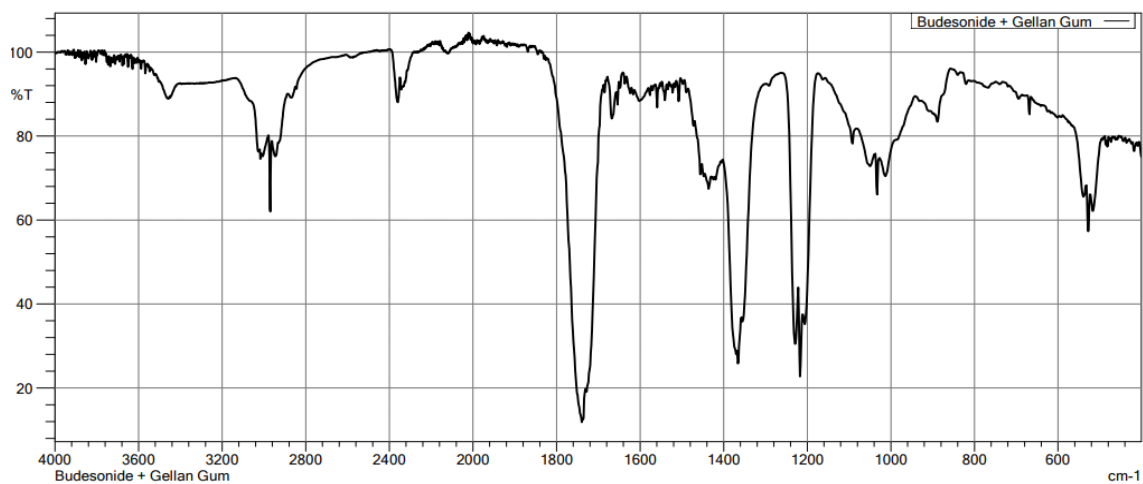


(c)

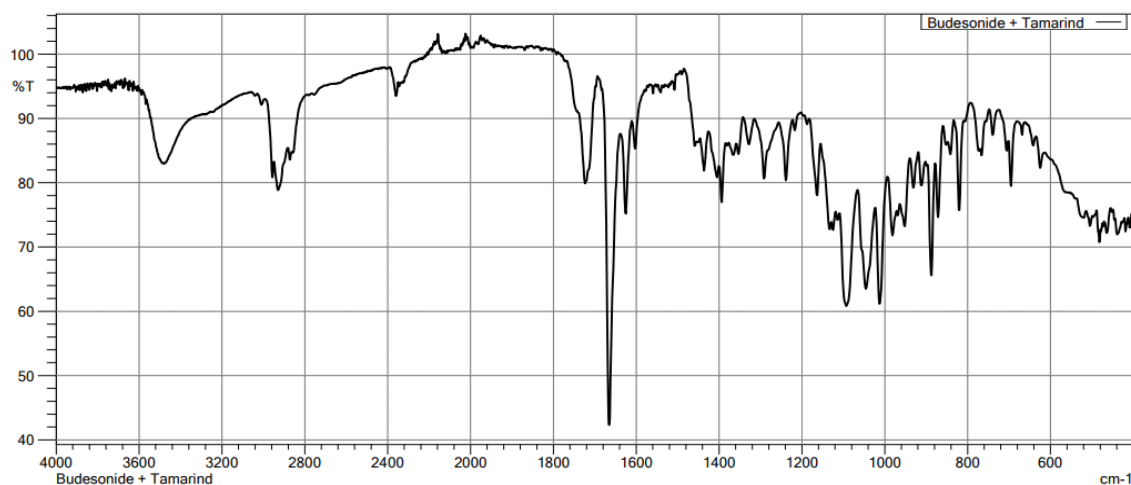
Figure 4.4: FTIR spectra of budesonide +(a) Pectin gum(b)Ghatti gum(c) Xanthan gum



(a)

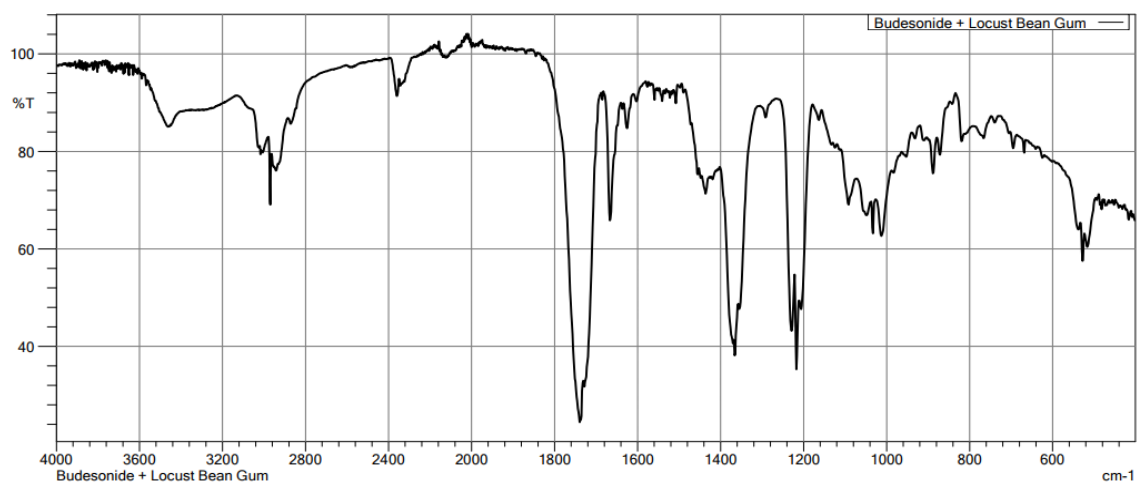


(b)

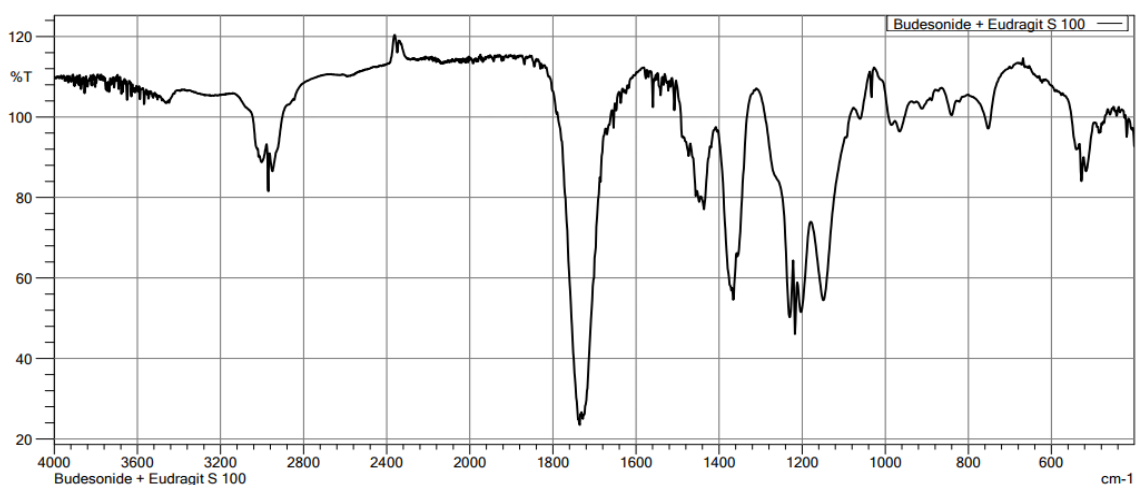


(c)

Figure 4.5: FTIR spectra of budesonide + (a) Karaya (b) Gellan (c) Tamarind gum



(a)



(b)

Figure 4.6: FTIR spectra of budesonide + (a) Locust Bean gum (b) Eudragit S 100

Table 4.4: FTIR characted peaks for drug and its mixtures with polymers

Sr. No	Functional Group	O-H stretching vibration	C-H stretching	C-O stretching	C=O Carbonyl group
1	Budesonide	3471.87	2933.73	1097.50	1666.50
2	Budesonide + Khaya gum	3480.00	2956.87	1093.64	1666.50
3	Budesonide + Pectin gum	3482.15	2969.98	1093.00	1666.68
4	Budesonide + Ghatti gum	3487.87	2875.86	1012.63	1666.50

5	Budesonide + Xanthan gum	3446.38	2945.66	1015.74	1669.54
6	Budesonide + Karaya gum	3481.51	2955.87	1091.71	1666.50
7	Budesonide + Gellan gum	3462.12	2947.09	1093.00	1668.11
8	Budesonide + Tamarind gum	3271.27	2931.80	1085.92	1666.50
9	Budesonide + Locust bean gum	3462.22	2955.87	1089.78	1666.50
10	Budesonide + eudragit s 100	3448.2	2885.51	1095.57	1627.92

The characteristics band were observed at 3471 cm⁻¹ (O-H stretching), 2933 cm⁻¹ (C-H stretching), and 1697 cm⁻¹ (C=O) for pure drug and same also were reflected in drug-excipient mixture as shown in Table 4.4 [21]. This eventually resulted in the conclusion that there was no interaction between the drug and the selected polymers.

4.3.3 Standard Calibration Curve of Budesonide in 0.1N HCl, Phosphate Buffer pH 7.4 & 6.8

A budesonide calibration curve was generated at 242 nm in 0.1 N HCl, representing a concentration range of 4-16 µg/ml. In Figure 4.7, the calibration curve is depicted. The calibration data that was acquired is presented in Table 4.5. The regression analysis was conducted, and the correlation coefficient for the calibration curve was calculated to be 0.9961.

Equation for the calibration curve in 0.1 N HCl is $Y = 0.05225 \cdot X + 0.018$

Table 4.5: standard calibration curve of Budesonide in 0.1 N HCl

0.1 N HCl (λ_{\max} = 242 nm)	
Concentration	Absorbance
0	0
4	0.24 ± 0.03
8	0.44 ± 0.05

12	0.67 ± 0.04
16	0.83 ± 0.06

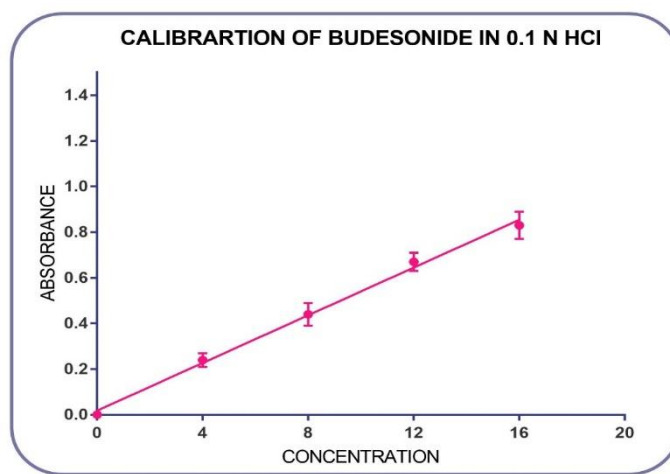
(*n=3, Mean \pm SD)

Figure 4.7: Standard calibration curve of Budesonide in 0.1 N HCl

A budesonide calibration curve was generated at 244 nm in phosphate buffer with a pH of 7.4, representing a concentration range of 4 to 16 $\mu\text{g/ml}$. For the calibration curve, see Fig. 4.8. The calibration data that was acquired is presented in Table 4.6. The regression analysis was conducted, and the correlation coefficient for the calibration curve was calculated to be 0.9952.

Equation for the calibration curve in Phosphate buffer pH 7.4 is $Y = 0.06375 \cdot X + 0.01$

Table 4.6: standard calibration curve f Budesonide in Phosphate buffer pH 7.4

Phosphate Buffer pH 7.4 ($\lambda_{\text{max}} = 244 \text{ nm}$)	
Concentration	Absorbance
0	0
4	0.28 ± 0.030
8	0.54 ± 0.050
12	0.73 ± 0.040
16	1.05 ± 0.060

(*n=3, Mean \pm SD)

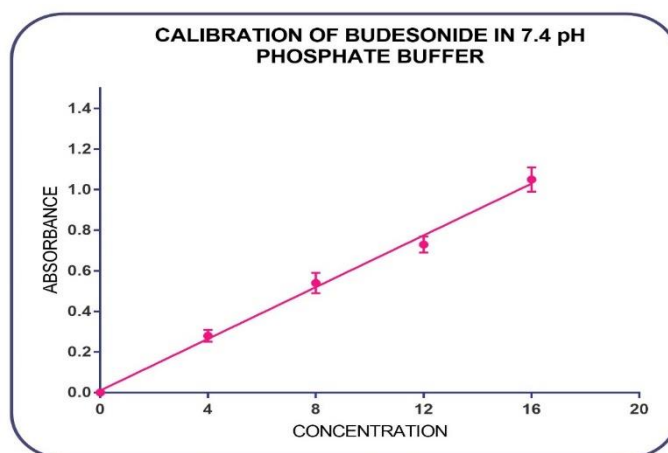


Figure 4.8: Standard calibration curve of Budesonide in Phosphate buffer pH 7.4

A budesonide calibration curve was generated at 244 nm in phosphate buffer with a pH of 6.8, representing a concentration range of 4 to 16 µg/ml. For the calibration curve, observe Fig. 4.9. The calibration data that was acquired is presented in Table 4.7. The regression analysis was conducted, and the correlation coefficient for the calibration curve was calculated to be 0.9955.

Equation for the calibration curve in Phosphate buffer pH 7.4 is $Y = 0.07425 \cdot X + 0.022$

Table 4.7: standard calibration curve of Budesonide in Phosphate buffer pH 6.8

Phosphate Buffer pH 6.8 ($\lambda_{\text{max}} = 244 \text{ nm}$)	
Concentration	Absorbance
0	0
4	0.32 ± 0.070
8	0.67 ± 0.090
12	0.89 ± 0.060
16	1.2 ± 0.080

(*n=3, Mean±SD)

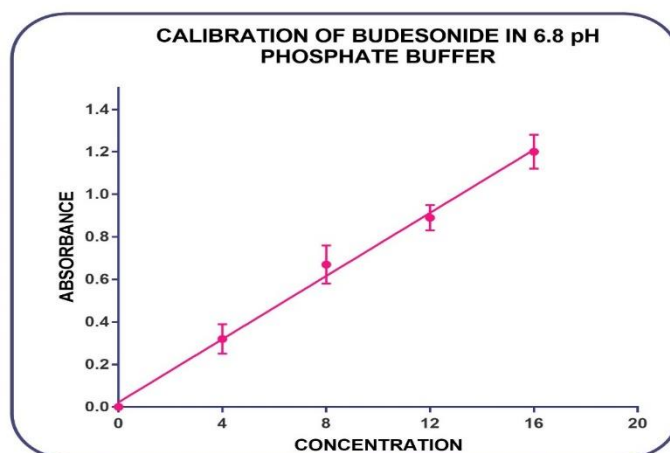


Figure 4.9: Standard calibration curve of Budesonide in Phosphate buffer pH 6.8

4.3.4 Screening of Natural Gums:

The determination of the appropriateness of natural gums for drug delivery applications is heavily influenced by their susceptibility to enzymatic degradation. In the present investigation, viscosity profiles were employed to assess the capacity of different natural gums in extending drug release within the upper gastrointestinal (GI) tract. The viscosity profiles of various natural gums were examined by measuring and analysing 1% solutions of these gums in a phosphate buffer with a pH of 6.8. The results indicated notable differences in viscosity among the tested natural gums are shown in Table 4.8 and Figure 4.10.

Table 4.8: Viscosity profile of 1 % solution of different gums

Name of polysaccharides	Viscosity Profile (cps) (mean \pm SD)
Khaya gum	20 \pm 0.6
Pectin gum	98 \pm 7
Gum ghatti	206 \pm 15.8
Xanthan gum	1730 \pm 36
Karaya gum	2400 \pm 54
Gellan gum	7440 \pm 86
Tamarind gum	8500 \pm 112
Locust bean gum	8700 \pm 138

(*n=3, Mean \pm SD)

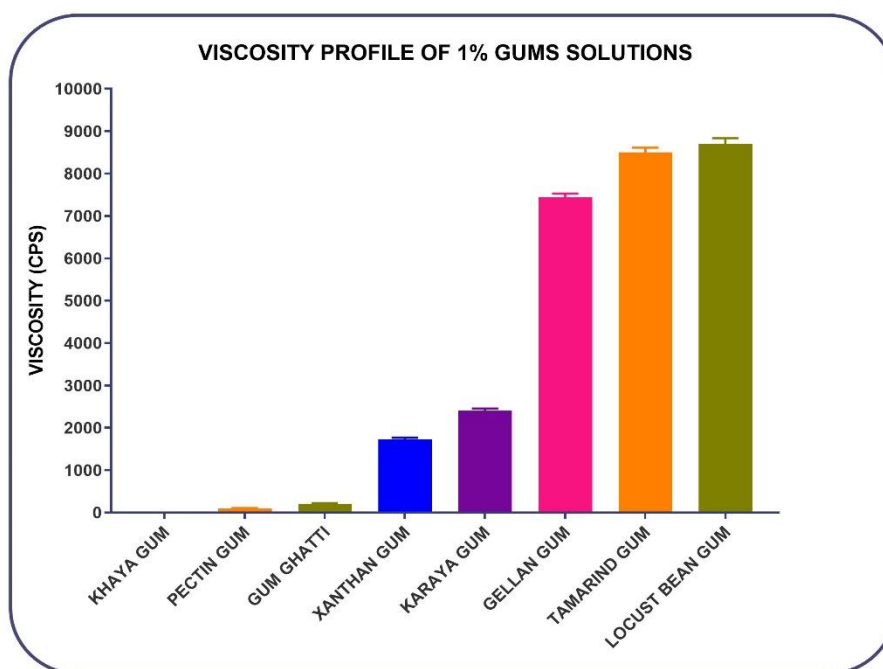


Figure 4.10: Viscosity profile of 1 % solution of different gums in Phosphate buffer pH 6.8.

Statistically significant viscosity profiles were observed in gellan gum, tamarind gum, locust bean gum, and karaya gum, among the screened natural gums. This suggests that these gums have the potential to effectively achieve the desired lag time for prolonged drug release because of dense crosslinking among the chains[18, 22]. The gums exhibited favourable viscosity properties, indicating their potential for use in the development of drug delivery systems intended to prolonged drug release in the upper gastrointestinal tract.

In order to evaluate the enzymatic vulnerability of the chosen natural gums, a viscometry technique was utilized that quantifies the degree of enzymatic degradation of polysaccharides using suitable enzymes which mimic gastric environment. This methodology offers significant insights into the influence of enzymes on the relaxation and depolymerization of polymer chains, presenting a direct and pertinent approach to investigating the effects of degrading enzymes on dispersions of polysaccharides[14].

Enzymatic degradation of polysaccharides can occur via two distinct mechanisms: terminal cleavage, which involves breaking the polysaccharide at its ends, and random cleavage, which involves breaking the polysaccharide at various points throughout its structure. The process of degradation can lead to the liberation of diverse substances, such as glucose and other metabolites, which can be utilized by the microorganisms present in the colon[13].

It is widely recognized that there exists a direct relationship between the viscosity of linear polymers and their molecular weight[15]. During the process of degradation, the polymer's viscosity experiences a significant decrease when the internal glycosidic bonds are

cleaved[23]. Conversely, in the case of terminal degradation, the viscosity either remains relatively stable or exhibits a gradual decrease. Hence, through the observation of alterations in viscosity, it becomes possible to deduce the specific enzymatic degradation process taking place in the natural gums.

The enzymatic degradation of polysaccharides in the colon is a multifaceted process[24]. The diversity of enzymes necessary for the breakdown of a polysaccharide is contingent upon its structural composition and level of complexity. The complete digestion of linear polysaccharides, even those composed of a single component, often necessitates the involvement of multiple enzymes[25].

A comparative investigation was carried out to assess the impact of enzymes obtained from rat cecal content and probiotic media on the viscosity of natural gum samples. Both enzyme systems exhibited the capacity to degrade natural gums by randomly breaking the polysaccharide bonds[26]. Initially, enzymatic degradation of gum solutions of tamarind gum and locust bean gum were evaluated using the different volume of probiotic medium which are shown in Figure 4.11.

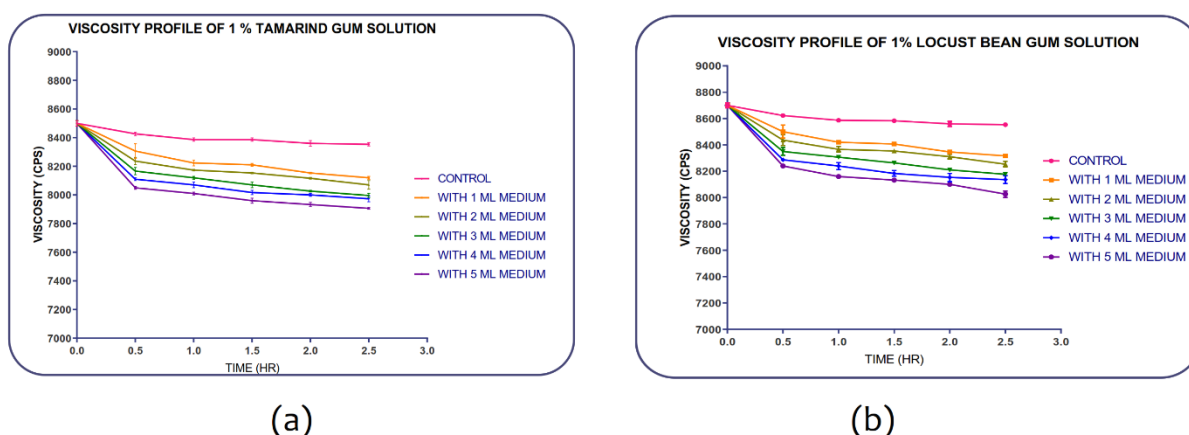


Figure 4.11: Enzymatic degradation of gums in presence of probiotic culture medium (a) Tamarind gum (b) Locust bean gum without CO₂ aeration

Based on the observed data, it was determined that there was a substantial degradation of the chain during the initial time period. However, subsequent analysis revealed that there was no notable decrease in viscosity, suggesting a decline in enzyme secretion due to the mortality of microorganisms that can only thrive in anaerobic conditions. Because of that reason, subsequent study was carried out with CO₂ aeration which was achieved by using INSTA 95g CO₂ Disposable Supply set, which is generally used for the aeration in aquarium.

Figure 4.12 depicts the enzymatic breakdown of natural gums in the presence of 4% rat cecal content and different volumes of probiotic culture medium.

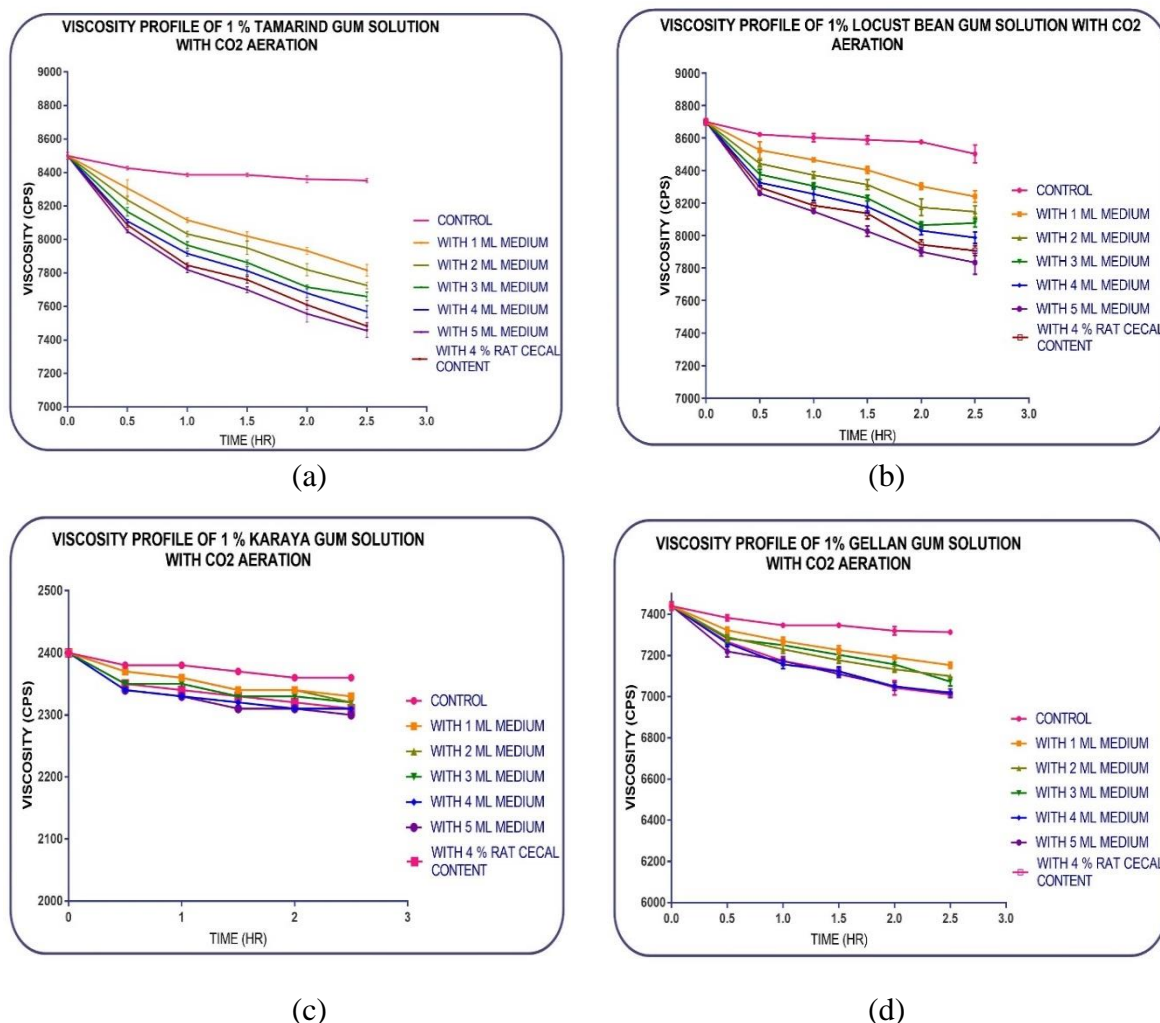


Figure 4.12: Enzymatic degradation of Natural gums in presence of 4 % rat cecal content and probiotic culture with respect to time (a) Tamarind gum (b) Locust bean gum (c) Karaya Gum (d) Gellan gum

The findings suggest that tamarind gum and locust bean gum demonstrated a comparatively greater susceptibility to secreted enzymes produced by the intestinal microflora in comparison to the remaining two gums. Based on the available data, it was observed that the response of 4 % rat cecal content exhibited a range between 4 ml and 5 ml of probiotic culture medium. This suggests that a probiotic culture medium with a volume of 4.5 ml produces a significant effect comparable to that of a 4 % concentration of rat cecal content, which has been previously established as a reliable mimic of the colonic environment according to existing literature[13, 27, 28].

The results of this study suggest that tamarind gum exhibits potential for the targeted delivery of drugs to the colon, as it possesses characteristics such as sustained release and susceptibility to enzymatic degradation.

4.4 References:

1. Hadi, M., Rao, N., & Rao, A. (2014). Formulation and Evaluation of pH-Responsive Mini-Tablets for Ileo-Colonic Targeted Drug Delivery. *Tropical Journal of Pharmaceutical Research*, 13(7), 1021. <https://doi.org/10.4314/tjpr.v13i7.3>
2. Buckton, G. (2011). Physical characterization of drugs and excipients. *Journal of Pharmacy and Pharmacology*, 50(Supplement_9), 60–60. <https://doi.org/10.1111/j.2042-7158.1998.tb02260.x>
3. Shah, J. P., Khan, A. I., Maurya, R., & Shukla, A. K. (2019). Formulation development and evaluation of Transfersosomal drug delivery for effective treatment of acne. *Advance Pharmaceutical Journal*, 4(1), 26–34. <https://doi.org/10.31024/apj.2019.4.1.4>
4. Vogel, I. (1989). *No Title. Practical textbook of organic chemistry*. LONGMAN GROUP LIMITED.
5. Aggarwal, A. K., & Singh, S. (2011). Physicochemical characterization and dissolution study of solid dispersions of diacerein with polyethylene glycol 6000. *Drug Development and Industrial Pharmacy*, 37(10), 1181–1191. <https://doi.org/10.3109/03639045.2011.563782>
6. Bandi, N., Wei, W., Roberts, C. B., Kotra, L. P., & Kompella, U. B. (2004). Preparation of budesonide– and indomethacin–hydroxypropyl- β -cyclodextrin (HPBCD) complexes using a single-step, organic-solvent-free supercritical fluid process. *European Journal of Pharmaceutical Sciences*, 23(2), 159–168. <https://doi.org/10.1016/j.ejps.2004.06.007>
7. Salve, P. S. (2011). Development and *in vitro* evaluation colon targeted drug delivery system using natural gums. *Asian Journal of Pharmaceutical Research*, 1(4), 91–101.
8. Mallikarjuna Gouda M, Ramakrishna Shabaraya. A, S. S. ., & Kumar, S. S. S. and P. R. (2011). Development and validation of selective UV spectro- photometric analytical method for budesonide pure sample. *Journal of Applied Pharmaceutical Science*, 1(7), 158–161.
9. Pani, N. R., Nath, L. K., Acharya, S., & Bhuniya, B. (2012). Application of DSC, IST, and FTIR study in the compatibility testing of nateglinide with different pharmaceutical excipients. *Journal of Thermal Analysis and Calorimetry*, 108(1), 219–226. <https://doi.org/10.1007/s10973-011-1299-x>
10. Raghu, M. S., Basavaiah, K., Ramesh, P. J., Abdulrahman, S. A. M., & Vinay, K. B. (2012). Development and validation of a UV-spectrophotometric method for the determination of pheniramine maleate and its stability studies. *Journal of Applied Spectroscopy*, 79(1), 131–138. <https://doi.org/10.1007/s10812-012-9574-6>
11. Patel, D. M., Sardhara, B. M., Thumbadiya, D. H., & Patel, C. N. (2012). Development and validation of spectrophotometric method for simultaneous estimation of paracetamol and lornoxicam in different dissolution media. *Pharmaceutical Methods*, 3(2), 98–101. <https://doi.org/10.4103/2229-4708.103885>
12. Kar, A. K., & Kar, B. (2020). In-Vitro Comparative Dissolution Study of Commercially Available Paracetamol Tablet. *Journal of Drug Delivery and Therapeutics*, 10(1), 18–23. <https://doi.org/10.22270/jddt.v10i1.3817>
13. Zhang, H., & Neau, S. H. (2002). *In vitro* degradation of chitosan by bacterial enzymes from rat cecal and colonic contents. *Biomaterials*, 23(13), 2761–2766. [https://doi.org/10.1016/S0142-9612\(02\)00011-X](https://doi.org/10.1016/S0142-9612(02)00011-X)
14. Zhang, H., Alsarra, I. A., & Neau, S. H. (2002). An *in vitro* evaluation of a chitosan-containing multiparticulate system for macromolecule delivery to the colon. *International Journal of Pharmaceutics*, 239(1–2), 197–205. [https://doi.org/10.1016/S0378-5173\(02\)00112-6](https://doi.org/10.1016/S0378-5173(02)00112-6)
15. Garcia-Ochoa, F., & Casas, J. A. (1992). Viscosity of locust bean (*Ceratonia siliqua*) gum solutions.

- Journal of the Science of Food and Agriculture*, 59(1), 97–100.
<https://doi.org/10.1002/jsfa.2740590114>
16. Turanlı, Y., & Acartürk, F. (2021). Fabrication and characterization of budesonide loaded colon-specific nanofiber drug delivery systems using anionic and cationic polymethacrylate polymers. *Journal of Drug Delivery Science and Technology*, 63, 102511. <https://doi.org/10.1016/j.jddst.2021.102511>
 17. Mishra, M. U., & Khandare, J. N. (2011). Evaluation of tamarind seed polysaccharide as biodegradable carrier for colon specific drug delivery. *International Journal of Pharmacy and Pharmaceutical Sciences*, 3(1), 139–142.
 18. Sirisha, V. N. L., Chinna Eswariah, M., & Sambasiva Rao, A. (2018). A novel approach of locust bean gum microspheres for colonic delivery of mesalamine. *International Journal of Applied Pharmaceutics*, 10(1), 86–93. <https://doi.org/10.22159/ijap.2018v10i1.22638>
 19. Wahlgren, M., Axenstrand, M., Håkansson, Å., Marefati, A., & Lomstein Pedersen, B. (2019). *In Vitro* Methods to Study Colon Release: State of the Art and An Outlook on New Strategies for Better In-Vitro Biorelevant Release Media. *Pharmaceutics*, 11(2), 95. <https://doi.org/10.3390/pharmaceutics11020095>
 20. Stojanov, S., Berlec, A., & Štrukelj, B. (2020). The Influence of Probiotics on the Firmicutes/Bacteroidetes Ratio in the Treatment of Obesity and Inflammatory Bowel disease. *Microorganisms*, 8(11), 1715. <https://doi.org/10.3390/microorganisms8111715>
 21. Bruni, G., Maggi, L., Tammaro, L., Canobbio, A., Di Lorenzo, R., D'aniello, S., ... Marini, A. (2015). Fabrication, Physico-Chemical, and Pharmaceutical Characterization of Budesonide-Loaded Electrospun Fibers for Drug Targeting to the Colon. *Journal of Pharmaceutical Sciences*, 104(11), 3798–3803. <https://doi.org/10.1002/jps.24587>
 22. Chourasia, M. K., & Jain, S. K. (2003). Pharmaceutical approaches to colon targeted drug delivery systems. *Journal of pharmacy & pharmaceutical sciences : a publication of the Canadian Society for Pharmaceutical Sciences, Societe canadienne des sciences pharmaceutiques*, 6(1), 33–66. Retrieved from <http://www.ncbi.nlm.nih.gov/pubmed/12753729>
 23. Visan, A. I., Popescu-Pelin, G., & Socol, G. (2021). Degradation Behavior of Polymers Used as Coating Materials for Drug Delivery—A Basic Review. *Polymers*, 13(8), 1272. <https://doi.org/10.3390/polym13081272>
 24. Tiwari, A., Verma, A., Panda, P. K., Saraf, S., Jain, A., & Jain, S. K. (2019). Stimuli-responsive polysaccharides for colon-targeted drug delivery. In *Stimuli Responsive Polymeric Nanocarriers for Drug Delivery Applications* (pp. 547–566). Elsevier. <https://doi.org/10.1016/B978-0-08-101995-5.00022-2>
 25. Lovegrove, A., Edwards, C. H., De Noni, I., Patel, H., El, S. N., Grassby, T., ... Shewry, P. R. (2017). Role of polysaccharides in food, digestion, and health. *Critical Reviews in Food Science and Nutrition*, 57(2), 237–253. <https://doi.org/10.1080/10408398.2014.939263>
 26. DHAWALE, S. C., DIAS, R. J., HAVALDAR, V. D., KAVITAKE, P. R., & MALI, K. K. (2017). Interpenetrating networks of carboxymethyl tamarind gum and chitosan for sustained delivery of aceclofenac. *Marmara Pharmaceutical Journal*, 21(4), 771–782. <https://doi.org/10.12991/mpj.2017.20>
 27. Patel, N., Patel, J., & Shah, S. (2010). Box-Behnken experimental design in the development of pectin-compritol ATO 888 compression coated colon targeted drug delivery of mesalamine. *Acta Pharmaceutica*, 60(1), 39–54. <https://doi.org/10.2478/v10007-010-0008-9>
 28. Prabhu, P., Ahamed, N., Matapady, H. N., Ahmed, M. G., Narayanacharyulu, R., Satyanarayana, D., & Subrahmanayam, E. (2010). Investigation and comparison of colon specificity of novel polymer khaya gum with guar gum. *Pakistan journal of pharmaceutical sciences*, 23(3), 259–65. Retrieved from <http://www.ncbi.nlm.nih.gov/pubmed/20566437>

CHAPTER 5

**Colon Targeted
Tablet dosage form**

CHAPTER 5

5. Colon Targeted Tablet dosage form

5.1 Experimental Methods

5.1.1 Precompression parameters

The following pre compression parameters were performed for lubricated powder mass and for lubricated granule mass of the Preliminary batches.

5.1.1.2: Bulk density

The powder mass being evaluated was passed through sieve no. 40, while the granule sample was passed through sieve no. 18. A 25 g sample was precisely weighed and transferred to a 100 ml graduated cylinder. The powder was levelled, and the unsettled volume, denoted as V_o , was recorded. The calculation of bulk density was performed using the formula.[1, 2]

$$\text{Bulk density } (\rho_o) = M/V_o$$

Where, M = Powder Mass

V_o = Unsettled volume

5.1.1.2: Tapped density

The powder sample that was being evaluated was passed through sieve no. 40, while the granule sample was passed through sieve no. 18. A 25g portion of the sample was then transferred into a 100 ml graduated cylinder. The cylinder was mechanically tapped 100 times with a Tapped Density Tester (Mfg: Singhala Scientific, Ambala) at a nominal rate of 50 drops per minute; the volume tapped, denoted as V_o , was recorded. As further tapping continued for an additional 50 times, the tapped volume V_b was recorded. Since the difference between two volumes that were tapped was below 2%, V_b was regarded as an equivalent tapped volume V_f . [3]

The tapped density was determined with the help of the formula.

$$\text{Tapped density } (\rho_t) = M / V_f$$

Where, M = Powder Mass

V_f = Tapped volume

5.1.1.3 Compressibility Index

Volumes of bulk and tapped were determined, and the compressibility index was computed utilizing the formula[3].

$$\text{Compressibility index} = \frac{100(V_o - V_f)}{V_o}$$

Where, V_o = Bulk volume

V_f = Tapped volume

5.1.1.4 Hausner ratio

Hausner discovered that the ratio $\rho_t/\rho_{\text{bulk}}$ was predictive of powder flow properties due to its correlation with interparticle friction.

The author demonstrated that powders characterized by low interparticle friction, like coarse spheres, possessed ratios of around 1.2.

Conversely, powders with higher cohesion and reduced mobility, like grains, exhibited values exceeding 1.6[1]

$$\text{Hausner's Ratio} = \rho_t / \rho_{\text{bulk}}$$

Where, ρ_{bulk} = Density of bulk

ρ_t = Density of tapped volume

5.1.1.5 Angle of Repose

The angle of repose is conceptualized as the greatest conceivable angle formed by the particle pile's surface and the horizontal plane. Utilizing the fixed funnel method, the angle of repose of the powder or granules was ascertained.

In order to evaluate the flow characteristics of the powder granules, the funnel's height was modified to the point where its tip just touched the apex of the powder or granules heap positioned to a sheet of paper laid out on a horizontal plane. The powder combination was measured and weighed precisely in a beaker. The substance was permitted to readily flow through the funnel onto the paper's surface, accumulating in the shape of a cone. The height (h) of the mound and the diameter (d) of the cone were recorded. In order to determine the radius (r), the diameter was used.

The angle of repose (θ) was determined by employing the formula provided below:[2]

$$\Theta = \tan^{-1} (h/r)$$

5.1.2 Preliminary batches of Tablets by Direct Compression method and wet granulation

For preliminary assessment, the measured amount of budesonide and all other excipients were passed via sieve number 60. PVP K 30 was utilized as a binder for both direct compression and wet granulation methods. The drug and excipients were thoroughly blended with talc and magnesium stearate for lubrication and to improve the flow properties of the powder mass. Using an 8/32" flat punch, a weighed amount of powder mass was compressed using a rotating tablet compression machine (12 station D tooling, Model No- PR-TCM-007, Mfg.: Karnavati Engineering, Ahmedabad, India).

Total 50 tablets were compressed per batch and the composition of the preliminary batches of tablets is reflected in Table 5.1. Table 5.2 displays the preliminary batches of tablets prepared with tamarind gum and carboxymethyl tamarind gum (CM tamarind gum) using PVP K 30 as a binder in wet granulation with water or isopropyl alcohol (IPA) as a bridging agent[4].

Table 5.1: Composition of Tablets for Preliminary formulation.

Ingredients	TD1 (mg)	TD2 (mg)	TD3 (mg)	TD4 (mg)	TW1 (mg)	TW2 (mg)	TW3 (mg)	TW4 (mg)
Budesonide	9	9	9	9	9	9	9	9
Tamarind gum	50	75	100	125	50	75	100	125
Lactose	125	100	75	50	125	100	75	50
PVP K30	10	10	10	10	10	10	10	10
Talc	4	4	4	4	4	4	4	4
Mg. Stearate	2	2	2	2	2	2	2	2
Total	200	200	200	200	200	200	200	200

* TD batches Prepared by Direct Compression

* TW Batches Prepared by Wet Granulation (PVP K30 in IPA as binder)

Table 5.2: Tablets prepared by PVP K 30 in IPA and water using tamarind gum and CM tamarind gum

Ingredients	IPA as bridging agent (Batch A)	Water as bridging agent (Batch B)	IPA as bridging agent (Batch C)	Water as bridging agent (Batch D)
Budesonide	9	9	9	9
Tamarind Gum	100	100	-	-
CM Tamarind Gum	-	-	100	100
Lactose	75	75	75	75
PVP K30	10	10	10	10
Talc	4	4	4	4
Mg. Stearate	2	2	2	2
Total	200	200	200	200

5.1.3 Post compression parameters for uncoated tablets dosage form

5.1.3.1 Weight Variation test

A total of twenty tablets were selected at random from each batch and weighed individually. The calculation was performed on the mean and standard deviation of twenty tablets' weights. The batch satisfies the weight variation test if no more than two samples of tablet weights deviate from the mean weight by an amount greater than the percentage specified in Table 5.3, and none of the samples deviate by more than twice the percentage shown in Table 5.3[2].

Table 5.3: Weight variation limit as per IP

Weight of tablet (Average) (X mg)	Percentage deviation
$X \leq 80 \text{ mg}$	10
$80 < X < 250 \text{ mg}$	7.5
$X \geq 250 \text{ mg}$	5

5.1.3.2 Friability

Friability denotes the degree to which a tablet is resistant to abrasion.

Utilising this measurement, one can ascertain the tablet's resistance to abrasion throughout the processes of handling, coating, packaging, and transportation.

The tablets are subjected to a combination of abrasion and stress in this apparatus through the use of a plastic chamber that rotates at a speed of 25 revolutions per minute. With each revolution, the tablets descend from a height of 6 inches. Twenty precisely weighed tablets were placed in the Roche friabilator for four minutes or one hundred revolutions before being removed, dedusted, and reweighed. The percentage of friability was computed utilising the formula[2].

$$\% F = \left\{ 1 - \left(\frac{W}{W_0} \right) \right\} \times 100$$

Where, % F = Friability in %

W₀ = Initial weight of the tablet W = Weight of tablets after test

5.1.3.3 Hardness

Tablets require a specific degree of rigidity or strength to endure the mechanical stresses associated with their production, packaging, and transportation. The definition of tablet hardness is the amount of force necessary to fracture a tablet during a diametric compressive test. All formulations' tablet hardness was evaluated employing a Monsanto hardness tester[1].

5.1.3.4 Thickness

The control of tablet thickness is a critical parameter in order to facilitate the packaging process. Tablet thickness exhibits variation in response to changes in die fill, particle size distribution, and packaging of the compressed particle mix, while thickness remains constant in response to changes in compressive load[2].

A thickness measurement was performed on three samples that were selected at random from each batch using a digital vernier calliper.

5.1.3.5 % Assay (Drug Content)

The drug percentage was determined by weighing and powdering twenty tablets. A precise volume of the powder, which corresponds to 10 mg of budesonide, was dispensed into 100 mL volumetric containers containing 50 mL of phosphate buffer with a pH of 7.4. Stirring the containers facilitated the solubilization of the drug. The volume was brought to 100 mL with the buffer, thoroughly mixed, and allowed to stand for 24 hours to assure complete drug solubility. Following filtration, 1 mL of the filtrate liquid was diluted appropriately and subjected to spectrophotometric analysis at 244 nm for the determination of budesonide content[5].

5.1.4 Coating of Tablets

5.1.4.1 Method of preparation of coating solution

Weighed quantity of polymer was dissolved in solvent in which good solubility by keeping it on magnetic stirrer at 50 rpm. After the complete solubilization of polymer, plasticizer (10 % of dry polymer weight) was added in the solution while stirring and later talc, titanium dioxide and colour were passed through 100 # sieve before use. The solution was filtered before use. The compositions of coating solution are given Table 5.4 [6].

Table 5.4: compositions of coating solution

Ingredients	Quantity for 100 ml
Eugragit S100	5 gm
Tri Ethyl Citrate	0.625 gm (12.5% w/w)
Talc (% w/v)	1%
TiO ₂ (% w/v)	0.5 %
Color	q.s
Acetone: IPA	50: 50 (100 mL)

Initially, the required quantities of tablets and some extra tablets were deposited in the coating pan and rotated at a speed of 40 revolutions per minute for five minutes. The tablets were then de-dusted, and a specific quantity of tablets were loaded for coating in coating pan as shown in figure 5.1. Previously optimized Process parameters for the coating of tablet dosage form are provided in the Table 5.5.

Table 5.5: Process parameters Fixed for coating of Tablets

Parameter	Condition
Inlet temperature (°C)	50-55
Spray rate (mL min ⁻¹)	0.7
Atomizing air (bar)	2
Pan speed (rpm)	35-40
Gun to Bed Distance	30 cm

The rotation speed of the coating pan (Model- CMTAC-1, Mfg: Cronimach Machinery, Ahmedabad) was then adjusted to 40 revolutions per minute, and the temperature was set to 50°C. Using a peristaltic pump, the previously optimize discharge rate was adjusted to obtain the desired coating. The process of coating tablets continued until the desired weight gain percentage was achieved.[7]



Figure 5.1: Coating pan assembly for coating of tablet dosage form.

5.1.5 Designing the Formulations by using Box-Behnken factorial design

Tablet dosage forms for colonic delivery were optimized using Box-Behnken design (Design Expert 11.0), containing the three-factor, three-level model to define main, interaction, and quadratic effects[8, 9] of independent variables like amount of CM Tamarind Gum, % water proportion, and % weight gain by Eudragit S100 on the selected responses (dependent variables), which were % drug release at 2 hours, % drug release at 5 hours and % drug release at 8 hours as shown in Table 5.6, and batches designed by Box-Behnken design as shown in Table 5.7 and 5.8.

Table 5.6: Independent variables and Dependent variables of Box Behnken design

Independent variables	levels			Dependent variables
	-1	0	+1	
X1=Amount of CM Tamarind Gum	75	100	125	Y_2 = % CDR at 2 Hours
X2= % Water Proportion	0	50	100	Y_5 = % CDR at 5 Hours
X3=% wt. Gain by Eudragit S100	2.5	5	7.5	Y_8 = % CDR at 8 Hours

Table 5.7: Formulation batches (F1 to F8) as per the Box Behnken Design

Ingredients	F1	F2	F3	F4	F5	F6	F7	F8
Budesonide (mg)	9	9	9	9	9	9	9	9
CM Tamarind Gum (mg)	100	100	125	125	75	100	100	100
Lactose (mg)	75	75	50	50	100	75	75	75
PVP K30 (mg)	10	10	10	10	10	10	10	10
Water: IPA Proportion	100:0	0:100	50:50	0:100	50:50	100:0	0:100	50:50
Talc (mg)	4	4	4	4	4	4	4	4
Mg. Stearate (mg)	2	2	2	2	2	2	2	2
Coating of tablet dosage form								
% Weight Gain	7.5	2.5	7.5	5	2.5	2.5	7.5	5

Table 5.8: Formulation batches (F1 to F8) as per the Box Behnken Design

Ingredients	F9	F10	F11	F12	F13	F14	F15
Budesonide (mg)	9	9	9	9	9	9	9
CM Tamarind Gum (mg)	75	100	75	75	125	125	100
Lactose (mg)	100	75	100	100	50	50	75
PVP K30 (mg)	10	10	10	10	10	10	10
Water: IPA Proportion	50:50	50:50	100:0	0:100	50:50	100:0	50:50
Talc (mg)	4	4	4	4	4	4	4
Mg. Stearate (mg)	2	2	2	2	2	2	2
Coating of tablet dosage form							
% Weight Gain	7.5	5	5	5	2.5	5	5

5.1.6 Dissolution Method

In-vitro drug release of colon-specific budesonide tablet was conducted in a USP Type II (Paddle) apparatus (VDA-8D (ARM) station unit, Veego Instruments Corporation, Mumbai, Maharashtra, India) at a rotation speed of 50 rpm and at $37 \pm 0.5^\circ\text{C}$. Initially, the test was done in 0.1 N HCl for 2 hours to mimic the environment of stomach[10]. The test was then conducted for three hours in phosphate buffer pH 7.4, which mimics the milieu of the small intestine[10]. Actually, the small intestine is divided into three sections: the duodenum (pH 5 to 6), the jejunum ($\text{pH } 6.63 \pm 0.53$), and the ileum ($\text{pH } 7.49 \pm 0.46$). The ileum is the longest section of the small intestine, and as a result, its mean pH is 7.3 ± 0.34 [11, 12]. The remaining investigation was conducted in biorelevant medium with a pH of 6.8, which is comparable to the mean pH of the large intestine (6.63 ± 0.04)[11, 12], and CO_2 aeration which was provided with the help of INSTA 95g CO_2 disposable Supply Set (Mfg. : INSTA, Taiwanese brand) shown in Figure 5.2 to provide an environment that is favourable for anaerobic bacteria.[13–15] Samples were collected at regular intervals and analysed spectrophotometrically at a wavelength of 242 nm[16].



Figure 5.2 Dissolution assembly with Insta CO_2 disposable set for creating the anaerobic environment in dissolution medium

5.1.7 Release kinetics of the formulations prepared by the experimental design

Dissolution studies offer valuable insights into the manner in which pharmaceuticals are released, and numerous mathematical kinetic models have been pu

blished to analyse this phenomenon. Several mathematical models are employed to describe drug release, including the Hixon-Crowell model, the Higuchi model, first order kinetics, and zero order kinetics. To interpret the mechanism of drug release, the Korsmeyer-Peppas

model and the Weibull model have been utilised. The kinetic models in question delineate the quantity of drug dissolved (C) from solid dosage form in relation to test time (t), denoted as $C=f(t)$. DD-solver, an Excel add-in, was utilised to ascertain the parameters of the mathematical models in the present study.

5.1.7.1 Zero-order kinetics

This model defines a drug release rate that remains constant irrespective of its concentration. This form of dissolution typically occurs in dosage forms that resist disaggregation and exhibits a delayed rate. Generally, the rate of drug release and the concentration of the drug in the blood remain constant during administration.

$$Q_t = Q_0 + K_0 t$$

Q_t = Amount of drug dissolved in time (t),

Q_0 = Initial amount of drug in the aqueous medium,

K_0 = Constant of zero order.

The cumulative quantity of substance versus time will be represented by a straight line with a K_0 as slope and zero as an intercept.

$$C = K_0 t$$

5.1.7.2 First order kinetics

Drug release from the formulation depends on the concentration of drug remain in the formulation at time t.

$$\frac{Dc}{Dt} = -K_1 C$$

K_1 = First order rate constant

$$\log Q_t = \log Q_0 - \frac{Kt}{2.303}$$

Q_t = Quantity of drug released at time (t)

Q_0 = Initial amount of drug present in formulation,

K = first order rate constant.

A straight-line graph can be generated by plotting the log cumulative % of drug remaining $[\log (Q_0 - Q_t)]$ against time $[t]$. The graph has a slope of $k/2.303$ and an intercept of $\log Q_0$ at $t=0$.

5.1.7.3 Higuchi model

It describes how the proportion of substance released is proportional to the square root of time. Drug release can occur through diffusion and dissolution processes.

Simplifying the equation above gives:

$$Q = K_H \times t^{1/2}$$

$$\frac{Mt}{M_\infty} = K_H \times t^{1/2}$$

M_t = Cumulative amount of drug released at time (t),

M_∞ = Cumulative amount of drug released at time (∞),

K_H = Higuchi constant.

The relationship between cumulative% of drug release (M_t/M_∞) and $t^{1/2}$ is represented by a linear trend with a slope of K_H . The occurrence of a diffusion release mechanism is indicated by a high correlation.

Certain assumptions are made, including the following: the solubility of the drug is less than its initial concentration, ideal sink conditions are maintained, the diffusivity of the drug remains constant, the enlargement of the polymer is negligible, and diffusion takes place in only one dimension (with minimal edge effect).

5.1.7.4 Hixon -Crowell model

The cube root law elucidates the mechanism by which drugs are released from dosage forms in which the surface area and diameter of granules or tablets diminish as a result of erosion. The particle's defined area is directly proportional to the cube root of its volume. This model is applicable to dispersible dosage forms, immediate release dosage forms, and conventional dosage forms. The drug release rate is believed to be constrained by the dissolution rate of the drug particles rather than by diffusion. The established concept was as follows:

$$W_o^{1/3} - W_t^{1/3} = K_{Hc}t$$

W_0 = Initial amount of drug in the dosage form (Drug amount remaining at time 0),

W_t = Quantity of drug present in formulation at time (t),

K_{HC} = Hixon- Crowell constant

The release kinetics can be represented graphically as the cube root of the drug's residual percentage over time.

5.1.7.5 Korsmeyer – Peppas model (Power Law)

The Higuchi plot determines whether a drug release occurred via diffusion, whereas the power law defines the mechanism of drug release. There are two types of drug release: Fickian and non-Fickian diffusion.

$$\frac{Mt}{M_{\infty}} = K_{KP} \times t^n$$

Mt/M_{∞} = Fraction of drug released at time (t)

$$\text{Log} \left(\frac{Mt}{M_{\infty}} \right) = \text{Log} K_{KP} + n \log t$$

M_t = Cumulative drug amount released at (t) time,

M_{∞} = Cumulative drug amount released at time (∞),

K_{KP} = Korsmeyer rate constant,

n = diffusional release exponent.

The relationship between log cumulative% drug release [$\log (Mt/M_{\infty})$] and log time [$\log t$] constitutes a release kinetics graph. The initial sixty percent of drug release data is modelled using the Korsmeyer-Peppas framework. The generic power law equation is typically applicable to short values of time ($Ct/C_{\infty} < 0.6$) and drug release occurs in a one-dimensional manner, among other assumptions.

5.1.7.6 Weibull Model

This has been used in various dosage forms. An empirical model supports it. The equation for it is:

$$\text{Log}[-\ln(1-m)] = \beta \log(t-T_i) - \log \alpha$$

m = amount of drug present formulation,

β = parameter of shape,

α = Parameter of scale,

Ti = Location parameter/ time lag usually zero,

t= Time in hours.

In the Weibull model, the α value represents the apparent rate constant or time scale, whereas the β value defines the curve's shape. When equals 1, the curve is exponential and its kinetics correspond to first order kinetics. A sigmoidal curve is characterised by an increase in the rate of drug release with increasing time ($\beta > 1$), whereas a parabolic curve is denoted by a decrease in the rate of drug release with increasing time. Log time versus log dissolved drug concentration produces a linear graph. β is computed by examining the gradient of the graph at time $t=1$, whereas α is determined by examining the y axis ($1/a$). α may be substituted with the parameter Td. Td is the time required for 63.2% of the substance to be released; it can be calculated from the y axis of $-\ln(1-m) = 1$ using the equation below.

5.1.8 Roentgenography study

The gastrointestinal (GI) transit of specific formulations was assessed through *in vivo* experiments conducted on White New Zealand Rabbits weighing between 1.5 and 2.5 kg.[17]. The Institutional Animal Ethics Committee, L. J. Institute of Pharmacy, LJ University, Ahmedabad, Gujarat, India (Proposal No. LJIP/IAEC/2022-23/02), granted approval for the research. To prepare for the experiment, the rabbits were fasted overnight prior to the administration of Tablets. The Tablet was carefully positioned in the animal's larynx using forceps, and a volume of 10-15 mL of water was administered down the neck to aid its passage into the oesophagus.[18] The same rabbit underwent repeated X-ray examinations at predetermined time intervals to monitor the movement of the formulations through the GI tract[19–21].

5.1.9 Stability Study

In the present study, the optimal batch (F14) from the Box Behnken Design was chosen for the stability study, which was conducted in accordance with ICH guidelines by keeping the sample at 40 ± 2 °C and 75 ± 5 % RH for six months in a stability chamber (Mfg. : Patel Instrument Pvt. Ltd.)[22–24]. The high density Polyethylene bottle is the container closure system used in this study[25]. The selected study intervals were the 1st, 3rd, and 6th months

from the Initial time. The Optimized tablet-based formulation was examined for Appearance (Description), Moisture Content, Drug Content, % CDR at 5th Hours, Friability, and microbial limit test.[26]

5.2. Results and Discussion

5.2.1 Precompression parameters of lubricated powder mass/granules

Precompression parameters of the premixture like powder and granule used for the preparation of preliminary batches were measure and are shown in Table 5.9.

According to the data presented in Table 5.9, it was determined that powder mass has a favourable flow property. Consequently, direct compression was initially favoured for tablet formulation. On the basis of the granule data, it was determined that the flow properties of the granule were excellent.

Table 5.9: Precompression parameters of premixture of Preliminary formulations

Formulation code	Bulk Density	Tapped Density	Compressibility Index	Housner Ratio	Angle of Repose
TD1 (Powder)	0.319±0.05	0.374±0.03	14.71	1.17	32.42±0.66
TD2 (Powder)	0.321±0.03	0.366±0.04	12.30	1.14	32.34±0.51
TD3 (Powder)	0.320±0.04	0.368±0.03	13.04	1.15	34.21±0.51
TD4 (Powder)	0.334±0.05	0.395±0.02	15.44	1.18	31.63±0.63
TW1 (Granule)	0.374±0.03	0.412±0.04	9.22	1.10	23.12±0.62
TW2 (Granule)	0.379±0.03	0.406±0.03	6.65	1.07	29.65±0.57
TW3 (Granule)	0.382±0.04	0.410±0.04	6.83	1.07	28.93±0.62
TW4 (Granule)	0.381±0.02	0.412±0.02	7.52	1.08	27.89±0.69

5.2.2 Post compression parameters of tablet dosage form

Post-compression parameters of the tablet dosage form of preliminary batches were measure and are shown in Table 5.10.

According to the data shown in table 5.10, it was found that the tablets exhibited an average weight of 200 mg and successfully met the criteria for weight variation testing. The hardness of the tablets exhibited a range of values between 4.1 kg/cm² and 4.6 kg/cm², while the friability of the granules varied from 0.08% to 0.80% (w/w). The drug content for all preliminary and experimental batches exhibited a range of percentages between 97.85 and 101.21 percent, with a maximum standard deviation of 1.23 percent.

Table 5.10: Precompression parameters of premixture of Preliminary formulation batches

Formulation code	Uniformity of weight	Friability	Hardness	Thickness	% Assay
TD1 (Powder)	Pass	0.85	4.3	4.11± 0.01	99.35
TD2 (Powder)	Pass	0.71	4.4	4.13±0.03	97.85
TD3 (Powder)	Pass	0.73	4.3	4.12±0.02	99.53
TD4 (Powder)	Pass	0.78	4.4	4.34±0.01	99.13
TW1 (Granule)	Pass	0.69	4.1	4.11±0.01	98.39
TW2 (Granule)	Pass	0.63	4.3	4.13±0.04	99.15
TW3 (Granule)	Pass	0.08	4.6	4.16±0.03	100.35
TW4 (Granule)	Pass	0.72	4.3	4.17±0.01	101.21

5.2.3 In-Vitro release studies

Dissolution data of preliminary batches prepared by direct compression and by wet granulation are shown in Table 5.11 and Table 5.12 respectively. Graphical representation of the dissolution data is reflected in Figure 5.3.

Table 5.11: *In vitro* release data of batches prepared by direct compression

Medium	Time (hour)	Cumulative % Drug Release			
		TD1	TD2	TD3	TD4
0.1 N HCl	1	64.64±3.22	49.56±3.07	44.19±1.69	37.70±1.95
	2	90.90±2.01	78.07±3.23	62.94±2.72	52.06±3.22
7.4 pH Phosphate Buffer	3	99.85±1.07	98.85±0.91	81.19±1.00	73.37±1.75
	4			99.30±0.46	90.92±1.39
	5				99.83±0.45
6.8 pH Phosphate Buffer with 4.5 mL of Culture Medium	6				
	7				
	8				
	9				
	10				

Table 5.12: *In vitro* release data of batches prepared by Wet granulation

Medium	Time (hour)	Cumulative % Drug Release			
		TW1	TW2	TW3	TW4
0.1 N HCl	1	48.18±2.04	38.02±2.53	30.74±2.01	24.74±1.54
	2	75.94±2.81	58.39±1.90	50.91±2.15	36.78±2.56
7.4 pH Phosphate Buffer	3	91.81±1.67	75.37±2.24	69.67±2.71	58.81±3.21
	4	98.81±0.89	92.10±0.43	82.62±3.24	71.37±1.30
	5		99.10±0.34	92.93±2.56	91.59±1.48
6.8 pH Phosphate Buffer with 4.5 mL of Culture Medium	6			99.93±2.01	98.59±0.94
	7				
	8				
	9				
	10				

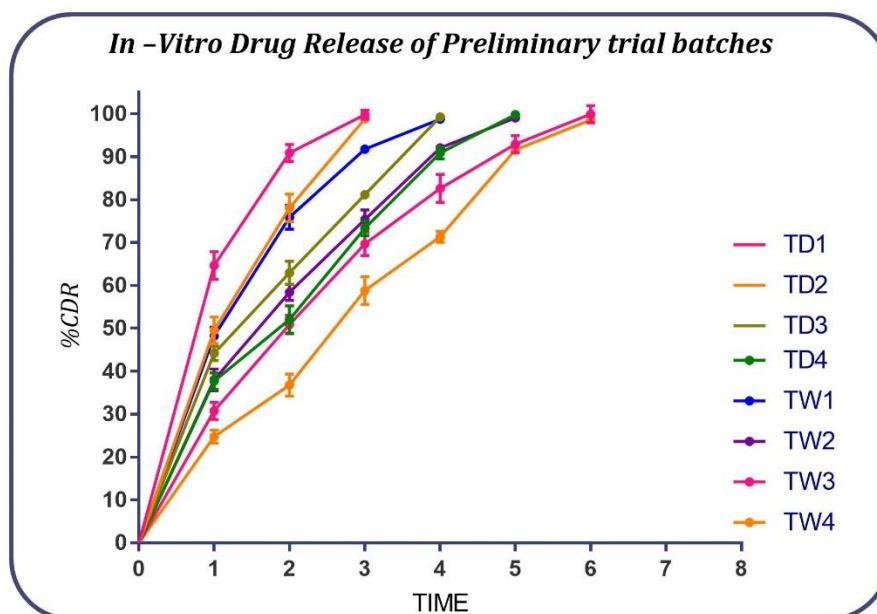


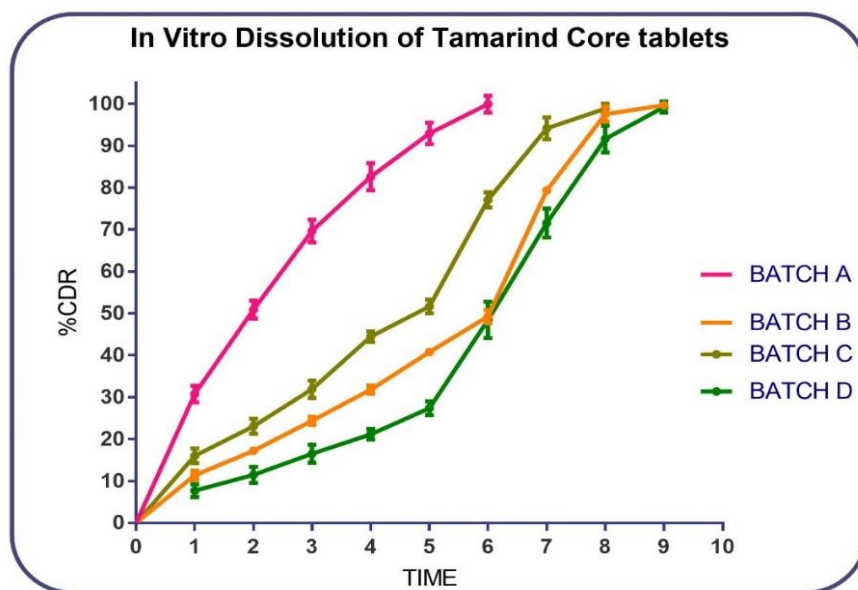
Figure 5.3: *In-Vitro* Drug Release study of Preliminary trial batches

From the dissolution data obtained from preliminary batches as illustrated in Figure 5.3, it was determined that wet granulation yields superior retardation compared to direct compression due to soaking of hydrophilic polymer. However, dissolution data obtained from tablet formulations made utilizing wet granulation exhibited inadequate outcomes., with release rates exceeding the desired limit. The desired *in vitro* release pattern for colon targeting stipulates that no more than 10% of the drug should be released by the end of the small intestine (5 hours), while more than 70% of the drug should be released within 8 hours. Consequently, Tamarind gum does not exhibit adequate retardation when tablets are prepared using PVP K 30 as a binder in IPA.

Based on the viscosity profile of Tamarind gum, it was concluded that Tamarind gum should demonstrate superior retardation compared to other natural polymers that were used for screening purposes. Consequently, a decision was made to substitute a portion of IPA with water during the granulation process to examine its impact on the retardation of drug release from the tablets.

Table 5.13: Dissolution profile of tablets prepared by the PVP K 30 in IPA and Water as bridging agent

Medium	Time (hours)	% CDR			
		Batch A	Batch B	Batch C	Batch D
0.1 N HCl	1	30.74±2.01	11.37±1.11	15.98±1.74	7.67±1.56
	2	50.91±2.15	17.21±0.79	23.03±1.84	11.45±1.94
7.4 pH Phosphate Buffer	3	69.67±2.71	24.34±1.02	31.89±2.10	16.49±2.13
	4	82.62±3.24	31.78±1.01	44.44±1.28	21.12±1.25
	5	92.93±2.56	40.78±0.93	51.65±1.64	27.35±1.64
6.8 pH Phosphate Buffer With 4.5 mL Probiotic Culture Medium	6	99.93±2.01	49.23±1.62	77.10±1.82	48.45±4.34
	7		79.34±0.76	94.15±2.63	71.56±3.45
	8		97.55±1.75	98.83±1.18	91.63±3.24
	9		99.67±0.90		99.24±1.34

Figure 5.4: *In –Vitro* Drug Release of Tablets prepared by PVP K 30 in IPA and water

Based on the dissolution data obtained from tablets formulated with PVP K 30 in both isopropyl alcohol (IPA) and water, as represented in Table 5.13 and illustrated in Figure 5.4, it has been determined that the presence of water in the tablet dosage form plays a crucial role in delaying the release of the drug. Consequently, water, functioning as a binder, is considered an influential independent factor in optimizing the dosage form through experimental design.

Nevertheless, it has been observed that the expected drug release retardation with the combination of PVP K 30 and water is not adequately achieved when utilizing tamarind gum. Therefore, it has been deemed necessary to explore an alternative approach by employing a modified form of tamarind gum. Among the several forms of grafted tamarind gum, carboxyl methyl tamarind gum was chosen due to its superior viscosity in comparison to conventional tamarind gum. Additionally, it demonstrates the capability to quickly develop a mucilaginous mass. This novel approach aims to minimize erosion and achieve the desired retardation of drug release.

To develop an optimized colon-targeted drug delivery system, it has been determined that a single microbial approach is insufficient. Consequently, a combination of approaches involving pH and microbial factors is required. In order to achieve this, it is imperative to coat the core tablet with a pH-dependent polymer. Eudragit S 100 has been selected as the pH-dependent polymer due to its superior pH threshold when compared to other available pH-dependent (enteric) polymers.

5.2.4 *In vitro* release profile of batches prepared by the Box-Behnken Experimental Design

Total 15 batches prepared by the Box-Behnken design were analyzed for the post compression parameter and it was concluded that data similar to preliminary batches and pass each test. Formulation batches were subjected for dissolution studies and the dissolution data for all the batches were reflected in Table 5.14, 5.15, and 5.16 and graphically represented in Figure 5.5, 5.6, and 5.7 respectively.

Table 5.14: *In vitro* release studies of experimental batches F1 to F5

Medium	Time (hours)	Cumulative % Drug Release				
		F1	F2	F3	F4	F5
0.1 N HCl	1	0.34±0.03	2.35±0.23	0.23±0.04	0.96±0.03	2.16±0.34
	2	0.93±0.05	4.57±0.54	0.67±0.07	1.54±0.05	4.21±0.89
7.4 pH Phosphate Buffer	3	1.52±0.08	12.38±0.92	1.45±0.9	3.12±0.8	10.9±1.23
	4	2.89±0.12	20.32±1.34	2.57±1.2	12.89±1.27	18.97±1.67
	5	6.75±0.34	32.45±2.34	8.94±1.78	21.31±2.13	28.56±2.43
6.8 pH Phosphate Buffer with 4.5 mL of Probiotic Culture Medium	6	18.79±0.89	67.89±3.42	19.79±1.89	47.54±2.78	51.23±3.89
	7	32.9±2.34	89.12±4.35	43.01±3.12	65.34±3.12	74.11±4.12
	8	63.31±3.45	99.99±1.23	62.87±3.89	85.55±3.89	89.79±3.23
	9	82.9±4.54		91.18±4.67	101.01±1.29	99.67±1.89
	10	99.98±3.45		98.31±2.12		

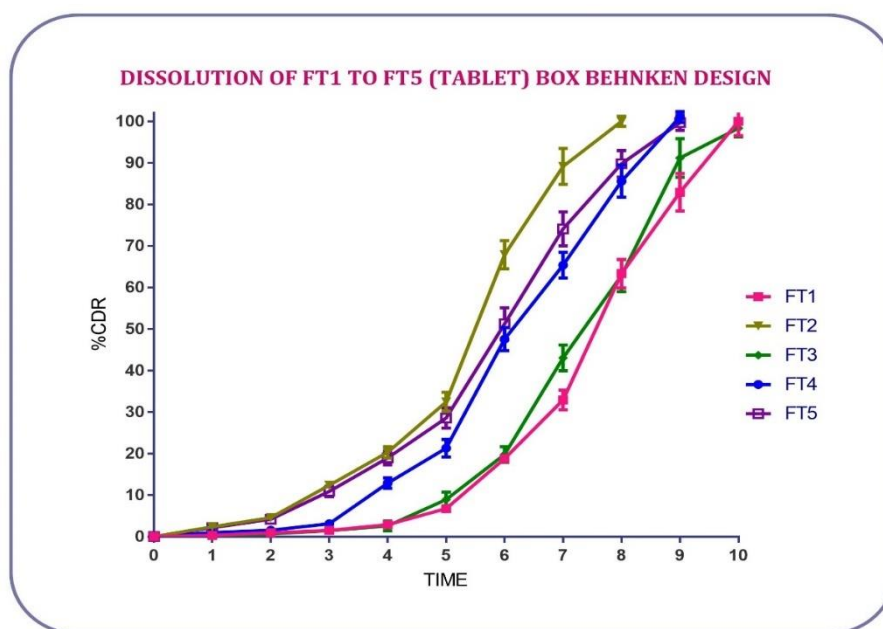
Figure 5.5: *In vitro* release of experimental batches F1 to F5

Table 5.15: *In vitro* release studies of experimental batches F6 to F10

Medium	Time (hours)	Cumulative % Drug Release				
		F6	F7	F8	F9	F10
0.1 N HCl	1	2.87±0.03	0.23±0.23	0.94±0.04	0.28±0.03	0.78±0.34
	2	4.56±0.05	0.92±0.54	1.78±0.07	0.95±0.05	1.58±0.89
7.4 pH Phosphate Buffer	3	7.45±0.08	1.23±0.92	3.23±0.9	1.26±0.8	2.56±1.23
	4	11.59±0.12	6.56±1.34	8.67±1.2	6.89±1.27	7.89±1.67
	5	18.43±0.34	12.34±2.34	15.7±1.78	14.82±2.13	15.5±2.43
6.8 pH Phosphate Buffer with 4.5 mL of Probiotic Culture Medium	6	43.23±0.89	45±3.42	39.94±1.89	47.54±2.78	41.19±3.89
	7	60.23±2.34	62.34±4.35	56.85±3.12	67.9±3.12	63.35±4.12
	8	88.43±3.45	85.79±1.23	81.23±3.89	90.94±3.89	83.17±3.23
	9	98.45±4.54	99.45±1.23	96.56±4.67	101.02±1.29	98.89±1.89
	10					

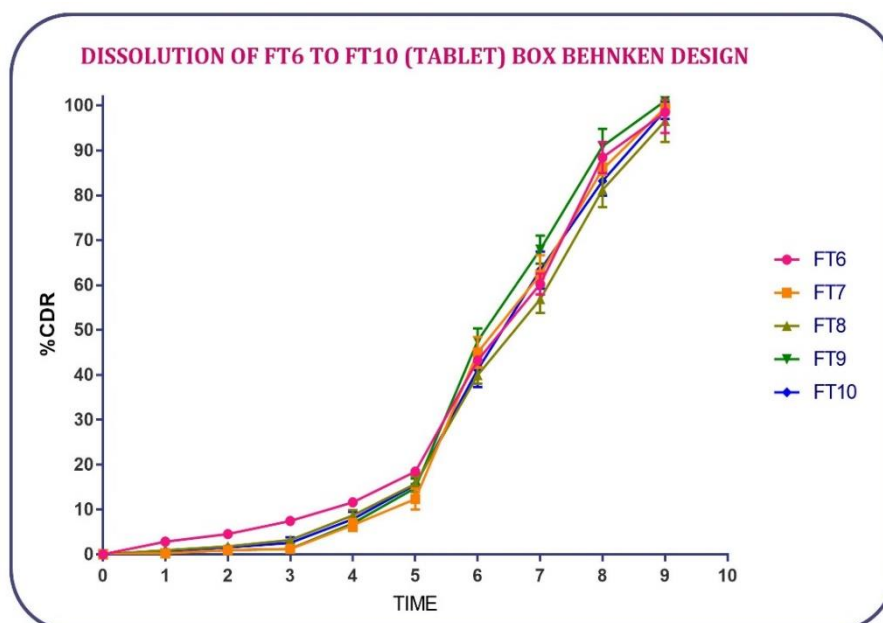
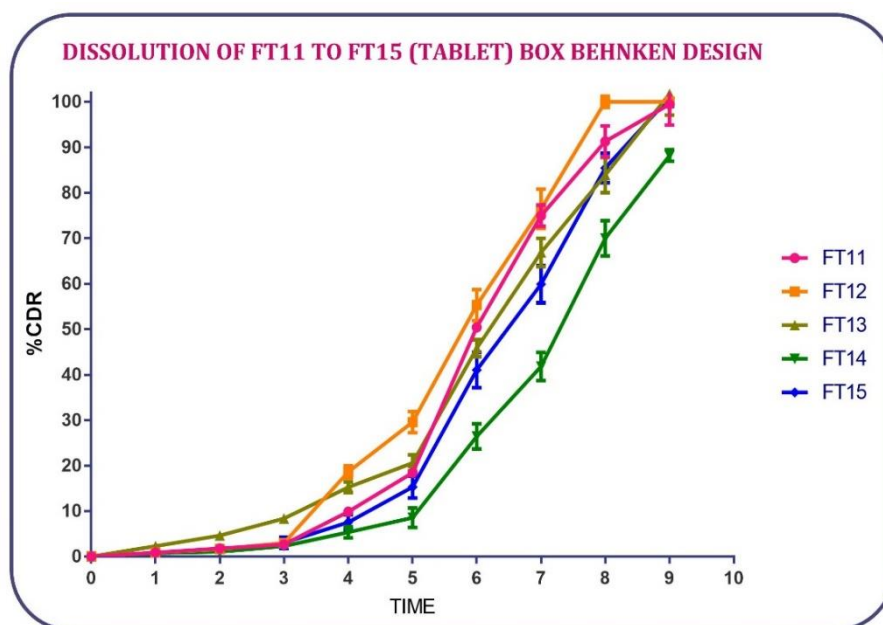
Figure 5.6: *In vitro* release of experimental batches F6 to F10

Table 5.16: *In vitro* release studies of experimental batches F11 to F15

Medium	Time (hours)	Cumulative% Drug Release				
		F11	F12	F13	F14	F15
0.1 N HCl	1	0.87±0.03	0.89±0.23	2.32±0.04	0.76±0.03	0.83±0.34
	2	1.82±0.05	1.67±0.54	4.63±0.07	1.07±0.05	1.21±0.89
7.4 pH Phosphate Buffer	3	2.67±0.08	2.99±0.92	8.39±0.9	2.32±0.8	3.02±1.23
	4	9.89±0.12	18.65±1.34	15.28±1.2	5.34±1.27	7.56±1.67
	5	18.45±0.34	29.56±2.34	20.59±1.78	8.56±2.13	15.31±2.43
6.8 pH Phosphate Buffer with 4.5 mL of Probiotic Culture Medium	6	50.43±0.89	55.29±3.42	45.84±1.89	26.45±2.78	41.01±3.89
	7	74.95±2.34	76.49±4.35	66.92±3.12	41.81±3.12	59.9±4.12
	8	91.32±3.45	100.02±1.23	83.9±3.89	70.01±3.89	85.45±3.23
	9	99.46±4.54	100.02±1.11	101.77±4.67	88.19±1.29	100.91±1.89
	10					

Figure 5.7: *In vitro* release of experimental batches F11 to F15

5.2.5 Statistical Assessment of Box-Behnken Experimental Design

The purpose of the 3-factors, 3-level experimental design was to analyse the impact and interaction of independent variables such as the amount of CM tamarind gum, the percentage of water Proportion, and the percentage of weight gain by Eudragit S 100 coating on Y2, Y5, and Y8, as shown in Table 5.17. The table revealed that Y2, Y5, and Y8 had respective values ranging from 0.67% to 4.67 %, 6.75% to 32.45%, and 62.87 % to 100.02%.

Table 5.17: Box-Behnken Experimental design Matrix and their responses.

Run	X1: quantity of tamarind (mg)	X2: % ratio of water: IPA content	X3: % weight gain	Y2 (% CDR at 2 hr)	Y5 (% CDR at 5 hr)	Y8 (% CDR at 8 hr)
1	100	100	7.5	0.93	6.75	63.31
2	100	0	2.5	4.57	32.45	99.99
3	125	50	7.5	0.67	8.94	62.87
4	125	0	5	1.54	21.31	85.55
5	75	50	2.5	4.21	28.56	89.79
6	100	100	2.5	4.56	18.43	88.43
7	100	0	7.5	0.92	12.34	85.79
8	100	50	5	1.78	15.7	81.23
9	75	50	7.5	0.95	14.82	90.94
10	100	50	5	1.58	15.5	83.17
11	75	100	5	1.82	18.45	91.32
12	75	0	5	1.67	29.56	100.02
13	125	50	2.5	4.63	20.59	83.9
14	125	100	5	1.07	8.56	70.01
15	100	50	5	1.21	15.31	85.45

5.2.5.1 Effect of X_1 , X_2 , and X_3 on % drug release at 2 (Y_2) hrs.

According to the results of the Analysis of variance shown in Table 5.18, the Model F-value of 56.53 indicates that the model was significant for Y_2 , % cumulative drug release (CDR) at 2, hours.

Table 5.18: Analysis of variance of independent variable Y2 (% CDR at 2 hours)

Source	Sum of Squares	df	Mean Square	F-value	p-value	
Model	31.60	9	3.51	56.53	0.0002	significant
A-Quantity of CM Tamarind	0.0685	1	0.0685	1.10	0.3419	
B - % Ratio of water: IPA content	0.0128	1	0.0128	0.2061	0.6689	
C-% weight gain	26.28	1	26.28	423.12	< 0.0001	
AB	0.0961	1	0.0961	1.55	0.2687	
AC	0.1225	1	0.1225	1.97	0.2192	
BC	0.0001	1	0.0001	0.0016	0.9695	
A ²	0.0152	1	0.0152	0.2448	0.6418	
B ²	0.0160	1	0.0160	0.2576	0.6333	
C ²	4.93	1	4.93	79.42	0.0003	
Lack of Fit	0.1433	3	0.0478	0.5711	0.6866	Not significant
Pure Error	0.1673	2	0.0836			
R ²			0.9903			
Adjusted R ²			0.9728			
Predicted R ²			0.9164			
Adeq Precision			19.9885			

Polynomial Equation

$$Y2 (\%CDR \text{ AT } 2 \text{ Hr}) = + 1.52 - 0.093X_1 - 0.040X_2 - 1.81X_3 - 0.155X_1X_2 - 0.175X_1X_3 + 0.005X_2X_3 - 0.064X_1^2 + 0.066X_2^2 + 1.16X_3^2$$

Design-Expert® Software

Factor Coding: Actual

Y2 (% CDR AT 2 Hr) (%)

● Design points above predicted value

○ Design points below predicted value

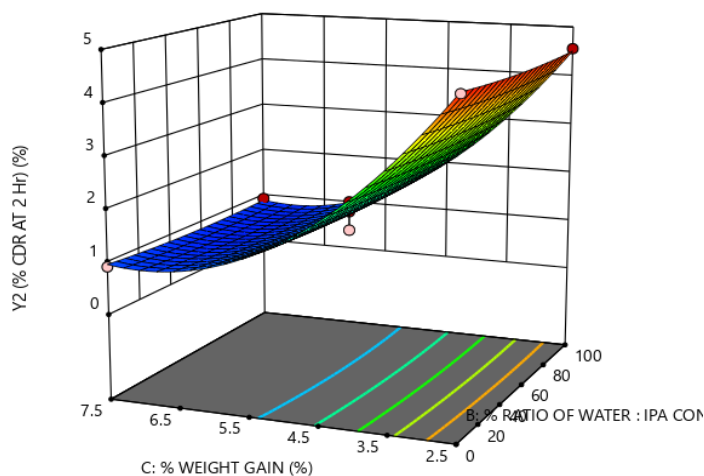
0.67 4.63

X1 = B: % RATIO OF WATER : IPA CONTENT

X2 = C: % WEIGHT GAIN

Actual Factor

A: QUANTITY OF CM TAMARIND = 100



(a)

Design-Expert® Software

Factor Coding: Actual

Y2 (% CDR AT 2 Hr) (%)

● Design Points

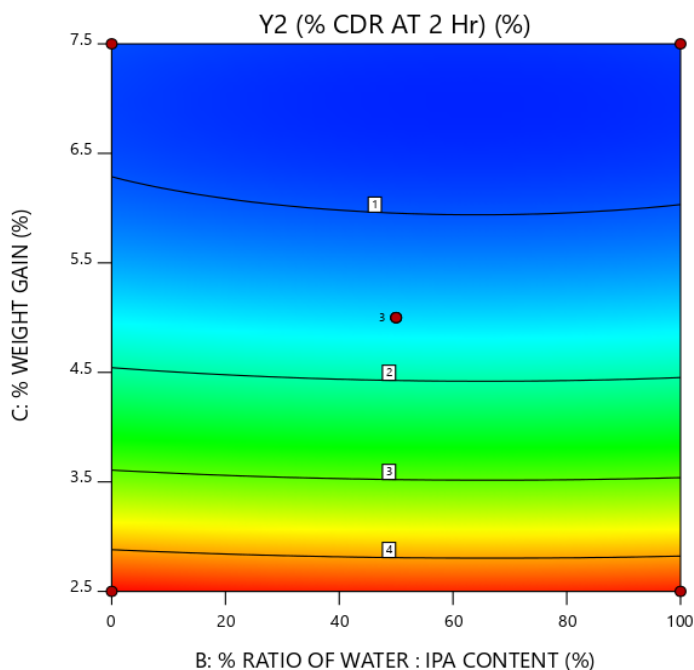
0.67 4.63

X1 = B: % RATIO OF WATER : IPA CONTENT

X2 = C: % WEIGHT GAIN

Actual Factor

A: QUANTITY OF CM TAMARIND = 100



(b)

Figure 5.8: 3D Response Graph (a) and Contour Plot (b) for % CDR at 2 hrs

Based on the polynomial equation, 3D response curve (Fig. 5.8a), and contour plot (Fig. 5.8b), it was determined that the percentage weight gain by coating tablets with Eudragit S 100 modulated Y2 significantly. As coating level (C) increases, drug release at 2 hours (Y2) decreases dramatically, and carboxymethyl tamarind gum amount (A) has the same negative impact on Y2. However, the impact of A on Y2 is much smaller than that of C. As B

increases, it gradually decreases drug release, but as coating thickness increases, the effect of B on drug release diminishes. As we investigated the impact of independent variables on % CDR at 2 hours (Y2%), we found that C, and C² were significant model terms. According to the significance explanation, the coating level of eudragit S 100 has a significant effect on Y2. A model F-value of 56.53 indicates that the model is statistically significant. P-values less than 0.05 indicate significant model terms. The minimal difference between the adjusted R² value (0.9728) and the predicted R² value (0.9164) indicates that the design has significant predictive power. However, by removing the insignificant terms from the model, the predictability of the model improved. The value of adequate precision was 19.98 indicated that model is capable to explore the design space.

5.2.5.2 Effect of X₁, X₂, and X₃ on % drug release at 5 (Y5) hrs.

According to the results of the Analysis of variance shown in Table 5.19, the Model F-value of 46.73 indicates that the model was significant for Y5, % cumulative drug release (CDR) at 5 hours

Table 5.19: Analysis of variance of independent variable Y5 (% CDR at 5 hours)

Source	Sum of Squares	df	Mean Square	F-value	p-value	
Model	820.43	9	91.16	46.73	0.0003	significant
A-Quantity of cm tamarind	127.92	1	127.92	65.57	0.0005	
B-% Ratio of water: IPA content	236.21	1	236.21	121.08	0.0001	
C-% weight gain	408.69	1	408.69	209.49	< 0.0001	
AB	0.6724	1	0.6724	0.3447	0.5827	
AC	1.09	1	1.09	0.5598	0.4880	
BC	17.77	1	17.77	9.11	0.0295	
A ²	20.41	1	20.41	10.46	0.0231	
B ²	9.64	1	9.64	4.94	0.0768	
C ²	0.5146	1	0.5146	0.2638	0.6294	
Lack of Fit	9.68	3	3.23	84.82	0.1117	Not significant
Pure Error	0.0761	2	0.0380			
R ²			0.9883			
Adjusted R ²			0.9671			

Predicted R ²	0.8133
Adeq precision	22.0640

Polynomial Equation:

$$Y5 (\% \text{ CDR AT 5 Hr}) = 15.50333 - 3.99875 X1 - 5.43375 X2 - 7.1475 X3 - 0.41 X1X2 + 0.5225 X1X3 + 2.1075 X2X3 + 2.350833 X1^2 + 1.615833 X2^2 + 0.373333 X3^2$$

Design-Expert® Software
Factor Coding: Actual

Y5 (% CDR AT 5 Hr) (%)

● Design points above predicted value

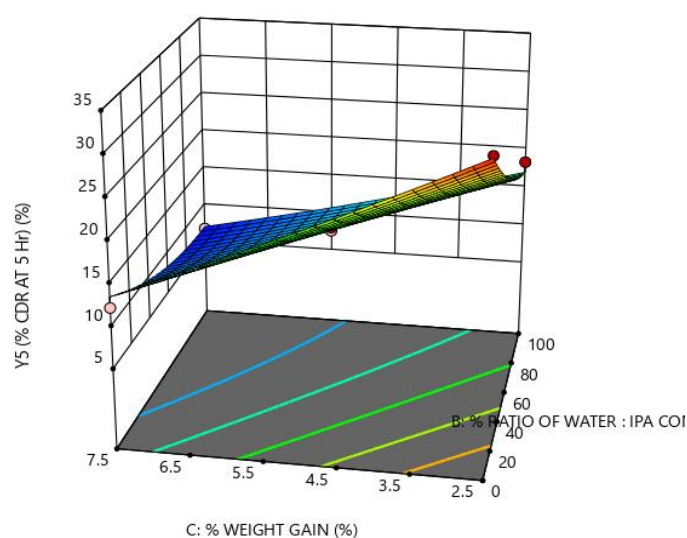
○ Design points below predicted value

6.75 32.45

X1 = B: % RATIO OF WATER : IPA CONTENT
X2 = C: % WEIGHT GAIN

Actual Factor

A: QUANTITY OF CM TAMARIND = 100



(a)

Design-Expert® Software
Factor Coding: Actual

Y5 (% CDR AT 5 Hr) (%)

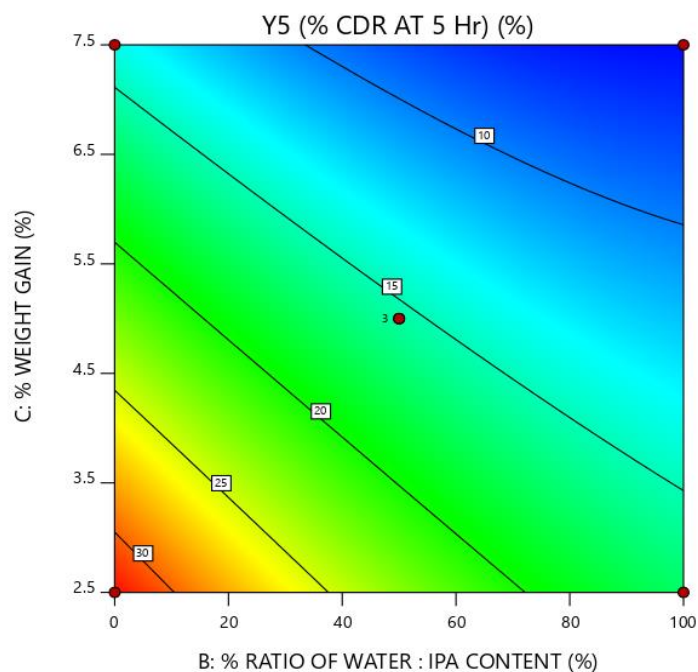
● Design Points

6.75 32.45

X1 = B: % RATIO OF WATER : IPA CONTENT
X2 = C: % WEIGHT GAIN

Actual Factor

A: QUANTITY OF CM TAMARIND = 100



(b)

Figure 5.9: 3D Response Graph (a) and Contour Plot (b) for % CDR at 5 hrs

On the basis of the polynomial equation, the 3D response (Fig. 5. 9a), and the contour plot (Fig. 5.9b), All three independent variables have a substantial influence on the rate of drug release at 5 hours. The drug formulations were subjected to a higher pH after two hours. As a result, the coating would dissolve more gradually, and the release rate would also be controlled by core pellet components such as CM tamarind gum and % ratio of water. According to the b1, b2, and b3 coefficient value of Polynomial equation, when the quantity of CM tamarind gum, % water ratio, and the percentage of weight gain increased, the percentage of drug release decreased.

According to the data in the ANOVA Table 5.19 for the dependent variable Y5, the model was significant based on the model F value, which was 46.73. Significant model terms in this instance are A, B, C, BC, and A². If your model has a large number of insignificant terms, model reduction may be able to enhance performance. From the values of adjusted R² (0.9671) and predicted R² (0.8133), it can be concluded that the design has significant predictive power. The adequate precision value was 22.06, indicating the model's capacity to explore the design space was adequate.

5.2.5.3 Effect of X₁, X₂, and X₃ on % drug release at 8 (Y8) hrs.

According to the results of the Analysis of variance shown in Table 5.20, the Model F-value of 18.44 indicates that the model was significant for Y8, % cumulative drug release (CDR) at 8, hours

Table 5.20: Analysis of variance of independent variable Y8 (% CDR at 8 hours)

Source	Sum of Squares	df	Mean Square	F-value	p-value	
Model	1635.10	6	272.52	18.44	0.0003	Significant
A-Quantity of cm tamarind	607.96	1	607.96	41.13	0.0002	
B-% Ratio of water: ipa content	424.57	1	424.57	28.72	0.0007	
C-% weight gain	438.08	1	438.08	29.64	0.0006	
AB	11.70	1	11.70	0.7913	0.3997	
AC	122.99	1	122.99	8.32	0.0204	

BC	29.81	1	29.81	2.02	0.1933	
Lack of Fit	109.33	6	18.22	4.08	0.2097	Not significant
Pure Error	8.92	2	4.46			
R ²	0.9326					
Adjusted R ²	0.8820					
Predicted R ²	0.6871					
Adeq precision	13.6895					

Polynomial Equation:

$$Y8 (\% \text{ CDR AT 8 Hr}) = +84.118 - 8.7175 X1 - 7.285 X2 - 7.4 X3 - 1.71 X1X2 - 5.545 X1X3 - 2.73 X2X3$$

Design-Expert® Software

Factor Coding: Actual

Y8 (% CDR AT 8 Hr) (%)

● Design points above predicted value

○ Design points below predicted value

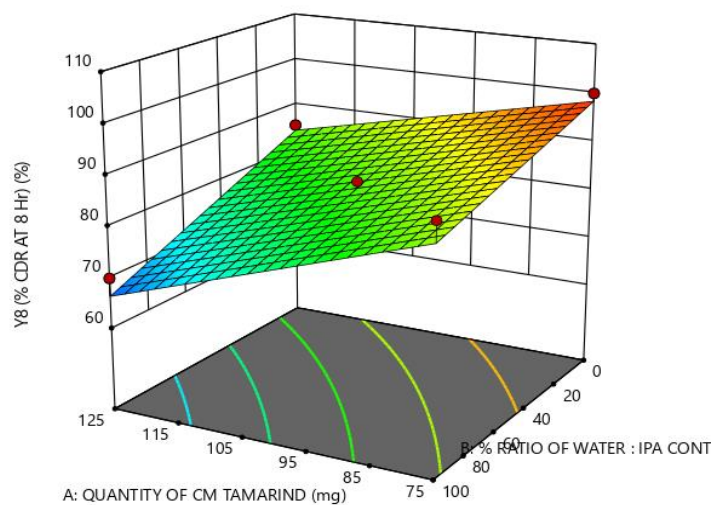
62.87 100.02

X1 = A: QUANTITY OF CM TAMARIND

X2 = B: % RATIO OF WATER : IPA CONTENT

Actual Factor

C: % WEIGHT GAIN = 5



(a)

Design-Expert® Software

Factor Coding: Actual

Y8 (% CDR AT 8 Hr) (%)

● Design Points

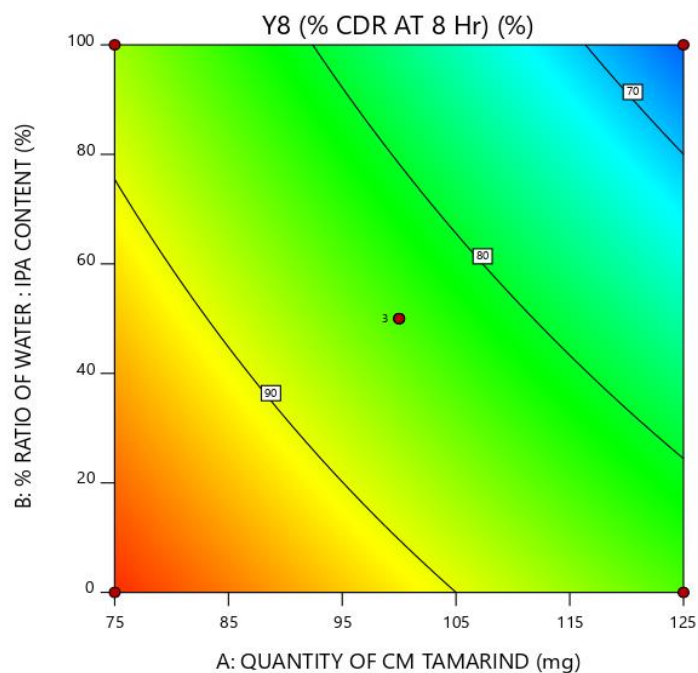
62.87 100.02

X1 = A: QUANTITY OF CM TAMARIND

X2 = B: % RATIO OF WATER : IPA CONTENT

Actual Factor

C: % WEIGHT GAIN = 5



(b)

Figure 5.10: 3D Response Graph (a) and Contour Plot (b) for CDR at 8 hrs

Based on the polynomial equation, 3D response graph (Fig. 5.10a), and contour plot (Fig. 5.10b), it was determined that as the amount of CM tamarind gum and percentage weight gain of the Eudragit S 100 coating increase, % water ratio, and the percentage of drug released at 8 hours (Y8) decreases. It was determined that CM tamarind gum, % water ratio, and % weight gain had a negative effect on the release of the drug until 8 hours after formulation. According to the coefficients of A, B, and C, the influence of A was greater than that of B and C, indicating that the release of the drug was impacted until around 8 hours after 5 hours due to the considerable breakdown of tamarind gum in the colonic area by enzymes released by the colonic microbiota.

Despite the fact that Eudragit's coat was no longer present after 5 hours, the cumulative effect of the coat on tablet in the upper gastrointestinal tract was responsible for the detection of this negative effect.

Design-Expert® Software

Factor Coding: Actual

Overlay Plot

Y2 (% CDR AT 2 Hr)

Y5 (% CDR AT 5 Hr)

Y8 (% CDR AT 8 Hr)

● Design Points

X1 = A: QUANTITY OF CM TAMARIND

X2 = C: % WEIGHT GAIN

Actual Factor

B: % RATIO OF WATER : IPA CONTENT = 100

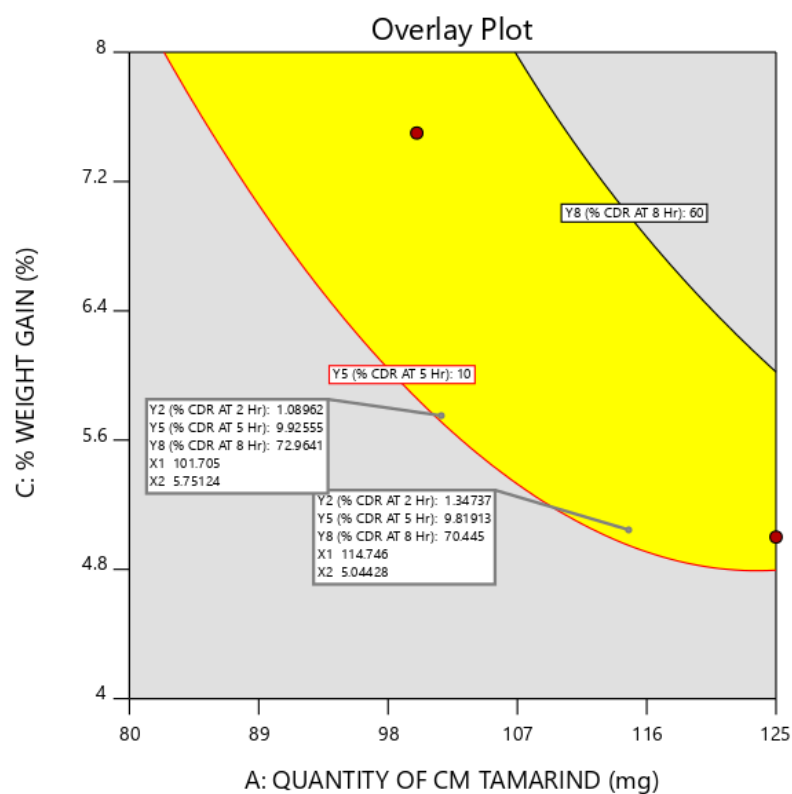


Figure 5.11: Design space (Overlay plot) of prepared with Operating ranges of B (% Ratio of Water: IPA content) at 100 (3rd level)

Design-Expert® Software

Factor Coding: Actual

Overlay Plot

Y2 (% CDR AT 2 Hr)

Y5 (% CDR AT 5 Hr)

Y8 (% CDR AT 8 Hr)

● Design Points

X1 = B: % RATIO OF WATER : IPA CONTENT

X2 = C: % WEIGHT GAIN

Actual Factor

A: QUANTITY OF CM TAMARIND = 100

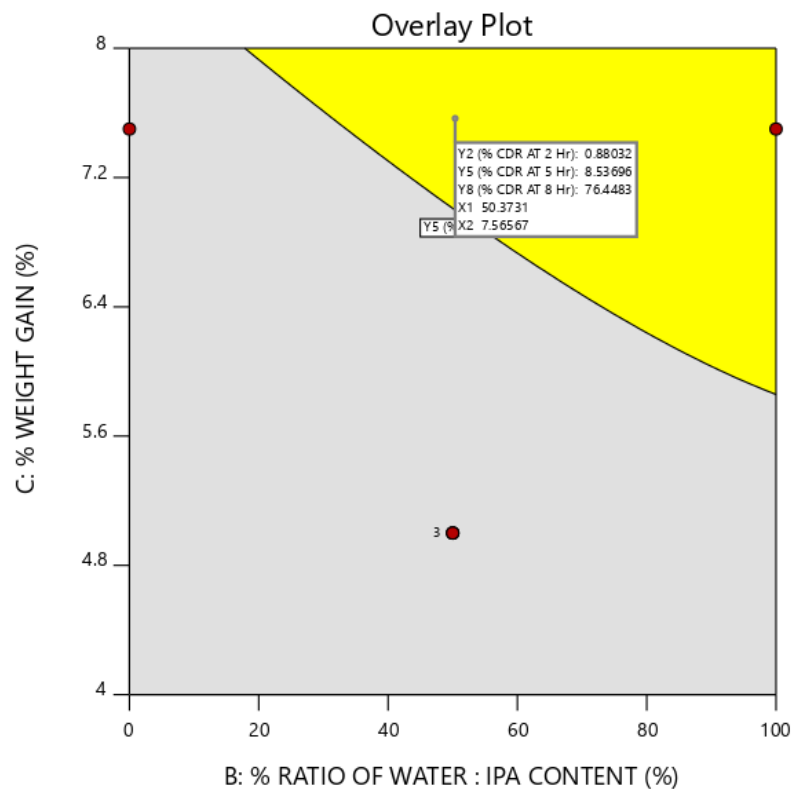


Figure 5.12: Design space (Overlay plot) of prepared with Operating ranges of A (Quantity of CM Tamarind gum) at 100 (2nd level)

In accordance with regulatory requirements, it may be stated that when modifications are made within the designated design space, they do not constitute a change. However, if changes extend beyond the established design space, it is likely necessary to adhere to the regulatory post-approval modification process. The applicant presents a conceptual framework that needs assessment and endorsement from regulatory authorities. In this study, the Design of Experiments (DOE) technique known as Response Surface Methodology (RSM) was used in combination with optimization methods. Contour plots were used to assess the influence of two independent variables on the dependent variables at a certain moment, while a third variable was held constant. Figure 5.11 illustrates the influence of variables A and C on outcomes Y2, Y5, and Y8, considering three different values of C. In cases where the percentage weight gain of the C's came between the range of 2.5% to 4.8%, it was seen that there was no expected development of DS, as shown in Figure 5.11. A design space was created by altering the value of components A, in response to the weight gain exceeding 4.8% of eudragit S 100. The yellow region, designated as the Design Space (DS) in Figure 5.11, is shown as an overlay plot that illustrates the spatial domain within which formulations meeting desired requirements might be generated.

Figure 5.12 illustrates the influence of variables B and C on the outcomes Y2, Y5, and Y9, while considering two different values of variable A. If the percentage weight increase of the subject was between the range of 2.5% to 5.8%, there was no observed establishment of DS as shown in Figure 5.12. A design space was created by modifying the values of components A, in response to the weight growth of eudragit S 100 exceeding 5.8%. The yellow region, referred to as the Design Space (DS), seen in Figure 5.12, serves as an overlay plot illustrating the spatial domain within which formulations meeting desired criteria might be constructed, as suggested by the Design-Expert 11.0 software.

In order to ensure the reliability and precision of the experimental design, five separate batches were selected within the Design Space (DS) to conduct a comparison between the predicted values and the observed values. Based on the findings shown in Table 5.21, it has been found that there is no significant difference seen in the data. Consequently, it has been concluded that the Selected Design has exceptional predictive capability.

Table 5.21: Predicated and Observed values for Dependent Variables of Checkpoint Batches

Batch No.	Independent Variables			Dependent Variables					
				Y2 (% CDR AT 2 Hr)		Y5 (% CDR AT 5 Hr)		Y8 (% CDR AT 8 Hr)	
	X1	X2	X3	Predicated	Observed	Predicted	Observed	Predicated	Observed
1	90	100	7.5	1.05	1.11	8.94	8.12	73.03	75.12
2	100	35	7.5	0.88	0.95	9.87	9.52	79.72	82.45
3	110	50	7	0.70	0.78	8.96	9.50	72.93	74.52
4	115	25	7.5	0.76	0.95	9.67	9.12	73.68	72.45
5	120	25	7.5	0.70	0.75	9.68	9.53	70.99	72.56

5.2.6 Release kinetics of formulation batches

The drug release from the dosage form depends upon the type of polymer and the other formulation parameter used. For finding out the mechanism of drug release from formulation release kinetics of all formulation batches were measure and are shown in Table 5.22 and 5.23.

Table 5.22: statistical parameter of all mathematical models (F1 to F8)

Model	Statistics	Formulations (Tablets)							
		F1	F2	F3	F4	F5	F6	F7	F8
Zero Order	R2	0.8223	0.9089	0.8453	0.9111	0.9393	0.8794	0.8692	0.8782
	AIC	80.07	57.79	79.22	65.47	61.67	67.58	69.33	67.40
	MSC	1.4457	2.0502	1.5839	2.1095	2.4910	1.8043	1.7232	1.7946
First Order	R2	0.5570	0.6516	0.5726	0.6384	0.6907	0.6311	0.5907	0.6150
	AIC	88.38	67.76	88.56	77.30	75.53	76.84	78.80	76.96
	MSC	0.6142	0.8043	0.6501	0.7949	0.9512	0.7749	0.6711	0.7322
Higuchi Model	R2	0.9672	0.9395	0.9792	0.9774	0.9452	0.9617	0.9893	0.9739
	AIC	63.17	54.52	59.13	53.15	60.74	57.25	46.81	53.53
	MSC	3.1353	2.4589	3.5924	3.4783	2.5940	2.9517	4.2254	3.3354
Hixson Crowell	R2	0.7093	0.7985	0.7311	0.8021	0.8398	0.7682	0.7556	0.7718
	AIC	84.99	64.14	84.74	72.68	70.40	73.46	74.96	73.05
	MSC	0.9534	1.2563	1.0313	1.3089	1.5205	1.1512	1.0980	1.1667
Korsmeyer Peppas	R2	0.9913	0.9676	0.9877	0.9916	0.9822	0.9775	0.9848	0.9913
	n	1.2310	1.4760	1.0640	1.2510	1.3720	1.5110	1.0670	1.2280
	AIC	50.57	50.06	54.60	44.81	51.24	53.07	50.54	44.28
	MSC	4.3951	3.0169	4.0459	4.4049	3.6498	3.4164	3.8107	4.3635
Weibull Model	β	7.2298	7.8164	7.0972	6.0995	6.8132	7.5891	3.4963	6.3603
	R2	0.9971	0.9922	0.9972	0.9946	0.9966	0.9909	0.9914	0.9959
	AIC	39.64	45.52	39.66	40.83	36.22	44.94	45.43	37.54
	MSC	5.4883	4.4706	5.5396	4.8476	5.3185	4.3194	4.3792	5.1117

Table 5.23: statistical parameter of all mathematical models (F9 to F15)

Model	Statistics	Formulations (Tablets)						
		F9	F10	F11	F12	F13	F14	F15
Zero Order	R2	0.8768	0.8786	0.8915	0.9275	0.9053	0.8129	0.8721
	AIC	69.48	68.13	68.23	64.86	65.45	69.24	68.84
	MSC	1.7827	1.7976	1.9097	2.3138	2.0466	1.3653	1.7457
First Order	R2	0.5927	0.6068	0.6163	0.6533	0.6538	0.5703	0.5977
	AIC	79.44	77.91	78.80	78.15	76.32	75.93	78.35
	MSC	0.6760	0.7111	0.7358	0.8371	0.8386	0.6225	0.6883
Higuchi Model	R2	0.9918	0.9835	0.9885	0.9581	0.9596	0.9679	0.9772
	AIC	45.05	50.16	48.03	59.93	57.79	53.38	53.33
	MSC	4.4973	3.7936	4.1544	2.8609	2.8982	3.1281	3.4681
Hixson Crowell	R2	0.7591	0.7673	0.7799	0.8220	0.7958	0.7177	0.7565
	AIC	84.99	64.14	84.74	72.68	70.40	73.46	74.96
	MSC	0.9534	1.2563	1.0313	1.3089	1.5205	1.1512	1.0980
Korsmeyer Peppas	R2	0.9913	0.9676	0.9877	0.9916	0.9822	0.9775	0.9848
	n	1.2310	1.4760	1.0640	1.2510	1.3720	1.5110	1.0670
	AIC	50.57	50.06	54.60	44.81	51.24	53.07	50.54
	MSC	4.3951	3.0169	4.0459	4.4049	3.6498	3.4164	3.8107
Weibull Model	β	7.2298	7.8164	7.0972	6.0995	6.8132	7.5891	3.4963
	R2	0.9971	0.9922	0.9972	0.9946	0.9966	0.9909	0.9914
	AIC	39.64	45.52	39.66	40.83	36.22	44.94	45.43
	MSC	5.4883	4.4706	5.5396	4.8476	5.3185	4.3194	4.3792

Upon evaluating the dissolution profiles of 15 different design batches, it was determined that batch 14 demonstrated the closest optimization in terms of release criteria and design space layout. Subsequently, after a 2-hour delay ($t_{lag} = 2$), the release kinetics observed in the study were analysed using various kinetic models (Table 5.22 & 5.23) through the DD solver[27], and using the adjusted R^2 values of 0.9914 and 0.9963 for the Korsmeyer-Peppas and Weibull models, respectively, it was determined that both models fit the data well. These high R^2 values indicate a significant correlation between the theoretical models and the observed data, confirming that the chosen models are appropriate for characterizing the release kinetics.

Applying the Korsmeyer-Peppas model to the release kinetics yielded an n value of 1.6270. This value implies a release mechanism consistent with super Case II, indicating extensive burst release after lag time. In contrast, the Weibull model yielded a β value of 6.2584, suggesting a failure in adequately controlling the release, as validated by a value of 1.

Furthermore, the Korsmeyer-Peppas model yielded an AIC value of 42.12, while the Weibull model resulted in an AIC value of 34.59 for batch 14. These values serve as indicators for model selection, with lower values suggesting a better fit to the data. Based on the AIC values, it can be concluded that the Weibull model is more suitable as a release mechanism for batch 14. The Weibull model exhibited the lowest AIC value, indicating a closer fit to the observed data compared to the Korsmeyer-Peppas model[28, 29]. The MSC values are used as a quantitative measure to assess the goodness of fit of different models. In this case, the lower MSC value of 4.37 for the Korsmeyer-Peppas model for batch 14 suggests that it exhibits a relatively poorer fit to the data. On the other hand, the higher MSC value of 5.21 for the Weibull model indicates a better fit, implying that the Weibull model captures the underlying patterns and behaviours in the observed data more accurately[30].

5.2.7 *In-vivo* study in rabbit

The figure 5.13 displaying the optimized colon-targeted formulation was analysed using X-ray imaging techniques to assess its behaviour within the gastrointestinal (GI) tract. The X-ray imaging results indicated that the formulation remained intact for a period of 5 hours. However, beyond this timeframe (at 7 hour), a burst release phenomenon was observed, suggesting that the formulation's contents release within the colon. This finding suggests that the optimised colon-targeted formulation exhibited delayed and targeted release characteristics, allowing the formulation to maintain its integrity till reach to the colon.

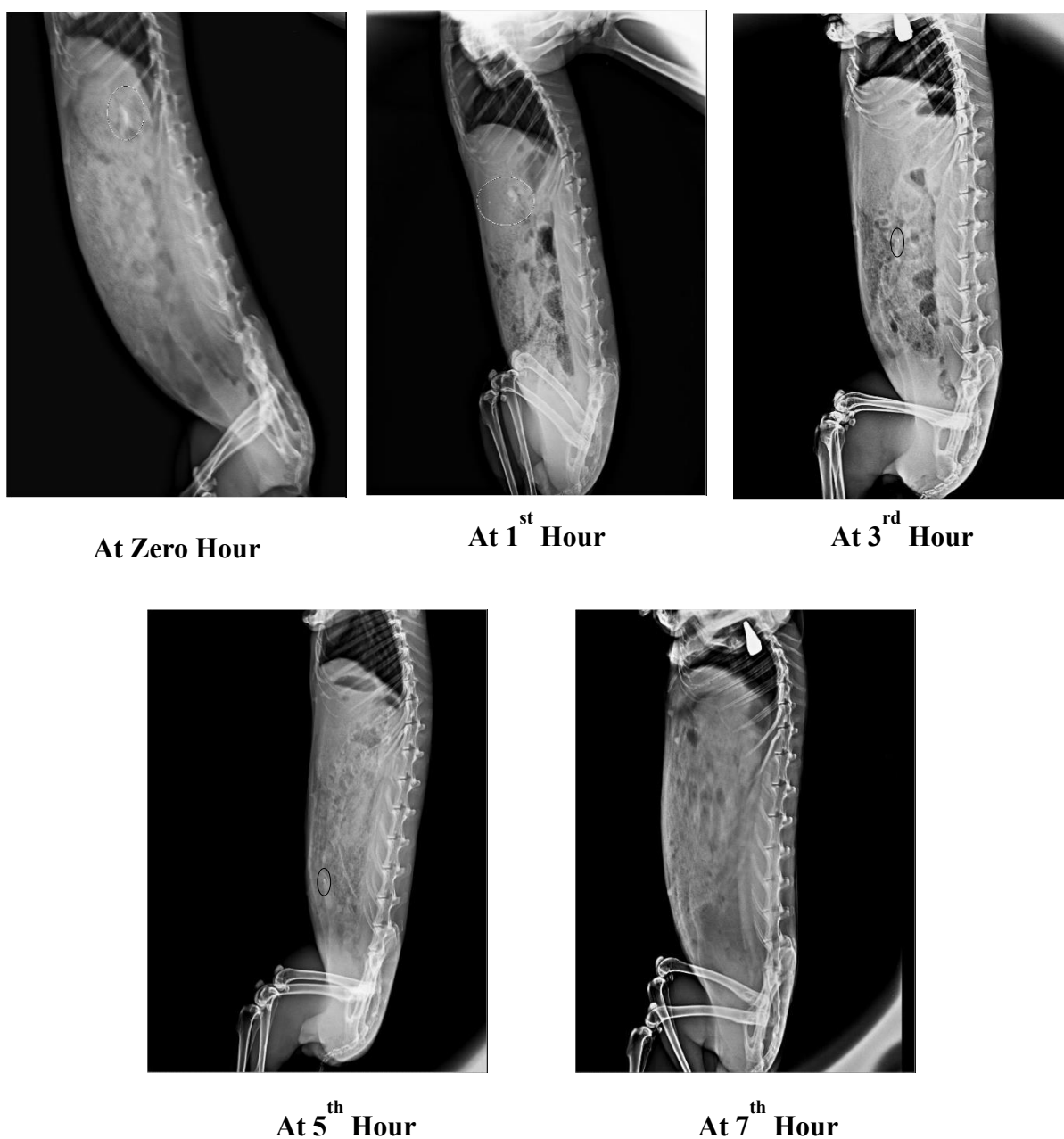


Figure 5.13: X – Ray imaging of Rabbit for Tablet dosage form

5.2.8 Stability Study

Stability study data for the optimized batch are shown in Table 5.24. As per the data, it was concluded that pellets dosage form was stable enough till 6 months under the accelerated conditions as per the ICH.

Table 5.24: Stability Study of Optimized Batch (F3) under accelerated Conditions as per ICH guideline

Test parameters	Specifications	Initial	1 st Month	3 rd Month	6 th Month
Description	Buff coloured coated spherical pellets	Buff coloured spherical pellets	No change	No change	No Change
Moisture content	NMT 2.5	1.23	1.26	1.32	1.45
Assay (Drug Content)	NLT 90% and NMT 110% of label claim	98.93% ±1.23	98.56%±1 .73	96.01%±2 .32	93.85%± 3.19
% CDR at 5 th hrs	NLT 90% and NMT 110% of label claim	7.98 % ± 1.214	7.83% ± 1.541	7.51% ± 1.862	8.93 % ± 1.49
Friability	Not greater than 1 %	0.23 %	0.25 %	0.56 %	0.12 %
Microbial limit test	Total count < 10 ² CFU (As per USP)	Complies	Complies	Complies	Complies

5.3. References

1. Devi, D., Ghosh, A., & Mandal, U. K. (2022). Sustained release matrix tablet of 100 mg losartan potassium: Formulation development and *in vitro* characterization. *Brazilian Journal of Pharmaceutical Sciences*, 58, 1–16. <https://doi.org/10.1590/s2175-97902022e20079>
2. PAWAR, S. S., Malpure, P. S., Surana, S. S., & Bhadane, J. S. (2019). Formulation and evaluation of sustained release matrix tablet of captopril. *Journal of Drug Delivery and Therapeutics*, 9(4-A), 260–268. <https://doi.org/10.22270/jddt.v9i4-A.3406>
3. Kanathe, P., Jain, R., Jain, N., & Jain, S. K. (2021). Formulation and Evaluation of Orodispersible Tablet of Fluvastatin Sodium. *Journal of Drug Delivery and Therapeutics*, 11(1), 42–47. <https://doi.org/10.22270/jddt.v11i1.4498>
4. Huanbutta, K., & Sittikijyothin, W. (2018). Use of seed gums from Tamarindus indica and Cassia fistula as controlled-release agents. *Asian Journal of Pharmaceutical Sciences*, 13(5), 398–408. <https://doi.org/10.1016/j.ajps.2018.02.006>
5. Pawar, P., Sharma, P., Chawla, A., & Mehta, R. (2013). Formulation and *in vitro* evaluation of Eudragit S-100 coated naproxen matrix tablets for colon-targeted drug delivery system. *Journal of Advanced Pharmaceutical Technology & Research*, 4(1), 31. <https://doi.org/10.4103/2231-4040.107498>
6. Khan, M. J., Huang, W.-C., Akhlaq, M., Raza, S., Hamadou, A. H., Yuning, G., ... Mao, X. (2022). Design, Preparation, and Evaluation of Enteric Coating Formulation of HPMC and Eudragit L100 on Carboxylated Agarose Hydrogel by Using Drug Tartrazine. *BioMed Research International*, 2022, 1–6. <https://doi.org/10.1155/2022/1042253>
7. Fude, C., Lei, Y., Jie, J., Hongze, P., Wenhui, L., & Dongmei, C. (2007). Preparation and *In Vitro* Evaluation of pH, Time-Based and Enzyme-Degradable Pellets for Colonic Drug Delivery. *Drug Development and Industrial Pharmacy*, 33(9), 999–1007. <https://doi.org/10.1080/03639040601150393>
8. Kan, S., Lu, J., Liu, J., Wang, J., & Zhao, Y. (2014). A quality by design (QbD) case study on enteric-coated pellets: Screening of critical variables and establishment of design space at laboratory scale. *Asian Journal of Pharmaceutical Sciences*, 9(5), 268–278. <https://doi.org/10.1016/j.ajps.2014.07.005>
9. Patel, N., Patel, J., & Shah, S. (2010). Box-Behnken experimental design in the development of pectin-compritol ATO 888 compression coated colon targeted drug delivery of mesalamine. *Acta Pharmaceutica*, 60(1), 39–54. <https://doi.org/10.2478/v10007-010-0008-9>
10. Ren, Y., Jiang, L., Yang, S., Gao, S., Yu, H., Hu, J., ... Zhou, Y. (2017). Design and preparation of a novel colon-targeted tablet of hydrocortisone. *Brazilian Journal of Pharmaceutical Sciences*, 53(1). <https://doi.org/10.1590/s2175-97902017000115009>
11. McCoubrey, L. E., Favaron, A., Awad, A., Orlu, M., Gaisford, S., & Basit, A. W. (2023). Colonic drug delivery: Formulating the next generation of colon-targeted therapeutics. *Journal of Controlled Release*, 353, 1107–1126. <https://doi.org/10.1016/j.jconrel.2022.12.029>
12. Evans, D. F., Pye, G., Bramley, R., Clark, A. G., Dyson, T. J., & Hardcastle, J. D. (1988). Measurement of gastrointestinal pH profiles in normal ambulant human subjects. *Gut*, 29(8), 1035–1041. <https://doi.org/10.1136/gut.29.8.1035>
13. Wahlgren, M., Axenstrand, M., Håkansson, Å., Marefati, A., & Lomstein Pedersen, B. (2019). *In Vitro* Methods to Study Colon Release: State of the Art and An Outlook on New Strategies for Better In-Vitro Biorelevant Release Media. *Pharmaceutics*, 11(2), 95. <https://doi.org/10.3390/pharmaceutics11020095>

14. Sathe, P. M., Tsong, Y., & Shah, V. P. (1996). In-Vitro Dissolution Profile Comparison: Statistics and Analysis, Model Dependent Approach. *Pharmaceutical Research*, 13(12), 1799–1803. <https://doi.org/10.1023/A:1016020822093>
15. Polli, J. E., Rekhi, G. S., Augsburger, L. L., & Shah, V. P. (1997). Methods to Compare Dissolution Profiles and a Rationale for Wide Dissolution Specifications for Metoprolol Tartrate tablets†. *Journal of Pharmaceutical Sciences*, 86(6), 690–700. <https://doi.org/10.1021/js960473x>
16. Varshosaz, J., Emami, J., Tavakoli, N., Minaian, M., Rahmani, N., Ahmadi, F., & Dorkoosh, F. (2011). Development and validation of a rapid HPLC method for simultaneous analysis of budesonide and its novel synthesized hemiesters in colon specific formulations. *Research in pharmaceutical sciences*, 6(2), 107–116. Retrieved from <http://www.ncbi.nlm.nih.gov/pubmed/22224094>
17. Patel, M. M. (2017). Formulation and development of di-dependent microparticulate system for colon-specific drug delivery. *Drug Delivery and Translational Research*, 7(2), 312–324. <https://doi.org/10.1007/s13346-017-0358-7>
18. Rao, K. P., Prabhashankar, B., Kumar, A., Khan, A., Biradar, S. S., Srishail, S. P., & Satyanath, B. (2003). Formulation and roentgenographic studies of naproxen-pectin-based matrix tablets for colon drug delivery. *The Yale journal of biology and medicine*, 76(4–6), 149–54. Retrieved from <http://www.ncbi.nlm.nih.gov/pubmed/15482652>
19. Prabhu, P., Ahamed, N., Matapady, H. N., Ahmed, M. G., Narayanacharyulu, R., Satyanarayana, D., & Subrahmanayam, E. (2010). Investigation and comparison of colon specificity of novel polymer khaya gum with guar gum. *Pakistan journal of pharmaceutical sciences*, 23(3), 259–65. Retrieved from <http://www.ncbi.nlm.nih.gov/pubmed/20566437>
20. Kshirsagar, S. J., Bhalekar, M. R., & Umap, R. R. (2009). *In vitro in vivo* comparison of two pH sensitive Eudragit polymers for colon specific drug delivery. *Journal of Pharmaceutical Sciences and Research*, 1(4), 61–70.
21. Shejawal, K. P., Randive, D. S., Bhinge, S. D., Bhutkar, M. A., Wadkar, G. H., Todkar, S. S., & Mohite, S. K. (2021). Functionalized carbon nanotube for colon-targeted delivery of isolated lycopene in colorectal cancer: *In vitro* cytotoxicity and *in vivo* roentgenographic study. *Journal of Materials Research*, 36(24), 4894–4907. <https://doi.org/10.1557/s43578-021-00431-y>
22. Bajaj, S., Singla, D., & Sakhuja, N. (2012). Stability testing of pharmaceutical products. *Journal of Applied Pharmaceutical Science*, 2(3), 129–138. <https://doi.org/10.7324/JAPS.2012.2322>
23. Pawar, P. K., & Gautam, C. (2016). Design, optimization and evaluation of mesalamine matrix tablet for colon drug delivery system. *Journal of Pharmaceutical Investigation*, 46(1), 67–78. <https://doi.org/10.1007/s40005-015-0214-z>
24. Dasankoppa, F., Patwa, S., Sholapur, H., & Arunkumar, G. (2012). Formulation and characterization of colon specific drug delivery system of prednisolone. *Saudi Journal for Health Sciences*, 1(3), 143. <https://doi.org/10.4103/2278-0521.106084>
25. Shedafa, R., Tibalinda, P., Manyanga, V., Sempombe, J., Temu, M., Masota, N., ... Bonsmann, C. (2016). Assessment of Moisture Permeability and Closure Systems of High Density Polyethylene Plastic Bottles Used as Primary Packaging Containers for Moisture Sensitive Medicines. *Pharmacology & Pharmacy*, 07(08), 321–325. <https://doi.org/10.4236/pp.2016.78039>
26. Shravani, D., Lakshmi, P. K., & Balasubramaniam, J. (2011). Preparation and optimization of various parameters of enteric coated pellets using the Taguchi L9 orthogonal array design and their characterization. *Acta Pharmaceutica Sinica B*, 1(1), 56–63. <https://doi.org/10.1016/j.apsb.2011.04.005>
27. Zhang, Y., Huo, M., Zhou, J., Zou, A., Li, W., Yao, C., & Xie, S. (2010). DDSolver: An Add-In Program for Modeling and Comparison of Drug Dissolution Profiles. *The AAPS Journal*, 12(3), 263–

-
271. <https://doi.org/10.1208/s12248-010-9185-1>
28. Pourtalebi Jahromi, L., Ghazali, M., Ashrafi, H., & Azadi, A. (2020). A comparison of models for the analysis of the kinetics of drug release from PLGA-based nanoparticles. *Heliyon*, 6(2), e03451. <https://doi.org/10.1016/j.heliyon.2020.e03451>
29. Romero, A. I., Villegas, M., Cid, A. G., Parentis, M. L., Gonzo, E. E., & Bermúdez, J. M. (2018). Validation of kinetic modeling of progesterone release from polymeric membranes. *Asian Journal of Pharmaceutical Sciences*, 13(1), 54–62. <https://doi.org/10.1016/j.ajps.2017.08.007>
30. Vora, C., Patadia, R., Mittal, K., & Mashru, R. (2013). Risk based approach for design and optimization of stomach specific delivery of rifampicin. *International Journal of Pharmaceutics*, 455(1–2), 169–181. <https://doi.org/10.1016/j.ijpharm.2013.07.043>

CHAPTER 6

Colon Targeted Pellets-based dosage form

CHAPTER 6

6. Colon Targeted Pellets-based dosage form

6.1 Experimental Methods

6.1.1 Preparation of Pellets dosage form

Budesonide (0.2 g), tamarind gum, microcrystalline cellulose (MCC), and lactose (q.s. to create 10 g) were thoroughly combined to form a homogenous powder. For uniformity, the powder mass would be passed through a 60-mesh sieve. The required quantity of water was added gently, and mixing was continued to achieve the desired consistency. Extrusion-spheronization was performed on the damp mass using an extruder (Make: Cronimach Machinery, Ahmedabad, Gujarat, India). The wet material was then extruded through a 1 mm mesh screen using an extruder to generate extrudate (needle-shaped). The extruded material was spheronized at 1,000 to 2,000 revolutions per minute using a spheronizer. The spheronization time ranged from 3 to 10 minutes. Different proportions of materials, equipment factors, and process parameters were used to determine the factors that influence pellet quality[1, 2].

6.1.2 Risk assessment

The primary benefit of risk assessment is the identification of CPPs and CMAs for selected CQAs in order to achieve the quality target product profile (QTPP) for the colon-targeted drug delivery system as per ICH Q8 R2 guideline[1, 3, 4].

Initially, the primary objective was to identify the CQAs for core pellets in order to achieve the pellets' quality and the desired drug release rate. Selected CQAs were aspect Ratio and particle size distribution, which reflect the quality of pellets in terms of sphericity, and the other was the percentage of drug release at 2 hours, which provides a general indication of the retardation of drug release in the upper portion of the gastrointestinal tract.

According to the ICH Q9 guideline, risk assessment consists of three steps: identification, analysis, and evaluation [5]. The primary objective of risk assessment was to identify risk factors that affect product quality. On the basis of the literature, previous work experience, and preliminary batch data, the Fishbone diagram was generated and potential identified risk parameters were arranged in a hierarchical fashion [6].

FMEA (Failure Mode and Effects Analysis), a risk management tool, was utilised to determine the RPN (risk priority number) for all potential risks [1, 7]. Multiplying S (severity), D (detectability), and P (probability) of risks yields the RPN.

The maximum value (5) denotes a prominent influence, while the minimum value (1) denotes no effect of a specific risk on the selected CQA [8]. A RPN value greater than 60 was used as a criterion for selecting factors for further research [6].

6.1.3 Screening of Pellets Parameters (Formulation and Process) by using 2^4 full factorial design

Based on the risk assessment data, amount of tamarind Gum, proportion of MCC in relation to lactose, speed of spheronizer, and time of spheronization were selected for further screening using 2^4 full factorial design. In this study, using design expert 11.0 (StatEase, Minneapolis, Minnesota (MN)) to build a four-factor, two-level full factorial design to assess the main, interaction, and quadratic effects of four components on selected responses, namely aspect ratio, particle size distribution, and % drug release at 2 hours [1], are outlined in Table 6.1.

In order to get the design space for attaining specified CQAs, a 2^4 Factorial design with 16 runs (factorial points) was used, as shown in Table 6.2 and 6.3.

Table 6.1: Dependent variables and independent variables with levels

Independent variables	levels		Dependent variables
	-1	+1	
A= Amount of Tamarind Gum	1	5	R1 = Aspect Ratio R2 = Particle Size Distribution (D50) R3 = % Drug Release at 2 Hrs
B= Proportion of MCC with respect to Lactose (%)	25	75	
C= Speed of Spheronizer	1000	1500	
D = Time for Spheronization	5	10	

Table 6.2: Experiment Batches as per 2⁴ factorial Design (FP1 TO FP8)

Ingredients	FP1	FP2	FP3	FP4	FP5	FP6	FP7	FP8
Budesonide	200 mg	200 mg	200 mg	200 mg	200 mg	200 mg	200 mg	200 mg
Tamarind Gum	1	5	1	5	1	1	1	5
MCC	25 %	75 %	75 %	75 %	75 %	25 %	75 %	75 %
Lactose	75 %	25 %	25 %	25 %	25 %	75 %	25 %	25 %
Total	10 gm	10 gm	10 gm	10 gm	10 gm	10 gm	10 gm	10 gm
Process Parameters								
Water- wet plastic mass	6 mL	6mL	6 mL	6 mL	6mL	6 mL	6mL	6 mL
Speed of Spheronizer	1000	1000	1500	1500	1000	1500	1000	1000
Spheronization Time	10	5	5	10	10	10	5	10

Table 6.3: Experiment Batches as per 2⁴ factorial Design (FP1 TO FP8)

Ingredients	FP9	FP10	FP11	FP12	FP13	FP14	FP15	FP16
Budesonide	200 mg	200 mg	200 mg	200 mg	200 mg	200 mg	200 mg	200 mg
Tamarind Gum	5	5	5	5	1	5	1	1
MCC	75 %	25 %	25 %	25 %	75 %	25 %	25 %	25 %
Lactose	25 %	75 %	75 %	75 %	25 %	75 %	75 %	75 %
Total	10 gm	10 gm	10 gm	10 gm	10 gm	10 gm	10 gm	10 gm
Process Parameters								
Water- wet plastic mass	6 mL	6mL	6 mL	6 mL	6mL	6 mL	6mL	6 mL
Speed of Spheronizer	1500	1500	1000	1000	1500	1500	1000	1500
Spheronization Time	5	10	5	10	10	5	5	5

6.1.3.1 Aspect Ratio of Pellets.

The sphericity or aspect ratio (AR) of pellets may be used to identify their shape. In this research, the overall shape of pellets was measured by determining their aspect ratio. Using digital vernier callipers, the diameter of a pellet was recorded in different directions, with the largest diameter being labelled as the Feret maximum. Feret minimum refers to the diameter measured at right angles to the feret maximum[1, 2].

The AR of the prepared pellet is calculated as follows:

$$\text{Aspect Ratio} = \frac{\text{Feret maximum}}{\text{Feret minimum}}$$

6.1.3.2 Average Particle size.

Using sieve analysis, the particle size distribution of dry pellets was determined. Each sample was shaken for 5 minutes using a sieve shaker with seven standard sieves ranging in size from 180 to 1700 μm . The D50, or Median diameter, was evaluated as a measure of particle Size distribution by plotting the percentage of pellet weight retained vs. sieve pore size [1]. D50, the Median diameter, and established criteria for attaining the desired and consistent pellet size were calculated[5].

6.1.3.3 In-vitro drug release at 2 hours

The dissolution study was carried out using the USP (United State Pharmacopeia) paddle apparatus. Pellets were introduced in 0.1 N HCl for 2 hours with a speed of 50 rpm at $37 \pm 0.5^\circ\text{C}$ in 900 ml of dissolution medium. At 2-hour intervals, a 5-ml sample was withdrawn from dissolving vessels and examined spectrophotometrically at 242 nm wavelength[9].

6.1.4 Coating of Pellets

In order to prevent release of drugs in the upper gastrointestinal (GI) tract and facilitate drug release specifically in the colonic area for targeted delivery, pellets were produced utilizing an experimental design and afterwards coated with an enteric polymer. Polymers containing methacrylic acid groups are often suggested for facilitating targeted administration to the

colon[1, 5, 10]. In the present study, the pellets were subjected to a coating process using Eudragit S 100, an agent having a pH threshold of 7[10, 11].

Table 6.4 displays the coating solution's composition. In the present study, pellets were coated using the pan coating process, and the optimal process parameters for pellet coating are shown in Table 6.5.

Table 6.4: Composition of enteric polymer Coating Solution

Ingredients	Quantity for 100 ml
Eudragit S100	5 gm
Talc	1%
TEC (Tri-ethyl citrate)	0.625 gm
Color	q.s
Acetone	50 ml
IPA	50 ml

Table 6.5: Process Parameters for pan coating of pellets

Parameter	Condition
Inlet temperature (°C)	50-55
Spray rate (mL min ⁻¹)	0.7
Atomizing air (bar)	2
Pan speed (rpm)	35-40
Gun to Bed Distance	30 cm

The pellet coating procedure was as follows:

- The required quantities of pellets, along with some excess pellets were fed into the coating pan and rotated at a speed of 40 revolutions per minute for 5 minutes. Pellets, were then subjected to de-dusting, and a fixed quantity of pellets were loaded for coating.
- The pan rpm was set at 40, and the temperature was adjusted to 50°C.
- For the appropriate coating, the peristaltic pump was used to adjust the previously optimized spray rate.
- Pellet coating was continued until the desired percentage weight gain was attained[12].

6.1.5 Formulation optimization by using Box-Behnken Factorial Design

The process parameters and formulation parameters for pellets were optimized using a 2^4 -factorial design. Subsequently, a Box-Behnken Design (Design Expert 11.0) was used to optimize pellets for colonic delivery. This design consisted of three factors with three levels each, allowing for the identification of main, interaction, and quadratic effects.[6, 13]

The study investigated the impact of various independent variables, including the quantity of tamarind gum, the proportion of MCC in relation to lactose, and the percentage weight gain by Eudragit S100, on the dependent variables of concern. These dependent variables were the percentage of drug release at 2 hours, 5 hours, and 9 hours.

The corresponding data for these variables can be found in Table 6.6. The experimental batches designed using the Box-Behnken design approach are presented in Table 6.7 and 6.8.

Table 6.6 Independent variables and Dependent variables of Box Behnken design

Independent variables	Levels			Dependent variables
	-1	0	+1	
X1= Amount of Tamarind Gum	2	2.5	3	Y2 = % Drug Release at 2 Hrs
X2= MCC proportion (%)	30	35	40	Y5 = % Drug Release at 5 Hrs
X3= % wt. Gain by Eudragit S100	2.5	5	7.5	Y9 = % Drug Release at 9 Hrs

Table 6.7: Experimental batches as per Box-Behnken Design (F1 to F8)

Ingredients	F1	F2	F3	F4	F5	F6	F7	F8
Budesonide	200 mg	200 mg	200 mg	200 mg	200 mg	200 mg	200 mg	200 mg
Tamarind Gum	2.5	2.5	2.5	3	3	2.5	2	2.5
MCC	35%	40%	35%	35%	35%	40%	30%	35%
Lactose	65 %	60 %	65 %	65 %	65 %	60 %	70 %	65 %
Total	10 gm	10 gm	10 gm	10 gm	10 gm	10 gm	10 gm	10 gm
Coating of Pellets by Eudragit S100								
% Weight Gain	5	7.5	5	2.5	7.5	2.5	5	5

Table 6.8: Experimental batches as per Box-Behnken Design (F1 to F8)

Ingredients	F9	F10	F11	F12	F13	F14	F15
Budesonide	200 mg	200 mg	200 mg	200 mg	200 mg	200 mg	200 mg
Tamarind Gum	2.5	2	2	2.5	2	3	3
MCC	30%	40%	35%	30%	35%	40%	30%
Lactose	70 %	60 %	65 %	70 %	65 %	60 %	70 %
Total	10 gm	10 gm	10 gm	10 gm	10 gm	10 gm	10 gm
Coating of Pellets by Eudragit S100							
% Weight Gain	2.5	5	2.5	7.5	7.5	5	5

6.1.6 Dissolution Method

In-vitro drug release of colon-specific Budesonide pellets was conducted in a USP Type II (Paddle) apparatus at a rotation speed of 50 rpm and at 37 ± 0.5 °C. Initially, the test was done in 0.1 N HCl for 2 hours to mimic the environment of stomach [14]. The test was then conducted for three hours in phosphate buffer pH 7.4, which mimics the milieu of the small

intestine [14]. In reality, the small intestine can be categorized into three distinct segments: the duodenum, which exhibits a pH range of 5 to 6; the jejunum, with a pH of approximately 6.63 ± 0.53 ; and the ileum, which maintains a pH level of around 7.49 ± 0.46 . The ileum is the longest section of the small intestine, and as a result, its mean pH is 7.3 ± 0.34 [15, 16]. The remaining investigation was conducted in biorelevant medium with a pH of 6.8, which is comparable to the mean pH of the large intestine (6.63 ± 0.04) [15, 16], and CO₂ aeration to create a favourable environment for anaerobic bacteria [17]. Samples were extracted at regular intervals and analysed spectrophotometrically at a wavelength of 242 nm.

6.1.7 Release kinetics of the formulations prepared by the experimental design

Dissolution investigations give significant insights into the profile of drug release, and numerous mathematical kinetic models have been established for the purpose of investigating drug release kinetics [18].

Various mathematical models are commonly used to characterize the process of drug release. The Hixon-Crowell model, the Higuchi model, first-order kinetics, and zero-order kinetics are among these models. In addition, the Weibull model and the Korsmeyer-Peppas model are frequently applied to the analysis of the mechanism of drug release [19].

Kinetic models can be employed to characterize the dissolution of drugs from solid dosage forms. In such models, the amount of drug dissolved (C) is represented as a function of the test time (t), denoted as $C=f(t)$ [20–22]. In current Study, DD-solver, Excel Add-in was used to determine the parameters of the mathematical models.

6.1.8 In vivo study

6.1.8.1 Animals and ethical approval

Eight weeks old male Wister rats weighting 250-280 g were acquired from ZyduS research centre, Ahmedabad, India. Animals were housed at animal house of L. J. Institute of Pharmacy, Ahmedabad, under controlled environmental conditions ($25^{\circ}\text{C} \pm 2^{\circ}\text{C}$ temperatures, $55 \pm 5\%$ humidity and 12 h light/dark cycle) for 2 weeks prior to study. Animals had free access to food and water throughout the study period. The study was approved by Institutional Animal Ethics Committee of L. J. Institute of Pharmacy with protocol number LJIP/IAEC/2022-23/02. All experimental procedures were conducted as per Committee for Control and Supervision of Experiments on Animals

(CCSEA) guidelines.

6.1.8.2 Induction of ulcerative colitis

Ulcerative colitis was induced as per the method described by Mousavizadeh et al [25] with modifications. Post overnight fasting, under light isoflurane anesthesia rats were administered 2 mL of 4% acetic acid solution rectally using a catheter (6 FG; 2 mm diameter) as shown in Figure 6.1. The tip of catheter was inserted up to 8 cm proximal to anus verge. Post administration, rats were maintained in supine Trendelenburg position for 1 min to prevent colonic acetic acid leakage and spread to other area. Post colitis induction animals were observed for diarrhoea. Animals with soft stool were selected and divided in various groups as shown below.

Post 24 hours of colitis induction, animals were treated with respective formulations as shown below for 5 days. Twenty-four hours after administration of the last dose of formulation, rats were sacrificed with high dose of isoflurane. The colon was removed, washed with ice-cold saline and used for histopathological examination and biochemical studies.

The rats were divided into seven groups (Figure 6.2) containing eight animals in each group as follows:

1. **Control group:** Received saline orally
2. **Sham Operated group:** Received 2 mL normal saline rectally
3. **Disease Control group:** Received 2 mL of acetic acid solution rectally (to induce colitis)
4. **Gum Treated group:** Post colitis induction received gum solution without drug orally.
5. **Test I group:** Post colitis induction received Budesonide pellets in 1% CMC solution (200 µg) orally
6. **Test II group:** Post colitis induction received Budesonide pellets in 1% CMC solution (300 µg) orally
7. **Standard group:** Post colitis induction received Marketed Budesonide pellets in 1% CMC solution (300 µg) orally



Figure 6.1: Catheter (Size: 6FG) used for instillation of 4% acetic acid in rectal cavity of rat

Dose Calculation:

Oral dose of Budesonide (Human): 9 mg/70Kg

Human dose per Kg: 9mg/70Kg

: 0.129 mg/Kg

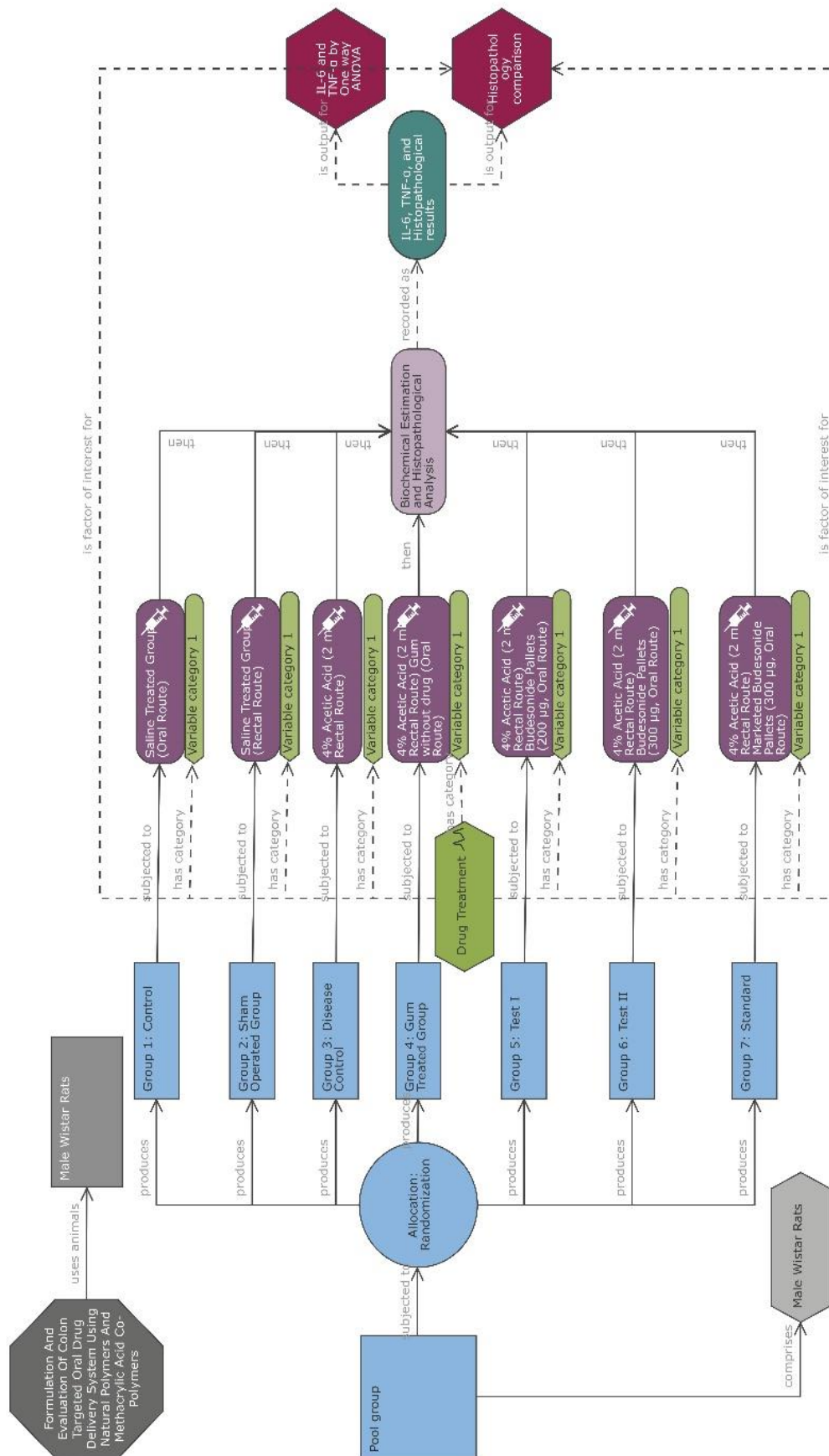
Rat dose per Kg: 0.129×6.2 (conversion Factor):

: 0.799 mg/Kg \approx 0.800 mg/Kg

Rat dose per 250 g (Standard weight of rat) = 0.319 mg \approx 0.300 mg = 300 μ g

6.1.8.3 Histopathological evaluation

The colon pieces were immersed in a solution of 10% neutral buffered formalin and allowed for fixation for 5 days. The colonic samples for histopathology were prepared using microtome; tissue was sectioned and fixed in paraffin wax blocks. The tissues underwent staining with haematoxylin and eosin, followed by mounting and microscopic observation to assess histological alterations. This evaluation was conducted by a pathologist in a blinded manner.



6.1.8.4 Preparation of tissue homogenate for biochemical estimation

Biochemical estimation including IL-6 and TNF- α was performed using colonic tissue homogenate. Tissue pieces weighed and then homogenized in phosphate buffer saline (tissue weight (g): PBS (mL) volume=1:9) with a glass homogenizer. To further breakdown the cells, suspension was subject it to freeze-thaw cycles. The homogenate was then centrifuged for 5-10 min at 5000 \times g at 2-8 °C to get the supernatant which was used for biochemical estimation.

Determination of TNF- α , and IL-6 levels

Inflammatory cytokines are known to play a crucial role in modulating mucosal immune system where the neutrophils and macrophages are responsible for disrupting epithelial integrity and causing colon injury. TNF- α and IL-6 levels in colonic supernatant were quantified using enzyme-linked immunosorbent assay (ELISA) (Sandwich Method). The results were expressed as pg/mL.

Reagent preparation

1. All reagents were brought to room temperature (18-25°C).
2. Wash Buffer: To prepare ash buffer 30 mL of concentrated wash buffer (provided with kit) was diluted up to 750 mL using distilled water.
3. Standard Working Solution: Post centrifugation (10,000 \times g for 1 min) of standard (provided with kit), 1.0 mL of reference standard and sample diluent was added and allowed to stand for 10 min. So prepared solution was mixed thoroughly using pipette. This reconstitution produced a working solution of 5000 pg/mL. Using serial dilution method concentrations including 5000, 2500, 1250, 625, 312.500, 156.250, 78.13, 0 pg/mL were prepared.
4. Biotinylated Detection Ab working solution: Required amount of solution was fixed before experiment (100 μ L/well). Concentrated Biotinylated Detection Ab was centrifuged at 800 \times g for 1 min, then diluted the 100 \times Concentrated Biotinylated Detection Ab to 1 \times working solution with Biotinylated Detection Ab Diluent (Concentrated Biotinylated Detection Ab: Biotinylated Detection Ab Diluent= 1: 99).
5. Concentrated HRP Conjugate working solution: Concentrated HRP Conjugate was centrifuged at 800 \times g for 1 min, then diluted the 100 \times Concentrated HRP Conjugate to 1 \times

working solution with HRP Conjugate Diluent (Concentrated HRP Conjugate: HRP Conjugate Diluent= 1: 99).

Assay procedure

1. Determined wells for diluted standard, blank and sample. Added 100 μ L each dilution of standard, blank and sample into the appropriate wells. Covered the plate with the sealer provided in the kit. Incubated for 90 min at 37°C.
2. Decanted the liquid from each well. Immediately added 100 μ L of Biotinylated Detection Ab working solution to each well. Covered the plate with a new sealer. Incubated for 1 hour at 37°C.
3. Decanted the solution from each well, added 350 μ L of wash buffer to each well. Soaked for 1 min and aspirated the solution from each well and pat it dry against clean absorbent paper. Repeated wash step 3 times.
4. Added 100 μ L of HRP Conjugate working solution to each well. Covered the plate with a new sealer. Incubated for 30 min at 37°C.
5. Decanted the solution from each well, repeated the wash process for 5 times as conducted in step 3.
6. Added 90 μ L of Substrate Reagent to each well. Covered the plate with a new sealer. Incubated for about 15 min at 37°C.
7. Added 50 μ L of Stop Solution to each well.
8. Determined the optical density (OD value) of each well at once with a micro-plate reader set to 450 nm.

6.1.9 Roentgenography study

The gastrointestinal transit of optimized formulation was assessed using White New Zealand Rabbits weighing between 1.5 and 2.5 kg[23]. The rabbits were fasted overnight prior to the administration of pellets. The pellets in capsule were carefully positioned in the animal's larynx using forceps, and a volume of 10-15 mL of water was administered down the neck to aid its passage into the oesophagus[24]. Post oral administration, rabbits were subjected to X-ray examination at predetermined time intervals to monitor the movement of the formulations through the GI tract[10, 25, 26].

6.1.10 Stability Study

In the present study, the optimal batch (F12) from the Box Behnken Design was chosen for the stability study, which was conducted in accordance with ICH (International Council on Harmonisation) guidelines by keeping the sample at 40 ± 2 °C and 75 ± 5 % RH for six months in a stability Chamber (Mfg.: Patel Instrument Pvt. Ltd., Ahmedabad, Gujarat, India) [27–29]. A high-density Polyethylene bottle is the container closure system used in this study. The selected study intervals were the 1st, 3rd, and 6th months from the Initial time. The optimized pellet-based formulation was examined for appearance (description), moisture content, drug content, % CDR (cumulative drug release) at 5 Hours, friability, and microbial limit test [30].

6.2. Result and Discussion

6.2.1 Risk assessment study for core pellets

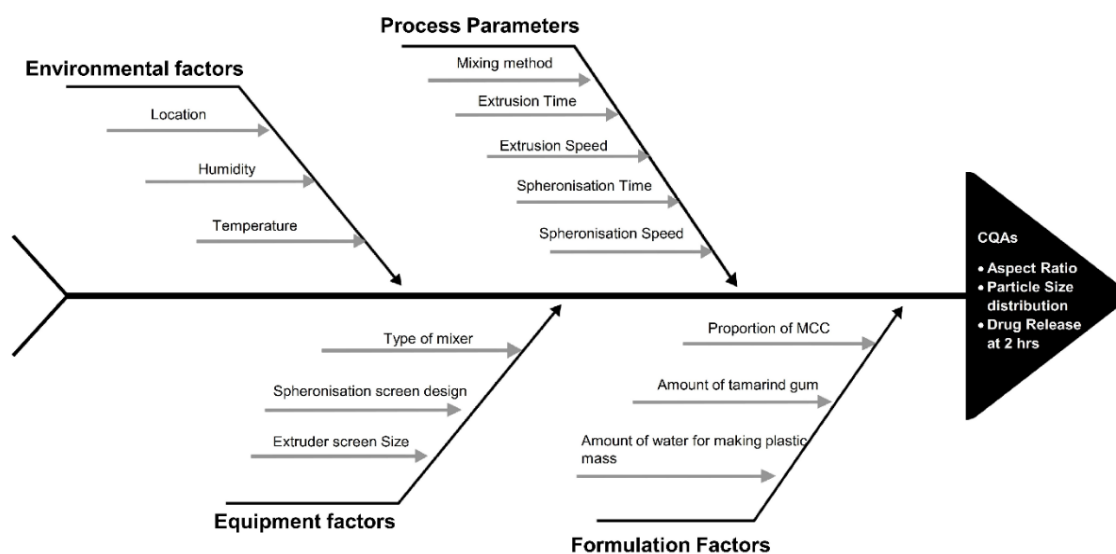


Figure 6.3: A Fishbone diagram illustrating factors that may have impact on the critical quality attributes (CQA)

Fig. 6.3 depicts a fishbone diagram for all potential risk factors, which reveals that formulation parameters and process parameters are more significant than equipment and environment factors [6]. Influence of environmental and equipment factors shown less significant because a research work was conducted at fixed laboratory setup.

The RPN scores for all potential risk factors, which were calculated by multiplying the S, D, and P of individual risk factors, are reflected in Table 6.9 and summarised in Figure 6.4,

indicating that five risk factors, the amount of tamarind gum, the ratio of MCC to lactose, the spheronizer speed, the spheronisation time, and the amount of water required to create plastic mass, have a significant impact on CQAs. On the basis of preliminary batches, it was determined that 6 ml was sufficient for all formulations; consequently, it was chosen as a constant variable for further research.

Table 6.9: RPN score of possible risk factors by Initial risk assessment study

Risk factors	S (severity)	D (detectability)	P (probability)	RPN Score
Proportion of MCC	4	4	5	80
Amount of tamarind gum	5	5	4	100
Amount of water for making plastic mass	5	4	3	60
Spheronisation Speed	4	5	4	80
Spheronisation Time	4	4	4	64
Extrusion Speed	4	3	3	36
Extrusion Time	4	2	3	24
Mixing method	3	2	3	18
Extruder screen Size	2	3	3	18
Spheronisation screen design	4	2	3	24
Type of mixer	2	2	3	12
Humidity	2	2	2	8
Temperature	2	1	1	2
Location	1	1	1	1

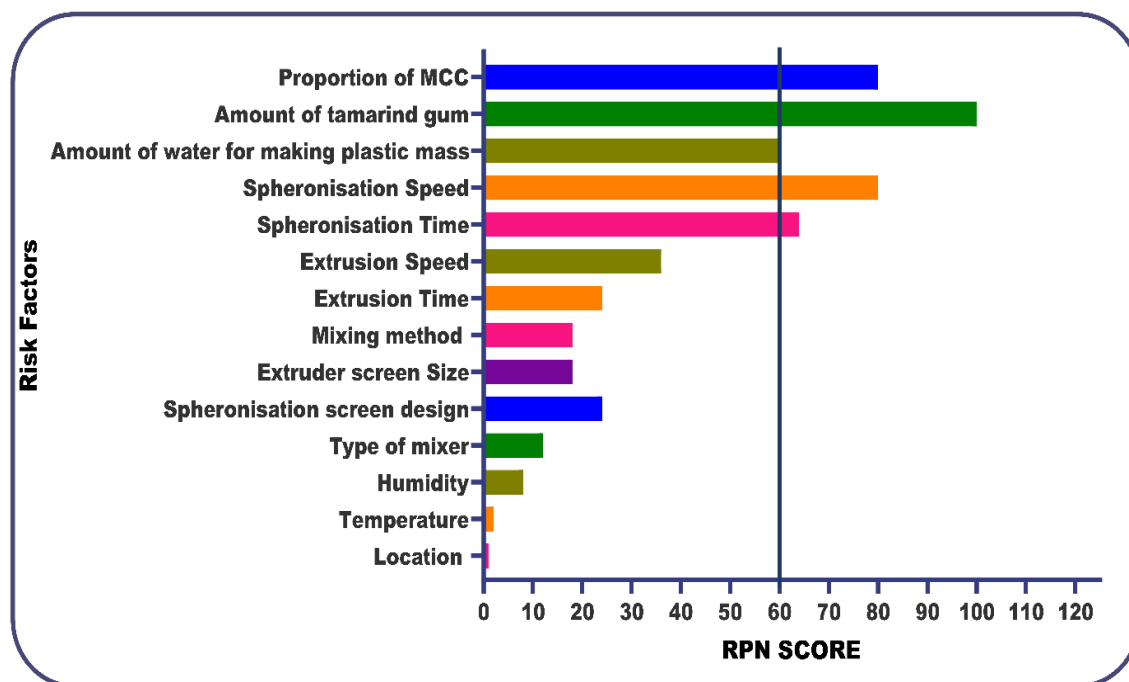


Figure 6.4: RPN score after FMEA risk assessment. RPN threshold of 60 was considered for selection of risk factor as potential high-risk factor.

6.2.2 Influence of formulation parameters and process parameters on dependent variables by using 2^4 screening factorial Design for core pellets

Table 6.10: Experimental runs obtained from 2^4 Factorial design and their responses.

Ru n	A: Amount of Tamarin d gum	B: %MCC	C: Spheronizat ion speed	D: time of Spheronizati on	Y1: aspect ratio	Y2: Particle size distribu tion	Y3: % CDR at 2 hrs
1	1	25	1000	10	1.07	1.123	33.08
2	5	75	1000	5	1.23	1.325	31.23
3	1	75	1500	5	1.01	1.03	40.32
4	5	75	1500	10	1.17	1.213	29.73
5	1	75	1000	10	1.03	1.092	44.19
6	1	25	1500	10	1.06	1.088	28.15
7	1	75	1000	5	1.01	1.075	42.23
8	5	75	1000	10	1.23	1.229	30.12
9	5	75	1500	5	1.2	1.201	30.32

10	5	25	1500	10	1.29	1.421	8.21
11	5	25	1000	5	1.34	1.51	9.17
12	5	25	1000	10	1.3	1.35	11.14
13	1	75	1500	10	1	1.03	44.34
14	5	25	1500	5	1.32	1.432	7.83
15	1	25	1000	5	1.1	1.129	31.33
16	1	25	1500	5	1.08	1.091	29.12

Utilizing a 2^4 full factorial design, the influence of various parameters on achieving the CQAs of core pellets was analysed. Table 6.10 presents the value of dependent variables for core pellets prepared using an experimental design. The aspect ratio of core pellets from batches 1 to 16 varied from 1 to 1.34, demonstrating that formulation and process variables had an effect on aspect ratio. Average particle diameters ranged from 1.03 mm to 1.51 mm, and % drug release at 2 hours ranged from 8.21 ± 1.45 to 44.34 ± 1.78 , indicating the impact of independent variables on the same.

6.2.2.1 Aspect Ratio of Pellets

Table 6.11 represents the value of Aspect ratio of all factorial batches prepared as per 2^4 factorial designs.

Values of the aspect ratio greater than 1 indicate pellets with a relatively elongated or rod-like shape, whereas values close to 1 indicate pellets with a spherical shape.

According to the pareto chart presented in Fig. 6.5, input factors like the amount of tamarind gum and the ratio of MCC to lactose have a greater influence on the aspect ratio than the spheronization speed and the time required for spheronization.

Table 6.11: Aspect ratio of all factorial batches

Batch	Aspect Ratio	Batch	Aspect Ratio
1	1.07	9	1.2
2	1.23	10	1.29
3	1.01	11	1.34
4	1.17	12	1.3
5	1.03	13	1
6	1.06	14	1.32

7	1.01	15	1.1
8	1.23	16	1.08

Design-Expert® Software

Aspect Ratio

A: Tamarind

B: MCC

C: spheronizer Speed

D: Time

Positive Effects

Negative Effects

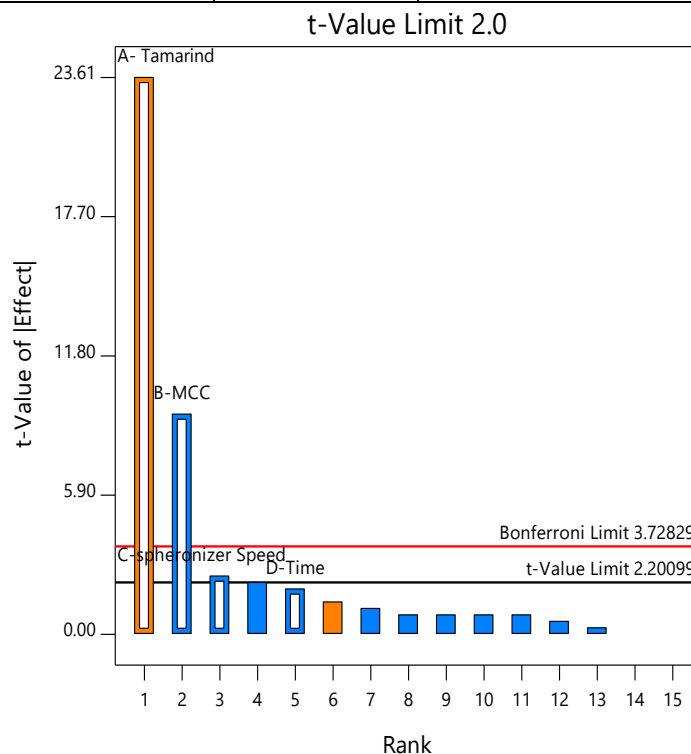


Figure 6.5: Pareto Charts for Aspect Ratio

The significance of the model is based on a considerably greater F-value, minimal variation between the adjusted and predicted R^2 values, and a significantly adequate precision value. Based on the data shown in Table 6.12, it was revealed that models can significantly explore design space.

Table 6.12: Analysis of variance for the Aspect Ratio (dependent variable)

Source	Sum of Squares	df	Mean Square	F-value	p-value	
Model	0.2170	4	0.0543	163.53	< 0.0001	significant
A-Tamarind gum	0.1849	1	0.1849	557.23	< 0.0001	
B-MCC	0.0289	1	0.0289	87.10	< 0.0001	
C-Spheronizer Speed	0.0020	1	0.0020	6.10	0.0311	
D-Time	0.0012	1	0.0012	3.69	0.0810	
Residual	0.0037	11	0.0003			

R ²	0.9835
Adjusted R ²	0.9774
Predicted R ²	0.9650
Adeq Precision	33.3890

According to ANOVA (Analysis of Variance) results, two variables have a substantial influence on the aspect ratio of pellets: the amount of tamarind gum ($P \leq 0.0001$) and the percentage of MCC ($P \leq 0.0001$), while spheronizer speed ($P = 0.0311$) has a marginal impact. Thus, the model retains factors A, B, and C.

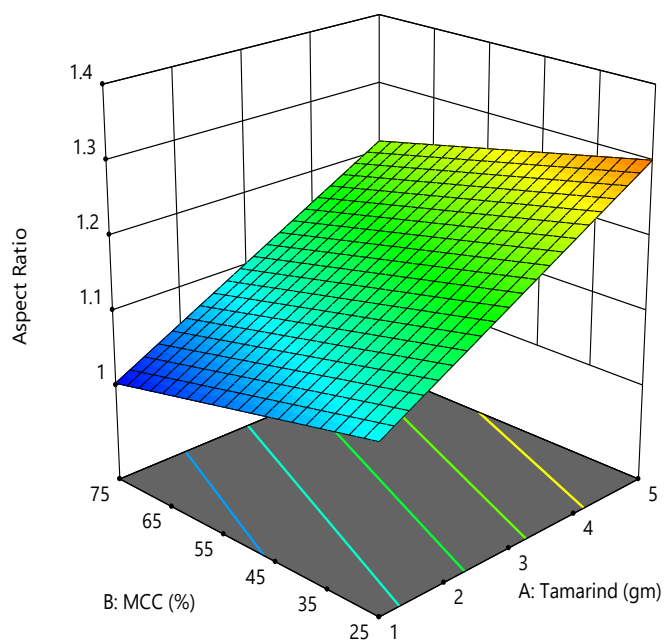
$$\text{Aspect Ratio} = 1.1525 + 0.1075 * A - 0.0425 * B - 0.01125 * C - 0.0087 * D$$

Design-Expert® Software
Factor Coding: Actual

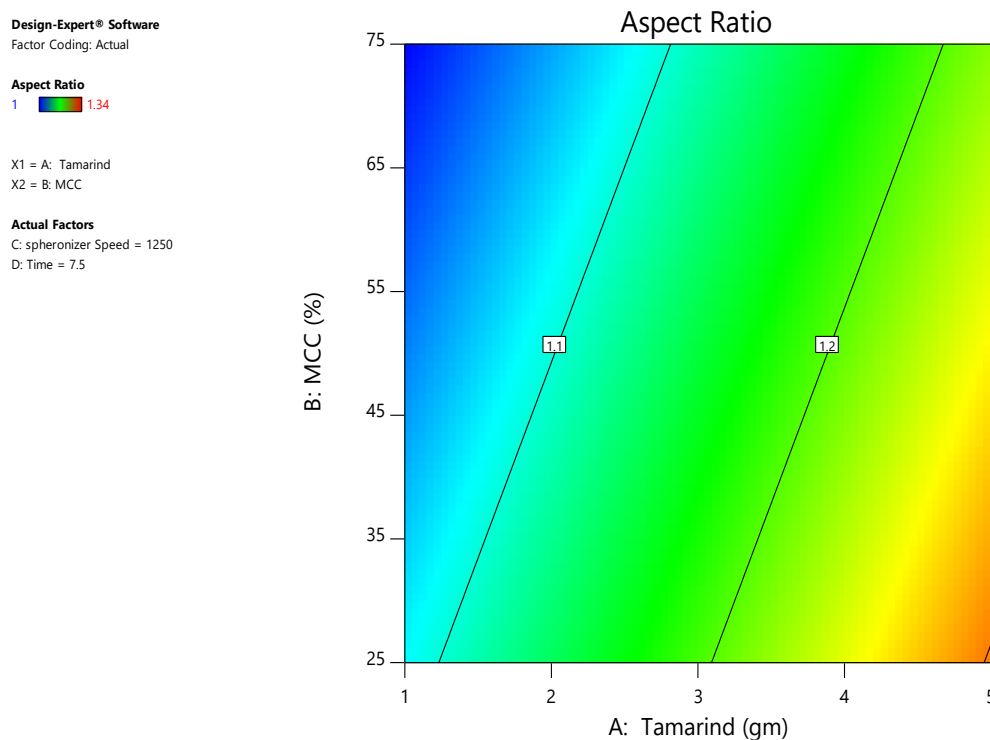
Aspect Ratio
1 1.34

X1 = A: Tamarind
X2 = B: MCC

Actual Factors
C: spheronizer Speed = 1250
D: Time = 7.5



(a)



(b)

Figure 6.6: 3D Response Graph (a) and Contour Plot (b) for Aspect Ratio

According to the 3D response graph (Fig. 6.6a) and contour plot (Fig. 6.6b) for aspect ratio, it can be inferred that as the amount of tamarind gum is increased, the aspect ratio will rise. However, when the aspect ratio exceeds 1.2, it is not suitable and indicates that sphericity is compromised, resulting in the formation of rod-shaped pellets. The aspect ratio reaches near 1 when the proportion of MCC increases in relation to lactose and the desired sphericity is attained. The same conclusion can be drawn from the data in Table 8, which shows that reducing the quantity of tamarind gum and increasing the fraction of MCC relative to lactose will result in an aspect ratio that is close to 1. Changing the spheronization speed between 1000 and 1500 rpm has little effect on the aspect ratio value. Observations indicate that raising the spheronization time from 5 to 10 minutes has no appreciable effect on the aspect ratio value of the pellets.

6.2.2.2 Particle size distribution

The particle size distribution was evaluated using the mean pellet diameter (D50). Table 6.13 represents D50 values for all factorial batches.

According to the pareto chart shown in Figure 6.7, the amount of tamarind gum and the ratio of MCC to lactose have a greater impact on the D50 than the spheronization speed and time required for spheronization. The D50, a measure of particle size distribution, should fall within the range of 1 to 1.3 for size uniformity.

Table 6.13: Particle Size Distribution data of batches as per 2^4 factorial designs

Batch	D50	Batch	D50
1	1.123	9	1.201
2	1.325	10	1.421
3	1.03	11	1.51
4	1.213	12	1.35
5	1.092	13	1.03
6	1.088	14	1.432
7	1.075	15	1.129
8	1.229	16	1.091

Design-Expert® Software

Particle size Distribution

A: Tamarind
B: MCC
C: spheronizer Speed
D: Time

Positive Effects
Negative Effects

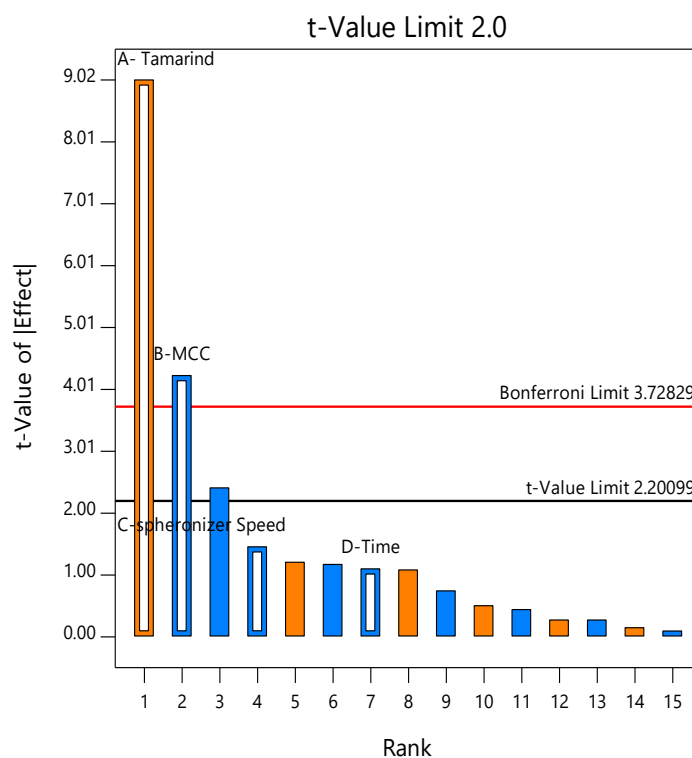


Figure 6.7: Pareto Charts for Particle Size Distribution

Table 6.14: Analysis of variance for the Particle size distribution (dependent variable)

Source	Sum of Squares	df	Mean Square	F-value	p-value	
Model	0.3226	4	0.0806	25.63	< 0.0001	significant
A- Tamarind	0.2558	1	0.2558	81.29	< 0.0001	
B-MCC	0.0563	1	0.0563	17.89	0.0014	
C-spheronizer Speed	0.0067	1	0.0067	2.12	0.1730	
D-Time	0.0038	1	0.0038	1.21	0.2945	
Residual	0.0346	11	0.0031			
R ²			0.9031			
Adjusted R ²			0.8679			
Predicted R ²			0.7950			
Adeq Precision			14.1356			

The Model is significant based on F-value of 25.63. A and B are important model terms in this case based on the P-value of those terms.

The predicted R² and the adjusted R² have minimal differences, as shown in Table 6.14, indicating that they correlate to one another. The ratio of signal to noise is 14.136, which is good. As a result, this model may be used to explore design space.

According to ANOVA results, two variables have a significant effect on the mean pellet diameter (D50) of pellets: the amount of tamarind gum ($P \leq 0.0001$) and the percentage of MCC ($P \leq 0.0001$). Thus, the model retains Factors A and B.

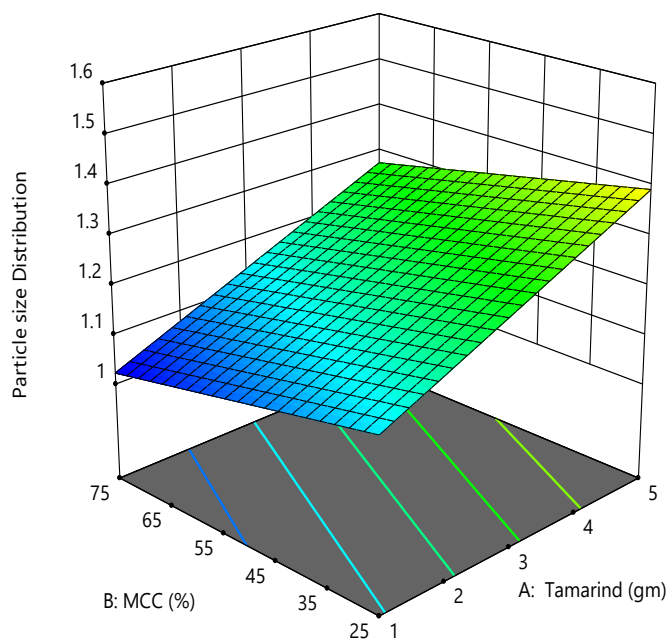
$$\text{Particle size distribution} = 1.20869 + 0.126438 * A - 0.0593125 * B$$

Design-Expert® Software
Factor Coding: Actual

Particle size Distribution
1.03 1.51

X1 = A: Tamarind
X2 = B: MCC

Actual Factors
C: spheronizer Speed = 1250
D: Time = 7.5



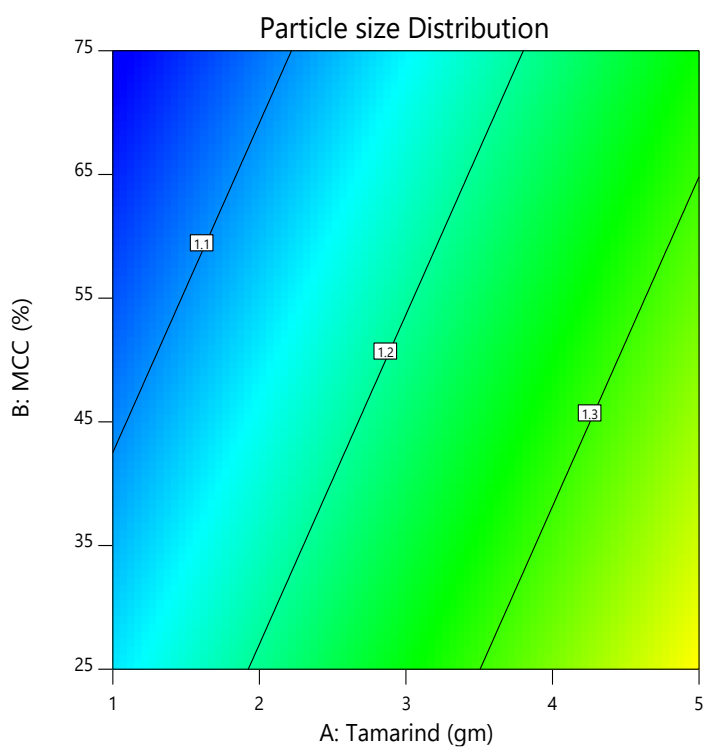
(a)

Design-Expert® Software
Factor Coding: Actual

Particle size Distribution
1.03 1.51

X1 = A: Tamarind
X2 = B: MCC

Actual Factors
C: spheronizer Speed = 1250
D: Time = 7.5



(b)

Figure 6.8: 3D Response Graph (a) and Contour Plot (b) for Particle size Distribution

Based on the 3D response graph (Fig. 6.8a) and contour plot (Fig. 6.8b), it was determined that as the amount of tamarind gum increased, the uniformity of size of the pellets decreased and their variation increased, and as the percentage of MCC increased in relation to lactose, the uniformity of size of the pellets increased, as predicted by the D50, whose value falls between 1 and 1.3. The identical results reported from the data interpretation of table 8 indicate that the desired D50 may be reached by decreasing the quantity of tamarind gum in the formulation and increasing the percentage of MCC relative to lactose. Spheronization speed between 1,000 and 1,500 rpm and spheronization time between 5 and 10 minutes showed negligible effects.

6.2.2.3 Percentage Cumulative Drug Release (% CDR) at 2 Hrs.

% Cumulative drug release at 2 hours for the factorial batches prepared as per 2^4 factorial design were shown in Table 6.15.

Table 6.15: % CDR at 2 hours for of the batches as per 2^4 factorial designs

Batch	%CDR	Batch	%CDR
1	33.08±1.02	9	30.32±1.23
2	31.23±1.89	10	8.21±1.45
3	40.32±2.01	11	9.17±1.33
4	29.73±1.34	12	11.14±2.11
5	44.19±2.11	13	44.34±1.78
6	28.15±1.01	14	7.83±2.12
7	42.23±2.29	15	31.33±2.81
8	30.12±2.12	16	29.12±2.53

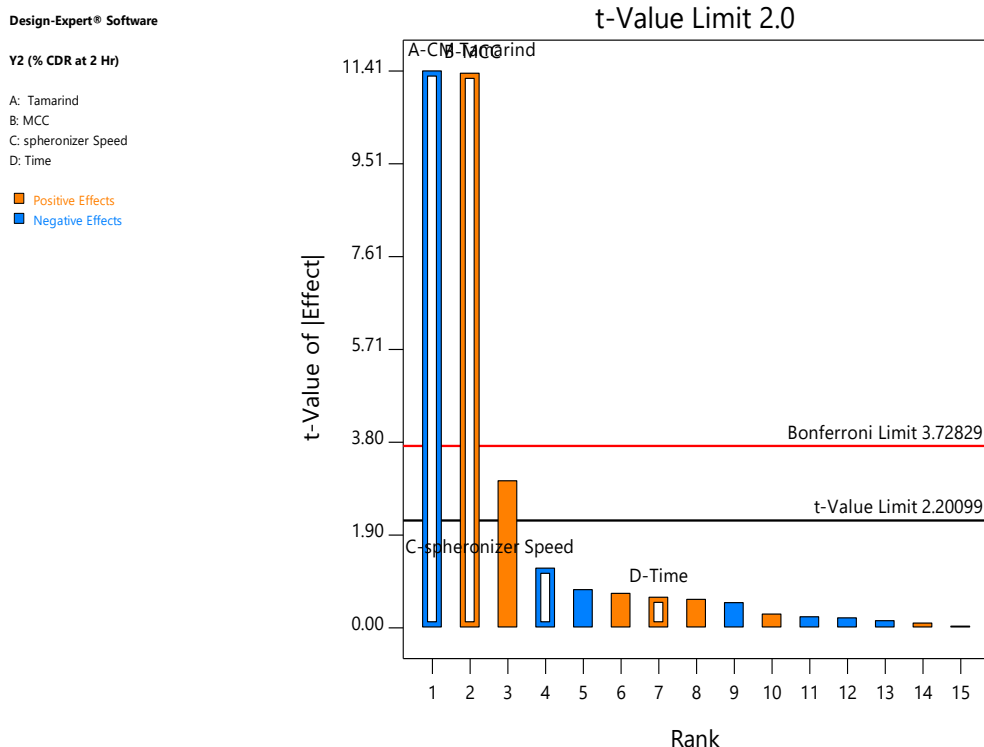


Figure 6.9: Pareto Charts for % CDR at 2 hours

As per the Pareto chart (Figure 6.9), it was concluded that as the factors A and B have a significant higher value than the Bonferroni limit (3.728), they have confirmed significant effect on the % CDR at 2 hrs. The factor D had lower value than the T-value limit (2.2), indicating that it is having confirmed non-significant effect. Whereas, Factor C having value between Bonferroni and T-value limits may or may not have significant effect on the outcome. Thus, the factors A & B were considered as significant factors for further study and factors C (spheronization speed) and D (spheronization time) were kept constant.

Table 6.16: Analysis of variance for the % cumulative drug release at 2 hours (dependent variable)

Source	Sum of Squares	df	Mean Square	F-value	p-value	
Model	2285.55	4	571.39	65.32	< 0.0001	significant
A- Tamarind	1139.23	1	1139.23	130.24	< 0.0001	
B-MCC	1129.80	1	1129.80	129.16	< 0.0001	
C-spheronizer Speed	13.09	1	13.09	1.50	0.2468	

D-Time	3.43	1	3.43	0.3923	0.5439	
Residual	96.22	11	8.75			
R ²	0.9596					
Adjusted R ²	0.9449					
Predicted R ²	0.9145					
Adeq Precision	22.0267					

Table 6.16 showed the Model F-value, predicted R², adjusted R², and adequate precision, indicating that the model has considerable predictive power and can be employed to explore the design space.

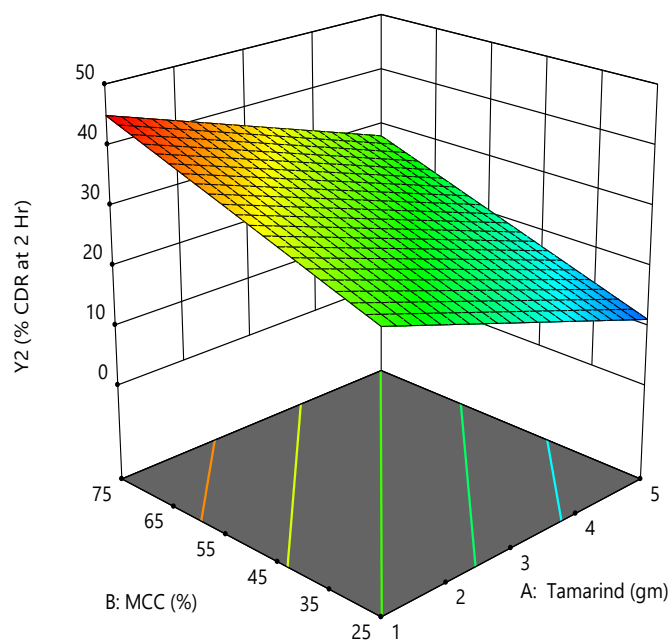
Core pellets would undergo enteric coating for colonic delivery; hence, core pellets should not release more than 25% of the formulation's drug. According to this criterion, it was observed that the quantity of tamarind and MCC has a crucial effect on retardation.

Design-Expert® Software
Factor Coding: Actual

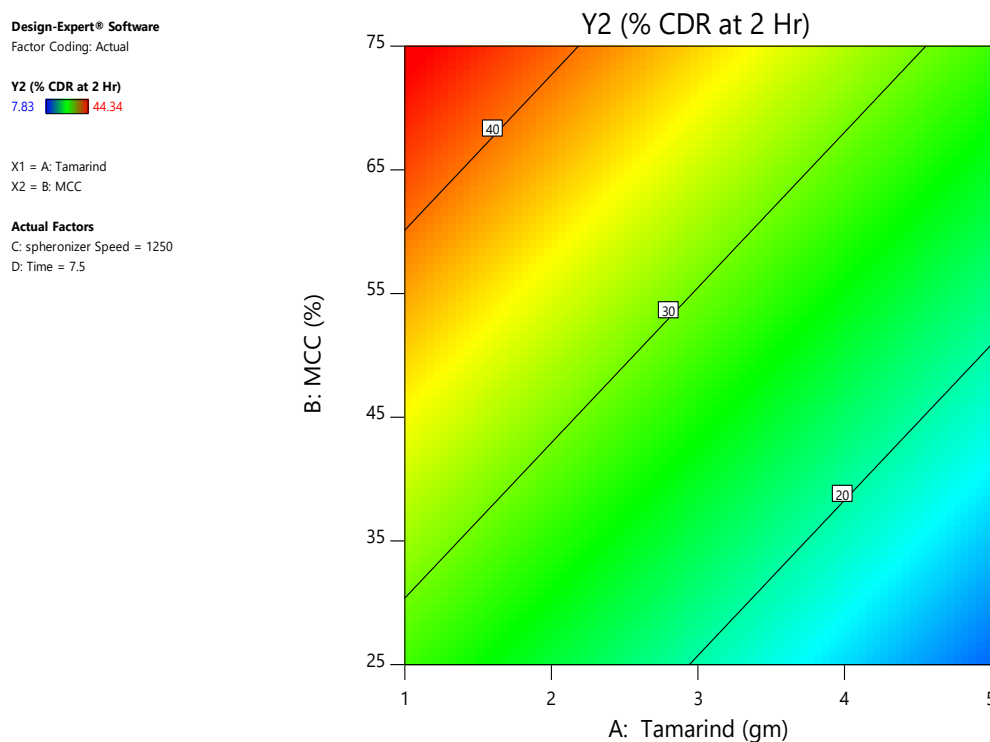
Y2 (% CDR at 2 Hr)
7.83 44.34

X1 = A: Tamarind
X2 = B: MCC

Actual Factors
C: spheronizer Speed = 1250
D: Time = 7.5



(a)



(b)

Figure 6.10: 3D Response Graph (a) and Contour Plot (b) for % CDR at 2 hours

We revealed from the 3D response graph (Fig. 6.10a) and contour plot (Fig. 6.10b) that the rate of drug release decreased as the amount of tamarind gum increased, but that an increase in the amount of MCC, which is the most frequently used spheronizing aid in a pellet formulation but also acts as a disintegrant, would increase the rate of drug release via formulation, and the same thing can also be deduced from Table 8. According to ANOVA results, two variables have a significant effect on the % CDR at 2 hours: the amount of tamarind gum ($P \leq 0.0001$) and the percentage of MCC ($P \leq 0.0001$). Thus, the model retains factors A and B.

$$\% \text{ CDR at 2 Hours} = 28.1569 - 8.43812 \cdot A + 8.40312 \cdot B$$

6.2.3 Creating the Design Space and reducing numbers and the range of independent variables for next Experimental Design

An ANOVA study for all three dependent variables suggests that both Factor A and Factor B had a substantial contribution, while Factors C and D did not significantly affect dependent variables within the defined range. This indicates that the optimal range has already been

determined via trial batches. Hence, the Design Expert Software suggested fixed values for spheronization speed (1250 revolution/min) and spheronization time (7.5 minutes).

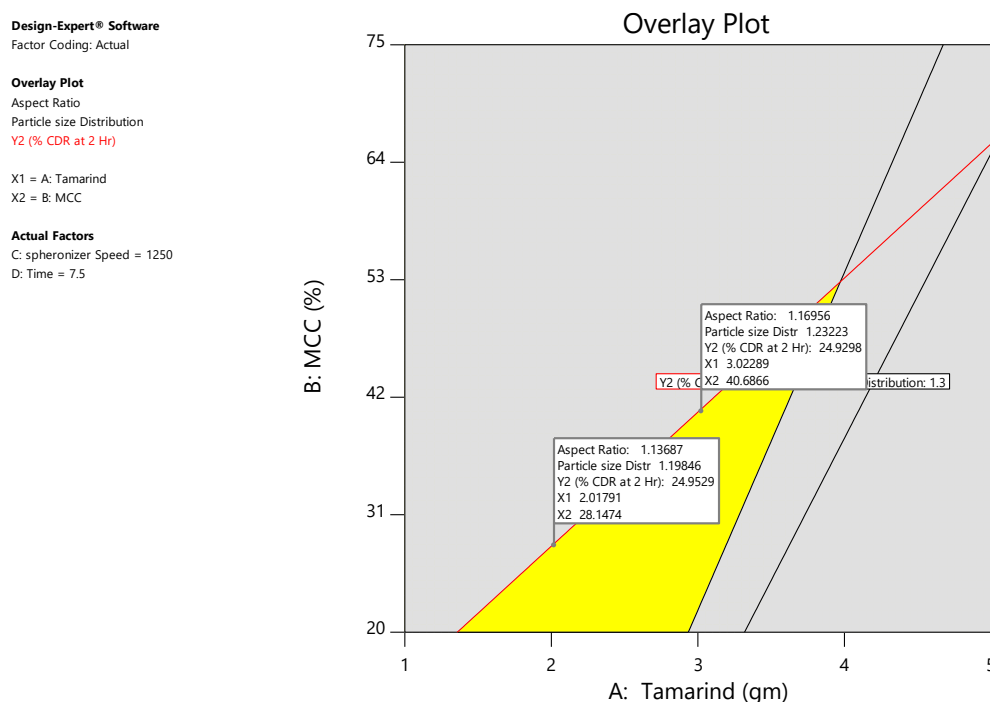


Figure 6.11: Design Space Generated By 2^4 Factorial Design

From the data of the 2^4 full factorial designs and design spaces (Figure 6.11), it can be determined that pellets with the desired characteristics may be produced by using tamarind gum in the range of 2 to 3 grams and MCC in the range of 30% to 40%. So, for the subsequent experimental design, we reduced the range of factors (A and B), while other factors of the 2^4 factorial study were kept constant and not included as independent variables in the subsequent box-Behnken experimental design.

6.2.4 Box-Behnken Design

The purpose of the 3-factor, 3-level experimental design was to analyse the impact and interaction of independent variables such as the amount of tamarind gum, the percentage of MCC in relation to lactose, and the percentage of weight gain by Eudragit S 100 coating on Y2, Y5, and Y9, as shown in Table 6.17. The table revealed that Y2, Y5, and Y9 had respective values ranging from 0.76% to 4.96%, 6.81% to 29.23%, and 72.34% to 101.23%.

Table 6.17: Experimental runs obtained from Box-Behnken Experimental design and their responses.

Runs	X1 –Quantity of tamarind Gum	X2- %MCC with respect to lactose	X3-% weight gain	Y2- %CDR at 2 hrs	Y5- %CDR at 5 Hrs	Y9-%CDR at 9 hrs
1	2.5	35	5	1.65	12.23	99.67
2	2.5	40	7.5	0.85	10.11	88.92
3	2.5	35	5	1.69	12.89	99.12
4	3	35	2.5	3.89	18.21	100.01
5	3	35	7.5	0.76	6.81	72.34
6	2.5	40	2.5	4.81	25.89	101.23
7	2	30	5	1.78	14.76	96.78
8	2.5	35	5	1.59	13.01	98.26
9	2.5	30	2.5	4.35	23.78	99.98
10	2	40	5	1.89	20.32	99.98
11	2	35	2.5	4.96	29.23	101.23
12	2.5	30	7.5	0.78	7.98	81.24
13	2	35	7.5	0.86	10.98	91.67
14	3	40	5	1.53	11.24	93.23
15	3	30	5	1.34	10.67	87.21

6.2.4.1 percentage cumulative drug release (% CDR) at 2 hours

Table 6.18: Analysis of variance for the % cumulative drug release at 2 hours (dependent variable)

Source	Sum of Squares	df	Mean Square	F-value	p-value	
Model	31.97	9	3.55	443.53	< 0.0001	significant
A-QUANTITY OF TAMARIND	0.4851	1	0.4851	60.58	0.0006	
B-% OF MCC	0.0861	1	0.0861	10.75	0.0220	
C-% WEIGHT GAIN	27.23	1	27.23	3400.48	< 0.0001	
AB	0.0016	1	0.0016	0.1998	0.6736	
AC	0.2352	1	0.2352	29.37	0.0029	

BC	0.0380	1	0.0380	4.75	0.0812	
A ²	0.0072	1	0.0072	0.8994	0.3865	
B ²	0.0047	1	0.0047	0.5920	0.4764	
C ²	3.83	1	3.83	478.12	< 0.0001	
Residual	0.0400	5	0.0080			
Lack of Fit	0.0350	3	0.0117	4.60	0.1837	not significant
R ²	0.9987					
Adjusted R ²	0.9965					
Predicted R ²	0.9822					
Adeq Precision	57.2414					

According to the results of the ANOVA analysis presented in Table 6.18, the Model F-value of 443.53 indicates that the model was significant for Y2 and % cumulative drug release (CDR) at 2 hours. P-values less than 0.05 indicate the statistical significance of model terms. Significant model terms in this instance are X1, X2, X3, X1X3, and X3². Y2 was represented by quadratic models with an adjusted R² of 0.9965, which was a more effective indication of the variance in responses. Theoretically, R² of 0.9983 represents the response variation that the model explains. However, when terms were added to the model, R² consistently increased. The predicted R² of 0.9822 represented the accuracy with which the model predicted future data. A reasonably high adjusted R² and predicted R² and a minimum difference between these two indicated that the model accurately predicted the response.

$$\% \text{ CDR at 2 hrs} = 1.63333 - 0.24375 \cdot X_1 + 0.0625 \cdot X_2 - 1.76125 \cdot X_3 + 0.1725 \cdot X_1 X_3 + 0.997083 \cdot X_3^2$$

Design-Expert® Software

Factor Coding: Actual

Y2 (% CDR AT 2 Hr) (%)

● Design points above predicted value

○ Design points below predicted value

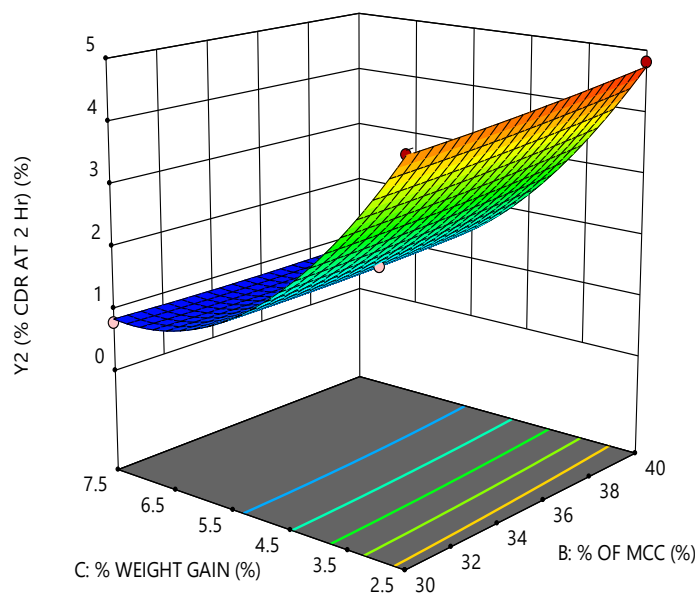
0.76 4.96

X1 = B: % OF MCC

X2 = C: % WEIGHT GAIN

Actual Factor

A: QUANTITY OF TAMARIND = 2.5



(a)

Design-Expert® Software

Factor Coding: Actual

Y2 (% CDR AT 2 Hr) (%)

● Design Points

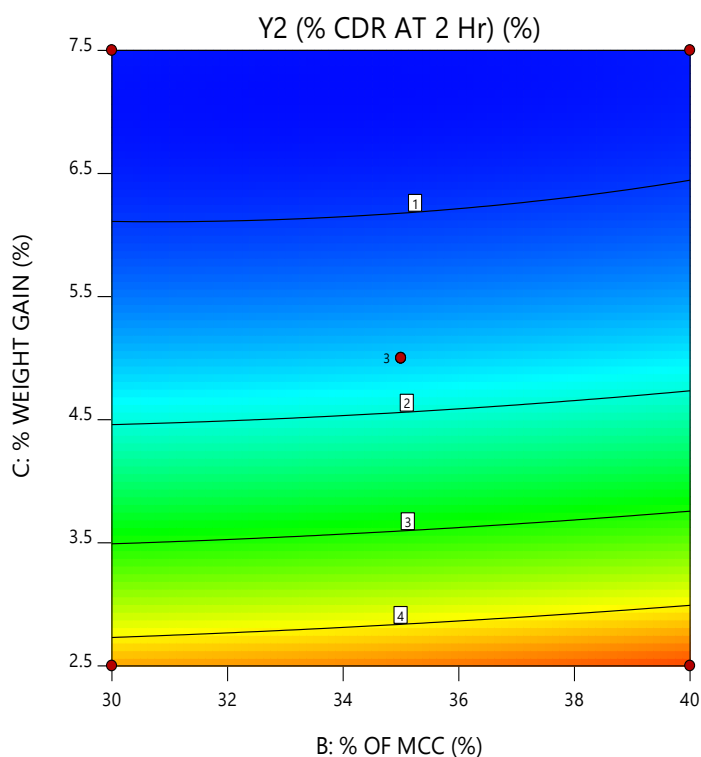
0.76 4.96

X1 = B: % OF MCC

X2 = C: % WEIGHT GAIN

Actual Factor

A: QUANTITY OF TAMARIND = 2.5



(b)

Figure 6.12: 3D Response Graph (a) and Contour Plot (b) for % CDR at 2 hrs

Based on the polynomial equation, 3D response curve (Figure 6.12a), and contour plot (Figure 6.12b), it was determined that the percentage weight gain by coating pellets with Eudragit S 100 modulated Y2 significantly. As coating level (X3) increases, drug release at 2 hours (Y2) decreases dramatically, and tamarind gum amount (X1) has the same negative impact on Y2. However, the impact of X1 on Y2 is much smaller than that of X3. As X2 increases, it gradually increases drug release, but as coating thickness increases, the effect of X2 on drug release diminishes.

6.2.4.2 percentage cumulative drug release (% CDR) at 5 hours

As the impact of independent variables was investigated on % CDR at 5 hours (Y%) as shown in Table 6.19, it was found that X1, X2, X3, X2², and X3² were significant model terms. A model F-value of 200.26 indicates that the model is statistically significant. P-values less than 0.05 indicate significant model terms. The minimal difference between the adjusted R² value (0.9923) and the predicted R² value (0.9633) indicates that the design has significant predictive power. However, by removing the insignificant terms from the model, the predictability of the model improved, as evidenced by the revised adjusted R² and predicted R² values of 0.9921 and 0.9736, respectively, and the increase in the value of adequate precision from 46.09 to 51.09. The modified model's F value of 252.48 indicates that the model is highly significant.

Table 6.19: Analysis of variance for the % cumulative drug release at 5 hours (dependent variable)

Source	Sum of Squares	df	Mean Square	F-value	p-value	
Model	639.82	9	71.09	200.26	< 0.0001	significant
A-Quantity of Tamarind gum	100.54	1	100.54	283.20	< 0.0001	
B-% of MCC	13.44	1	13.44	37.87	0.0016	
C-% weight gain	468.64	1	468.64	1320.13	< 0.0001	
AB	6.23	1	6.23	17.54	0.0086	
AC	11.73	1	11.73	33.04	0.0022	
BC	0.0001	1	0.0001	0.0003	0.9873	

A ²	0.7560	1	0.7560	2.13	0.2043	
B ²	4.35	1	4.35	12.24	0.0173	
C ²	36.52	1	36.52	102.88	0.0002	
Residual	1.77	5	0.3550			
Lack of Fit	1.42	3	0.4741	2.69	0.2828	not significant
R ²	0.9972					
Adjusted R ²	0.9923					
Predicted R ²	0.9633					
Adeq Precision	46.0399					

Polynomial equation:

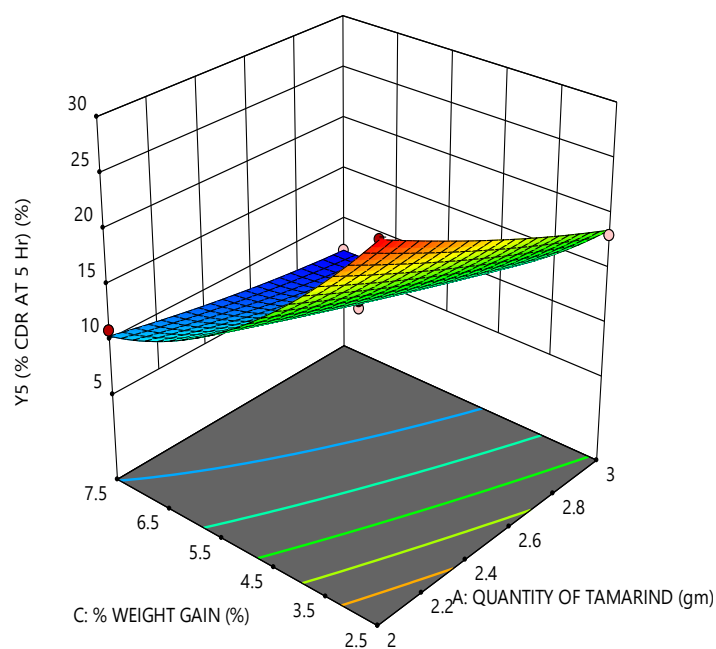
$$\% \text{ CDR at 5 hrs} = 12 - 4 \cdot X_1 + 2.625 \cdot X_2 - 8.125 \cdot X_3 + 2.625 \cdot X_2^2 + 6.625 \cdot X_3^2$$

Design-Expert® Software
Factor Coding: Actual

Y5 (% CDR AT 5 Hr) (%)
● Design points above predicted value
○ Design points below predicted value
6.81 29.23

X1 = A: QUANTITY OF TAMARIND
X2 = C: % WEIGHT GAIN

Actual Factor
B: % OF MCC = 35



(a)

Design-Expert® Software
Factor Coding: Actual

Y5 (% CDR AT 5 Hr) (%)

● Design Points

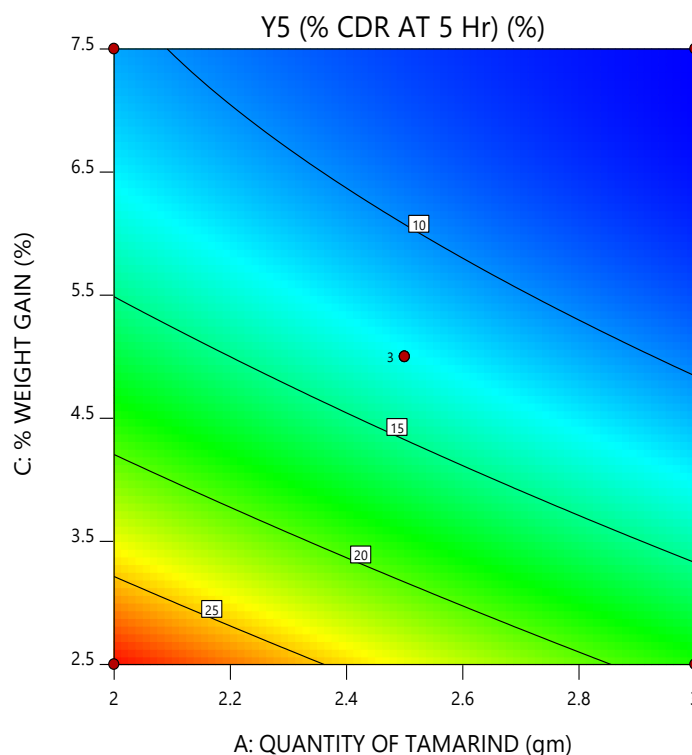
6.81 29.23

X1 = A: QUANTITY OF TAMARIND

X2 = C: % WEIGHT GAIN

Actual Factor

B: % OF MCC = 35



(b)

Figure 6.13: 3D Response Graph (a) and Contour Plot (b) for % CDR at 5 hrs

On the basis of the polynomial equation, the 3D response (Fig. 6.13a), and the contour plot (Fig. 6.13b), All three independent variables have a substantial influence on the rate of drug release at 5 hours. The drug formulations were subjected to a higher pH after two hours. As a result, the coating would dissolve more gradually, and the release rate would also be controlled by core pellet components such as tamarind gum and MCC. According to the data, when the quantity of tamarind gum and the percentage of weight gain increased, the percentage of drug release decreased, but the reverse impact was found with the % of MCC in the formulation.

6.2.4.3 percentage cumulative drug release (% CDR) at 9 hours

Table 6.20: Analysis of variance for the % cumulative drug release at 9 hours (dependent variable)

Source	Sum of Squares	df	Mean Square	F-value	p-value	
Model	998.25	9	110.92	69.05	0.0001	significant
A-Quantity of Tamarind gum	169.92	1	169.92	105.79	0.0001	
B-% of MCC	41.18	1	41.18	25.64	0.0039	
C-% weight gain	582.77	1	582.77	362.81	< 0.0001	
AB	1.99	1	1.99	1.24	0.3165	
AC	81.99	1	81.99	51.05	0.0008	
BC	10.34	1	10.34	6.44	0.0521	
A ²	36.02	1	36.02	22.42	0.0052	
B ²	9.37	1	9.37	5.84	0.0604	
C ²	77.48	1	77.48	48.24	0.0010	
Residual	8.03	5	1.61			
Lack of Fit	7.02	3	2.34	4.63	0.1826	not significant
R ²				0.9920		
Adjusted R ²				0.9777		
Predicted R ²				0.8861		
Adeq Precision				27.4422		

According to the data in the ANOVA Table 6.20 for the dependent variable Y9, the model was significant based on the model F value, which was 69.05. Significant model terms in this instance are X1, X2, X3, X1X3, X1², and X3². If your model has a large number of insignificant terms, model reduction may be able to enhance performance. From the values of adjusted R² (0.9777) and predicted R² (0.8861), it can be concluded that the design has significant predictive power. The adequate precision value was 27.44, indicating the model's capacity to explore the design space was adequate.

$$\% \text{ CDR at 9 hrs} = 97.7977 - 4*X_1 + 2.75*X_2 - 8*X_3 - 4.75*X_1X_3 - 3.69846*X_1^2 - 4.69846*X_3^2$$

Design-Expert® Software

Factor Coding: Actual

Y9 (% CDR AT 9 Hr) (%)

● Design points above predicted value

○ Design points below predicted value

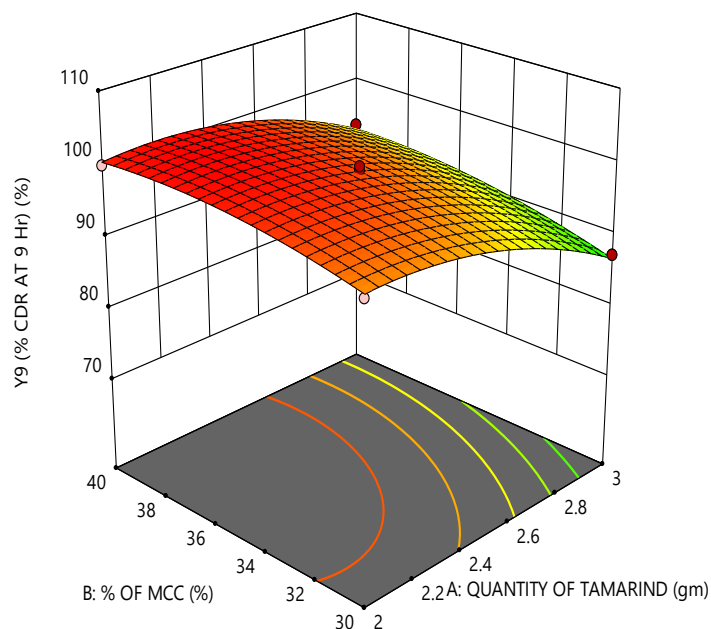
72.34 101.23

X1 = A: QUANTITY OF TAMARIND

X2 = B: % OF MCC

Actual Factor

C: % WEIGHT GAIN = 5



(a)

Design-Expert® Software

Factor Coding: Actual

Y9 (% CDR AT 9 Hr) (%)

● Design Points

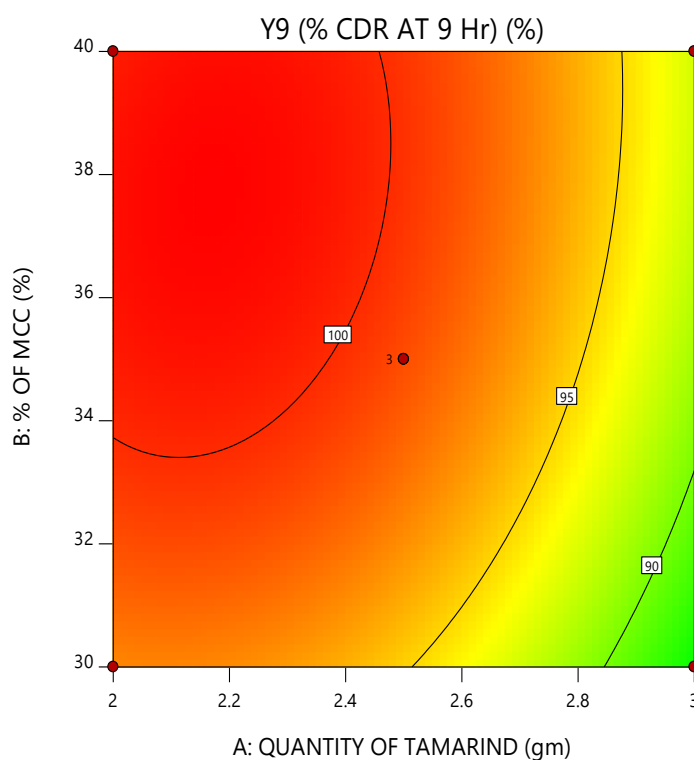
72.34 101.23

X1 = A: QUANTITY OF TAMARIND

X2 = B: % OF MCC

Actual Factor

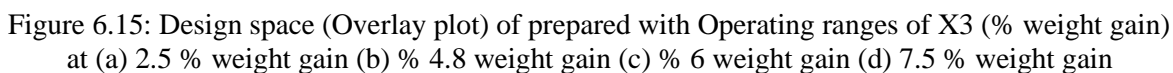
C: % WEIGHT GAIN = 5



(b)

Figure 6.14: 3D Response Graph (a) and Contour Plot (b) for % CDR at 5 hrs

Although the Eudragit coating was no longer observed after a duration of 5 hours, the combined impact of the coating on the pellets inside the upper gastrointestinal system was accountable for the identification of this negative effect.



According to regulatory requirements, if adjustments are made within the design space, no change is necessary; if adjustments are made outside the design space, the post-approval modification procedure must be followed. The applicant proposes a design space, which must be evaluated and approved by regulators. In this research, DS (design space) was set up using RSM (response surface methodology) in conjunction with optimization. Response contour plots (design Space) were utilized to evaluate the impact of 2 factors on the Dependent variables at a given time while a third variable was maintained constant. Figure 6.15 depicts the impact of X1 and X2 on Y2, Y5, and Y9 at 3 levels of X3. If the X3's % weight gain was between 2.5% and 4.8%, there was no projected DS formation (Figure 6.15a and 6.15b). The yellow area (Design Space-DS) in Fig. 6.15c and 6.15d, is an overlay plot demonstrating a medium and high level of % weight gain by Eudragit S 100, as proposed by the Design-Expert 11.0 in order to produce the optimal dosage form towards the desired criteria. If all variables were within the DS, colon-targeted pellets would satisfy the compliance requirements.

For the robustness and accuracy of the experimental design, five distinct confirmatory batches were chosen within DS to compare the predicted value to the observed value. Based on the information revealed in Table 6.21, it was determined that there is no substantial difference between the data, and it was therefore determined that the selected design had excellent prediction power.

Table 6.21: Predicated and Observed values for Dependent Variables of Confirmatory batches

Independent Variables			Dependent Variables					
			Y2 (% CDR AT 2 Hr)		Y5 (% CDR AT 5 Hr)		Y9 (% CDR AT 9 Hr)	
X1	X2	X3	Predicated	Observed	Predicted	Observed	Predicated	Observed
2.5	32	6	1.06	1.10	9.36	9.21	92.10	93.01
2.5	35	6	1.09	1.12	9.81	10.12	94.96	94.14
2.5	35	7	0.86	0.92	9.74	9.78	89.43	90.67
2.6	35	6	1.05	1.07	9.11	9.23	93.62	92.12
2.6	35	7	0.84	0.93	9.07	9.67	87.72	88.12

6.2.5 Release kinetics of formulation batches

The drug release from the dosage form depends upon the type of polymer and the other formulation parameter used. For finding out the mechanism of drug release from formulation

release kinetics of all formulation batches were measure and are shown in Table 6.22 & 6.23.

Table 6.22: Statistical parameter of all mathematical models (F1 to F8)

Model	Statistics	Formulations (pellets)							
		F1	F2	F3	F4	F5	F6	F7	F8
Zero Order	R2	0.8452	0.8651	0.8514	0.8480	0.8411	0.8839	0.8662	0.8568
	AIC	69.81	77.74	69.29	70.55	77.80	67.73	68.80	68.86
	MSC	1.55	1.72	1.60	1.57	1.56	1.84	1.70	1.63
First Order	R2	0.5845	0.5946	0.5923	0.6049	0.5835	0.6534	0.6061	0.5983
	AIC	77.89	87.92	77.58	78.35	86.62	76.78	77.72	77.35
	MSC	0.66	0.70	0.67	0.71	0.68	0.84	0.71	0.69
Higuchi Model	R2	0.9735	0.9809	0.9714	0.9296	0.9724	0.9004	0.9745	0.9715
	AIC	53.91	58.22	54.47	63.62	60.31	66.35	53.89	54.34
	MSC	3.32	3.67	3.24	2.34	3.31	2.00	3.36	3.25
Hixson Crowell	R2	0.7320	0.7510	0.7400	0.7282	0.7364	0.7670	0.7554	0.7474
	AIC	74.75	83.87	74.33	75.78	82.87	74.00	74.23	73.97
	MSC	1.01	1.11	1.04	0.99	1.05	1.15	1.10	1.07
Korsmeyer Peppas	R2	0.9925	0.9887	0.9918	0.9495	0.9934	0.9527	0.9809	0.9904
	n	1.3470	1.2790	1.3180	1.7690	1.4310	2.1900	1.1400	1.2510
	AIC	43.14	53.57	43.82	61.24	46.64	60.26	51.89	45.17
	MSC	4.52	4.14	4.43	2.61	4.67	2.67	3.58	4.26
Weibull Model	β	6.9645	6.9018	6.7650	8.7069	5.7007	8.3279	6.8640	6.0436
	R2	0.9948	0.9987	0.9943	0.9781	0.9886	0.9646	0.9970	0.9931
	AIC	39.80	32.18	40.52	53.72	52.09	57.65	35.17	42.13
	MSC	4.89	6.28	4.79	3.44	4.13	2.96	5.44	4.60

Table 6.23: Statistical parameter of all mathematical models (F9 to F15)

Model	Statistics	Formulations (Pellets)						
		F9	F10	F11	F12	F13	F14	F15
Zero Order	R2	0.8768	0.8234	0.8921	0.8599	0.8631	0.9015	0.8922
	AIC	67.71	72.18	66.71	77.19	78.39	75.11	75.65
	MSC	1.78	1.42	1.92	1.68	1.71	2.04	1.95
First Order	R2	0.6516	0.5723	0.6677	0.5957	0.5905	0.6339	0.6255
	AIC	76.27	79.34	76.04	86.96	88.53	87.42	87.28
	MSC	0.83	0.63	0.88	0.71	0.69	0.80	0.78
Higuchi Model	R2	0.9007	0.9427	0.8832	0.9851	0.9780	0.9793	0.9858
	AIC	65.77	62.06	67.43	54.76	60.12	59.49	55.40
	MSC	2.00	2.55	1.84	3.93	3.53	3.60	3.97
Hixson Crowell	R2	0.7635	0.7051	0.7783	0.7527	0.7456	0.7920	0.7836
	AIC	73.58	76.79	73.19	82.87	84.59	82.59	82.62
	MSC	1.13	0.91	1.20	1.12	1.09	1.29	1.25
Korsmeyer Peppas	R2	0.9583	0.9443	0.9573	0.9953	0.9833	0.9845	0.9860
	n	2.4600	1.3460	2.3140	1.0030	1.2590	0.9920	1.0350
	AIC	58.57	62.40	58.99	43.96	58.01	57.28	55.88
	MSC	2.80	2.51	2.77	5.01	3.74	3.82	3.92
Weibull Model	β	8.1814	8.9201	8.0652	4.6338	7.5974	5.1468	3.3937
	R2	0.9675	0.9760	0.9608	0.9978	0.9986	0.9961	0.9956
	AIC	56.34	54.84	58.20	36.48	33.35	43.40	44.24
	MSC	3.05	3.35	2.86	5.75	6.21	5.21	5.09

Upon evaluating the dissolution profiles of 15 different design batches, it was determined that batch 12 demonstrated the closest optimization in terms of release criteria and design space layout. Subsequently, after a 2-hour delay ($t_{lag} = 2$), the release kinetics observed in the study were analysed using various kinetic models (Table 6.22 and 6.23) through the DD solver[31], and using the adjusted R^2 values of 0.9953 and 0.9978 for the Korsmeyer-Peppas and Weibull models, respectively, it was determined that both models fit the data well. These high R^2 values indicate a significant correlation between the theoretical models and the observed data, confirming that the chosen models are appropriate for characterizing the release kinetics.

Applying the Korsmeyer-Peppas model to the release kinetics yielded an n value of 1.0030. This value implies a release mechanism consistent with Case II, indicating controlled release after lag time. In contrast, the Weibull model yielded a β value of 4.633, suggesting a failure in adequately controlling the release, as validated by a value of 1.

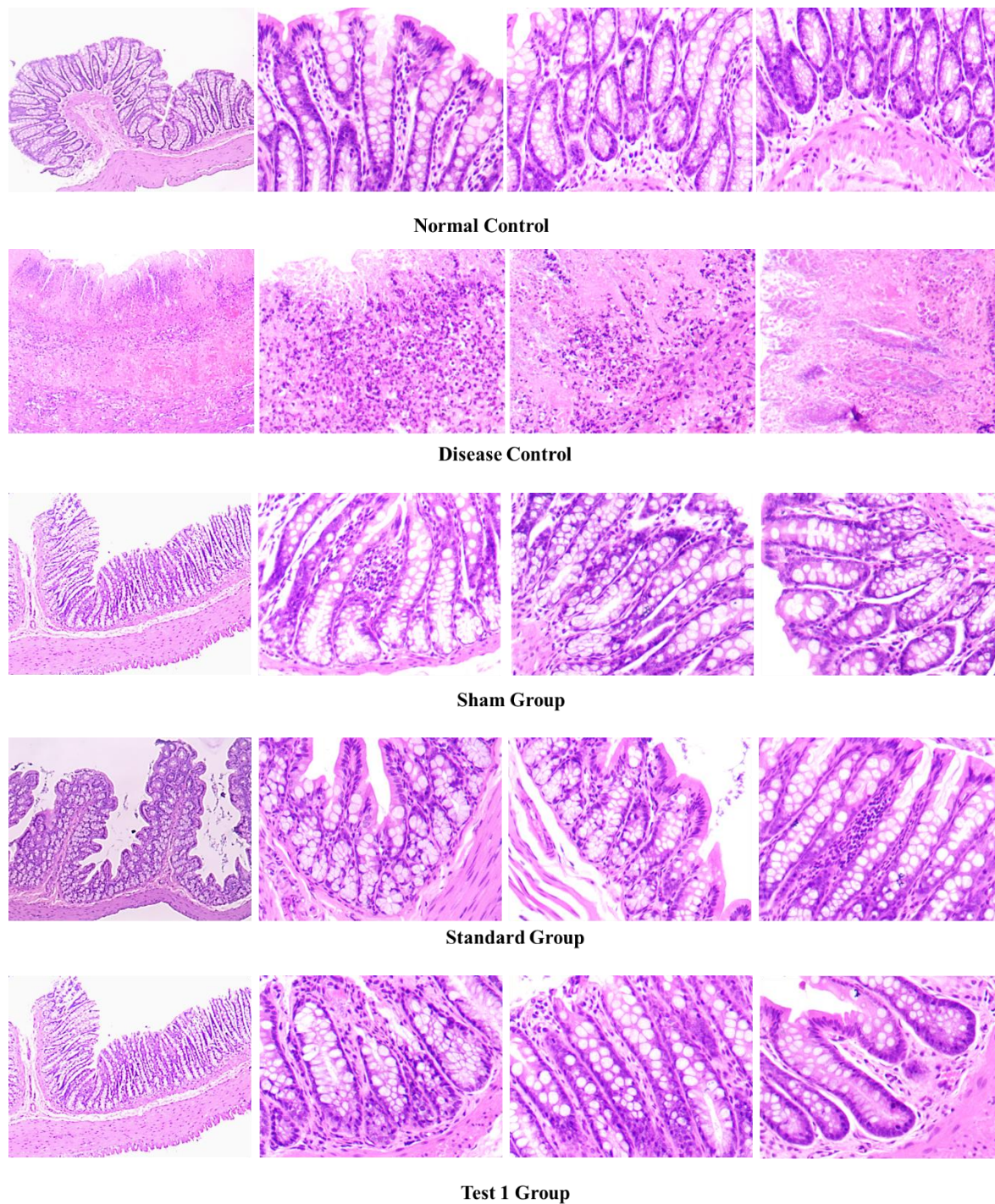
Furthermore, the Korsmeyer-Peppas model yielded an AIC value of 43.96, while the Weibull model resulted in an AIC value of 36.47 for batch 12. These values serve as indicators for model selection, with lower values suggesting a better fit to the data. Based on the AIC values, it can be concluded that the Weibull model is more suitable as a predication of release mechanism for batch 12. The Weibull model exhibited the lowest AIC value, indicating a closer fit to the observed data compared to the Korsmeyer-Peppas model[32, 33]. The MSC values are used as a quantitative measure to assess the goodness of fit of different models. In this case, the lower MSC value of 5.00 for the Korsmeyer-Peppas model for batch 12 suggests that it exhibits a relatively poorer fit to the data compared to the higher MSC value of 5.75 for the Weibull model indicates a better fit, implying that the Weibull model captures the underlying patterns and behaviours in the observed data more accurately[8]

6.2.6 In vivo study

6.2.6.1 Histopathological assessment of the colon

Four factors were used to score histological damage: inflammation intensity, inflammation extent, crypt damage, and % of participation. The concept of total colitis included many factors, including the intensity of inflammation, the area of inflammation, and the degree of crypt destruction. The administration of budesonide pellets to rats resulted in a reduction in all histology scores associated with colitis. Notably, there was a significant difference seen

between the control group and the other treatment groups in terms of crypt damage and overall colitis. The results shown in Figure 6.16 illustrate the impact of the administered therapy on the development of colitis.



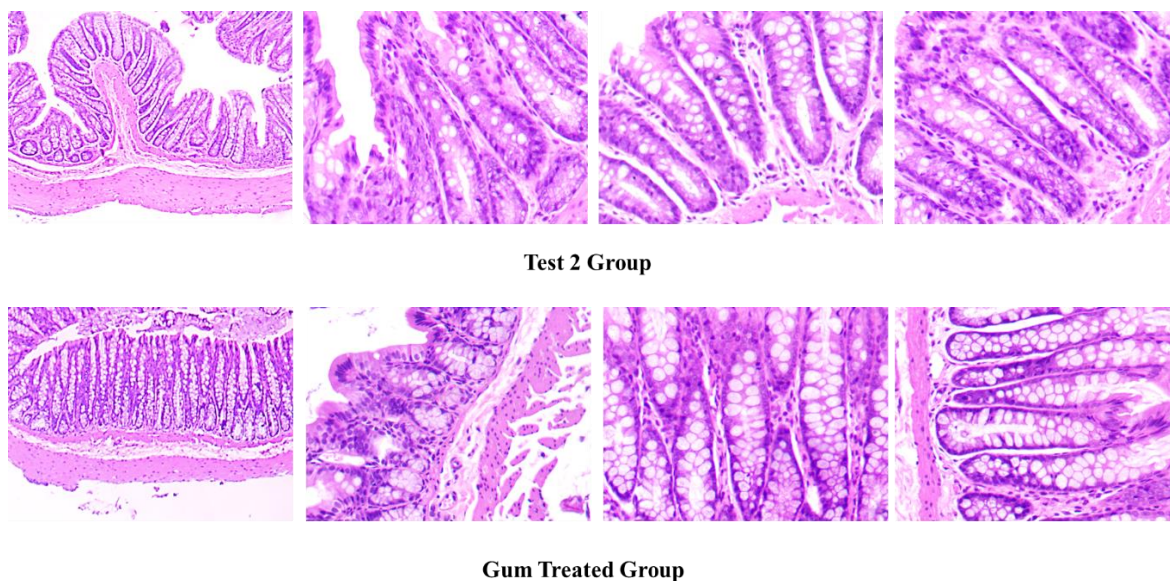


Figure 6.16: Histopathological Evaluation for different animal groups

Figure 6.16 illustrates histopathological alterations together with the degree to which they occurred. a harmless benign mucosal epithelium composed of tall columnar epithelial cells and goblet cells is seen on a slide from the **Normal control group**.

The **Disease Control (Acetic Acid-induced) group** had a prevalent manifestation of active colitis, as shown by histological examination. The mucosal layer exhibited significant erosion, ulcerations, and necrosis, accompanied by edema, hyperplasia of goblet cells, and lymphoid follicular hyperplasia. In addition, there was a presence of lymphocytes and plasma cells infiltrating the whole thickness of the tissue, along with a small population of neutrophilic cells in the connective tissue.

The **sham group** had a slightly degraded mucosal epithelium composed of tall columnar epithelial cells including goblet cells. This observation supports the conclusion that the approach used for the rectal delivery of the chemical did not result in any substantial injury.

Upon histological examination, the tissue sample from the **Standard group** revealed the existence of epithelial cells that were undergoing moderate healing. Dispersed superficial lesions accompanied these cells; these ulcers were lined with colonic glands that exhibited reparative epithelial alterations. Hyperchromatic characteristics were observed in the nuclei of these cells, while mitotic activity was comparatively infrequent. Additionally, a reduction in the quantity of goblet cells was observed, accompanied by transmucosal infiltration of lymphocytes and plasma cells into the stromal tissue through an edematous milieu.

The histological slide from the **Test 1 group** (with less dose) revealed the presence of an intestinal rat specimen that exhibited a lining composed of healing epithelial cells. These cells displayed a tall columnar morphology, with superficial shredded epithelial cells. The surface of the specimen appeared to be less eroded, and there was evidence of minimal inflammatory edema and necrosis. Additionally, the colonic gland displayed repairing epithelial changes, suggesting a substantial recovery as a result of the treatment administered.

The group receiving **the normal dosage of budesonide therapy (Test 2)** had a superior healing response and improvement in the intestinal mucosa when compared to the positive control group. The positive control group showed just a few instances of mucosal lymphoplasmacytic infiltration inside stromal edema.

The histopathological slide of the **gum treated group** revealed the presence of superficial, small eroded mucosa accompanied by mucosal hemorrhage, edema, and the infiltration of acute and chronic inflammatory cells around the colonic glands. Additionally, repairing epithelial alterations and a limited number of goblet cells were seen.

6.2.6.2 Biochemical estimation of cytokines, IL 6 and TNF- α

Standard Calibration curve for the TNF- α and IL 6

Table 6.24 and Table 6.25 represents the data for the standard calibration curve for TNF - α and IL-6 respectively.

calibration curve for both TNF - α and IL-6 are illustrated in Figure 6.17 and 6.18 respectively.

Table 6.24: Standard calibration curve data for the TNF- α

Concentration	Optical Density
0	0.1414
15.63	0.2193
31.25	0.3209
62.5	0.5176
125	0.9117
250	1.417
500	2.4989
1000	4.21

OD -Mean value (n=3*)

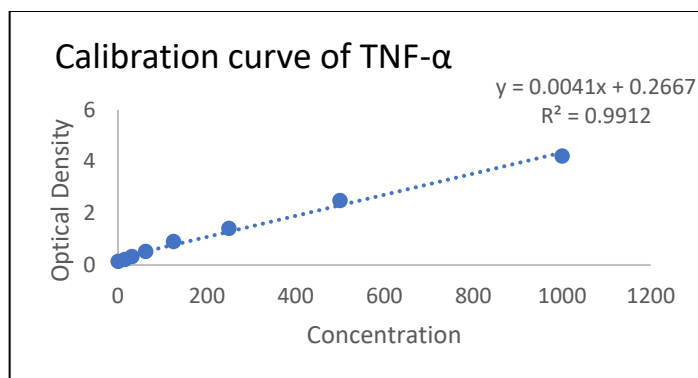
Figure 6.17: Standard calibration curve of TNF- α

Table 6.25: Standard calibration curve data for the IL-6

Concentration	Optical Density
0	0.0514
12.5	0.1236
25	0.1645
50	0.2072
100	0.3099
200	0.4132
400	0.8851
800	1.666

OD -Mean value (n=3*)

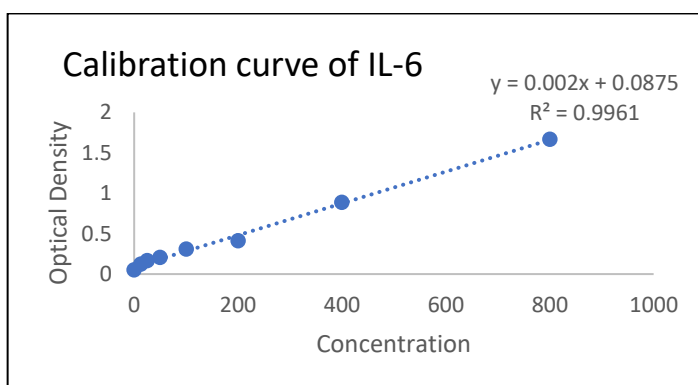


Figure 6.18: Standard calibration curve of IL-6

Table 6.26: Values of IL6 for each experimental animal group

IL -6 Reading for Six Rats per group							
Groups	Control	Sham Operated	T1	T2	STD	Gum Treated	Disease group
1	26.46	30.60	44.66	39.30	66.23	103.12	163.89
2	23.22	34.22	41.78	32.34	57.12	97.23	148.97
3	30.23	35.23	47.22	36.23	74.35	110.23	178.23
4	22.95	27.67	48.22	46.78	68.23	115.25	162.34
5	29.34	30.12	38.45	48.23	74.34	92.34	157.84

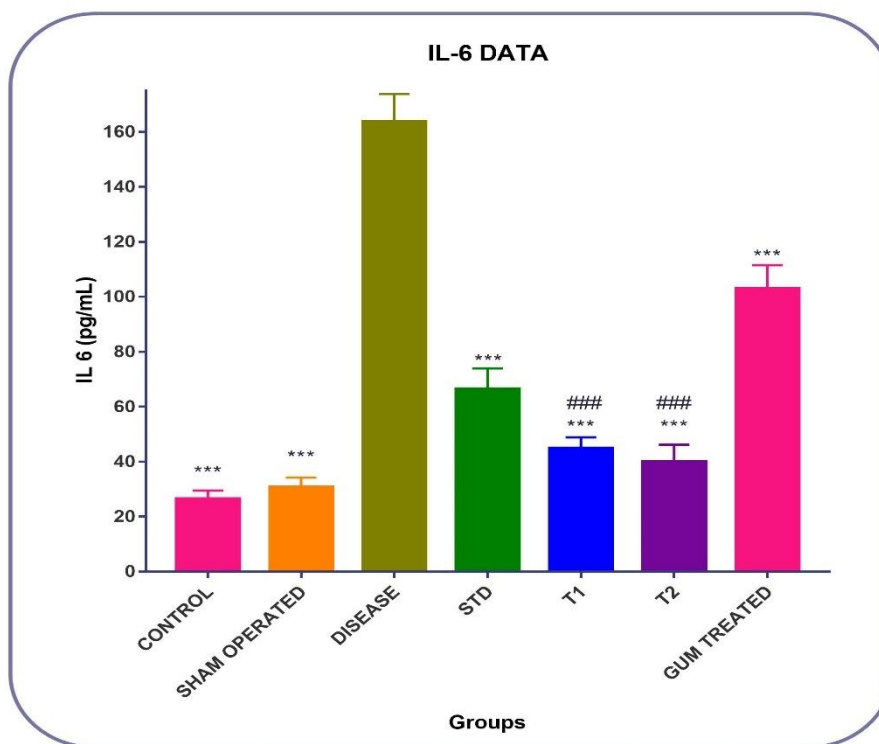
6	26.67	26.19	48.54	36.27	58.23	100.12	170.76
Average	26.4783	30.67167	44.81167	39.85902	66.416	103.0483	163.6717
S.D.	2.7497	3.23455	3.67428	5.78601	6.8616	7.71965	9.25705

Table 6.27: Values of TNF- α for each experimental animal group

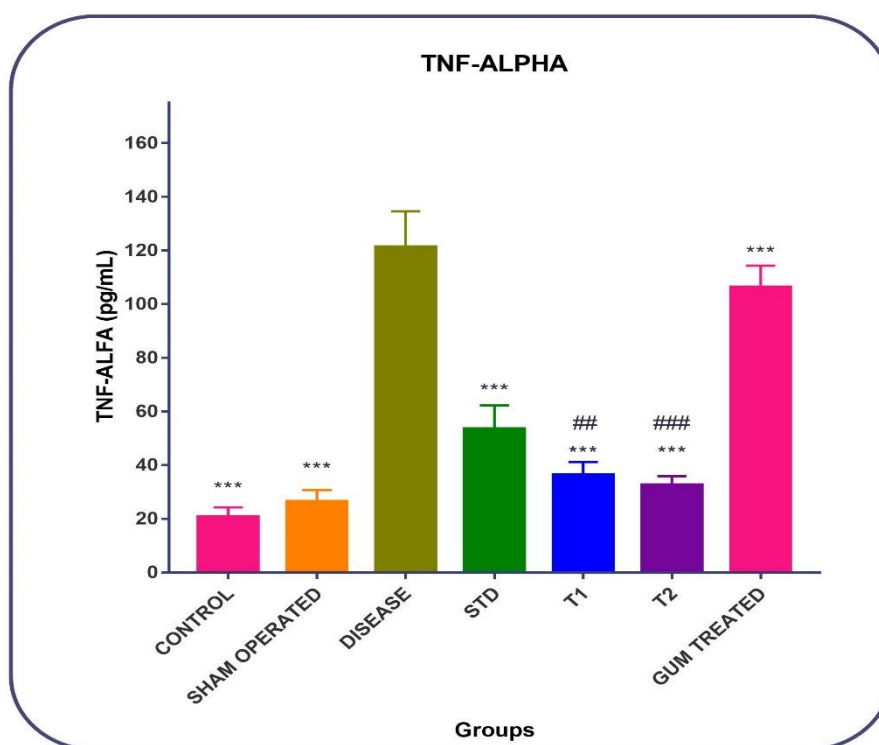
TNF - α DATA							
Groups	Control	Sham Operated	T1	T2	STD	Gum Treated	Disease group
1	20.77	26.68	36.40	32.74	53.22	106.05	121.17
2	18.78	21.24	33.81	33.43	43.84	98.34	138.38
3	24.97	30.21	38.12	31.23	45.98	95.47	135.47
4	16.43	27.4	28.56	36.78	67.34	110.27	113.56
5	17.9	31.64	37.78	26.78	59.45	112.56	115.45
6	24.97	21.43	43.23	34.32	51.29	115.6	104.27
Average	20.63667	26.43333	36.31661	32.54667	53.52	106.3817	121.3833
S.D.	3.321795	3.965937	4.465491	3.078732	7.976781	7.327022	12.08747

The disease group exhibited significantly ($P < 0.05$ and $P < 0.01$) elevated levels of TNF- α and IL-6 in the colon tissue compared to the control group, confirming the induction of inflammation. Histopathological analysis revealed evidence of epithelial cell necrosis, edema, and neutrophil infiltration, further supporting the inflammatory response in the disease group.

In contrast, the treatment group receiving budesonide colon targeted formulation (T1 & T2) showed a significant reduction in the levels of TNF- α and IL-6 compared to both the disease group and the group receiving budesonide solution in a 1% CMC solution.



(a)



(b)

Figure 6.19: Biochemical estimation of (a) IL 6 and (b) TNF- α in different animal group

6.2.7 SEM analysis for optimised Formulation

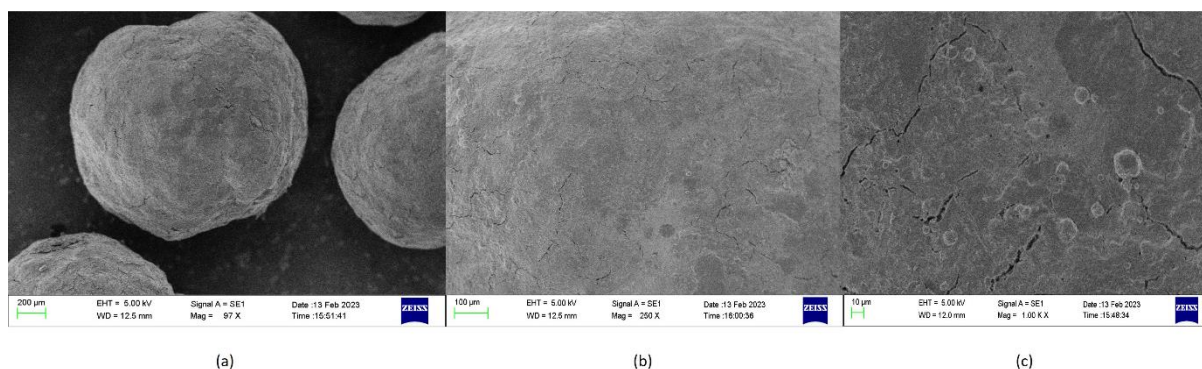


Figure 6.20: SEM Picture of surface of Optimized Pellets (1) Magnification with 97X (b) Magnification with 250X (c) Magnification with 1000X

A scanning electron microscopy (SEM) picture was captured to examine the surface of the optimized batch. The image revealed that the pellet exhibited a nearly spherical shape, as seen in Figure 6.20a. The magnifications of 250x and 1000x in Figures 6.20b and 6.20c, respectively, provided insights into the small nature of the detected fissures. That indicates challenges in water penetration and restricted water admission. Water penetration is facilitated mostly at elevated pH levels, since this causes the dissolution of the coating and the widening of fissures, ultimately resulting in the relaxation of the polymer covering. The reduced release of the medication was seen during the early hours, which may be attributed to the low pH conditions that were not favourable for the dissolving of the coating. Over the course of time, there was an observed increase in the release of the drug, which may be related to the gradual raise in pH levels. This rise in pH levels had a significant role in favouring the dissolution of the coating layer.

6.2.8 Stability Study

Stability study data for the optimized batch are shown in Table 6.28. As per the data, it was concluded that the pellet dosage form is stable enough for 6 months under the accelerated conditions as per the ICH.

Table 6.28: Stability Study of Optimized Batch (F12) under accelerated Conditions as per ICH guideline

Test parameters	Specifications	Initial	1 st Month	3 rd Month	6 th Month
Description	Buff coloured coated spherical pellets	Buff coloured spherical pellets	No change	No change	No Change
Moisture content	NMT (Not more than) 2.5	1.23	1.26	1.32	1.45
Assay (Drug Content)	NLT (Not less than) 90% and NMT 110% of label claim	98.93% ±1.23	98.56%±1 .73	96.01%±2 .32	92.85%± 3.19
% CDR at 5 th hrs	NLT 90% and NMT 110% of label claim	7.98 % ± 1.214	7.83% ± 1.541	7.51% ± 1.862	7.42 % ± 1.49
Friability	Not greater than 1 %	0.23 %	0.25 %	0.56 %	0.12
Microbial limit test	Total count < 10 ² CFU (Colony forming units) (As per USP)	Complies	Complies	Complies	Complies

6.3 References

1. Wang, J., Kan, S., Chen, T., & Liu, J. (2015). Application of quality by design (QbD) to formulation and processing of naproxen pellets by extrusion–spheronization. *Pharmaceutical Development and Technology*, 20(2), 246–256. <https://doi.org/10.3109/10837450.2014.908300>
2. Saripella, K. K., Loka, N. C., Mallipeddi, R., Rane, A. M., & Neau, S. H. (2016). A Quality by Experimental Design Approach to Assess the Effect of Formulation and Process Variables on the Extrusion and Spheronization of Drug-Loaded Pellets Containing Polyplasdone® XL-10. *AAPS PharmSciTech*, 17(2), 368–379. <https://doi.org/10.1208/s12249-015-0345-6>
3. Pallagi, E., Ismail, R., Paál, T. L., & Csóka, I. (2018). Initial Risk Assessment as part of the Quality by Design in peptide drug containing formulation development. *European Journal of Pharmaceutical Sciences*, 122, 160–169. <https://doi.org/10.1016/j.ejps.2018.07.003>
4. Hales, D., Tefas, L. R., Tomuță, I., Moldovan, C., Gulei, D., Munteanu, R., & Porfire, A. (2020). Development of a Curcumin-Loaded Polymeric Microparticulate Oral Drug Delivery System for Colon Targeting by Quality-by-Design Approach. *Pharmaceutics*, 12(11), 1027. <https://doi.org/10.3390/pharmaceutics12111027>
5. Veerubhotla, K., & Walker, R. B. (2020). Application of Quality by Design Principles for Optimizing Process Variables of Extrusion and Spheronization of a Captopril Pellet Formulation. *Indian Journal of Pharmaceutical Sciences*, 82(1). <https://doi.org/10.36468/pharmaceutical-sciences.624>
6. Kan, S., Lu, J., Liu, J., Wang, J., & Zhao, Y. (2014). A quality by design (QbD) case study on enteric-coated pellets: Screening of critical variables and establishment of design space at laboratory scale. *Asian Journal of Pharmaceutical Sciences*, 9(5), 268–278. <https://doi.org/10.1016/j.ajps.2014.07.005>
7. Mundada, P. K., Sawant, K. K., & Mundada, V. P. (2017). Formulation and optimization of controlled release powder for reconstitution for metoprolol succinate multi unit particulate formulation using risk based QbD approach. *Journal of Drug Delivery Science and Technology*, 41, 462–474. <https://doi.org/10.1016/j.jddst.2017.09.001>
8. Vora, C., Patadia, R., Mittal, K., & Mashru, R. (2013). Risk based approach for design and optimization of stomach specific delivery of rifampicin. *International Journal of Pharmaceutics*, 455(1–2), 169–181. <https://doi.org/10.1016/j.ijpharm.2013.07.043>
9. Varshosaz, J., Emami, J., Tavakoli, N., Minaian, M., Rahmani, N., Ahmadi, F., & Dorkoosh, F. (2011). Development and validation of a rapid HPLC method for simultaneous analysis of budesonide and its novel synthesized hemiesters in colon specific formulations. *Research in pharmaceutical sciences*, 6(2), 107–16. Retrieved from <http://www.ncbi.nlm.nih.gov/pubmed/22224094>
10. Kshirsagar, S. J., Bhalekar, M. R., & Umap, R. R. (2009). *In vitro in vivo* comparison of two pH sensitive Eudragit polymers for colon specific drug delivery. *Journal of Pharmaceutical Sciences and Research*, 1(4), 61–70.
11. Sinha, V. R., & Kumria, R. (2003). Coating polymers for colon specific drug delivery: a comparative *in vitro* evaluation. *Acta pharmaceutica (Zagreb, Croatia)*, 53(1), 41–7. Retrieved from <http://www.ncbi.nlm.nih.gov/pubmed/14769251>
12. Fude, C., Lei, Y., Jie, J., Hongze, P., Wenhui, L., & Dongmei, C. (2007). Preparation and *In Vitro* Evaluation of pH, Time-Based and Enzyme-Degradable Pellets for Colonic Drug Delivery. *Drug Development and Industrial Pharmacy*, 33(9), 999–1007. <https://doi.org/10.1080/03639040601150393>
13. Patel, N., Patel, J., & Shah, S. (2010). Box-Behnken experimental design in the development of pectin-compritol ATO 888 compression coated colon targeted drug delivery of mesalamine. *Acta Pharmaceutica*, 60(1), 39–54. <https://doi.org/10.2478/v10007-010-0008-9>
14. Ren, Y., Jiang, L., Yang, S., Gao, S., Yu, H., Hu, J., ... Zhou, Y. (2017). Design and preparation of a novel colon-targeted tablet of hydrocortisone. *Brazilian Journal of Pharmaceutical Sciences*, 53(1). <https://doi.org/10.1590/s2175-97902017000115009>

15. McCoubrey, L. E., Favaron, A., Awad, A., Orlu, M., Gaisford, S., & Basit, A. W. (2023). Colonic drug delivery: Formulating the next generation of colon-targeted therapeutics. *Journal of Controlled Release*, 353, 1107–1126. <https://doi.org/10.1016/j.jconrel.2022.12.029>
16. Evans, D. F., Pye, G., Bramley, R., Clark, A. G., Dyson, T. J., & Hardcastle, J. D. (1988). Measurement of gastrointestinal pH profiles in normal ambulant human subjects. *Gut*, 29(8), 1035–1041. <https://doi.org/10.1136/gut.29.8.1035>
17. Wahlgren, M., Axenstrand, M., Håkansson, Å., Marefati, A., & Lomstein Pedersen, B. (2019). *In Vitro* Methods to Study Colon Release: State of the Art and An Outlook on New Strategies for Better In-Vitro Biorelevant Release Media. *Pharmaceutics*, 11(2), 95. <https://doi.org/10.3390/pharmaceutics11020095>
18. Školáková, T., Slámová, M., Školáková, A., Kadeřábková, A., Patera, J., & Zámostný, P. (2019). Investigation of Dissolution Mechanism and Release Kinetics of Poorly Water-Soluble Tadalafil from Amorphous Solid Dispersions Prepared by Various Methods. *Pharmaceutics*, 11(8), 383. <https://doi.org/10.3390/pharmaceutics11080383>
19. Mircioiu, C., Voicu, V., Anuta, V., Tudose, A., Celia, C., Paolino, D., ... Mircioiu, I. (2019). Mathematical Modeling of Release Kinetics from Supramolecular Drug Delivery Systems. *Pharmaceutics*, 11(3), 140. <https://doi.org/10.3390/pharmaceutics11030140>
20. Ekenna, I. C., & Abali, S. O. (2022). Comparison of the Use of Kinetic Model Plots and DD Solver Software to Evaluate the Drug Release from Griseofulvin Tablets. *Journal of Drug Delivery and Therapeutics*, 12(2-S), 5–13. <https://doi.org/10.22270/jddt.v12i2-S.5402>
21. Costa, P., & Sousa Lobo, J. M. (2001). Modeling and comparison of dissolution profiles. *European Journal of Pharmaceutical Sciences*, 13(2), 123–133. [https://doi.org/10.1016/S0928-0987\(01\)00095-1](https://doi.org/10.1016/S0928-0987(01)00095-1)
22. Askarizadeh, M., Esfandiari, N., Honarvar, B., Sajadian, S. A., & Azdarpour, A. (2023). Kinetic Modeling to Explain the Release of Medicine from Drug Delivery Systems. *ChemBioEng Reviews*. <https://doi.org/10.1002/cben.202300027>
23. Patel, M. M. (2017). Formulation and development of di-dependent microparticulate system for colon-specific drug delivery. *Drug Delivery and Translational Research*, 7(2), 312–324. <https://doi.org/10.1007/s13346-017-0358-7>
24. Rao, K. P., Prabhashankar, B., Kumar, A., Khan, A., Biradar, S. S., Srishail, S. P., & Satyanath, B. (2003). Formulation and roentgenographic studies of naproxen-pectin-based matrix tablets for colon drug delivery. *The Yale journal of biology and medicine*, 76(4–6), 149–54. Retrieved from <http://www.ncbi.nlm.nih.gov/pubmed/15482652>
25. Prabhu, P., Ahamed, N., Matapady, H. N., Ahmed, M. G., Narayanacharyulu, R., Satyanarayana, D., & Subrahmanayam, E. (2010). Investigation and comparison of colon specificity of novel polymer khaya gum with guar gum. *Pakistan journal of pharmaceutical sciences*, 23(3), 259–65. Retrieved from <http://www.ncbi.nlm.nih.gov/pubmed/20566437>
26. Shejawal, K. P., Randive, D. S., Bhinge, S. D., Bhutkar, M. A., Wadkar, G. H., Todkar, S. S., & Mohite, S. K. (2021). Functionalized carbon nanotube for colon-targeted delivery of isolated lycopene in colorectal cancer: *In vitro* cytotoxicity and *in vivo* roentgenographic study. *Journal of Materials Research*, 36(24), 4894–4907. <https://doi.org/10.1557/s43578-021-00431-y>
27. Bajaj, S., Singla, D., & Sakhuja, N. (2012). Stability testing of pharmaceutical products. *Journal of Applied Pharmaceutical Science*, 2(3), 129–138. <https://doi.org/10.7324/JAPS.2012.2322>
28. Sirisha, V. N. L., Chinna Eswariah, M., & Sambasiva Rao, A. (2018). A novel approach of locust bean gum microspheres for colonic delivery of mesalamine. *International Journal of Applied Pharmaceutics*, 10(1), 86–93. <https://doi.org/10.22159/ijap.2018v10i1.22638>
29. Bhatt, H., Naik, B., & Dharamsi, A. (2014). Solubility Enhancement of Budesonide and Statistical Optimization of Coating Variables for Targeted Drug Delivery. *Journal of Pharmaceutics*, 2014, 1–13. <https://doi.org/10.1155/2014/262194>
30. Shravani, D., Lakshmi, P. K., & Balasubramaniam, J. (2011). Preparation and optimization of various parameters of enteric coated pellets using the Taguchi L9 orthogonal array design and their characterization. *Acta Pharmaceutica Sinica B*, 1(1), 56–63.

- <https://doi.org/10.1016/j.apsb.2011.04.005>
31. Zhang, Y., Huo, M., Zhou, J., Zou, A., Li, W., Yao, C., & Xie, S. (2010). DDSolver: An Add-In Program for Modeling and Comparison of Drug Dissolution Profiles. *The AAPS Journal*, 12(3), 263–271. <https://doi.org/10.1208/s12248-010-9185-1>
 32. Pourtalebi Jahromi, L., Ghazali, M., Ashrafi, H., & Azadi, A. (2020). A comparison of models for the analysis of the kinetics of drug release from PLGA-based nanoparticles. *Heliyon*, 6(2), e03451. <https://doi.org/10.1016/j.heliyon.2020.e03451>
 33. Romero, A. I., Villegas, M., Cid, A. G., Parentis, M. L., Gonzo, E. E., & Bermúdez, J. M. (2018). Validation of kinetic modeling of progesterone release from polymeric membranes. *Asian Journal of Pharmaceutical Sciences*, 13(1), 54–62. <https://doi.org/10.1016/j.ajps.2017.08.007>

CHAPTER 7

**Comparison of Dissolution
profiles between Tablet and
Pellets dosage form**

CHAPTER 7

7. Comparison of dissolution profiles between Tablet and Pellets dosage form

7.1 Statistical Methods

Dissolution profiles of dosage forms may only be evaluated for similarity or difference by statistical comparison[1]. The goal is to provide a quantitative evaluation of the data to support conclusions about the performance of different dosage forms, such as tablets and pellets[2].

Type of the statistical methods commonly used for comparison of dissolution profile are[3]:

(a) Model independent Methods (b) Model dependent methods.

7.1.1 Model Independent Models [4]:

Model-independent models may be further classified into two categories:

1. Pair-wise procedures.
2. Ratio tests

(1) Pairwise procedure:

The difference factor (f1), the similarity factor (f2), and the Rescigno index are part of the pairwise procedure test.

The pairwise Procedure (fit factors) provide to compare the dissolving rate of the active pharmaceutical ingredient (API) between a pellets formulation and a tablet formulation. The FDA (Food and Drug Administration, 1997) has acknowledged the acceptance of fit factors[5]. Additionally, the European Medicines Agency (EMA), Committee for Medicinal

Products for Human Use (CHMP) (European Medicines Agency, 2010), and the World Health Organization (WHO) (World Health Organization, 2006) have also adopted the similarity factor as a criterion for evaluating the similarity between two *in vitro* dissolution profiles[6].

Across all time periods, the percentage error between two trajectories is quantified by the difference factor (f1).

$$f_1 = \frac{\sum_{j=1}^n |R_j - T_j|}{\sum_{j=1}^n R_j}$$

In the given context, the variable "n" represents the sample number, while "R" and "T" denote the percentage of dissolution for the reference and test items, respectively, at each time point "j". The percentage error is 0 when the dissolution profiles of the test and drug reference are equal, and it increases proportionately as the dissimilarity between the two profiles increases[7].

To calculate f2, we use the logarithm of the total squared error of differences between test T_j and reference products R_j throughout every point in time.

$$f_2 = 50 \times \log \left\{ \left[1 + \left(\frac{1}{n} \right) \sum_{j=1}^n w_j |R_j - T_j|^2 \right]^{-0.5} \times 100 \right\}$$

The variable "w" represents an optional weight factor. The similarity factor is constrained to the range of 0 to 100. The similarity score between the test and reference profiles is 100 when they are identical, and decreases towards 0 as the dissimilarity between them grows. This approach is seen more suitable for conducting comparisons of dissolution profiles in cases when there are more than three or four time points available for dissolution analysis. Equation (43) is applicable under the condition that the mean discrepancy between R and T does not exceed 100. If the discrepancy exceeds 100, it is necessary to adjust the data[7].

Rescigno introduced a bioequivalence index as a means of quantifying the difference between a reference product and a test product, using plasma concentration over time as the determining factor. The Rescigno index, denoted by the variables j and i, may also be used in the context of dissolved drug concentrations.

$$\xi_i = \left\{ \frac{\int_0^\infty |d_R(t) - d_T(t)|^i dt}{\int_0^\infty |d_R(t) + d_T(t)|^i dt} \right\}^{1/i}$$

In this context, let $d(t)$ represent the amount of the reference product dissolved, $d(t)$ represents the amount of the test product dissolved at each time point of sampling, and i denote any positive integer. The dimensional index consistently represents values ranging from 0 to 1, inclusively, and measures the differences seen between two dissolution profiles. The index value is 0 when comparing the disintegration characteristics of the two releases. The index value of 0 is assigned when neither the release from the test nor the reference dosage form. An increase in the value of i will result in a greater emphasis being placed on the magnitude of the concentration change rather than its duration[8].

(2) Ratio-tests

The ratio tests involve comparing parameters derived from the release assay of the pellet's formulation and the release assay of the tablet product conducted simultaneously.

The **mean dissolution time** is determined from the accumulative curves of dissolved API as function of time.

The calculation of the mean dissolution time may be ascertained by using the below mathematical expression:

$$MDT = \frac{\sum(t_i \cdot \Delta Q_i)}{Q_\infty}$$

where t_i represents an intermediate time within the intervals of sampling time, ΔQ_i denotes the quantity of API (Active Pharmaceutical Ingredient) dissolved at each time interval, and Q_∞ represents the highest amount of API dissolved[2].

% Dissolution Efficiency (% DE) is a metric introduced by Khan and Rhodes in 1972 to assess the efficiency of drug release from pharmaceutical dosage forms. It quantifies the extent to which a drug is released from a dosage form within a specified time frame, relative to the theoretical maximum release at that same time point. % DE is particularly useful for comparing and evaluating the performance of different drug formulations.

The formula for calculating the percentage dissolution efficiency is as follows:

$$DE\% = \frac{AUC_0^T}{Q_{100.T}} \times 100$$

The comparison between the results of dissolution efficiency (DE) and mean dissolution time (MDT) for the pellets and tablet dosage forms was conducted using a one-way analysis of variance (ANOVA)[9]. The study was conducted using the DD-solver, an Excel Add-in.

7.1.2 Model dependent Models:

The model-dependent technique serves as an alternate tool for assessing the similarity of dissolution profiles in situations when the usual f_2 measure may not be suitable. This methodology involves applying regression models to characterise the dissolution characteristics of two separate kinds of drug. Based on the analysis presented in chapters 5 and 6, it was determined that the dissolving characteristics of the tablet dosage form and pellet dosage form were most accurately represented by the both Weibull model and the Korsemeyer-Pappas model [10].

In order to conduct a more comprehensive comparison of these dissolution profiles, the maximum multivariate statistical distance (MSD) approach was used. The approach used in this study included using Multivariate Statistical Distance (MSD) to analyse the model parameters of the Weibull model and the Korsemeyer-Pappas model in the context of optimised batch processes[11].

7.2 Result and Discussion

Based on the predetermined parameters outlined for the colon-targeted formulation in the present investigation, it was determined that the drug release should not exceed 10% during a duration of 5 hours, while a minimum of 80% of the medication should be released over a 9-hour interval. Upon examination, it was observed that batch 12 and batch 2, formulated as pellet dosage forms, along with batch 3 and batch 14, formulated as tablet dosage forms, met the optimized criteria outlined for drug release.

Subsequently, a comparative analysis of the in-vitro dissolution profiles was conducted for these optimized batches employing fit factors, the values of which are documented in Table

7.1. Notably, the calculated f_2 value, which amounted to 72.87 for the given formulation, surpassed the threshold of 50. This finding suggests that a significant degree of similarity exists between the drug release patterns of the different formulations[5].

Conversely, the dissimilarity factor (f_1) was determined to be 5.9, a value well below the stipulated limit of 15, signifying a high degree of similarity in drug release profiles. Furthermore, the Rescigno index values for i_1 and i_2 were ascertained to be 0.0335 and 0.0386, respectively. These values, being in proximity to zero, suggest a substantial likeness between the various formulations, whereas a value of 1 would indicate dissimilarity. In light of these various fit factor values, it can be inferred that the drug release profiles of both the tablet and pellet dosage forms exhibit a high degree of similarity in their release patterns[12]

Table 7.1: In-vitro Dissolution Profile Comparison using Fit Factors (Pairwise Procedures)

Time	% Dissolved of Optimized Pellet formulation	% Dissolved of Optimized Tablet formulation	Similarity factor: f_2	Difference factor: f_1	Rescigno index
1	0.78	0.23	72.87 (Is greater than 50)	5.9 (Is less than 15)	$i_1 =$ 0.0335 (Is near to zero)
2	1.18	0.67			
3	1.97	1.45			
4	4.35	2.57			
5	7.98	8.94			
6	22.01	19.79			$i_2 =$ 0.0386 (Is near to zero)
7	43.23	43.01			
8	64.23	62.87			
9	81.24	91.18			
10	97.23	98.31			

Determining the DE and MDT values are practical approaches for simplifying each curve to an independent value, denoted as the dissolution rate constant. The percentage dissolution efficiency (% DE) and mean dissolution time (MDT) values for the optimized batch have been documented in Table 7.2. These values were calculated utilizing the DD-solver, an Excel add-in tool. The utilization of DD-solver, an established computational tool, ensures

accuracy and consistency in these calculations, contributing to the comprehensive assessment of the optimized formulation's dissolution properties.

In statistical hypothesis testing, when the F-critical value is greater than the observed f value, it typically signifies that the null hypothesis, which in this case suggests no significant difference between the % DE values and MDT values of the two dosage forms, can be accepted[13].

Table 7.2: % Dissolution efficiency (%DE) comparison using One way ANOVA study

BATCH	% Dissolution Efficiency		Mean Dissolution Time (MDT)	
	Pellets	Tablets	Pellets	Tablets
1	27.34	26.03	6.53	7.40
2	29.45	42.12	7.06	5.21
3	27.57	27.99	6.50	7.15
4	33.35	32.08	6.00	6.14
5	25.58	36.64	7.42	5.69
6	37.41	31.78	5.67	6.09
7	29.82	29.35	6.23	6.34
8	27.74	28.51	6.46	6.34
9	35.52	31.23	5.80	6.22
10	30.53	29.50	6.25	6.32
11	37.78	33.35	5.64	5.98
12	27.56	37.29	7.17	5.64
13	30.36	33.20	7.00	6.06
14	33.86	29.41	6.61	7.04
15	32.17	29.42	6.78	6.38

One way ANOVA data for % DE and MDT are presented in Table 7.3. For % DE, The F-critical value, which has been calculated to be 4.19, exceeds the calculated f value of 0.29. This statistical observation leads to the interpretation that there exists a similarity between the percentage dissolution efficiency (% DE) values of the optimized batch for both the pellets and tablet dosage forms.

For MDT, The F-critical value, which has been calculated to be 4.20, exceeds the calculated f value of 1.01. This statistical observation leads to the interpretation that there exists a similarity between the Mean dissolution time (MDT) values of the optimized batch for both the pellets and tablet dosage forms.

Table 7.3: One way ANOVA study for the % DE and MDT

% DE (%) dissolution efficiency)	Source of Variation	SS	df	MS	F	P-value	F crit
	Between Groups	4.68896 1	1	4.68896 1	0.2917 3	0.59338 4	4.19597 2
	Within Groups	450.042 1	28	16.0729 3			
	Total	454.731	29				
MDT (Mean Dissolution time)	Source of Variation	SS	df	MS	F	P-value	F crit
	Between Groups	0.32	1.00	0.32	1.01	0.32	4.20
	Within Groups	8.90	28.0 0	0.32			
	Total	9.22	29.0 0				

In the current investigation, Mahalanobis Distance (MSD) calculations were applied to assess the Weibull and Korsmeyer-Pappas parameters of the optimized batches. A diminished MSD value denotes a pronounced resemblance between the dissolution profiles of the two formulations, signifying a close alignment of data points representing the release of the active component within the multivariate space. Conversely, an elevated MSD value signifies notable dissimilarity in the dissolution profiles of the two formulations[11]. It is noteworthy that, in this study, the calculation of MSD values was facilitated through the utilization of the DD-solver, an Excel add-in tool, offering a robust quantitative approach for evaluating the multivariate distances between data points[14]. Values for MSD parameters for Weibull Model and Korsmeyer Pappas of optimized batches are shown in Table 7.4.

Table 7.4: In-vitro Dissolution Profile Comparison using MSD (Multivariate Statistical distance) test

<i>Model</i>	<i>Weibull</i>	<i>Korsmeyer Pappas</i>
<i>Statistics</i>	<i>Value</i>	<i>Value</i>
p (N of parameters)	4	4
K (scaling factor)	1.6741	1.6741
F _p (p, n1+n2-p-1,0.90)	2.1842	2.1842

Hotelling's T^2	11.2014	18.9213
Mahalanobis Distance (MSD)	1.2221	1.5883
Lower_90_CR_MSD	0.0799	0.4461
Upper_90_CR_MSD	2.3643	2.7306
Max_MSD	11.8200	11.8200
Is Upper_90 \leq Max_MSD	Yes	Yes
Similarity of R and T (R=PELLETS & T= TABLETS)	Accept	Accept

This F-statistic is associated with hypothesis testing. It is used to assess the statistical significance of parameters in the model. In this case, it indicates a value of 2.1842, which is used for making inferences about the model's goodness of fit.

A Mahalanobis Distance (MSD) value of 1.2221 and 1.5883 indicates a that this value is not exceptionally high, it suggests that there are no noticeable differences in the drug release behaviour between the two formulations[15].

Based on the findings of the dissolution profile comparison study, it has been determined that a notable similarity exists between the optimized batches of pellets and tablet dosage forms. This implies that both formulations exhibit a proficient capacity to deliver a substantial quantity of the drug to the colonic region.

Furthermore, when considering an economic perspective, it becomes evident that the tablet dosage form incorporates CM tamarind gum as an ingredient, while the pellets dosage form is exclusively reliant on tamarind gum. This difference in ingredient composition suggests that the production cost of pellets may be notably more cost-effective.

The experimental design has indicated that the tablet dosage form comprises CM tamarind gum within the range of 37.5% to 62.5%, whereas the tamarind gum content in the pellet's dosage form falls within the range of 20% to 30%. As a result, the data suggests that the total ingredient cost for the pellets is expected to be considerably lower. This reduction in ingredient costs may justify the potentially higher processing expenses associated with the production of pellets.

In light of these considerations, it can be reasonably concluded that the pellets dosage form may offer certain advantages over the tablet dosage form, particularly from an economic

standpoint. These findings underscore the importance of assessing both the pharmaceutical performance and the economic feasibility of drug delivery systems when making formulation decisions.

7.3 References

1. Wang, Y., Snee, R. D., Keyvan, G., & Muzzio, F. J. (2016). Statistical comparison of dissolution profiles. *Drug Development and Industrial Pharmacy*, 42(5), 796–807. <https://doi.org/10.3109/03639045.2015.1078349>
2. Muselík, J., Komersová, A., Kubová, K., Matzick, K., & Skalická, B. (2021). A Critical Overview of FDA and EMA Statistical Methods to Compare *In Vitro* Drug Dissolution Profiles of Pharmaceutical Products. *Pharmaceutics*, 13(10), 1703. <https://doi.org/10.3390/pharmaceutics13101703>
3. Gomez-Mantilla, J. D., Schaefer, U. F., Casabo, V. G., Lehr, T., & Lehr, C. M. (2014). Statistical Comparison of Dissolution Profiles to Predict the Bioequivalence of Extended Release Formulations. *The AAPS Journal*, 16(4), 791–801. <https://doi.org/10.1208/s12248-014-9615-6>
4. Khan, F., Li, M., & Schlindwein, W. (2013). Comparison of *In Vitro* Dissolution Tests for Commercially Available Aspirin Tablets. *Dissolution Technologies*, 20(1), 48–58. <https://doi.org/10.14227/DT200113P48>
5. Diaz, D. A., Colgan, S. T., Langer, C. S., Bandi, N. T., Likar, M. D., & Van Alstine, L. (2016). Dissolution Similarity Requirements: How Similar or Dissimilar Are the Global Regulatory Expectations? *The AAPS Journal*, 18(1), 15–22. <https://doi.org/10.1208/s12248-015-9830-9>
6. Costa, P. (2001). An alternative method to the evaluation of similarity factor in dissolution testing. *International Journal of Pharmaceutics*, 220(1–2), 77–83. [https://doi.org/10.1016/S0378-5173\(01\)00651-2](https://doi.org/10.1016/S0378-5173(01)00651-2)
7. Simionato, L. D., Petrone, L., Baldut, M., Bonafede, S. L., & Segall, A. I. (2018). Comparison between the dissolution profiles of nine meloxicam tablet brands commercially available in Buenos Aires, Argentina. *Saudi Pharmaceutical Journal*, 26(4), 578–584. <https://doi.org/10.1016/j.jsps.2018.01.015>
8. Costa, P., & Sousa Lobo, J. M. (2001). Modeling and comparison of dissolution profiles. *European Journal of Pharmaceutical Sciences*, 13(2), 123–133. [https://doi.org/10.1016/S0928-0987\(01\)00095-1](https://doi.org/10.1016/S0928-0987(01)00095-1)
9. Solis-Cruz, B., Hernandez-Patlan, D., Morales Hipólito, E. A., Tellez-Isaias, G., Alcántara Pineda, A., & López-Arellano, R. (2023). Discriminative Dissolution Method Using the Open-Loop Configuration of the USP IV Apparatus to Compare Dissolution Profiles of Metoprolol Tartrate Immediate-Release Tablets: Use of Kinetic Parameters. *Pharmaceutics*, 15(9), 2191. <https://doi.org/10.3390/pharmaceutics15092191>
10. I, M. R., & Damodharan, N. (2020). Mathematical Modelling of Dissolution Kinetics in Dosage forms. *Research Journal of Pharmacy and Technology*, 13(3), 1339. <https://doi.org/10.5958/0974-360X.2020.00247.4>
11. Cardot, J.-M., Roudier, B., & Schütz, H. (2017). Dissolution comparisons using a Multivariate Statistical Distance (MSD) test and a comparison of various approaches for calculating the measurements of dissolution profile comparison. *The AAPS Journal*, 19(4), 1091–1101. <https://doi.org/10.1208/s12248-017-0063-y>
12. Kassaye, L., & Genete, G. (2013). Evaluation and comparison of in-vitro dissolution profiles for different brands of amoxicillin capsules. *African Health Sciences*, 13(2), 1–16.

<https://doi.org/10.4314/ahs.v13i2.25>

13. Shreffler, J., & Huecker, M. R. (2023). *Hypothesis Testing, P Values, Confidence Intervals, and Significance*. (Jacob Shreffler; Martin R. Huecker., Ed.)*StatPearls*. StatPearls Publishing LLC. Retrieved from <http://www.ncbi.nlm.nih.gov/pubmed/12003508>
14. Hoffelder, T. (2019). Equivalence analyses of dissolution profiles with the Mahalanobis distance. *Biometrical Journal*, 61(5), 1120–1137. <https://doi.org/10.1002/bimj.201700257>
15. Hoffelder, T. (2019). Author response to the Letter to the Editor “Equivalence analyses of dissolution profiles with the Mahalanobis distance: A regulatory perspective and a comparison with a parametric maximum deviation-based approach.” *Biometrical Journal*, 61(5), 1138–1140. <https://doi.org/10.1002/bimj.201900047>

CHAPTER 8

Conclusion

CHAPTER 8

8. Conclusion

- This research successfully developed Microbial and pH-triggered Colon-targeted Budesonide Tablet and Pellet Dosage forms using the Quality by Design (QbD) approach for the treatment of ulcerative colitis.
- The utilization of viscometric analysis allowed for the evaluation of natural gums by examining their viscosity profiles. This assessment provided valuable information regarding their capacity to delay the release of drugs within the upper gastrointestinal tract.
- The enzymatic susceptibility of natural gums was investigated, with a focus on the non-specific cleavage of polysaccharide bonds by enzymes obtained from rat cecal content and probiotic media.
- Tamarind gum had emerged as highly promising candidate due to their notable characteristics, including elevated viscosity and heightened susceptibility to enzymes found in the intestinal microflora.
- It was also concluded that probiotic culture medium with a quantity of 4.5 ml emerged as a promising alternative to 4% rat cecal content through a study that was conducted to investigate the potential of tamarind gum in the delivery of drugs to the colonic region.
- The tablet dosage form incorporated Carboxymethyl (CM) Tamarind Gum and was coated with Eudragit S 100 to retard the release of Budesonide in the upper gastrointestinal tract.
- The optimized tablet formulation, achieved through the Box Behnken Design, exhibited controlled drug release with less than 10% released in the initial 5 hours and more than 70% released within the first 8 hours. These findings demonstrate the potential of this novel drug delivery system for targeted treatment of colon-related disease.
- For the pellet dosage form, process parameters and initial formulation parameters were screened using a 2^4 full factorial design for pellet size and shape uniformity, and

optimised factors and ranges were used to prepare a colon-targeted formulation using a Box-Behnken optimization design.

- Based on the design space, it was concluded that tamarind gum can be used to develop a targeted formulation with desired constraints.
- The QbD approach employed in these studies offers a systematic and effective approach for the development of colon-targeted drug delivery systems.
- The pellets formulation was evaluated by *in-vivo* model of ulcerative colitis. Both biochemical parameters (IL-6 and TNF- α) and histopathological evaluation indicated that the formulations effectively reduced inflammation in the colonic tissues at 600 $\mu\text{g/Kg}$ compared to conventional formulation (800 $\mu\text{g/Kg}$).
- GI transit studies in rabbits confirmed the successful passage of both tablet and pellet formulations through the GI tract and delivered to colonic region.
- Both tablet and pellet optimised formulations were found to be stable under accelerated stability conditions for six months, meeting ICH guidelines
- The release profile of tablet and pellet formulations were compared to assess their comparative efficiency in delivering the dosage form to colon. The results of the dissolution profile comparison analysis indicated that there was a significant similarity between the optimized batches of pellets and tablet dosage forms.
- Based on type and amount of ingredients used, it may be safely inferred that the use of pellets as a dosage form may have distinct benefits compared to tablets, especially in terms of cost consideration.

CHAPTER 9

List of Publications

List of publications

1. Patel, J., Patel, K., & Shah, S. (2023). Fabrication of a Dual-Triggered Natural Gum-Based Multi-Particulate Colon-Targeted Drug Delivery System of Budesonide Using the QbD Approach. *Journal of Pharmaceutical Innovation*.
<https://doi.org/10.1007/s12247-023-09764-z>
(Scopus and Web of science indexed, Clarivate Impact Factor – 2.6)
2. Patel, J., Patel, K., & Shah, S. (2023). Quality by Design Approach for Optimization of Microbial and pH-Triggered Colon-Targeted Tablet Formulation Using Carboxymethyl Tamarind Gum. *ASSAY and Drug Development Technologies*, 21(7), 297–308.
<https://doi.org/10.1089/adt.2023.066>
(Scopus and Web of science indexed, Clarivate Impact Factor – 1.8)



Fabrication of a Dual-Triggered Natural Gum-Based Multi-Particulate Colon-Targeted Drug Delivery System of Budesonide Using the QbD Approach

Jaymin Patel^{1,2} · Kaushika Patel¹ · Shreeraj Shah¹

Accepted: 29 July 2023

© The Author(s), under exclusive licence to Springer Science+Business Media, LLC, part of Springer Nature 2023

Abstract

Purpose To develop microbial and pH-triggered colon-targeted budesonide pellets utilising the Quality by Design (QbD) approach. Several polysaccharide-based natural gums selected using a retrospective research strategy were screened for their efficacy in developing a microbial degradation-based colon-targeted Drug Delivery System (DDS).

Methods The viscosity profiles were generated in the presence of a prebiotic culture medium that simulated the effect of 4% rat cecal content. Critical process parameters (CPPs) such as spheronization speed and time and formulation variables (CMAs) such as proportion of tamarind gum and microcrystalline cellulose (MCC):lactose were selected as independent variables for screening design 2⁴ FFD (full factorial design) to sort out the crucial parameters for the further optimization of pellets. The significant dependent variables were aspect ratio, particle size distribution, and % CDR (cumulative drug release) at 2 h. Pellets were super coated with the enteric polymer Eudragit S100. The screened range was further revealed to Box Behnken Design (BBD) for response surface optimization.

Results On the basis of viscometric analysis, tamarind gum was selected for formulation development. Based on the screening design, considering the constraints of aspect ratio, particle size distribution, and % CDR at 2 h in the range of 1–1.2, 1–1.3, and < 25%, respectively, the independent variables selected for Box Behnken Design (BBD) were proportion of gum and % MCC in the ranges of 2–3 g and 30–40%, respectively. The optimization design space was generated based on the criteria of LT 10% of the drug in the first 5 h and MT 80% in the first 9 h to achieve colon targeting.

Conclusion Tamarind gum is efficient for colon targeting, and its proportion of 2.5–3 g along with an enteric coating of 6% leads to an optimised formulation.

Keywords Budesonide · Tamarind gum · pH and microbial approach · QbD · Probiotic culture medium · Colon-targeted pellets · Box-Behnken design

Introduction

Inflammatory bowel disease (IBD) or inflammatory bowel syndrome (IBS) is a prevalent worldwide health issue with a consistently rising occurrence [1].

Despite the fact that 5-ASA (5-amino salicylic acid) drugs have been the preferred treatment for CD (Crohn's disease) and UC (ulcerative colitis), there is contradictory

information about their efficacy in individuals with Crohn's disease, particularly as long-term treatment. Antibiotics have a minimal role in colonic CD therapy [2]. Corticosteroids remain the preferred therapy for acute diseases unresponsive to more conservative treatment [3].

Unfortunately, corticosteroids may result in undesirable side effects [4]. Budesonide is a relatively recent steroid drug that undergoes rapid hepatic metabolism, thereby minimising corticosteroid-associated implications [5]. Budesonide is much more effective than placebo or mesalamine in the treatment of severe ulcerative colitis [6–8].

Budesonide is a corticosteroid with a considerable anti-inflammatory effect at the site of application but limited systemic activity due to significant hepatic degradation [4, 9]. Because of this, conventional oral formulations are

✉ Shreeraj Shah
Shreeraj.Shah@ljinstitutes.edu.in

¹ L. J. Institute of Pharmacy, LJ University,
 Ahmedabad 382210, India

² Gujarat Technological University, Ahmedabad, India



ORIGINAL ARTICLES

Open camera or QR reader and scan code to access this article and other resources online.



Quality by Design Approach for Optimization of Microbial and pH-Triggered Colon-Targeted Tablet Formulation Using Carboxymethyl Tamarind Gum

Jaymin Patel,^{1,2} Kaushika Patel,¹ and Shreeraj Shah¹

¹L. J. Institute of Pharmacy, LJ University, Ahmedabad, India.

²Research Scholar, Gujarat Technological University, Ahmedabad, India.

ABSTRACT

The purpose of this study was to apply the quality by design (QbD) approach in the development of a microbial and pH-triggered colon-targeted budesonide tablet. A retrospective research strategy was used to select various polysaccharide-based natural gums such as tamarind gum, gellan gum, karaya gum, gum ghutti, and khaya gum, which were then evaluated for their effectiveness in microbial degradation and targeting the colon. Viscosity profiles were generated in the presence of a prebiotic culture medium prepared by using the Velgut capsule that mimicked the impact of 4% rat cecal content and helpful in screening of natural polymer. Based on the cumulative drug release data of preliminary batches, carboxymethyl (CM) tamarind gum was identified as a superior and an excellent polymer over the tamarind gum for formulation development. The presence of water as a bridging agent in wet granulation also played an important role in the retardation of drug release. Tablets were supercoated with the enteric polymer, Eudragit S100. The Box-Behnken design was utilized, where the selected independent variables were the proportion of CM tamarind gum, % water proportion, and % weight gain of Eudragit S 100 to optimize the formulation. The optimized design space was generated with the criteria that a drug release should be of

less than 5% within the first 2 h, less than 10% within the first 5 h, and more than 70% within the first 8 h, to achieve colon targeting. The optimized batch F3 was found stable as per International Council for Harmonisation guidelines. The roentgenography study for optimized formulation demonstrated that it remained intact for 5 h and, at 7 h, was disseminated completely. CM tamarind gum is efficient for colon targeting, and its proportion in 100 mg along with an enteric coating of 6% led to the optimized formulation.

Keywords: budesonide, pH and microbial triggered, carboxymethyl tamarind gum, Box-Behnken design, colon-targeted drug delivery

INTRODUCTION

In recent years, the pharmaceutical research community has devoted considerable attention to the development of targeted drug delivery systems.^{1,2} One such promising approach is the use of natural polymers as carriers for drug delivery.³


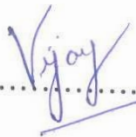

The targeted delivery of drugs to the colon is a highly desired objective in the field of drug delivery due to its numerous benefits in treating various gastrointestinal (GI) disorders such as ulcerative colitis (UC), Crohn's disease (CD), amebiasis, colonic cancer, and other colonic pathologies.⁴

One of the prominent symptoms of UC is a frequent occurrence of blood and mucus in association with fecal matter, accompanied with lower abdominal cramping that reaches its maximum severity during the act of defecation.^{5,6} CD, in

Appendix A- CPCSEA Approval protocol for *in vivo* study

Certificate

This is to certify that the project proposal no . *LJIP/IAEC/2022-23/02* entitled "*Formulation And Evaluation Of Colon Targeted Oral Drug Delivery System Using Natural Polymers And Methacrylic Acid Co-Polymers*" submitted by **Mr. Jaymin Patel** has been approved/recommended by the IAEC of L. J. Institute of Pharmacy in its meeting held on 15/10/2022 and Wistar Rat -56, Rabbit- 2 have been sanctioned under this proposal for a duration of next 12 months.

Authorized by	Name	Signature	Date
Chairman:	Dr. Shreeraj Shah		15/10/2022
Member Secretary:	Mr. Vijay Kevlani		15/10/22
Main Nominee of CPCSEA:	Dr. Surajit Baksi		15/10/22



(Kindly make sure that minutes of the meeting duly signed by all the participants are maintained by Office)